

**YEDİTEPE UNIVERSITY
INSTITUTE of HEALTH SCIENCES
DEPARTMENT OF PHARMACEUTICAL TECHNOLOGY
MASTER'S PROGRAM IN COSMETOLOGY**



**DEVELOPMENT of LIPOSOMAL CARRIER
SYSTEMS of HYDROLYZED COLLAGEN,
RESVERATROL, RETINOL and INVESTIGATION
of THEIR PENETRATIONS**

MASTER OF SCIENCE THESIS

HAKAN SEVİNÇ

ISTANBUL, 2020

**YEDİTEPE UNIVERSITY
INSTITUTE of HEALTH SCIENCES
DEPARTMENT OF PHARMACEUTICAL TECHNOLOGY
MASTER'S PROGRAM IN COSMETOLOGY**



**DEVELOPMENT of LIPOSOMAL CARRIER
SYSTEMS of HYDROLYZED COLLAGEN,
RESVERATROL, RETINOL and INVESTIGATION
of THEIR PENETRATIONS**

MASTER OF SCIENCE THESIS

HAKAN SEVİNÇ




**SUPERVISOR
DR. YASEMİN YAĞAN UZUNER
Bsc. Pharm., Ph. D**

İSTANBUL, 2020

THESIS APPROVAL FORM

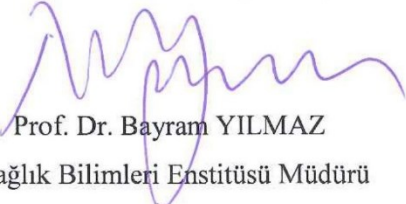
Kurum : Yeditepe Üniversitesi Sağlık Bilimleri Enstitüsü
Program : Kozmetoloji Yüksek Lisans Programı
Tez Başlığı : Development of Liposomal Carrier Systems of Hydrolyzed Collagen,
Resveratrol, Retinol and Investigations of Their Penetrations
Tez Sahibi : Hakan SEVİNÇ
Sınav Tarihi : 17/01/2020 - 10⁰⁰

Bu çalışma jürimiz tarafından kapsam ve kalite yönünden Yüksek Lisans Tezi olarak kabul edilmiştir.

	Unvanı, Adı-Soyadı (Kurumu)	İmza
Jüri Başkanı:	Prof.Dr. Gülgün YENER (İstanbul Ün. Ecz.Fak. Farmasötik Teknoloji AD)	
Tez danışmanı:	Dr.Öğr.Üyesi Yasemin UZUNER (Acıbadem Mehmet Ali Aydınlar Ün. Ecz.Fak. Farmasötik Teknoloji AD)	
Üye:	Prof.Dr. Çetin TAŞ (Yeditepe Ün. Ecz.Fak. Farmasötik Teknoloji AD)	
Üye:		
Üye:		

ONAY

Bu tez Yeditepe Üniversitesi Lisansüstü Eğitim-Öğretim ve Sınav Yönetmeliğinin ilgili maddeleri uyarınca yukarıdaki jüri tarafından uygun görülmüş ve Enstitü Yönetim Kurulu'nun 17/01/2020 tarih ve 2020/01-30 sayılı kararı ile onaylanmıştır.


Prof. Dr. Bayram YILMAZ
Sağlık Bilimleri Enstitüsü Müdürü

DECLARATION

I declare that this thesis is my work and that according to the best of my belief and knowledge, it does not contain previously published material nor material that is written by another person nor material that had been accepted for another degree award except where due acknowledgment has been made in the text.



18.08.2019

Hakan Sevinç

This thesis is dedicated to my family with love



ACKNOWLEDGMENTS

I want to thank my supervisor Dr. Yasemin Uzuner for her continuous support and motivation during my MSc study. I want to express my gratitude to her for spending her precious time every time I consulted her, offering me the best she could in order to help, with patience and high interest.

I would also like to thank my dear colleague and director, Prof. Dr. Murat Türkođlu, for continuously guiding me in terms of my research topics and methods, and providing me with the resources and also sharing his valuable information with me.

I would also like to thank my General Manager, Cihat Dünder, for encouraging me to enroll in this graduate program.

Moreover, I would like to thank very much every one of my other university professors and teachers in the Faculty of Chemical and in this MSc program for everything they have contributed to me during my 4-year undergraduate university education, during the theoretical and practical studies for teaching me all of the invaluable information and the skills that made me who I am now in life.

Finally, I would like to express my gratitude and exceptional thanks to my family, which has been the most significant change I had in my life, for their unlimited support and trust in me.

HAKAN SEVİNÇ

TABLE of CONTENTS

THESIS APPROVAL FORM.....	iii
DECLARATION	iv
ACKNOWLEDGMENTS	vi
TABLE of CONTENTS	vii
ABBREVIATIONS	xiii
LIST of TABLES	xv
LIST of FIGURES.....	xvii
LIST of GRAPHS.....	xviii
ABSTRACT.....	xxii
ÖZET.....	xxiii
1. INTRODUCTION.....	1
2. SKIN and COSMETICS	3
2.1. SKIN.....	3
2.1.1. EPIDERMIS	4
2.1.1.1. NATURAL MOISTURIZING FACTOR (NMF)	5
2.1.1.2. SEBACEOUS GLANDS.....	6
2.1.1.3. ECCRINE GLANDS.....	6
2.1.1.4. MELANOCYTES	6
2.1.1.5. LANGERHANS' CELLS	7
2.1.1.6. MERKEL CELLS	7
2.1.1.7. PROPERTIES and FUNCTIONS of the SKIN BARRIER.....	7
2.1.2. DERMIS	8
2.1.3. HYPODERMIS.....	9
2.1.4. SKIN AGING	9
2.1.4.1. EFFECT of AGING on COLLAGEN	11
2.1.4.2. ELASTIN, GLYCOSAMINGLYCANS, and GLYCOPROTEINS on AGING	13
3. COSMECEUTICAL PRODUCTS.....	14
3.1. ANTI-AGING ACTIVES/INGREDIENTS	16
3.1.1. VITAMIN A, RETINOIDS and RETINOL.....	18
3.1.1.1. TRETINOIN.....	21
3.1.1.2. ISORETINOIN.....	22
3.1.1.3. RETINOL.....	22
3.1.1.4. RETINALDEHYDE.....	25
3.1.2. RESVERATROL.....	25

3.1.3.	COLLAGEN	27
3.1.3.1.	OTHER COMMONLY USED ANTI-AGING ACTIVES	28
3.1.3.1.1.	ALPHA LIPOIC ACID	28
3.1.3.1.2.	COENZYME Q10.....	28
3.1.3.1.3.	VITAMIN C.....	29
3.1.3.1.3.1.	COLLAGEN FORMATION	30
3.1.3.1.3.2.	FREE RADICALS SCAVENGING AND TOXINS OXIDANT DISPOSING	30
3.1.3.1.3.3.	INHIBITION of MELANOGENESIS.....	30
3.1.3.1.3.4.	INTERACTION with CELL SIGNALLING PATHWAYS	31
3.1.3.1.4.	BIOTIN	32
3.1.3.1.5.	CAFFEINE.....	32
4.	DELIVERY SYSTEMS in COSMETIC INDUSTRY	33
4.1.	CARRIER SYSTEMS	33
4.1.1.	LIPOSOMES	35
4.1.1.1.	STRUCTURE of LIPOSOMES	37
4.1.1.2.	LIPOSOMES ADVANTAGES.....	38
4.1.1.3.	CLASSIFICATION of LIPOSOMES	38
4.1.1.4.	PREPARATION of LIPOSOMES	39
4.1.1.4.1.	PASSIVE LOADING TECHNIQUE.....	40
4.1.1.4.1.1.	MECHANICAL DISPERSION METHOD.....	40
4.1.1.4.1.2.	SOLVENT DISPERSING METHOD	42
4.1.1.4.1.3.	DETERGENT CLEANING METHOD	43
4.1.1.4.2.	ACTIVE LOADING TECHNOLOGY	43
4.1.1.4.3.	DETERGENT DIALYSIS	44
4.1.1.4.4.	MICROFLUIDIZER METHOD	44
4.1.1.5.	CHARACTERIZATION of LIPOSOMES	46
4.1.1.5.1.	DETERMINATION of ENCAPSULATION EFFICIENCY.....	46
4.1.1.5.2.	DETERMINATION of LAMELLAR STRUCTURE.....	46
4.1.1.5.3.	DETERMINATION of SIZE DISTRIBUTION and SURFACE CHARGE DETERMINATION	47
4.1.1.5.4.	TRANSMISSION ELECTRON MICROSCOPY	48
4.1.1.5.5.	APPEARANCE.....	48
4.1.1.5.6.	STABILITY of LIPOSOMES.....	48
4.1.1.6.	ETHOSOMES	50
4.1.1.6.1.	PRODUCTION of ETHOSOMES	51
4.1.2.	LIPIDS	52
4.1.3.	PHOSPHOLIPIDS	52
4.1.4.	LIPOSOMES and SKIN	54

5.	FRANZCELL.....	55
6.	DIFFUSION.....	59
6.1.	FICK'S 1 st LAW.....	60
6.2.	FICK'S 2 nd LAW.....	60
6.3.	STEADY-STATE.....	61
7.	MATERIALS and METHODS.....	61
7.1.	MATERIALS.....	61
7.1.1.	CHEMICALS.....	61
7.1.1.1.	PBS (PHOSPHATE BUFFERED SOLUTION).....	62
7.1.2.	INSTRUMENTS/EQUIPMENT.....	63
7.1.2.1.	MICROFLUIDIZER HIGH-PRESSURE HOMOGENIZER.....	63
7.1.2.2.	HIGH-PRESSURE LIQUID CHROMATOGRAPHY DEVICE (HPLC).....	64
7.1.2.3.	PARTICLE SIZE ANALYZER.....	64
7.1.2.4.	FRANZCELL.....	64
7.1.2.5.	UV-VIS SPECTROPHOTOMETER.....	65
7.1.2.6.	THE FOURIER TRANSFORM INFRARED SPECTROMETER.....	65
7.1.2.7.	ZETA POTENTIAL DEVICE.....	65
7.1.2.8.	MICROPLATE ABSORBANCE READER.....	65
7.1.2.9.	CRYO-SEM of LIPOSOMAL DELIVERY SYSTEMS.....	66
7.2.	METHODS.....	66
7.2.1.	FT-IR SPECTRUM ANALYSIS of ACTIVE SUBSTANCES.....	66
7.2.2.	STUDIES on RESVERATROL.....	67
7.2.2.1.	HPLC ANALYSIS PROCEDURE.....	67
7.2.2.1.1.	LINEARITY.....	68
7.2.2.1.2.	ACCURACY.....	68
7.2.2.1.3.	PRECISION.....	68
7.2.2.1.3.1.	REPEATABILITY 1.....	69
7.2.2.1.3.2.	REPEATABILITY 2.....	69
7.2.2.1.4.	LIMIT of DETECTION (LOD).....	69
7.2.2.1.5.	LIMIT of QUANTITATION (LOQ).....	69
7.2.2.1.6.	RANGE.....	70
7.2.2.1.7.	ROBUSTNESS.....	70
7.2.2.1.8.	SPECIFICITY.....	70
7.2.2.1.9.	DETERMINATION OF SOLUBILITY OF RESVERATROL.....	71
7.2.3.	STUDIES on RETINOL.....	71
7.2.3.1.	HPLC ANALYSIS PROCEDURE.....	71
7.2.3.1.1.	LINEARITY.....	72
7.2.3.1.2.	ACCURACY.....	72

7.2.3.1.3.	PRECISION	72
7.2.3.1.3.1.	REPEATABILITY 1	73
7.2.3.1.3.2.	REPEATABILITY 2	73
7.2.3.1.4.	LIMIT of DETECTION (LOD)	73
7.2.3.1.5.	LIMIT of QUANTITATION (LOQ).....	73
7.2.3.1.6.	RANGE	74
7.2.3.1.7.	ROBUSTNESS	74
7.2.3.1.8.	SPECIFICITY	74
7.2.3.1.9.	DETERMINATION OF SOLUBILITY OF RETINOL	75
7.2.4.	STUDIES on HYDROLYZED COLLAGEN.....	75
7.2.4.1.	HYDROLYZED COLLAGEN ANALYSIS.....	75
7.2.4.2.	LINEARITY.....	76
7.2.4.3.	ACCURACY.....	76
7.2.4.4.	PRECISION	77
7.2.4.4.1.	REPEATABILITY 1	77
7.2.4.4.2.	REPEATABILITY 2.....	77
7.2.4.5.	LIMIT of DETECTION (LOD)	78
7.2.4.6.	LIMIT of QUANTITATION (LOQ).....	78
7.2.4.7.	RANGE	78
7.2.4.8.	ROBUSTNESS	79
7.2.4.9.	SPECIFICITY	79
7.2.4.10.	DETERMINATION of the SOLUBILITY of HYDROLYZED COLLAGEN.....	79
7.2.5.	PREPARATION of LIPOSOMES and ETHOSOMES	79
7.2.5.1.	REDUCING the SIZES of LIPOSOMES and ETHOSOMES	80
7.2.6.	STUDIES CONDUCTED on LIPOSOMES and ETHOSOMES	81
7.2.6.1.	DETERMINATION of ETHOSOMES ENCAPSULATION EFFICIENCY	81
7.2.6.2.	PARTICLE SIZE ANALYSIS.....	81
7.2.6.3.	UV-VIS SPECTROPHOTOMETER ANALYSIS.....	81
7.2.6.4.	ZETA POTENTIAL ANALYSIS of ETHOSOMES	82
7.2.6.5.	IMAGING of ETHOSOMES BY SCANNING ELECTRON MICROSCOPE	82
7.2.6.6.	PH MEASUREMENT.....	82
7.2.6.7.	CONDUCTIVITY MEASUREMENT.....	82
7.2.6.8.	DENSITY MEASUREMENT.....	83
7.2.6.9.	CONDUCTING STABILITY STUDIES.....	83
7.2.6.10.	CYTOTOXICITY ANALYSIS.....	83
7.2.6.11.	FRANZCELL <i>in-vitro</i> DIFFUSION TESTS.....	84
7.2.7.	STATICAL ANALYSIS.....	85
8.	RESULTS	85
8.1.	RESULTS of LIPOSOME FORMULATION STUDIES.....	85

8.2.	RESULTS of the RESVERATROL	91
8.2.1.	RESULTS of ANALYTICAL VALIDATION of RESVERATROL ASSAY	91
8.2.1.1.	FT-IR SPECTRUM	91
8.2.1.2.	LINEARITY	91
8.2.1.3.	ACCURACY	92
8.2.1.4.	PRECISION	93
8.2.1.4.1.	REPEATABILITY 1	93
8.2.1.4.2.	REPEATABILITY 2	93
8.2.1.5.	LIMIT of DETECTION (LOD)	94
8.2.1.6.	LIMIT of QUANTITATION (LOQ)	94
8.2.1.7.	ROBUSTNESS	94
8.2.1.8.	SPECIFICITY	95
8.2.1.9.	SOLUBILITY	95
8.2.2.	FORMULATIONS of RESVERATROL ETHOSOMES	95
8.2.2.1.	PARTICLE SIZE and STABILITY of ETHOSOMES FORMULATIONS	96
8.3.	RESULTS of the RETINOL	97
8.3.1.	RESULTS f ANALYTICAL VALIDATION of RETINOL ASSAY	97
8.3.1.1.	FT-IR SPECTRUM	97
8.3.1.2.	LINEARITY	98
8.3.1.3.	ACCURACY	98
8.3.1.4.	PRECISION	99
8.3.1.4.1.	REPEATABILITY 1	99
8.3.1.4.2.	REPEATABILITY 2	100
8.3.1.5.	LIMIT of DETECTION (LOD)	100
8.3.1.6.	LIMIT of QUANTITATION (LOQ)	101
8.3.1.7.	ROBUSTNESS	101
8.3.1.8.	ORIGINALITY, SELECTIVITY	101
8.3.1.9.	SOLUTION STUDY	102
8.3.2.	FORMULATIONS of RETINOL ETHOSOMES	102
8.3.2.1.	PARTICLE SIZE and STABILITY of RETINOL ETHOSOMES FORMULATIONS	102
8.4.	RESULTS of the HYDROLYZED COLLAGEN	104
8.4.1.	RESULTS of ANALYTICAL VALIDATION of HYDROLYZED COLLAGEN ASSAY	104
8.4.1.1.	FT-IR SPECTRUM	104
8.4.1.2.	LINEARITY	104
8.4.1.3.	ACCURACY	105
8.4.1.4.	PRECISION	106
8.4.1.4.1.	REPEATABILITY 1	106
8.4.1.4.2.	REPEATABILITY 2	106

8.4.1.5.	LIMIT of DETECTION (LOD)	107
8.4.1.6.	LIMIT of QUANTITATION (LOQ).....	107
8.4.1.7.	ROBUSTNESS	107
8.4.1.8.	SPECIFICITY	108
8.4.1.9.	SOLUTION STUDY	108
8.4.2.	FORMULATIONS of HYDROLYZED COLLAGEN ETHOSOMES.....	108
8.4.2.1.	PARTICLE SIZE and STABILITY of ETHOSOMES FORMULATIONS	109
8.5.	CHARACTERIZATION of ETHOSOMES FORMULATIONS.....	110
8.5.1.	DETERMINATION of PH, CONDUCTIVITY, DENSITY and ZETA POTENTIALS of ETHOSOMES FORMULATIONS.....	110
8.5.2.	ELECTRON MICROSCOPY (SEM) IMAGES of ETHOSOMES FORMULATIONS.	111
8.5.3.	DETERMINATION of CYTOTOXICITY of ETHOSOMES FORMULATIONS	112
8.5.4.	INFRARED FOURIER TRANSFORMATION SPECTROSCOPY (FT-IR) ANALYSIS of ETHOSOMES FORMULATIONS.....	114
8.5.5.	MEASUREMENT of ACTIVE SUBSTANCE CONTENT in ETHOSOMES FORMULATIONS.....	115
8.5.6.	<i>In-vitro</i> RELEASE STUDIES of ETHOSOME FORMULATIONS.....	115
9.	DISCUSSION	119
9.1.	The CHOICE of ACTIVE SUBSTANCES, IDENTIFICATION, and VALIDATION STUDIES	119
9.2.	The ETHOSOMES FORMULATION of <i>trans</i> -RESVERATROL, RETINOL, and HYDROLYZED COLLAGEN.....	123
9.3.	STABILITY STUDIES of ETHOSOME FORMULATIONS	124
9.4.	EVALUATION of ENTRAPMENT EFFICACIACY, POLY DISPERSITY INDEX, PARTICLE SIZE, ZETA POTENTIAL, and ELECTRON MICROSCOPY IMAGES.....	124
9.5.	EVALUATION of <i>in-vitro</i> RELEASE STUDIES on FRANZCELL.....	126
9.6.	CONCLUSION.....	128
10.	REFERENCES	130
11.	ANNEX A: DEVICE OUTPUTS of ANALYZES	143
12.	ÖZGEÇMİŞ.....	169

ABBREVIATIONS

A	: Average
ALA	: Alpha-lipoic acid
ATR	: Attenuated total reflectance
CEM	: Cryo-electron microscopy
CMC	: Critical Micelle Concentration
CRABP	: Cellular Retinoic Acid Binding Protein
DLS	: Dynamic light scattering
DPPC	: Dipalmitoyl Phosphatidylcholine
DSPC	: Distearyl Phosphatidylcholine
EE	: Encapsulation efficiency
FDA	: The American Food, Drug, and Cosmetic Act
GAG	: Glycosaminoglycans
HA	: Hyaluronic acid
HLE	: Human leukocyte elastase
LOD	: Limit of detection
LOQ	: Limit of quantitation
LUV	: Large unilamellar vesicles
MLV	: Multicellular vesicles
MM	: Mixed micelles
MMP	: Matrix metalloproteinase
MWCO	: Molecular weight cut-off
NF	: Nuclear factor
NMF	: Natural Moisturizing Factor
OTC	: Over-the-counter

PA	: Phosphatidic acid
PC	: Phosphatidylcholine
PC	: Phosphatidylcholine
PC	: Positive control
PCA	: Pyrrolidone carboxylic acid
PE	: Phosphatidylethanolamine
PI	: Phosphatidylinositol
PPG	: Phosphatidylglycerol
PS	: Phosphatidylserine
RA	: Retinoic acid
RAR	: Retinoic acid receptor
ROL	: All-trans-retinol
ROS	: Reactive oxygen species
RR	: Reliability Range
RXR	: retinoid X receptor
SC	: Stratum corneum
SIRT	: Sirtuin gene
SM	: Sphingomyelin
SUV	: Small layered vesicles
T _c	: Critical phase transition temperature
T _m	: Phase transition temperature
V	: Coefficient of Variation
Z	: Zeta potential (ζ)
σ	: Standard deviation

LIST of TABLES

Table 1.Types of collagen found in the dermiş	13
Table 2.Vitamins and their functions in photoaging summary	18
Table 3.Summary of some of the potential effects of vitamin C on the skin	31
Table 4.Different carrier vesicle systems	34
Table 5.Disciplines using liposomes	36
Table 6.Advantages and disadvantages of liposome	38
Table 7.Liposome carrier types	39
Table 8.Liposome stability tests	49
Table 9.Comparison of different characteristics of liposomes, transfersomes, and ethosomes	51
Table 10.Summary of the synthetic membrane properties. All values are nominally provided by manufacturers (ρ -membrane porosity, τ -membrane tortuosity)	56
Table 11.Properties of cellulose nitrate filter (ρ -membrane porosity, τ -membrane tortuosity)	58
Table 12.Total diffusion flow of cellulose nitrate filter	58
Table 13.Chemical materials	62
Table 14.Instruments used in the study	63
Table 15.Formulations of liposomes obtained with different sources of lecithin	86
Table 16.Particle Size and Uniformity Analysis of Empty liposomes	87
Table 17.Ethosome formulations with suitable Lipoid P75	89
Table 18.Particle Size and Uniformity Analysis for Empty liposome formulations and ethosomes with lipoid P75	89
Table 19.Accuracy of trans-resveratrol in ethyl alcohol	92
Table 20.Trans-resveratrol repeatability test results in ethyl alcohol	93
Table 21.Trans-resveratrol repeatability test results in ethyl alcohol	94
Table 22.Trans-resveratrol stability test results in ethyl alcohol	94
Table 23.Empty and loaded ethosomes formulations	95
Table 24.Particle size and uniformity of ethosome formulations	96
Table 25.Results of the accuracy test of retinol in ethyl alcohol	99
Table 26.Retinol repeatability test results in ethyl alcohol	100
Table 27.Retinol recoverability test results in ethyl alcohol	100
Table 28.Trans-resveratrol stability test results in ethyl alcohol	101

Table 29.Empty and loaded retinol ethosomes formulations	102
Table 30.Particle size and uniformity of retinol ethosomes formulations	102
Table 31.Data on the accuracy test of Hydrolyzed Collagen	105
Table 32.Hydrolyzed Collagen repeatability test results in PBS.....	106
Table 33.Hydrolyzed collagen repeatability test results in PBS.....	107
Table 34.Hydrolyzed collagen stability test results in PBS.....	107
Table 35. Empty and loaded hydrolyzed collagen ethosomes formulations	108
Table 36.Particle size and uniformity of hydrolyzed collagen ethosomes	109
Table 37.The pH, conductivity and Zeta potential values of ethosomes formulations	111
Table 38.PDI values of ethosomes formulations	112
Table 39.% amount of encapsulated active ingredient of ethosomes and the solutions	115



LIST of FIGURES

Figure 1.Diagram of the Skin	3
Figure 2.Layer of the Epidermis	5
Figure 3.Groups of fat cells separated by collagen.....	9
Figure 4.Bill McElligott, truck driver, massive sun damage on one side of his face	10
Figure 5.Illustration of collagen weakening with age	12
Figure 6.Chemical structures of retinoids.....	20
Figure 7.Active retinol	24
Figure 8.Dispersion method with an organic solvent (Burgess,).....	41
Figure 9.Dimensioning of liposomes by sonication	42
Figure 10.Glycerophospholipids (185)	53
Figure 11.Sphingolipids.....	53
Figure 12.Structure of the cell membrane (88)	54
Figure 13.Franzcell diffusion cell	57
Figure 14.Cryo-SEM images of the active substance-free ethosomes	112
Figure 15.Cryo-SEM images of the active substance containing ethosomes (T12, T16, T20).....	112
Figure 16.Light refraction image of bilayer layer with a microscope of ethosome.....	167
Figure 17.Light refraction image of bilayer layer with a microscope of ethosome.....	167
Figure 18.Light refraction image of bilayer layer with a microscope of ethosome.....	168

LIST of GRAPHS

Graph 1.Day-Particle Size Graph of liposomes.....	88
Graph 2.Uniformity graph of liposomes.....	88
Graph 3.Particle size graph of formulations made with Lipoid P75	90
Graph 4.Uniformity graph of formulations made with lipoid P75	90
Graph 5.IR spectrum of resveratrol	91
Graph 6.The standard line of trans-resveratrol obtained by HPLC method	92
Graph 7.Trans-resveratrol peak in HPLC	95
Graph 8.The particle size of Resveratrol ethosome formulations vs empty ethosomes .	96
Graph 9.Uniformity of ethosomes formulations.....	97
Graph 10.IR spectrum of retinol	97
Graph 11.The standard line of retinol obtained by HPLC method.....	98
Graph 12.Retinol peak in HPLC.....	101
Graph 13.Particle size of retinol ethosomes formulations.....	103
Graph 14.Uniformity of retinol ethosomes formulation.....	103
Graph 15.IR spectrum of hydrolyzed collagen.....	104
Graph 16.The standard line of hydrolyzed collagen obtained by lowry method.....	105
Graph 17.Hydrolyzed collagen in Uv-Vis	108
Graph 18.Particle size of hydrolyzed collagen ethosomes	109
Graph 19.Uniformity of hydrolyzed collagen ethosomes.....	110
Graph 20.PH-Conductivity-Zeta potential measurements of ethosomes.....	110
Graph 21.Cytotoxicity results of actives on HaCaT cells.....	113
Graph 22.Cytotoxicity results of ethosomes on HaCaT cells.....	113
Graph 23.FT-IR absorbances of T12, T16, T20, T24 formulations	114
Graph 24.FT-IR absorbances of T12, T16, T20, T24 formulations and PBS	114
Graph 25.Graph of trans-resveratrol Franzcell Diffusion T16 formulation	116
Graph 26.Graph of Retinol Franzcell Diffusion T20 formulation.....	117
Graph 27.Graph of Hydrolyzed collagen Franzcell Diffusion T12 formulation	118
Graph 28.T9 1st-day particle size analysis	143
Graph 29.T9 5th-day particle size analysis.....	143
Graph 30.T9 15th-day particle size analysis.....	143
Graph 31.T9 180th-day particle size analysis.....	144
Graph 32.T10 1st-day particle size analysis	144

Graph 33.T10 5th-day particle size analysis.....	144
Graph 34.T10 15th-day particle size analysis.....	144
Graph 35.T10 180th-day particle size analysis.....	144
Graph 36.T11 1st-day particle size analysis	145
Graph 37.T11 5th-day particle size analysis.....	145
Graph 38.T11 15th-day particle size analysis.....	145
Graph 39.T11 180th-day particle size analysis.....	145
Graph 40.T12 1st-day particle size analysis	146
Graph 41.T12 5th-day particle size analysis.....	146
Graph 42.T12 15th-day particle size analysis.....	146
Graph 43.T12 180th-day particle size analysis.....	146
Graph 44.T13 1st-day particle size analysis	147
Graph 45.T13 5th-day particle size analysis.....	147
Graph 46.T13 15th-day particle size analysis.....	147
Graph 47.T13 180th-day particle size analysis.....	147
Graph 48.T14 1st-day particle size analysis	148
Graph 49.T14 5th-day particle size analysis.....	148
Graph 50.T14 15th-day particle size analysis.....	148
Graph 51.T14 180th-day particle size analysis.....	148
Graph 52.T15 1st-day particle size analysis	149
Graph 53.T15 5th-day particle size analysis.....	149
Graph 54.T15 15th-day particle size analysis.....	149
Graph 55.T15 180th-day particle size analysis.....	149
Graph 56.T16 1st-day particle size analysis	150
Graph 57.T16 5th-day particle size analysis.....	150
Graph 58.T16 15th-day particle size analysis.....	150
Graph 59.T16 180th-day particle size analysis.....	150
Graph 60.T17 1st-day particle size analysis	151
Graph 61.T17 5th-day particle size analysis.....	151
Graph 62.T17 15th-day particle size analysis.....	151
Graph 63.T17 180th-day particle size analysis.....	151
Graph 64.T18 1st-day particle size analysis	152
Graph 65.T18 1st-day particle size analysis	152
Graph 66.T18 1st-day particle size analysis	152

Graph 67.T18 1st-day particle size analysis	152
Graph 68.T19 1st-day particle size analysis	153
Graph 69.T19 5th-day particle size analysis.....	153
Graph 70.T19 15th-day particle size analysis.....	153
Graph 71.T19 180th-day particle size analysis.....	153
Graph 72.T20 1th day particle size analysis	154
Graph 73.T20 5th-day particle size analysis.....	154
Graph 74.T20 15th-day particle size analysis.....	154
Graph 75.T20 180th-day particle size analysis.....	154
Graph 76.T21 1st-day particle size analysis	155
Graph 77.T21 5th-day particle size analysis.....	155
Graph 78.T21 15th-day particle size analysis.....	155
Graph 79.T21 180th-day particle size analysis.....	155
Graph 80.T22 1st-day particle size analysis	156
Graph 81.T22 5th-day particle size analysis.....	156
Graph 82.T22 15th-day particle size analysis.....	156
Graph 83.T22 180th-day particle size analysis.....	156
Graph 84.T23 1st-day particle size analysis	157
Graph 85.T23 5th-day particle size analysis.....	157
Graph 86.T23 15th-day particle size analysis.....	157
Graph 87.T23 180th-day particle size analysis.....	157
Graph 88.T24 1st-day particle size analysis	158
Graph 89.T24 5th-day particle size analysis.....	158
Graph 90.T24 15th-day particle size analysis.....	158
Graph 91.T24 180th-day particle size analysis.....	158
Graph 92.T9-T10-T11-T12 1st-day zeta potentials	159
Graph 93.T13-T14-T15-T16 1st-day zeta potentials	159
Graph 94.T17-T18-T19-T20 1st-day zeta potentials	160
Graph 95.T21-T22-T23-T24 1st-day zeta potentials	160
Graph 96.T21-T22-T23-T24 1st-day zeta potentials	161
Graph 97.T13-T14-T15-T16 7th-day zeta potentials	161
Graph 98.T17-T18-T19-T20 7th-day zeta potentials	162
Graph 99.T21-T22-T23-T24 7th-day zeta potentials	162
Graph 100.T9-T10-T11-T12 15th-day zeta potentials	163

Graph 101.T13-T14-T15-T16 15th-day zeta potentials	163
Graph 102.T17-T18-T19-T20 15th-day zeta potentials	164
Graph 103.T21-T22-T23-T24 15th-day zeta potentials	164
Graph 104.T9-T10-T11-T12 30th-day zeta potentials	165
Graph 105.T13-T14-T15-T16 30th-day zeta potentials	165
Graph 106.T17-T18-T19-T20 30th-day zeta potentials	166
Graph 107.T21-T22-T23-T24 30th-day zeta potentials	166



ABSTRACT

Sevinç, H. (2020), “Development of Liposomal Carrier Systems of Hydrolyzed Collagen, Resveratrol, Retinol, and investigation of Their Penetrations.” Yeditepe University, Institute of Health Sciences, Department of Pharmaceutical Technology, MSc Thesis, İstanbul.

In recent years, not only for cosmetic products but also for the administration of drugs, transdermal delivery is becoming an important route of administration. Percutaneous permeation of molecules is controlled by the diffusion laws and is a big challenge in biomedical sciences. Transdermal delivery systems have many advantages such as avoidance of the first-pass metabolism, sustained-release opportunity and less frequent dosing, ease of application, and better user compliance.

Ethosome is one of these new and promising delivery systems, which is a new generation of liposome and because of the presence of alcohol in its structure, it offers an increased solubility for hydrophilic, hydrophobic and amphiphilic active materials. Also, the smaller and more flexible structure makes ethosome a better carrier than liposome. Resveratrol, retinol and hydrolyzed collagen ethosomes were prepared as a possibility of developing new delivery systems with these anti-aging ingredients. The results of the studies showed that the ethosomes were easy to produce and stable at the duration of the tests (180 days at $25^{\circ}\text{C}\pm 2^{\circ}\text{C}$), no phase separation or bottom precipitation was observed; the changes in the measurements of particle size, size distribution, poly-dispersity index, zeta potential, pH, density, and conductivity were within acceptable intervals. The presence of alcohol increased the solubility of the ingredients resulting in good entrapment of respective active materials in ethosomes at a minimum of 86 % and retained the entrapped actives at a minimum of 71% level after 180 days. *In-vitro* release studies by Franzcell diffusion system were performed with the ethosome formulations using two different synthetic membranes; Strat-M® (layered skin mimicking) and 12-14KD cellulose acetate dialysis membrane. The release rates of the actives from ethosomes were compared with the simple solutions of the actives at 1,5%. The results clearly showed that ethosomes released the actives in a sustained release manner and the release rates were slower when Strat-M® was used.

Keywords: Retinol, hydrolyzed collagen, resveratrol, liposomes, ethosomes, in-vitro tests, franzcell

ÖZET

Sevinç, H. (2020), “Hidrolize kolajen, resveratrol ve retinol taşıyıcı liposomal sistemlerin geliştirilmesi ve bunların penetrasyonlarının incelenmesi “Yeditepe Üniversitesi, Sağlık Bilimleri Enstitüsü, Farmasötik Teknoloji Departmanı, Yüksek Lisans Tezi

Son yıllarda, sadece kozmetik ürünler için değil, aynı zamanda ilaçların uygulanması için de transdermal uygulama önemli bir uygulama yolu haline gelmiştir. Moleküllerin perkütan yolla geçişi difüzyon yasaları tarafından kontrol edilir ve biyomedikal bilimler açısından hala önemli derecede zordur. Transdermal taşıma sistemlerinin karaciğerden ilk geçiş metabolizmasına maruz kalınmaması, uzun süre ve sürekli salım fırsatı, daha az sayıda dozlama, uygulama kolaylığı ve kullanıcı uyumu gibi konularda avantajları vardır.

Etozom, yeni nesil bir lipozom olup yeni ve umut verici taşıyıcı sistemlerden biridir ve yapısındaki alkol nedeniyle hidrofilik, hidrofobik ve amfifilik aktif maddeler için daha fazla çözünebilirlik olasılığı sunar. Ayrıca, daha küçük ve daha esnek yapısı, etozomu lipozomdan daha etkin bir taşıyıcı yapar. Resveratrol, retinol ve hidrolize kollajen etozomlar, bu yaşlanma karşıtı bileşenlerle yeni dağıtım sistemleri geliştirme olasılığı olarak hazırlandı. Çalışmaların sonuçları, testler sırasında (25 toC ± 2°C'de 180 gün) etozomların üretilmesinin kolay ve stabil olduğunu, faz ayrılmasının veya taban çökmesinin gözlenmediğini; partikül büyüklüğü, boyut dağılımı, poli dağılımı indeksi, zeta potansiyeli, pH, yoğunluk ve iletkenlik ölçümlerindeki değişiklikler kabul edilebilir aralıklardaydı. Alkolün varlığı, bileşenlerin çözünürlüğünü arttırdı, bununla birlikte, ilgili aktif materyallerin, etozomlara en az% 86 oranında iyi tutulması sağlandı ve tutulan aktif maddeleri, 180 gün sonra minimum % 71 seviyesinde tuttu. Franzcell difüzyon sistemi kullanılarak yapılan *in-vitro* salım çalışmaları, iki farklı sentetik zar kullanılarak yapılmıştır; Strat-M® (katmanlı cilt taklit eden membran) ve 12-14KD selüloz asetat diyaliz membranı. Aktiflerin etozomlardan salım oranları aktiflerin %1,5'lük basit çözeltileriyle karşılaştırılmıştır. Sonuçlar, etozomların aktifleri sürekli salım şeklinde serbest bıraktıklarını açıkça gösterdi. Strat-M® kullanıldığında salım oranları daha yavaştı.

Anahtar kelime: Retinol, hidrolize kolajen, resveratrol, liposomes, etozom, *in-vitro* test, franzcell

1. INTRODUCTION

Liposomes, which are composed of biomembrane like double-layer structures, are used as drug/active material carrier systems in many industries such as pharmaceutical, cosmetic, and food. Due to their low toxicity, biodegradability, and also ability to penetrate the lower layers of the skin, liposomes have been used as delivery systems successfully. It is possible to encapsulate water and fat-soluble active substances into liposomes and transfer these to the lower layers of the skin to provide higher bioavailability of the actives. Ethosomes are third-generation liposomes with the advantages of their softness, malleability, and smaller sizes facilitating enhanced delivery. The amount of alcohol used in ethosome formulation makes it unique because of its known effect in disturbing the skin lipid bilayer, therefore increasing the penetration through stratum corneum. Additionally, ethosomes are known for their better stability and ease in their production (1).

In this thesis, ethosomes formulations will be developed for three common anti-aging active materials, and their effectiveness as topical delivery systems will be studied. Many researchers have studied liposomes and found that their stability was one of the main problems. These studies indicated that the stability problem of liposomal encapsulation could be overcome by making smaller liposomes. Another major problem with liposomes is the difficulties of conventional liposome preparation methods. The film method or reverse-phase evaporation method cannot be applied easily to large scale production due to the necessity of using organic solvents and the costly and laborious removal of these solvents from the final vesicular systems. As an alternative, one step liposome preparation methods have been tried by using a high-pressure homogenizer, and very successful results have been achieved, not only the penetration of ethosomes is simpler than liposomes but also there was no need to form a thin film or to evaporate large amounts of solvents during the process (2).

In this study, the ethosomes by entrapping resveratrol, retinol, and hydrolyzed collagen will be prepared, and their stability, entrapping efficiency as well as the release properties will be investigated. The release studies will be conducted by using the Franz cell diffusion systems with two different synthetic membranes and the amounts of actives released to the receptor solution will be monitored against time by using the validated spectrophotometric methods (3).

The characterization studies that are planned as part of our studies will reveal many features of ethosomes, such as average particle size and distribution, zeta potential, encapsulation efficiency. The microscopic imaging under normal and crossed polarized light and SEM will also help to investigate the structure, size, and shape of the ethosomes.

At the conclusion of this study, the following achievements are expected:

- a. The development of a reliable production method for these three ethosome formulations to entrap resveratrol, retinol, and hydrolyzed collagen.
- b. The development of analytical methods to measure the quantity of these three active anti-aging materials and validation of these methods. These validated methods will be used to measure the entrapment efficiency of the ethosomes as well as to monitor the release profiles of the actives with Franzcell diffusion tests.
- c. The characterization of the three ethosomes formulations where average particle size, size distribution, polydispersity index, and shape will be investigated.
- d. The stability of ethosomes will be monitored by repeating the characterization test at the predetermined time points (1, 7, 14, 30, 180 days). All of the samples will be kept at $25\pm 2^\circ\text{C}$.
- e. The determination of the *in-vitro* release profiles of each ethosome formulations. These studies will be conducted using the Franzcell diffusion system. Two different synthetic membranes will be used; Strat-M and cellulose acetate (12-14 KD) membrane. The Strat-M membrane has been studied by many other researchers, and it is said to be more resembling the human skin (4, 5). The ethosome formulations will be tested by comparing the release patterns of the simple solutions of the actives in order to see how ethosomes affect the release patterns. A retarded and sustained release pattern is expected from the ethosome formulations (6).

2. SKIN and COSMETICS

2.1. SKIN

Human skin is composed of layered, cellular epidermis and underlying connective tissue (7). The skin consists of three layers: epidermis, dermis, and hypodermis. Each layer has its characteristics and functions. The epidermis is the most superficial layer of the skin and is a multilayered epithelial tissue that is divided into several layers and known as the cover of the outer surface of our body (8). It has great importance since it provides the overall cosmetic appearance of the skin of a person's skin color. The stratum corneum (SC), located at the outermost side of this structure, is covered with organelle-free keratinocytes. This barrier forms an epidermal permeability barrier to prevent water and electrolyte loss. In Figure 1. the epidermis, the different layers of the epidermis and other structural components of the epidermal barrier, is shown downwards, granular layer, spinous layer, basal layer, respectively. Under these layers, the dermis begins (8, 22).

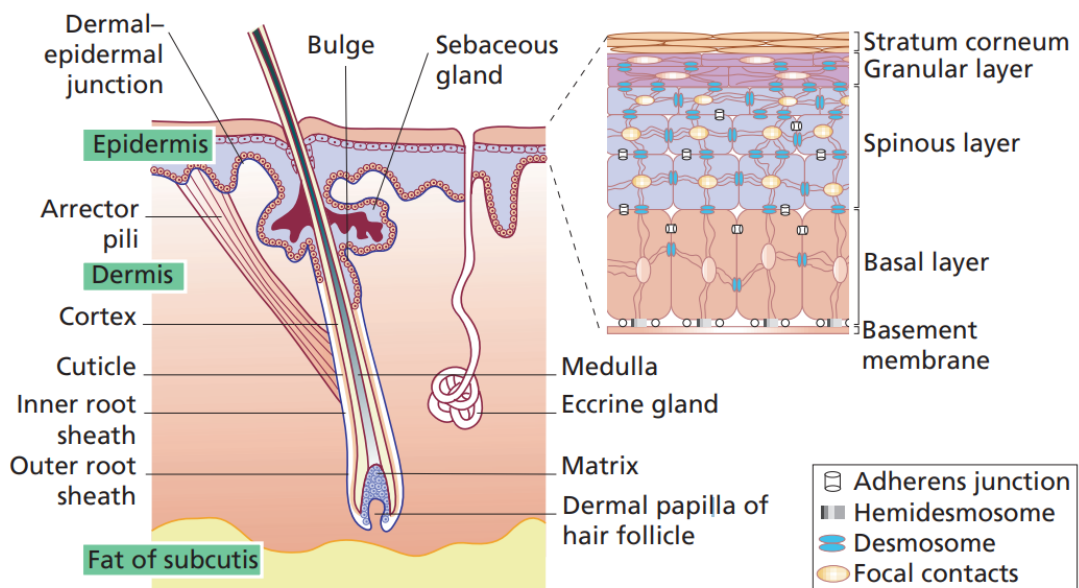


Figure 1. Diagram of the Skin (9)

2.1.1. EPIDERMIS

The healthy epidermis is a terminally differentiated, layered squamous epithelium. The primary cell constituting 95% of the total is keratinocyte, which passes through the epidermal basement membrane during the transition and proceeds towards the surface of the skin and forms several well-defined layers. Thus, on simple morphological grounds, the epidermis can be divided into four separate layers: stratum basale or stratum germinativum, stratum spinosum, stratum granulosum, and stratum corneum. The term Malpighian layer includes both basal and pointed cells. Other cells in the epidermis include melanocytes, Langerhans cells, and Merkel cells (10, 11).

The stratum basale is a continuous layer defined in the skin and hyperproliferative epidermis, generally only one cell thick but perhaps two or three cells thick. Basal cells are small and cuboidal (10-14 μm) and have large, dark-colored nuclei, dense cytoplasm with many ribosomes, and dense bundles of tonofilament. Immediately above the basal cell layer, the epibasal keratinocytes expand to form the spunk prickle cell layer or the stratum spinosum (10).

Stratum spinosum, stratum granulosum, or granular layer. Dense keratohyalin granule mass from a human at high magnification (12).

The epidermis has irregularly shaped particles of approximately 2 μm in length and has a randomly occurring particle structure in rows or cages (12).

The cytoplasm of the cells of the upper, pointed layer, and granule cell layer also contains smaller lamellar granules of an average size of 100-300 nm, known as lamellar granules or bodies, membrane coating granules or Odland bodies (11).

They are numerous in the cells at the top of the pointed layer and migrate around the cells as they enter the granular cell layer. They discharge lipid components into the intracellular space, play an essential role in barrier function, and promote intercellular association within the stratum corneum. The outermost layer of the epidermis is the stratum corneum, where cells have lost nuclei and cytoplasmic organelles. The cells become flattened, and the keratin filaments align into disulfide cross-linked macrofibres, under the influence of filaggrin, the

protein component of the keratohyalin granule, responsible for keratin filament aggregation (13)

Stratum corneum consists of terminally differentiated keratinocytes (corneocytes) and secreted contents of lamellar bodies (14).

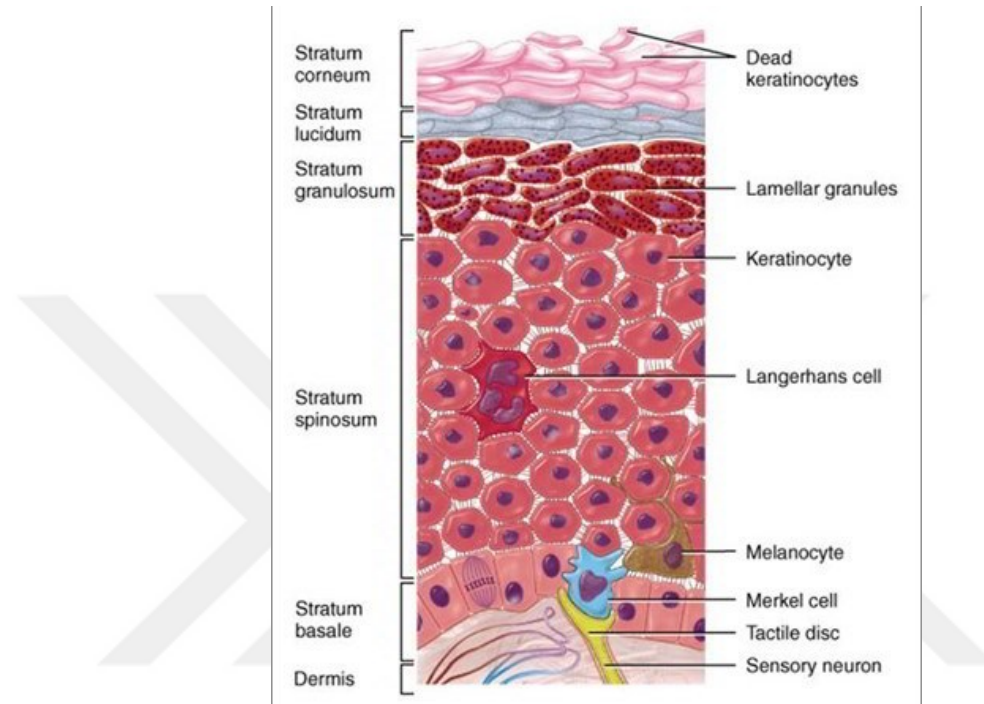


Figure 2. Layer of the Epidermis

2.1.1.1. NATURAL MOISTURIZING FACTOR (NMF)

Natural Moisturizing Factor (NMF) skin moisturizing; the primary function of NMF is to maintain adequate skin hydration and is composed principally of free amino acids, derivatives of these amino acids, like Pyrrolidone carboxylic acid (PCA), urocanic acid, and inorganic salts, sugars, as well as lactic acid and urea. The NMF components are highly efficient humidifiers that draw and bind water from the atmosphere and attract them to corneocytes. This process can even be as low as 50% relative humidity, which allows the corneocytes to maintain sufficient water levels in low humidity environments. Water absorption is so efficient that NMF is mostly dissolved in the water it absorbs. Hydrated NMF particularly neutral and essential amino acids form ionic interactions with keratin fibers, reducing intermolecular forces between the fibers and thereby increasing the

flexibility of the stratum corneum. This flexibility helps keep the skin looking healthy and supple and prevent cracking or spillage due to mechanical stress. Besides, NMF allows it to compensate for the osmotic pressure exerted by the intracellular "cement" surrounding the corneocyte cells. It is essential to keep the dissolution concentrations stable, to prevent excessive water flow, as seen in the wrinkled skin of someone who has been in the bath for too long, or the water flow to cause contraction of the corneocytes (15).

2.1.1.2. SEBACEOUS GLANDS

Sebaceous glands are an organelle of the epidermis, even though they are in the dermis itself (16).

Firstly, they are trustworthy, hemispherical protrusions on the rear surfaces of the hair clips. The cells contain a moderate amount of glycogen, but soon the central cells lose it and become more significant and foamy when they accumulate lipid droplets. The sebaceous glands differ in 13-15 weeks and are then large and functional. Sebum forms part of the vernix caseosa. At the end of fetal life, the sebaceous glands are well developed and usually significant. After birth, the size shrinks rapidly and grows to be functional again only after puberty (17).

2.1.1.3. ECCRINE GLANDS

The sweat gland found in almost every part of our body is called eccrine glands. These are the right sweat glands in terms of helping to regulate body temperature. In other words, sweating causes loss of body temperature and therefore cools us down on a hot day or during a compelling exercise. This is because as the water in the sweat evaporates, it takes body temperature with it (18).

2.1.1.4. MELANOCYTES

In the presence of different skin colors in the world; genetic factors, skin pigments, exposure to ultraviolet (UV) rays, and environmental factors, while melanin in the epidermis is accepted as the primary pigment affecting the skin color and the number of melanocytes that enable melanin synthesis, melanogenic activity, melanin type, size, quantity and distribution

of melanosomes are mentioned as active factors in the formation of skin color. Two forms of melanin; pheomelanin (yellow/red) and eumelanin (brown/black) and is considered the leading cause of ethnic skin color differences in the world. Melanin is synthesized in lysosome-like organelles called melanosomes in melanocyte cells (19).

2.1.1.5. LANGERHANS' CELLS

Langerhans cell in the skin is dendritic cells that take up microbial antigens in the skin to transform into antigen-presenting cells and provides immunity by interacting with T cells (20).

2.1.1.6. MERKEL CELLS

They occur on the hairless skin of the fingertips, lips, gums, nail bed, and a few other areas in about 16 weeks of the fetus (21).

2.1.1.7. PROPERTIES and FUNCTIONS of the SKIN BARRIER

Human skin is continuously exposed to a hostile environment: changes in relative humidity, extreme temperatures, environmental toxins, and daily topical products. Exposure to regular soap and other household chemicals can damage skin barrier properties and cause unhealthy skin conditions. Prolonged exposure to surfactants eliminates the epidermal barrier lipids and increases desquamation leading to impaired barrier properties. Allergic reactions to topical products may result in allergic or irritant contact dermatitis, resulting in redness of the itchy and scaly skin and leads to barrier disorders (22).

The stratum corneum, the outermost part of the epidermis, is an integral part of the skin that controls the permeability of the skin. This barrier property is caused by a unique lipid mixture between the cells. The lipid mixture consists of phospholipids, glycolipids, and cholesterol, as well as a small amount of cholesterol sulfate and cholesterol esters. The stratum corneum is about 50, 25, and 10 percent of the lipid mass is the ceramides, cholesterol, and fatty acids (23).

- a. Epidermal barrier is one of the most known and most important properties of stratum corneum.

- b. Mechanical barrier; It gives strength to the epidermis, protects the epidermis against injury. It provides mechanical strength with a specially modified cross-linked amino acid.
- c. Antimicrobial barrier; acts as a physical barrier, protects against organisms that want to penetrate the skin
- d. NMF, skin moisturizing; The lipid layer surrounding the corneocytes provides moisture by preventing NMF loss
- e. Environmental toxins and topical drugs; SC, has the task of preventing the penetration of toxic substances and topically applied drugs into the skin.
- f. UV barrier; protects against UV light, photoaging, and damage (22, 24).

2.1.2. DERMIS

The dermis, between the fat layer and the epidermis, is a structure responsible for the skin thickness and has essential responsibilities for skin cosmetics. The main functions are preserving and repairing, skin coloration, temperature controls, moisture retention, immune provision, storage for skin organelles, absorption, and vitamin D synthesis. This middle layer of the skin contains a minimal amount of collagen and collectively elastin-shaped connective tissue with abundant blood circulation (25).

The moisture and thickness of this layer are reduced with age. Cell types found in the dermis are fibroblasts, mast cells, and histocytes. Hair follicles, nerves, lymphatic veins, and sweat glands are also found in the dermal layer of the skin. This part is rich in nerve and blood vessels (26).

The dermis has three layers:

- a. Papillary layer: The dermal where the fiber components are thin and supplied with capillaries and sensory nerve endings are mainly located here
- b. Subpapillary layer: This is the area that underly the epidermis, and the same components are also present here as in the papillary layer.
- c. Reticular layer: This part is the most significant part of the dermis and composed of very dense connective tissue and fiber components. The lower part of the dermis is in contact with the subcutaneous fatty tissue (26).

The fibrous tissue and matrix formed by cells are the interstitial components which mainly consist of collagen fibers (types I and III), with smaller amounts of elastic fibers, reticular fibers, and matrix which consists of extracellular matrix and ground substance made up of proteoglycans and gelatin (26).

2.1.3. HYPODERMIS

This fat layer under the dermis serves as a buffering layer to protect vital internal organs from mechanical traumas, as well as an insulation layer to protect against cold. Besides, fat is a famous energy store for the body. The amount and distribution of fat depend largely on hereditary factors, diet, and physical activity. The groups of fat cells are separated by rigid portions consisting mainly of collagen fibers, as shown in the following Figure 3 (242).

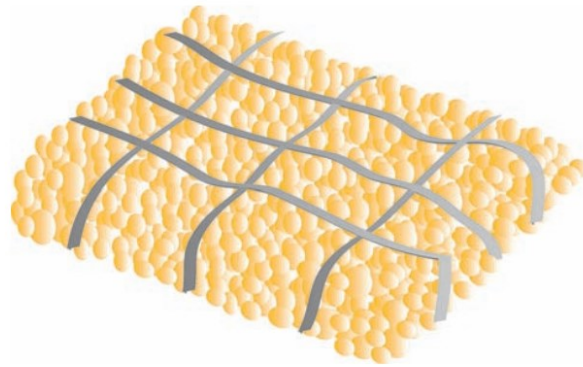


Figure 3. Groups of fat cells separated by collagen

2.1.4. SKIN AGING

Skin aging is a complex biological process caused by internal and external factors. Internal factors can be referred to as hormonal changes and physiological changes caused by aging. Photoaging, smoking, and all other environmental factors can be grouped as external factors (27).

Premature or natural aging, changes occur in the skin like fine wrinkles, pale skin tone, reduced elasticity, and occasional exaggerated expression lines are evident (28) also there is a reduction in the thickness of the dermal layer, along with fewer fibroblasts and mast cells, less collagen production, reduced vascularisation degradation of the extracellular matrix components, particularly elastin, collagen and glycosaminoglycans (29).

There are several studies conducted to investigate the effects of hormonal changes with increasing age in the skin (30).

Hormonal changes with increasing age in humans are associated with changes in the skin (31).

Although males get older, the cosmetic world is interested in the symptoms of the aging of women. Most of the research revealed that dryness of skin, thinning, wrinkle, and disappeared elasticity due to hormonal changes in women. Although the causes of these changes are related to estrogen, no mechanism has been found for the thickness and dryness of the skin (32).

However, the decrease in the amount of collagen with aging has been shown to be directly related to skin collagen and skin thickness, therefore, signs of aging such as sagging and wrinkles (32, 33).



Figure 4. Bill McElligott, truck driver, massive sun damage on one side of his face (34)

Due to the visible signs, it can easily be pointed out the difference between the sun-exposed skin covering the areas like face, hands, feet, and legs, and skin that is not exposed to the sun. Although the sun is not the only reason for skin aging, it is the most critical environmental element of aging. Internal change is chronically age-related and is inextricably related to genetics and is irreversible. Environmental factors caused by external factors can be reduced by the measures taken personally.

Early aging has been reported to be due to 80% of premature aging has been reported to be due to exposure to UV rays, in other words, due to environmental factors (35) shown in Figure 4.

2.1.4.1. EFFECT of AGING on COLLAGEN

Collagen, elastic fibers and hyaluronic acid (HA) are the main structural components of the dermal extracellular matrix. Collagen may comprise 70% of the dry weight of normal human skin dermis. The dermis is morphologically composed of two different layers: the dermis of fine collagen fibers and the reticular dermis of thick, coarse collagen bundles. Skin elastic fibers consist of an inner core of elastin cross-linked with outer fibril layers in microfibrils. The HA content of the dermis is much higher than that of the epidermis, and the papillary dermis has significantly higher HA levels than the reticular dermis (33).

Collagen is a primary material that has been the focus of many anti-aging studies. It consists of 18 amino acids and is located in the dermis shown in Table 1.

Collagen, one of the most potent natural proteins known, plays a structural role in the dermis. The structure known as the hypodermis or subcutaneous structure is located below the dermis. In particular, this layer contains collagen of type I, type III, and type V. With age, collagen in this part decreases, and sagging occurs, appearing as signs of aging. Collagen fibers develop in the dermis (36).

Fibroblasts produce procollagen molecule, a specific helical polypeptide chain. Then, the cell secretes the fibroblasts, which turns into collagen fibrils. The standard amino acids glycine, hydroxyproline, and hydroxylysine profoundly enrich collagen. The fibrillar collagens found in the skin comprise the dominant group and are the most abundant proteins in the body. The principal constituent of the dermis is type I collagen. Loosely positioned collagen fibers are found in the papillary and adventitial dermis, whereas hefty collagen bundles are noted in the reticular dermis. There are four types of collagen found in the basement membrane zone, and the major structural component of anchoring fibrils is collagen type V, which is produced primarily by keratinocytes (36).

The elastic fiber differs both structurally and chemically from collagen and consists of two components: protein filaments and elastin, an amorphous protein. The fibroblast fuses elastic fiber to the extracellular matrix of the dermis, which is composed of glycosaminoglycans. The fibers are beautiful in the papillary dermis and coarse in the reticular dermis. Hyaluronic

acid is a minor component of the normal dermis but is the major mucopolysaccharide that accumulates in pathologic states (36).

The amino acids glycine, hydroxyproline, and hydroxylysine are abundantly used in collagen synthesis. First, procollagens are synthesized as precursor molecules in the fibroblasts, and then synthesis continued to transform this ed into collagen (37). In this production, iron, vitamin c, and alpha-ketoglutarate are needed for the reactions. The principal constituent of the dermis is type I collagen. Loosely positioned collagen fibers are found in the papillary and adventitial dermis, whereas hefty collagen bundles are noted in the reticular dermis. Collagen is a significant stress-resistant material of the skin, whereas elastic fibers play a role in maintaining elasticity but do very little to resist deformation and tearing of the skin (36).

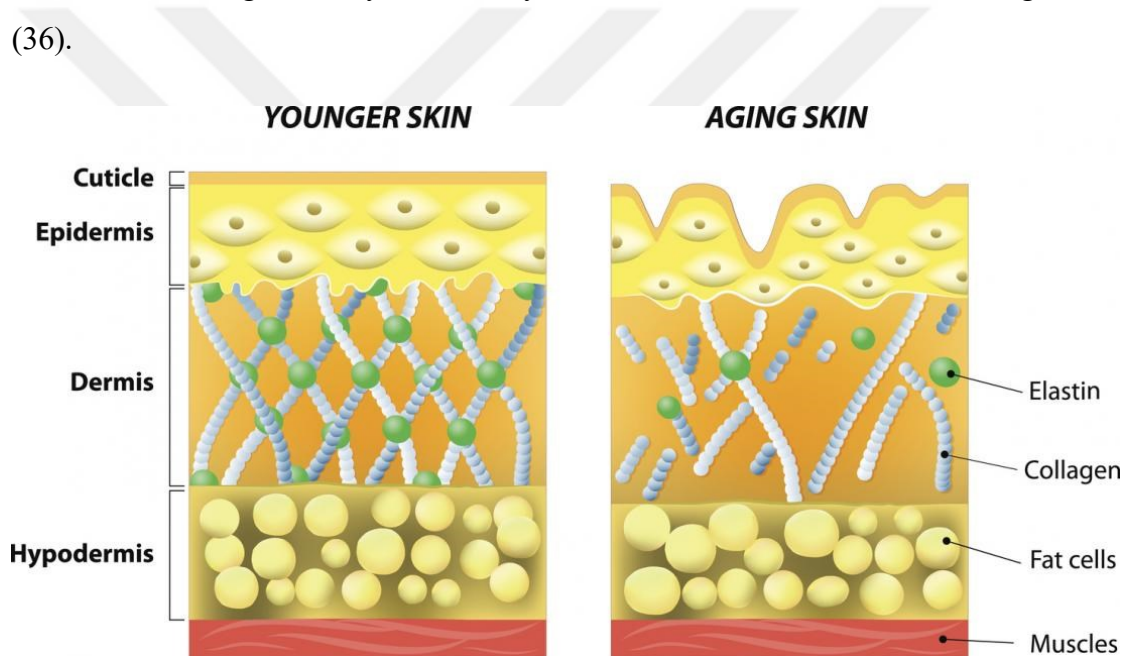


Figure 5. Illustration of collagen weakening with age (38)

All types consist of 3 peptide chains. Procollagen is synthesized as precursor molecules in fibroblasts and then synthesized into collagen with transformation reactions. In this process, iron, vitamin c, and alpha-ketoglutarate are needed for reactions. Skin aging that is associated with decreased collagen production is shown in Figure 5.

UV-induced damage also affects the matrix metalloproteinases (MMP), an increase of collagenase enzymes, including MMP-1, MMP-8, and MMP-13, have been reported by

many researchers. Changes made by MMPs may contribute to skin wrinkling, a feature of early skin aging (35, 39).

Table 1. Types of collagen found in the dermis (25)

TYPE	LOCALIZATION	% of DERMIS	RELATED SITUATIONS
I	Bone, Tendon, Skin	80%	Aging
III	Dermis	15%	Aging
IV	Basal Membranes		
V	Diffuse, Dermis	4,50%	
VII	Fibrils		
XVII	Hemidesmozo		Dystrophic EB

2.1.4.2. ELASTIN, GLYCOSAMINGLYCANS, and GLYCOPROTEINS on AGING

Elastin fibers are located around the collagen bundles and reinforce the skin with recoil properties. These fibers are assembled on bundles of microfibrils composed of fibrillin. Elastic fibers are degraded by the elastolytic enzymes such as human leukocyte elastase (HLE). With significant levels of sun exposure, elastin degrades and is seen as an amorphous substance in the dermis when viewed by light microscopy. This resultant “elastosis” is a hallmark of photoaged skin (25).

One of the critical signs of photo-aging is dermal solar elastosis, which can be described as the production of thickened, tangled, poorly organized, and granular amorphous elastin structures (40).

Some studies showed that the production of elastin increased due to UV radiation, which may have an explanation of the massive amounts of abnormal elastic material found in the skin during aging and photoaging. Although the mechanism of the accumulation of elastin and elastomers in the dermis is unclear, it has been shown that the amount of elastosis is proportional to the degree of sun exposure (41).

UV irradiation has been shown to induce the expression of MMPs, which degrade the extracellular matrix materials elastin and collagen. Some of the research indicated that UVA

exposure both during indoor activities as well as more severe exposure during outdoor activities contributes to the release of lysozyme enzyme which can interact with and reduce the elastolysis which in turn causes the accumulation of damaged elastin fibers (42).

Glycosaminoglycans (GAG) are a family of highly sulfated, sophisticated, versatile linear polysaccharides that exhibit a variety of critical biological roles. Based on the diversity of repetitive disaccharide units containing GAG's, they can be divided into four main groups: heparin/heparan sulfate, chondroitin sulfate/dermatan sulfate, keratan sulfate and hyaluronan (25).

Together with the deposition of abnormal elastic tissue, there are essential changes in dermal GAGs. Accumulation of GAGs as a result of photoaging has been shown in both humans and animal models of photoaging. In one of the studies, GAGs, especially hyaluronic acid and chondroitin sulfate amounts, were investigated, and a significant increase in GAG staining in sun-damaged vs. sun-protected skin from the same individuals was demonstrated (43).

Also, the increased dermal GAGs in sun-damaged skin were found to be deposited on the elastotic material of the superficial dermis of photodamaged skin and not between collagen and elastic fibers as in healthy skin (43).

Inadequate hydration of proteins and turgor capacity contributes to the dry appearance of photo-aged skin (44).

3. COSMECEUTICAL PRODUCTS

Cosmetic products are products that do not require testing or approval because they do not have biological activity. The European Community defines the cosmetic product as “any substance or mixture intended to be placed in contact with the external parts of the human body (epidermis, hair system, nails, lips, and external genital organs) or with the teeth and the mucous membranes of the oral cavity with a view exclusively or mainly to cleaning them, perfuming them, changing their appearance, protecting them, keeping them in good condition or correcting body odors. The American Food, Drug, and Cosmetic Act (FDA) in 1938 defines cosmetics as “articles intended to be rubbed, poured, sprinkled, or sprayed on, introduced into, or otherwise applied to the human body for cleansing, beautifying,

promoting attractiveness, or altering the appearance. On the other hand, drugs are the substances used in the prevention, diagnosis, or treatment of the disease” (45, 46).

Although the term "cosmeceutical" was coined by Albert Kligman, an MD, back in the 1980s to explain skincare products that are more than a cosmetic product, the Egyptians were the first to recognize the health-giving properties of cosmetics as shown by the Ebers (medical papyruses) in 1600 BC. Cosmeceuticals are not quite like the drugs, and the word is a blend of the words: cosmetics and pharmaceuticals. The concept owner Dr. Albert Kligman stated that “The Cosmeceuticals are topical agents that are distributed across a broad spectrum of materials lying somewhere between pure cosmetics they partake of both categories (47).

Both cosmetics and cosmeceuticals are applied topically. Cosmeceuticals contain ingredients that influence the skin’s biological function to a certain extent. Cosmeceuticals are meant to improve the appearance by delivering nutrients necessary for keeping healthy skin. Cosmeceuticals are the fastest-growing segment of the natural personal care industry. The “active ingredients” used in cosmeceutical products are quite many, which can be classified under different functions. Such ingredients’ mechanisms of action, formulations, necessary concentrations, penetration, and retention behaviors in the skin are critical issues for both the manufacturers and consumers. Generally, *in-vitro* and *in-vivo* tests, as well as some clinical tests, have to be performed to substantiate their claims (46, 48-49).

The cosmeceuticals are more expensive products than ordinary mass-market cosmetics (more than 1USD per gram as a finished product), but the consumers are willing to pay higher prices for such products that meet consumer's high expectations in terms of aesthetics and elegance, as well as efficacy. In order to meet consumer demands, formulators must choose appropriate cosmetic active ingredients that will be compatible with the suitable vehicle or delivery system (50).

There are several ingredients, both synthetic chemicals and herbal, are used in cosmetics/cosmeceuticals for their different functions (51). Herbal ingredients are used because of their many functional properties. Some of such herbal ingredients are well researched and tested for their mechanism of action efficacy, biodegradability, toxicity, but not all are tested in such detail (52).

The formulator has to choose from those hundreds of different ingredients and formulate the product appropriately that would deliver the necessary ingredient to the skin at the required amounts and meet the consumers' expectations. This process becomes even more complicated when the necessary clinical and technical data about the "active" ingredients are not enough or available (50).

Many cosmeceutical products on the market today can make claims like "the product can make the skin look younger and more beautiful or moisturize it better." The claims are generally based on the ingredients the products contain (45).

However, not only the ingredients in the formulation but also the delivery systems carrying these actives are also crucial for the overall effectiveness of the product (52).

In cases where direct administration or loss of effect of the active ingredients is involved, the effects of the active ingredients in the carrier systems have been examined and have introduced the cosmetic definition into the literature by demonstrating the effects of macromolecular carrier systems that assist in the subcutaneous transport of large-molecule active substances, such as liposomes (46).

3.1. ANTI-AGING ACTIVES/INGREDIENTS

Physiological skin aging is a result of damage that accumulates throughout life and is due to both intrinsic factors and extrinsic factors (29).

As a result of aging not only molecular, cell-related, and morphological changes but also some physiological effects occur, including excessive dryness and formation or deepening wrinkles, dyspigmentation (53), fragility and difficulty to heal injuries (54), alteration in skin permeability to drugs impaired ability to sense and respond to mechanical stimuli (55), skin irritation and tumor incidence (54).

Due to the technological advances in medicine to prevent and cure many diseases help to increase life expectancy. The percentage of the elderly population is increasing in most countries, especially in developing and developed countries. Skin aging will come inevitably, but a youthful appearance and keeping the right health conditions are going to remain significant. This is why a wide range of skin-care products and their uses have

become very extensive. It is generally difficult to quantify the amount of the effects because there are many variables: test methods, equipment, the sensitivity of the methods and equipment, the difference in endpoints measured, and even the body sites where the product effect is applied. The creation of 3 groups of strategies for planning the treatment and prevention of aging skin is suggested (56).

- a.** The first approach aims the preventing photoaging by using sunscreens with chemical or physical broadspectrum filters and educating the population to gain more conscious behavior to photo-exposure.
- b.** The use of formulations with active substances to try to prevent or reduce the signs and symptoms of aging. Retinoic acid, alpha-hydroxy acids, antioxidants, estrogens, and growth factors have been used to enable the application of this strategy.
- c.** Anti-aging approaches requiring more invasive mechanisms, like chemical peeling with specific acids and higher acid concentrations, use of injected fillers and botulinum toxin and similar medical approaches.
- d.** Focusing on derma cosmetics having anti-aging actives that are effective to improve the feeling and appearance of the skin. For this strategy, and many anti-aging ingredients are used like retinoids, alpha hydroxy acids, antioxidants.

One of the most commonly studied mechanisms by which premature skin aging develops is UV exposure (photoaging). Acute and chronic exposure have specific results on the skin. Chronic sun exposure is characterized by fine and coarse wrinkles, telangiectasias, mottled pigmentation, and rough textures (57).

Histologically, elastosis; disorganized collagen fibrils and an abnormal amorphous elastin-containing material increase in the dermis and thinning of the stratum corneum and flattening of the dermo-epidermal junction are the most common outcomes of UV exposure and excessive, long-term exposure causes actinic keratosis nonmelanoma and melanoma skin cancers (57).

In vitro studies clearly showed that human skin exposed to UV irradiation forms reactive oxygen species (ROS), levels of hydrogen peroxide begin to increase within 15 minutes of UV exposure and continue to increase for up to 60 minutes after the exposure has

ceased. These ROS stimulate transcription factor nuclear factor (NF)- κ B, leading to increases in proinflammatory cytokines and up-regulation of MMPs (58).

The skin has its enzymes that function as antioxidants, but when ROS levels increase rapidly, the antioxidants cannot scavenge these ROSs effectively. The primary skin anti-oxidants are copper-zinc superoxide dismutase, manganese superoxide dismutase, and catalase, which are found in higher concentrations in the epidermis than in the dermis (59).

Acute and chronic UV exposures reduce levels of antioxidants in the skin; therefore, oxidative damage of proteins is inevitable, and replacement of the antioxidants helps reversal or slowing down of the clinical and histopathologic signs of photoaging (60).

Table 2. Vitamins and their functions in photoaging summary

	Function
Vitamin A - Carotenoids - Retinoids	<ul style="list-style-type: none"> - May prevent UV-induced collagen breakdown - Increases fibroblast growth and collagen production in clinical trials - Increases epidermal thickness, thus reducing appearance of fine wrinkles - Reduces levels of MMP, which catalyze collagen and elastin degradation in clinical trials - Chemopreventive effect in skin cancer by reducing keratinocyte and melanocyte cell atypia in clinical trials
Vitamin C	<ul style="list-style-type: none"> - Confers increased stability and decreased heat sensitivity to collagen - Stimulates collagen production both in vitro and in clinically controlled trials - Theoretically may protect skin from UV-induced photodamage through antioxidant properties
Vitamin E	<ul style="list-style-type: none"> - Acts as an antioxidant when applied before sun exposure to protect skin from UV-induced photodamage in both in vitro and clinically controlled trials - Regulates collagen and elastin breakdown through its effect on MMPs, demonstrated for in vitro trials
Vitamin B ₃	<ul style="list-style-type: none"> - Increases collagen production in in vitro studies - Reduces skin hyperpigmentation in clinical studies
Vitamin D	<ul style="list-style-type: none"> - Protects against UV-induced skin wrinkling and epidermal thickening in vivo in mice studies
Vitamin K	<ul style="list-style-type: none"> - Reduces vascular manifestations of photoaging

MMP, Matrix metalloproteinase; UV, ultraviolet.

Several review papers summarize the anti-aging vitamins and other ingredients that are used in cosmetics and derma cosmetics/cosmeceuticals (61). The most common vitamins used in such products are listed in Table 2.

3.1.1. VITAMIN A, RETINOIDS and RETINOL

The use of the retinoids in therapy dates back some 3000 years to ancient Egypt, where the liver was used to treat endemic night blindness. The modern history of retinoids began in the early 1900 when an essential factor for keeping the embryo viable, vitamin A was rediscovered in the fatty extract of egg yolk. The importance of retinol (vitamin A) was

realized again during World War I, and several researchers showed that its deficiency causes xerosis and follicular hyperkeratosis. In 1928, Green and Mellandy reported that vitamin A could improve the anti-inflammatory response of organisms and called vitamin A as “anti-inflammation vitamin” (62).

In the 1950s and 1960s, vitamin A was used more extensively, and to improve its clinical efficacy and safety, many new derivative compounds were synthesized in the retinoid family by chemical manipulation of vitamin A molecule. These new retinoids were introduced into the treatment of dermatoses, including photoaging (63).

In the later years, in the 1980s and 1990s, another effect, such as the anti-inflammatory capacity of vitamin A, was also discovered. The retinoid family comprises of vitamin A and its natural derivatives such as retinol, retinaldehyde, retinoic acid, and retinyl esters, as well as a large number of synthetic derivatives (64).

The body can not synthesize vitamin A; it has to be taken from the external sources and stored as retinyl esters in the liver. Retinoids are required for a vast number of biological processes, such as embryogenesis, reproduction, vision, growth, inflammation, differentiation, proliferation, and apoptosis. Not all physiological functions of retinoids (such as routine vision and reproductive requirements) can be provided by retinoic acid (65).

Based on the structural properties, retinoids can be classified into various generations, as shown in Figure 6.

Mechanism of action of topical retinoids are very well known in many of the their interaction with mediates cellular processes and these effects specific cellular and nucleic acid receptors; such as:

- a.** The cellular or cytoplasmic receptors include the Cellular Retinoic Acid Binding Protein (CRABP) types I and II
- b.** Cellular retinol-binding protein in the circulation
- c.** The nucleic acid receptors (which were discovered in 1987 which revealed the mechanism of action) (66),
- d.** Tretinoin specific gene transcription factor (discovery of this also showed that tretinoin is a hormone).

- e. Retinol receptors comprise two families, each of which are encoded by three genes. The nuclear retinoic acid receptor family called RARs was the first to be described and consisted of three forms (RAR- α , RAR- β , RAR- γ) that are activated by retinoic acid receptor (RAR) specific all-*trans*-retinoic acid (tretinoin). RARs have specific DNA and retinoid-binding domains, and they function in pairs. In the human skin, RARs partner with retinoid X receptors (RXRs) to form heterodimers (67),

The retinoid X receptors or RXRs are nuclear receptors that interact with 9-*cis* retinoic acid. Both RARs and RXRs are present in the healthy skin and provide the necessary machinery for the retinoid repair process of the photodamaged skin. RAR- γ and RXR- α regulate healthy human skin. The heterodimer requires only RAR specific retinoid (tretinoin) to bind to RARE and initiate transcriptional activity; the presence of an RXR binding retinoid (9-*cis* retinoic acid) does not confer additional trans-activation induced by the RAR retinoid.

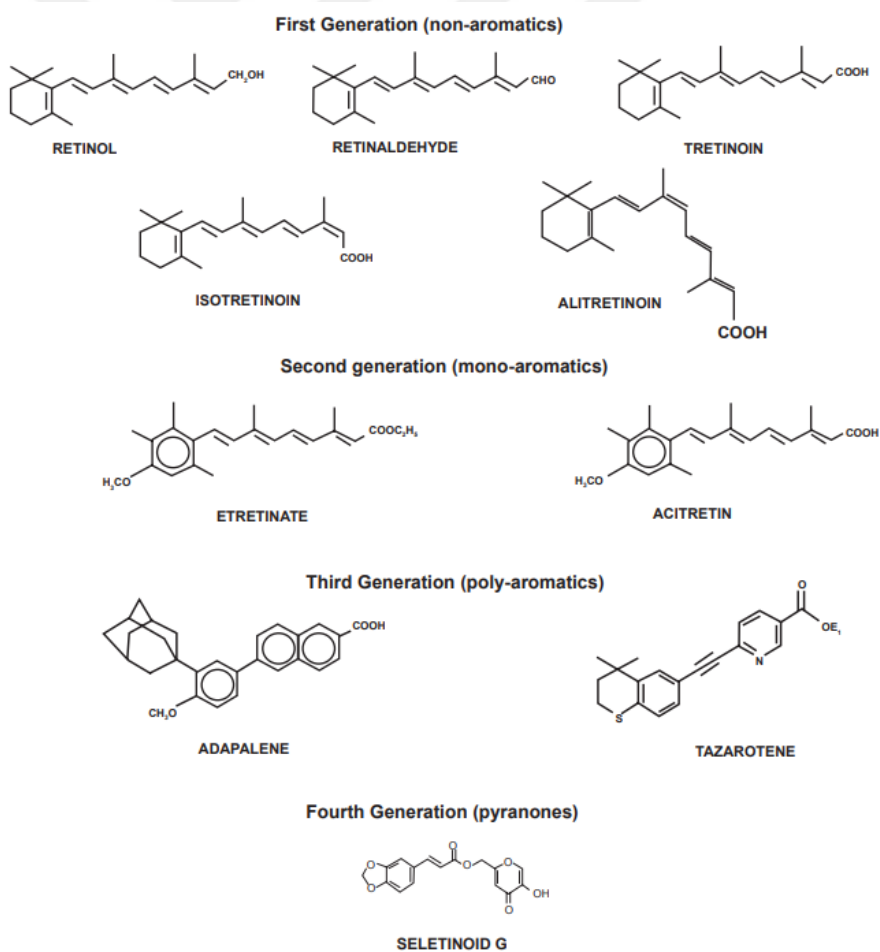


Figure 6. Chemical structures of retinoids

The following processes summarise the mechanism of action that topical retinoids improve photoaged skin by modifying the cellular differentiation programs:

- a. Initiating the increase of epidermal proliferation leading to epidermal thickening;
- b. Compaction of the stratum corneum
- c. Biosynthesis and deposition of the glycosaminoglycans (68),

Retinoic acid has been accepted as a drug since it passes from the womb to the circulation of the fetus. Therefore, only esters of alcohol form are allowed in cosmetics. Two retinoids that are commonly used in cosmetic products are retinol and retinyl palmitate. Retinoids are as effective as tretinoin at the appropriate concentrations and in the appropriate carrier systems. Retinol at 0.25% is as effective as 0.025% retinoic acid; however, it produces less irritation. As it is shown in Figure 7, the conversion of the active retinol molecule to the ester bond, first to retinol and then to topical application to retinoic acid, is necessary (45).

Many studies have reported that retinoids topically improve photoaging conditions such as wrinkles, pigmentation changes, examinations have shown an increase in epidermal thickness with the formation of new collagen (69).

Retinoids cause epidermal hyperproliferation, accumulation of glycosaminoglycans in the epidermis, formation of collagen in the dermis, and also increase the production of collagenase inhibitors that slows down collagen degradation rate (70-72).

3.1.1.1. TRETINOIN

Tretinoin, commonly known as retinoic acid, is used more than the other retinoids in the treatment of physiological and photoaging since the 1950s by the studies of Kligman and his colleagues (73).

The same group of researchers, as well as the other researchers, extensively investigated the potential of tretinoin in the treatment of photoaging. All of the results of the studies research results indicated that by blockage of the synthesis of interstitial collagenase and gelatinases, which results in the prevention of:

- a. Collagen degradation
- b. Deposition of reticulin fibers
- c. New dermal collagen formation (type I and III) accompanied by angiogenesis in the papillary dermis.

The results of many other studies conducted in the following years confirmed the clinical efficacy of tretinoin in the treatment of photoaging, repair of photoaged skin damage (removing wrinkles, lightening skin color). Retinoic acid was also used in medical treatments to reduce acne and erythema (74, 75).

3.1.1.2. ISORETINOIN

Clinical studies conducted with both animals and patients showed that topical isotretinoin (13-cis retinoic acid) has a dose-dependent effect on wrinkles (76).

In a large multi-centered, double-blind, and placebo-controlled clinical study, Maddin and his co-workers found that daily usage of 0.1% isotretinoin cream for 36 weeks improved the overall appearance of the skin, fine wrinkles, texture, coarse wrinkling, and hyperpigmented macules. There were, no significant changes were seen in other histological parameters, such as dermal elastosis, the thickness of the dermis, epidermal melanin content, number of fibroblasts, melanocyte dysplasia and keratinocyte atypia (69).

Unwanted effects were severe irritation on facial skin was seen in 10 % of the patients, while other participants experienced only mild irritation. In another 6-month, multicentered, randomized, double-blind, parallel-group, and vehicle-controlled study, 0.05 % isotretinoin was applied once daily in combination with. At the end of the study, a significant improvement in fine wrinkles of photoaged skin was observed (77).

3.1.1.3. RETINOL

Retinol is the most popular substance known as a moisturizer in cosmeceutical aging products. It is a derivative of vitamin A. Vitamin A in plants is a substance that captures free radicals to protect against UV radiation damage (70).

Retinol is a Vitamin A alcohol or all-trans-retinol, which is another member of endogenous natural retinoids 1 and it is a starting ingredient for synthesis of endogenous retinal and retinoic acid. Figure 6. Although all-trans-retinol has been used in over-the-counter (OTC) cosmetic products since 1984 (78), its potential in the treatment of photoaging was first realized by Kang et al. (79).

In other studies, the clinical, histologic, and molecular responses of healthy human skin to all-trans-retinol (ROL) application was investigated and compared to those induced by topical all-trans-retinoic acid (RA), and ROL-derived metabolites were measured. The results demonstrated that ROL application:

- a. Produces trace erythema not significantly different from the vehicle, whereas RA causes erythema
- b. Induces epidermal thickening and enhances expression of CRABP-11 and CRBP mRNAs and proteins as does RA
- c. Causes marked accumulation of retinyl ester
- d. Does not significantly increase RA levels

Natural and synthetic derivatives of vitamin A are called retinoids. Although retinoids are widely used in cosmetics, they have many biological effects; they reduce the activity of cell division of epithelial cells, stimulate collagen synthesis and the immune system, and reduce keratinization, pigmentation, and inflammation. Tretinoin, commonly known as retinoic acid, repairs photoaged skin damage, removes wrinkles, and lightens skin color. Retinoic acid also used in medical treatments to reduce acne and erythema (74, 75).

In a human study, the photoprotective effect of topical retinyl palmitate 2% has been shown to be as efficient as a sunscreen with a sunscreen factor 20 in preventing UVB-induced erythema and DNA photo diagnosis the authors also observed that retinol showed only minimal signs of erythema and irritation unlike tretinoin (80).

In another study, an *ex-vivo* human and rat skin mounted on Franz perfusion cells was used as a predictive model of *in-vivo* human metabolism. The study demonstrated that freshly excised skin mounted on Franz diffusion cells proved to be an attractive alternative method to study the epidermal profile of topical retinoids in human skin. Topical retinal penetrated

well into the epidermis, induced a slight increase of endogenous retinoids as retinol and retinyl esters, and a small part was oxidized into retinoic acid; topical retinol and its palmitic ester highly increased endogenous retinoids, whereas no oxidized retinoid as retinol and retinoic acid was found (64).

In another study (n=6; duration=14 days), Fluhr and colleagues (1999) confirmed that retinol produces considerably less transepidermal water loss, erythema, and scaling than retinoic acid. Interestingly, Fisher and colleagues (1996, 1997) further demonstrated that retinol inhibits UV induction of MMP and stimulates collagen synthesis in photoaged skin. However, it was observed that retinol is 20 times less potent than tretinoin, and it requires further conversion to retinoic acid to demonstrate its action (79).

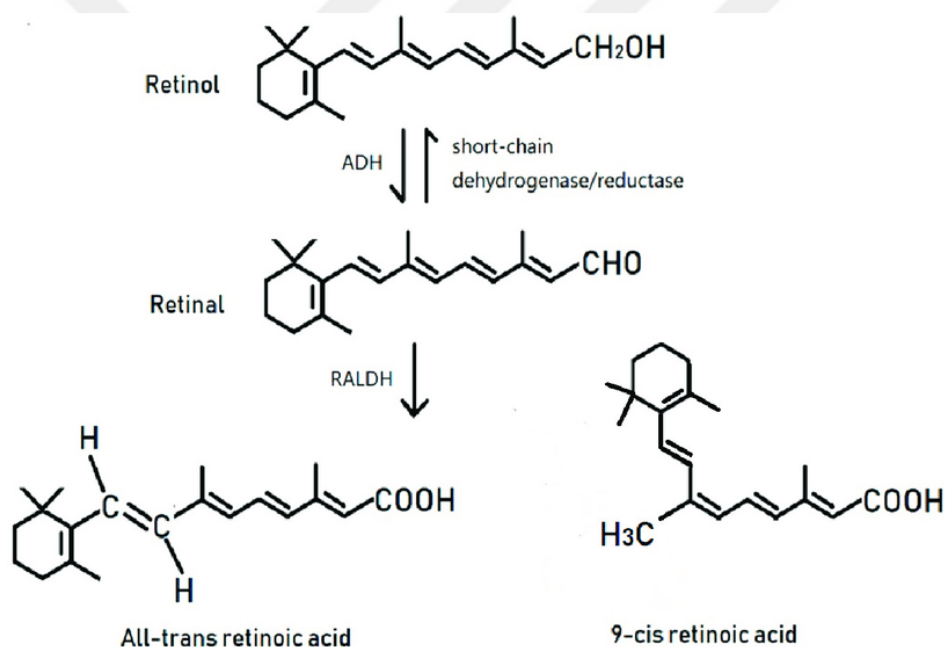


Figure 7.Active retinol (2)

Duell and colleagues (1996) demonstrated that retinol could be as active as retinoic acid in producing 'retinoid mediated histological changes' (like epidermal thickening and keratinocyte proliferation), but with much less irritancy. Pierard-Franchimont and colleagues (1998) first conducted a controlled clinical trial with retinol formulation and observed that retinol formulation resulted in significant improvement in fine wrinkles after 12 weeks of treatment. Subsequently, Varani and colleagues (2000) studied the effect of topical application of 1% retinol in 53 individuals with aged skin. The authors observed that

retinol application for seven days reduced MMP, collagenase, and gelatinase expression with a concomitant increase in fibroblast growth and collagen synthesis in the studied tissue specimens.

Based on the research results as summarized above, it can be concluded that retinol is useful in the treatment of aged and photoaged skin. However, the vehicle used for retinol delivery would play a crucial role in eliciting its efficacy, as well as to protect retinol, which is extremely unstable and easily gets degraded to biologically inactive forms on exposure to light and air.

3.1.1.4. RETINALDEHYDE

Retinaldehyde is a retinoic acid precursor and an intermediate metabolite in the transformation of retinol to retinoic acid in the epidermis. This metabolism occurs only in keratinocytes during the differentiation process (243).

3.1.2. RESVERATROL

Resveratrol (3,5,4-trihydroxystilbene) is a chemical compound which is present in fruits, mainly in the skins of fruits such as grapes, berries, also in peanuts, tea, and red wine. Resveratrol is known to be a phytoalexin produced by plants, especially as a result of the plant-pathogen attack, injury, or UV exposure (82).

The effect of free radicals on aging was first accepted by a theory put forward in 1956 (83). The free radicals are also oxygen derivatives and are formed by combining with other molecules to gain electrons. Molecules with an even number of electrons are stable, while odd numbers that are causing damage to tissues as electrons are reactive (84).

UV-induced skin damage and aging have been related to reactive oxygen. Although vitamins C and E, Glutathione, CoQ10, and Alpha-Lipoic acid are known as essential antioxidants today, resveratrol contents have recently been found in many cosmetic products. The potent antioxidant properties of resveratrol in the grape peel are 50 times more than vitamin E and 30 times more than vitamin C. Resveratrol binds to binding sites in human skin and delays the normal process of skin aging by blocking mitochondrial dysfunction in keratinocytes and apoptotic events (85).

The studies with human keratinocyte cells have shown that trans-resveratrol is capable of inhibiting hydrogen peroxide production. In addition to the protective effect of trans-resveratrol against UVA radiation in humans, it also improves the clinical signs of aging (86).

In the last decade, science dealing with aging has increasingly focused on a group of genes called sirtuins that are believed to protect many organisms, including mammals (87).

This effect of sirtuins is achieved by increasing insulin sensitivity, enhancing the enzymatic activity of the sirtuin gene (SIRT), as well as increasing the number of mitochondria and antioxidant effects. It inhibits tissue damage and cellular proliferation by its anti-inflammatory effect (88).

In another 2013 study, researchers showed that resveratrol, a red wine compound, directly activates a protein that promotes health and longevity in animal models (89).

Besides, researchers have uncovered the molecular mechanism of this interaction and have now shown that a stronger class of drugs acts similarly in clinical trials (90).

Evidence has shown that resveratrol increases the activity of a specific sirtuin, SIRT1. The SIRT1 gene increases the speed of mitochondria and protects the body from diseases (88, 91).

Resveratrol is the first molecule to prolong cell life. Studies have shown that resveratrol prolongs cell survival in fungi in response to caloric restriction by activation of sirtuin SIRT2, the human SIRT1 homolog. Also, studies showed that resveratrol activates sirtuins in human and animal models (92).

Resveratrol, as an antioxidant and anti-mutagen, blocks cell changes leading to cancer formation and prevents the formation of unwanted tissues in the body. Resveratrol is naturally found in peanuts, raspberries, mulberries, plums, blackberries, and some other vegetables and fruits and is one of the ingredients utilized in “Ayurveda” in ancient India. Polyphenols are divided into two parts as flavonoid and nonflavonoid. Flavonoids are the most common polyphenols found in fruits and vegetables. Stilbens form a small portion. Resveratrol, a natural stilbene, is the most biologically active phenol as nonflavonoid (82).

3.1.3. COLLAGEN

Collagens are the most abundant proteins in mammals. The collagen family comprises 28 members that contain at least one triple-helical domain. Collagens are deposited in the extracellular matrix, where most of them form supramolecular assemblies. Four collagens are type II membrane proteins that also exist in a soluble form released from the cell surface by shedding. Collagens play structural roles and contribute to mechanical properties, organization, and shape of tissues. They interact with cells via several receptor families and regulate their proliferation, migration, and differentiation. Some collagens have a restricted tissue distribution and hence, specific biological functions (93).

Fibrillary collagen is the most common collagen found in vertebrates, where they play a structural role by contributing to the molecular architecture, shape, and mechanical properties of tissues such as tensile strength in the skin and tensile strength in ligaments (94).

A few collagens, once called “small” collagen, are very important for tissue integrity, although they are present in tiny amounts. Collagen IX, 1% collagen in adult articular cartilage (95), and collagen VII, which are crucial for skin integrity, constitute only 0.001% of total collagen in the skin (96).

Collagen type I is the most abundant protein in mammals. It gives mechanical stability, strength, and toughness to a range of tissues, from tendons and ligaments to skin, cornea, bone, and dentin. These tissues have quite different mechanical requirements, and some need to be elastic or store mechanical energy; others need to be rigid. This demonstrates the versatility of collagen as a building material. In some cases bone and dentin, hardness is increased with the incorporation of the mineral, while mechanical properties are generally adapted from a different chemical composition by modification of the hierarchical structure (97).

The common structural feature of collagen is the presence of a triple helix, which can vary from most of its structure (96% for collagen I) to less than 10% (collagen XII). As described in the discussion below, the diversity of the collagen family is further enhanced by the presence of several α chains, several molecular isoforms and supramolecular structures for a single collagen type, and the use of alternative promoters and alternative splices (93).

The classical fibril-forming collagens include collagen types I, II, III, V, and XI. These collagens are characterized by their ability to assemble into highly orientated supramolecular aggregates with a characteristic suprastructure, the typical quarter-staggered fibril-array with diameters between 25 and 400nm in the electron microscope, the fibrils are defined by a characteristic binding pattern with a periodicity of about 70 nm called the D-period based on a staggered arrangement of individual collagen monomers (98).

The collagen type I triple helix is usually formed as a heterotrimer by two identical $\alpha 1(I)$ -chains and one $\alpha 2(I)$ -chain. The triple-helical fibers are, *in-vivo*, mostly incorporated into composite containing either type III collagen in the skin and reticular fibers (99) or type V collagen in bone, tendon, cornea (100).

3.1.3.1. OTHER COMMONLY USED ANTI-AGING ACTIVES

3.1.3.1.1. ALPHA LIPOIC ACID

Alpha-lipoic acid (ALA), which also is known as thioctic acid, helps to prevent the signs of aging as well as helps to improve the signs of aging. ALA is found naturally in the mitochondria portion of our cells, as part of an enzyme system that helps energy production which is necessary during the cell repair and also reduces inflammation, which is a significant cause of aging. It is lipid and water-soluble, meaning that it is easily absorbed through the lipid layers of the skin and works well as a free-radical fighter in the cell plasma membrane as well. ALA, when concentrates on the cell plasma membrane, scavenges the free radicals, and by moving into the cell plasma, it can also neutralize the free radicals there and prevent activation of other pro-inflammatory chemicals (85, 101).

World-famous dermatologist Dr. Perricone recommends supplementing with ALA every day, along with a liberal application of topical ALA formulations for optimum cellular protection of the skin (102).

3.1.3.1.2. COENZYME Q10

Coenzyme Q10, also known as ubiquinone, is present in every cell of the body together with vitamins A, C, and E, and it provides powerful endogenous antioxidant protection and

collagen-boosting capabilities. Coenzyme Q10 is used widely in topical products which are sold as a skin energizer, against skin aging, skin repairer and an anti-wrinkling agent. Two forms of coenzyme Q10 were investigated in a commercial vehicle. Coenzyme Q10 absorption in the stratum corneum was determined after a 1h application, and ethanol extraction was used to determine the absorbed amounts of Q10. Significantly more yeast coenzyme Q10 was absorbed than the pure coenzyme Q10, and the middle-aged subjects absorbed about twice as much coenzyme Q10 as did the younger subjects. Skin antioxidant levels were significant, while peroxides declined in the stratum corneum after twice daily application of coenzyme Q10 with both forms. The older subjects had significantly higher baseline levels of lipid peroxides than did the younger group, indicating an increase in skin oxidative damage with age. The yeast coenzyme Q10 is the superior form of coenzyme Q10 for human skin applications (103). In another study, it was shown that topical Q10 treatment increases the augmentation of cellular energy metabolism and antioxidant effects. In this study, in the deeper layers of the epidermis, the ubiquinone level was significantly increased, indicating effective supplementation, and the results demonstrated that stressed skin benefits from the topical Q10 treatment by reduction of free radicals and an increase in antioxidant capacity (104).

3.1.3.1.3. VITAMIN C

Vitamin C is an antioxidant that protects the skin from environmental pollutants, including UV exposure, increasing skin's collagen, making it appear plumper while reducing wrinkles and fine lines. Healthy skin contains reasonably high vitamin C concentration, which is more than the plasma level indicating active accumulation from the blood circulation, with levels comparable to other body tissues and well above plasma concentrations, suggesting active accumulation from the circulation. Most of the vitamin C in the skin appears to be in intracellular compartments, with concentrations likely to be in the millimolar range (105).

Vitamin C is transported into cells from the blood vessels present in the dermal layer. Many different researchers have reported vitamin C levels in epidermis and dermis, and the high concentrations of vitamin C in the skin layers show that it has essential functions in the biological processes (106).

3.1.3.1.3.1. COLLAGEN FORMATION

Vitamin C is a co-factor in the structure of proline and lysine hydroxylases, which stabilize the tertiary structure of the collagen, and it also starts collagen production, which is done by fibroblasts (107).

Some animal studies with the vitamin-C-deficient mouse showed that collagen stability depended on the availability of vitamin C (108), and vitamin C also stimulates collagen mRNA production by fibroblasts (109).

3.1.3.1.3.2. FREE RADICALS SCAVENGING AND TOXINS OXIDANT DISPOSING

Vitamin C is a potent antioxidant that can neutralize and remove ROS produced due to external factors like after UV exposure to ultraviolet radiation, which is particularly crucial in the epidermis (110, 111).

Vitamin C works together with enzymatic catalase, glutathione peroxidase, and superoxide dismutase as well as non-enzymatic vitamin E, glutathione, uric acid, and other putative antioxidants such as carotenoids like antioxidants. Vitamin C is especially effective at reducing oxidative damage to the skin when it is used in conjunction with vitamin E, because it is also a generator of oxidized vitamin E. Effective recycling of vitamin E which is an essential lipid-soluble radical scavenger, and it limits oxidative damage to cell membrane structures (112).

3.1.3.1.3.3. INHIBITION of MELANOGENESIS

Vitamin C derivatives have been shown to decrease melanin synthesis both in cultured melanocytes and *in-vivo*, which may be due to its ability to interfere with the action of tyrosinase, the rate-limiting enzyme in melanogenesis (113, 114).

3.1.3.1.3.4. INTERACTION with CELL SIGNALLING PATHWAYS

Vitamin C has roles in the differentiation of keratinocytes and improved ultrastructural organization of the stratum corneum, helping the establishment of enhanced barrier function (115).

Vitamin C also levels of the late differentiation marker filaggrin, which appeared to be due to altered gene expression and promotes synthesis and organization of barrier lipids and increased cornified envelope formation during differentiation (116).

Table 3. Summary of some of the potential effects of vitamin C on the skin (106)

Study Description	Measured Parameters	Outcome and Comment
Effects on collagen and elastin synthesis		
Vitamin C affects collagen and elastin synthesis in human skin fibroblasts and vascular smooth muscle cells.	Monitored vitamin C time of exposure and dose on collagen synthesis and gene expression, and elastin synthesis and gene regulation.	Vitamin C exposure increased collagen, decreased elastin. Stabilization of collagen mRNA, lesser stability of elastin mRNA, and repression of elastin gene transcription.
Effect of vitamin C on collagen synthesis and SVCT2 expression in human skin fibroblasts. VitaminC added to the culture medium for five days.	VitaminC uptake measured into cells, collagen I, and IV measured with RT-PCR and ELISA and RT-PCR for SVCT2.	VitaminC increased collagen I and IV and increased SVCT2 expression.
Effect of vitamin C on elastin generation by fibroblasts from healthy human skin, stretch-marked skin, keloids, and dermal fat.	Immunohistochemistry and western blotting for the detection of elastin and precursors.	50 and 200 µM vitamin C increased elastin production. 800 µM inhibited. No measures of vitamin C uptake into cells.
Effects on morphology, differentiation and gene expression		
VitaminC addition to cultures of rat keratinocytes (REK).	Effect on differentiation and stratum corneum formation.	Morphology showed enhanced stratum corneum structure, increased keratohyalin granules, and organization of intercellular lipid lamellae in the interstices of the stratum corneum: increased profilaggrin and filaggrin.
Effect of vitamin C on human keratinocyte (HaCaT) cell line differentiation in vitro.	Systematic development of cornified envelope (CE), gene expression.	CE formation and keratinocyte differentiation induced by vitamin C, suggesting a role in the formation of stratum corneum and barrier formation in vivo.
Effect of vitamin C supplementation on gene expression in human skin fibroblasts.	Total RNA nano assay for genetic profiling, with and without vitamin C in the culture medium.	Increased gene expression for DNA replication and repair and cell cycle progression. Increased mitogenic stimulation and cell motility in the context of wound healing. Faster repair of damaged DNA bases.
Effect of vitamin C on the dermal-epidermal junction in skin model (keratinocytes and fibroblasts).	Keratinocyte organisation, fibroblast number, basement membrane protein deposition and mRNA expression.	VitaminC improved keratinocyte and basement membrane organization. Increased fibroblast number saw the deposition of basement membrane proteins.
Effect of vitamin C on cultured skin models—combined human epidermal keratinocytes and dermal fibroblasts.	Monitored morphology, lipid composition.	VitaminC, but not vitamin E, improved epidermal morphology, ceramide production, and phospholipid layer formation.

Protective effects against UV irradiation		
Effect of vitamin C on UVA irradiation of primary cultures of human keratinocytes.	VitaminC added in low concentrations, monitored MDA, TBA, GSH, cell viability, IL-1, IL-6 generation.	VitaminC improved resistance to UVA, decreased MDA and TBA levels, increased GSH levels, decreased IL-1, and IL-6 levels.
Effect of vitamin C uptake into human keratinocyte (HaCaT) cell line on the outcome of UV irradiation.	Accumulation of vitamin C in keratinocytes, antioxidant capacity by DHDCF, and apoptosis induction by UV irradiation.	Keratinocytes accumulated mM levels of vitamin C, increasing antioxidant status, and protecting against apoptosis.
Effect of UVB on vitamin C uptake into human keratinocyte cell line (HaCaT) and effects on inflammatory gene expression.	Cellular vitamin C measured by HPLC, mRNA expression for chemokines, western blotting for SVCT localization.	VitaminC uptake was increased with UVB irradiation, and chemokine expression decreased with vitamin C uptake.
Protective effects against ozone exposure		
Effect of antioxidant mixtures of vitamin C, vitamin E, and ferulic acid on the exposure of cultured normal human keratinocytes to ozone.	Cell viability, proliferation, HNE, protein carbonyls, Nrf2, NFkappaB activation, IL-8 generation.	VitaminC-containing mixtures inhibited toxicity. The presence of vitamin E provided additional protection against HNE and protein carbonyls.
Protection of cultured skin cells against ozone exposure with vitamin C, vitamin E, and resveratrol. 3-D culture of the human dermis—fibroblasts with collagen I + III.	Cell death, HNE levels, expression of transcription factors Nrf-2 and NfkappaB	Extensive protection against cell damage with mixtures containing vitamin C. Increased expression of antioxidant proteins. An additional effect of vitamin E + C. No effect with VitaminE alone.

3.1.3.1.4. BIOTIN

As part of B-complex vitamins, commonly known as biotin, also known as Vitamin B7 or Vitamin H, is a water-soluble vitamin that serves as an essential cofactor for carboxylase enzymes in multiple metabolic pathways. Due to its relatively low cost and easy availability in the market place, biotin has become the new trend for cosmetic products promoting stronger hair, skin, and nails. It is naturally found in nuts, soybeans, eggs, avocado, and cauliflower. Biotin's role in skin health is not well understood. However, it is known that if there is biotin deficiency, the skin gets red, scaly skin rashes occur (117). Some studies show that biotin deficiency may sometimes cause a skin disorder called seborrheic dermatitis, also known as cradle cap (118).

There is no evidence showing that biotin improves skin health in people who are not deficient in this vitamin (119).

3.1.3.1.5. CAFFEINE

Many researchers believe that caffeine can reduce the appearance of cellulite by constricting the blood vessels and giving a firmer appearance to the skin. According to a study published in the *Skin Pharmacol Physiol* journal, “Caffeine has potent antioxidant properties protecting the cells against UV radiation, therefore slows down the photoaging process of the skin” (120).

Other studies showed that adding caffeine to sunscreen formula can increase its protective effect against UV radiation, reducing the formation of free radicals in skin cells and therefore preventing UV-induced skin cancers (121).

Studies are indicating that Caffeine affects the UV-damaged human skin cells' proliferation process and cause apoptosis before they begin to transform into cancer cells (122). In another study, caffeine was shown to be an effective scavenger of hydroxyl, alkoxy radicals, and a poor scavenger of other free radicals (123).

4. DELIVERY SYSTEMS in COSMETIC INDUSTRY

4.1. CARRIER SYSTEMS

In recent years, many new cosmetic delivery systems have been introduced in addition to solutions, emulsions, lotions, gels, and aerosols, which are known as conventional delivery systems. Multiple emulsion systems, vesicular, and particulate systems are among the most commonly used new delivery systems (124).

Many advantages of liposomes and niosomes that are a vesicular system have been demonstrated (125). In addition to controlled release, it has been shown that the increased penetration through the skin, providing a longer-lasting effect, ensuring the stability of the active components, reducing the undesirable effects and irritation are the beneficial effects of the liposomes (126, 127).

Liposomes, resemble the biological membranes and are biodegradable (128). Because the method of preparation affects the behavior of liposomes, as well as the lipids used, the method of preparation, and the composition of the liposomes should be carefully selected (129).

Niosomes, colloidal particles made from nonionic surfactants, and cholesterol. The structure of the niosomes is similar to liposomes that have a concentric double layer surrounding an aqueous compartment (130).

Table 4. Different carrier vesicle systems (131)

VESICLE	COMPOUND
Liposome	Phospholipids and cholesterol
Niosome	Consists of non-ionic amphiphiles (surfactants)
Transferosome	Phospholipids, cholesterol
Ethosome	Phospholipid, ethanol, and water
Flexosome	Contains phospholipid in, positively or negatively charged lipids
Invasome	Phosphatidylcholine, ethanol, and terpene
Vesosome	Large lipid bilayers surrounding many small liposomes
Ufasome	Fatty acid vesicles
Polymer-some	Diblock and triblock copolymers vesicles

Transferosomes, offer not only a versatile delivery concept to enhance the potential use of a wide range of active compounds but also on improved stability. They are metastable, which makes the vesicle membrane ultra-flexible; therefore, the vesicles can easily deform when applied topically that they do not block the pores in the stratum corneum, even less than a tenth of their diameter. Thus, transferosomes with sizes up to 200–300nm can penetrate intact skin (132).

Flexosome is a self-regulating lipid-based non-invasive drug carrier for targeted delivery of agents into and through the skin, comprising biocompatible membrane emollients in the liposomal bilayer. Flexosome crosses the skin barrier by opening the intracellular hydrophilic pathways of the skin. This process takes place due to the originating from the transdermal hydration gradient, while deforming is membranes to fit such passages with high flexibility (133).

Invasomes, are soft, flexibles, liposomal vesicles with very high membrane fluidity. They contain ethanol and terpenes, which play a role in penetration enhancement. The skin penetration mechanism of invasomes is similar to ethosomes (134).

Vesosome, an alternative to liposomes, are new structures that are multilamellar and large systems. These new constructs are controlled include controlled-sized multicellular liposomes and giant multicellular liposomes that act as depot-type drug delivery systems. Multiple membranes and multiple compartments significantly increase degrees of freedom in optimizing such structures for drug delivery or other applications (135).

Ufasome, a closed lipid bilayer membrane colloidal suspension, consists of fatty acid vesicles, fatty acids, and ionized species (soap, anionic fatty acids). The formation of these unsaturated fatty acid vesicles was first reported by Gebicki and Hicks in 1973 and was termed “ufasome” (136).

Polymer-some is hollow shell nanoparticles that can be used for drug delivery. Biodegradable polymers for loading, delivering, and cytosolic uptake of drug mixtures have been shown to benefit from the thick membrane and aqueous lumens of these block copolymer vesicles, the drug can be released in the manner of pH-induced release in endosomes. Target-specific and biodegradable polymers break down in acidic environments and release drugs into tumor cell endosomes. Unlike cell membranes and liposomes formed from a pair of phospholipid layers, a polymer consists of two synthetic polymer layers, in which the individual polymers are substantially more significant than the individual phospholipids but have the same chemical properties (137).

4.1.1. LIPOSOMES

Liposomes are versatile structures for research, therapeutic, and analytical applications. They consist of the hydrophobic chains of lipids forming the two layers and a lipid bilayer with polar groups of lipids directed into the extravascular solution and the inner cavity. Its structure is similar to cells and can, therefore, be used as a more natural method on target organisms to study the interactions between membrane lipids and the permeability of biomolecules, ions, and drugs, and to elucidate the mechanism of action of antibiotics (138).

For the first time in 1964, Bangham et al. observed that phospholipids in the aqueous medium formed a closed bilayer structure (139) In 1968, Weissmann and colleagues called the name of these spheres’ “liposomes”.

Liposomes can be used to transport macromolecules, cosmetic raw materials to targeted areas in topical and pharmaceutical applications. They are lipid bilayer structures with a hollow spherical shape that can easily encapsulate hydrophilic substances (140).

For the first time as a cosmetic preparation, “Capture” under the brand name Christian Dior was introduced into the market in 1987. After that has been on the market after that, many cosmetic companies have developed products containing liposomes. Today, the cosmetic

industry produces and markets its products in pharmaceutical quality to increase the cosmetic benefits by trapping the active ingredients in the liposomes (141).

Liposomes are spherical, closed, double lipid layers and are colloidal sized vesicles, which are capable of binding solvent in which they float freely. They are mainly composed of phospholipids. They have various features and can be useful in many applications. Liposomes exhibit several specific biological properties, including interactions with biological membranes and various cells. They can be made entirely from natural materials and are therefore non-toxic, biodegradable, and non-immunogenic. The areas where liposomes are used are shown in Table 5. Liposome offers beneficial models in topology, membrane biophysics, photophysics, and photochemical sciences, colloidal interactions, cell function, signal transduction, and many other studies (3).

Table 5. Disciplines using liposomes (3)

DISCIPLINE	APPLICATION AREA
Mathematics	Topology
Physics	Aggregation behavior, soft and high hardness materials
Biochemistry	Permeability, phase transitions in two dimensions, photophysics
Chemistry	Photochemistry, artificial layers
Biology	Protein permeability of artificial membranes
Pharmaceuticals	Drug action studies
Medicine	Carrier and medical diagnostics, gene therapy

Many pharmacological and medical applications of liposomes have been investigated by many researchers (131). Therapeutic and diagnostic applications of liposomes containing drugs or various markers, their use as a model instrument or reagent to investigate the mode of action of certain substances have been investigated (142). Many cosmetic products have a narrow therapeutic window (131), whereas liposomes can reduce toxicity and increase efficacy. The benefits and limitations of drug delivery liposomes depend on the fate of liposomes after *in-vivo* administration. *In-vivo* and *in-vitro* studies have shown that the interaction of liposomes with cells is through a simple adsorption process (3).

Liposomes have been the subject of intensive research in the last few years as carrier systems in pharmaceutical and cosmetic products. Furthermore, the superiority of liposomes as drug carriers is now widely accepted (143).

Significant basic and clinical research has facilitated final regulatory approval from many companies. Many liposome formulations, such as AmbiSome[®] and Stealth[®] liposome (DOXIL[®]), are now commercially available (144).

4.1.1.1. STRUCTURE of LIPOSOMES

It is a group of chemical compounds that occur in living organisms such as liposomes, lipids, fats, and waxes, and their solubility in water is very low. Phospholipids, on the other hand, can be defined as a particular lipid containing a phosphate group. Phospholipids are the building blocks of liposomes and cell membranes. Like other parts of our body, our skin consists of a combination of cells and the cell membrane that forms the skin needs to be healthy and durable in order to function as desired. Liposomes are formed by adding cholesterol to both synthetic and natural phospholipids. The formulations have been preferred for historical reasons or analogy to natural membrane compositions. Phosphatidylcholine (Lecithin) is most commonly used in the preparation of liposomes. Each type of phospholipid is characterized by a gel-liquid transition temperature (T_c). Below this temperature, the fatty acid chains are almost in a crystal plane. Above this temperature, the chains are in a more liquid phase. As the chain melts, the thickness of the bilayer decreases, and the area per molecule increases. These changes have been investigated by various physical techniques such as X-ray diffraction, nuclear magnetic resonance, electron spin resonance, differential scanning calorimetry, and fluorescence depolarization. In general, the T_c value can be reduced by reducing the chain length by not saturating the leading chains by large side groups and by the branching of the actual chain. Polar bond groups also affect the transition temperature, but not as effective as the leading chains. Natural phospholipids (e.g., egg phosphatidylcholine) contain a complex of saturated and unsaturated leading chains and are characterized by a wide range of low-temperature transitions. All T_c values given in the table belong to the studies performed with multilamellar vesicles (145).

4.1.1.2. LIPOSOMES ADVANTAGES

Some of the advantages of the liposome are as follows in Table 6.

Table 6. Advantages and disadvantages of liposome (131)

ADVANTAGES of LIPOSOME	DISADVANTAGES of LIPOSOME
Liposomes increased efficacy and therapeutic index of a drug (actinomycin-D)	Low solubility
Liposome increased stability via encapsulation	Short half-life
Liposomes are non-toxic, flexible, biocompatible, completely biodegradable, and non-immunogenic for systemic and non-systemic administrations	Sometimes phospholipid undergoes oxidation and hydrolysis-like reaction
Liposomes reduce the toxicity of the encapsulated agent (amphotericin B, Taxol)	Leakage and fusion of encapsulated drug/molecules
Liposomes help reduce the exposure of sensitive tissues to toxic drugs	Production cost is high
Site avoidance effect	Fewer stables
Flexibility to couple with site-specific ligands to achieve active targeting	

4.1.1.3. CLASSIFICATION of LIPOSOMES

Liposomes vary in size from 0.025 μ m to 2.5 μ m. They can be classified according to their sizes, also according to their structures, like single, double, or multi-layer liposomes, as shown in Table 7. Vesicle size is an acute parameter in determining the circulating half-life of liposomes, and both the size and the number of bilayers affect the amount of active substance encapsulation in the liposomes. Based on their size and double number, liposomes can also be classified into one of two categories multicellular vesicles (MLV) and unicellular vesicles. Unilamellar vesicles can also be classified into two categories: large unilamellar vesicles (LUV) and small unilamellar vesicles (SUV). Several new types of vesicles are shown in Table 7, depending on the additives used for vesicle preparation (131).

The technology used to produce liposomes has been progressing considerably over the years that the liposome technology has now come to the ‘second-generation liposomes’ phase, in which long-circulating liposomes are obtained, which are different and more sophisticated than the conventional ones (131).

Table 7. Liposome carrier types

TYPES	ABBREVIATION	SIZE
Unilamellar vesicles	UV	Whole size range
Oligolamellar vesicles	OLV	0.1-1 μm
Multicellular vesicles	MLV	$>0.5 \mu\text{m}$
Small single-layer vesicles	SUV	20-40 nm
Medium single-layer vesicles	MUV	40-80 nm
Large unilamellar vesicles	LUV	$>100 \text{ nm}$
Giant unilamellar vesicles	GUV	Diameter of vesicles $>1 \mu\text{m}$
Multiple vesicular vesicles	MVV	Generally large $> 1 \mu\text{m}$

4.1.1.4. PREPARATION of LIPOSOMES

Liposomes are widely used as carriers for a large number of molecules in the cosmetic and pharmaceutical industries. Besides, the food and agricultural industries have extensively explored the use of liposome encapsulation to enhance delivery systems that can retain unstable compounds and retain their function (131).

Liposomes can entrap both hydrophobic and hydrophilic compounds, which can be released at specified targets. When phospholipids are dispersed in aqueous solutions, due to their amphipathic nature, they have a strong tendency to form membranes (146). However, additional steps are often required to alter the size distribution and lamellae of the liposomes (1).

Many different methods for accurate structure, size, high entrapment yield, and reproducibly, the low release of encapsulated material during shelf-life have been studied (1).

Liposome preparation consists of three main steps: vesicle formation, vesicle size reduction, and purification. Various preparation methods have been studied based on a production scale, active encapsulation activity, physicochemical properties of the active substance, and other aspects such as route of administration (147).

The main production techniques can be divided into two: passive loading techniques and active loading techniques (148).

4.1.1.4.1. PASSIVE LOADING TECHNIQUE

The passive loading technique consists of three main methods, which are mechanical dispersion, solvent dispersion, and detergent removal methods (149).

4.1.1.4.1.1. MECHANICAL DISPERSION METHOD

As shown in Figure 11 is the oldest and the most widely used liposome preparation method, which involves lipid hydration and exchange of organic solvents in an aqueous medium 3. This method, also known as Bangham's method, consists of a creation of a vortex or manual mixing, followed by lipid hydration, whereby the lipids are dissolved in a suitable organic solvent such as chloroform or methanol. Then the solvent is removed by evaporation under an evaporator at low vapor pressure until a thin film is formed. The thin film is hydrated above the phase transition temperature in an aqueous medium, resulting in the formation of MLV. This is the method of vesicle formation; however, it is limited in use due to its low encapsulation ability (139).

The preparation of lipid hydrates starts with homogeneous mixing of all lipids and hydrophobic materials, and these are kept homogeneously in an organic solvent. The drying step involves drying the solution in a glass container under reduced pressure by a rotary evaporator. Generally, this step is carried out by using chloroform: methanol mixtures. A lyophilizer can also be used to achieve complete dryness (149).

The dispersion of the solid residue obtained in the previous step is then achieved by the addition of an aqueous medium into the glass container. If the substances to be retained are hydrophilic, they are dissolved and added with this aqueous medium. This method is beneficial for the encapsulation of hydrophobic substances, while the yield of hydrophilic substances is low, 5-15% (1). For the production of larger volumes, the organic solvent should be removed through the evaporator to give a thin lipid film on the sides of a round bottom flask, and the lipid film is dried thoroughly by placing the flask on a vacuum pump throughout the day to remove the organic solvent. If chloroform is inconvenient, the lipids could be dissolved in tertiary butanol or cyclohexane. After drying the film, hydration of the dry lipid film/cake is carried out by adding an aqueous medium to the dry lipid container and shaking. The temperature of the humidifying medium should be above the highest gel-

liquid crystal transition temperature (T_c or T_m) of the lipid before being added to the dry lipid. After the addition of the solvent water medium, the lipid suspension should be kept above T_m for the duration of the hydration. For high pass lipids, this can be easily accomplished by transferring the lipid suspension to a round bottom flask and placing the flask in a vacuum-free rotary evaporation system (150).

Rotating the round-bottom flask in a warm water bath maintained at a temperature above the T_m of the lipid suspension allows the lipid to liquefy in the liquid phase with sufficient agitation. The hydration time may vary slightly between lipid types and structure, but a 1-hour hydration time with vigorous shaking or stirring is highly recommended. It is further believed that allowing the vesicle suspension to remain overnight before reduction facilitates the sizing process and improves the homogeneity of the size distribution. Heating is not recommended for high-pass lipids because of lipid hydrolysis increases at high temperatures (149-151).

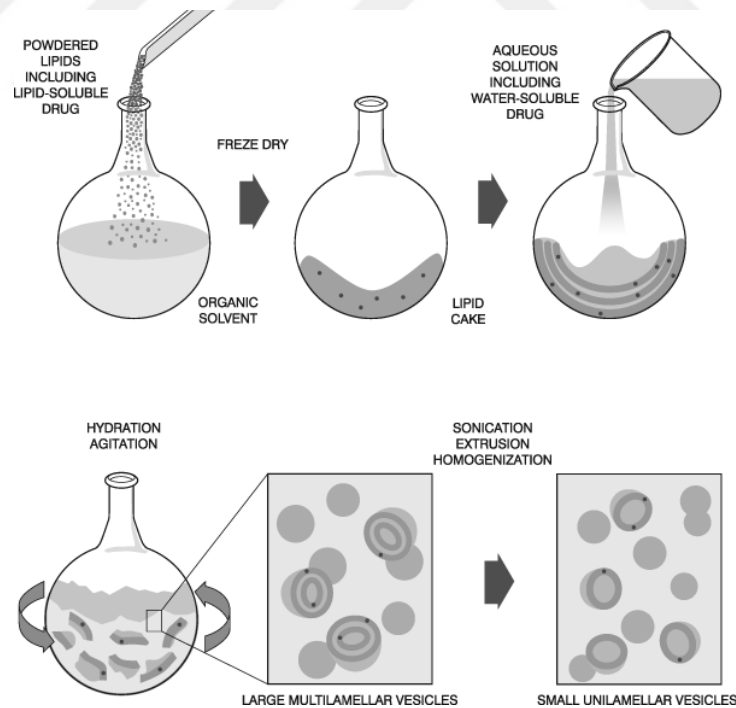


Figure 8. Dispersion method with an organic solvent (Burgess, 1998)

The size adjustment of the lipid suspension can be made by sonication. Sonication involves disruption of MLV) suspensions using sonic radiation energy and is often used to produce

small-layer vesicles (SUVs) with diameters in the range of 20-100nm (131). The most commonly used tools for this process are bath and probe end sonicators. While bath sonicators are applied for large volume diluted MLVs, the probe end sonicators (like stylus) is more suitable for a smaller suspension volume requiring high energy input to disintegrate vesicles. The size adjustment of liposomes by sonication is an open system that involves the risk of contamination from both the medium and the metal tip (metal contamination) of the probe, as seen in Figure 12 The presence of MLV together with SUV, possible degradation of phospholipids and compounds to encapsulate, elimination of large molecules can be listed as essential disadvantages of sonication (131). In this sizing method, the average size and distribution of the vesicles are influenced by many factors such as composition, concentration, temperature, sonication time and power, volume and sonicator setting (152, 153).

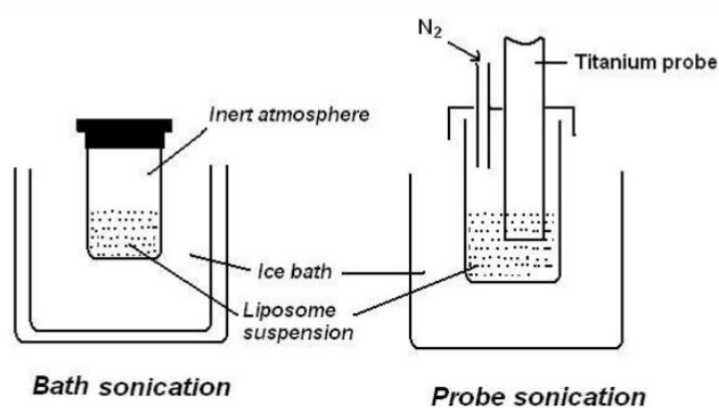


Figure 9. Dimensioning of liposomes by sonication (4)

4.1.1.4.1.2. SOLVENT DISPERSING METHOD

It involves the injection of the dissolved organic lipid solution into the aqueous medium containing the materials entering it. MLVs are formed immediately at the interface between the organic and aqueous regions (153).

The main disadvantages of this method include heterogeneous size distribution of liposomes and difficulties in removing possible azeotropes of water with organic solvents (153)

This method has three different techniques. These are ether injection, ethanol injection, and reverse-phase evaporation. In ether injection, a lipid solution dissolved in diethyl ether or

ether-methanol mixture is gradually injected into the aqueous solution of the material to be encapsulated at 55 °C to 65 °C, or under high pressure. The solvent (ether) is then removed under vacuum, so causing liposomes to form (153).

The ethanol injection method proceeds as the same procedure as for the ether injection method wherein ethanol is used as the organic solvent. The disadvantage of this method is that the liposomes are much diluted (152).

The reverse-phase evaporation method is based on the formation of reverse micelles, which are formed by sonication of a buffered aqueous phase mixture comprising water-soluble molecules to be encapsulated in liposomes and an organic phase in which the amphiphilic molecules are dissolved. The slow elimination of the organic solvent leads to the conversion of these inverted micelles into a viscous gel form (131).

4.1.1.4.1.3. DETERGENT CLEANING METHOD

Detergents at critical micelle concentrations (CMC) are used to solubilize lipids. When the detergent is removed, the micelles become increasingly rich in phospholipids and to form LUV. Although this method is best for obtaining repeatable liposomes, further processing is required to remove the detergent residues within the liposomes.

To summarise, thanks to the repeatability and applicability, the mechanical dispersion method is the simplest and easiest way to produce homogeneously sized liposomes among all three methods (131).

Following the formation of MLV's, a variety of sizing methods is applied to reduce vesicle sizes because they are too large to work and are highly heterogeneous in the population. Ultra-sonication and extrusion are the most preferred techniques for size reduction (149).

4.1.1.4.2. ACTIVE LOADING TECHNOLOGY

Industrial production of liposomes requires additional attention because sterility and stability problems, repeatability, size distribution are becoming more critical for the end products. Removal of carcinogenic raw material and solvent residues are the other obstacles to be

overcome in large scale manufacturing. In order to prevent this situation, suitable methods for the industry have been developed (155).

4.1.1.4.3. DETERGENT DIALYSIS

Detergents can be defined as a subgroup of certain surfactants whose lipid membranes are soluble. A sufficient amount of detergent leads to the rearrangement of the lipid layers to form smaller, soluble detergent-lipid pellets of various forms, called mixed micelles (MMs). Conversely, when the amount of detergent in the MMs is reduced, it causes the MMs to expand repeatedly. In a critical detergent-lipid ratio, membrane duplexers are formed, which are inherently vesicular to form liposomes. In different intermediate phases of detergent-membrane lipid aggregation, membrane proteins can be regenerated into membrane bilayers (156).

Detergent removal for the liposome preparation is inherently superior to other methods when unilamellar liposomes are needed. This is important for their use as model membranes to study the diffusion rate of compounds through bilayers or to measure transmembrane transport of compounds through reconstituted membrane proteins. In this context, the spherical shape of the liposomes is also desirable; this is better than mechanical procedures such as extrusion after removal of the detergent. The production of unique and homogeneous liposomes can be more easily achieved by removing the detergent. Besides, even if sterile liposome dispersions are required, for example, for parenteral administration by infusion or injection, liposomes more giant than 200nm may, in principle be used, since the initial micelle solution can be purified from microorganisms through a sterile channel. Filters with porosities of 0.2 μ m or less. Finally, some methods for removing the detergent allow the concentration of liposome dispersions in a second step without changing the preparation equipment (156). Unfortunately, aqueous dispersions of liposomes often tend to aggregate or fuse and may be susceptible to hydrolysis and oxidation (157).

4.1.1.4.4. MICROFLUIDIZER METHOD

Microfluidic methods include all new techniques using microscopic channels (size 5-500 μ m). In this method, the lipids are dissolved in a suitable organic solvent (ethanol or isopropanol), and the resulting solution is pushed perpendicularly or inversely to the aqueous

medium in the microchannels. Continuous axial mixing of the organic and aqueous solutions leads to liposome formation due to local diffusion of phospholipids in the aqueous phase, which promotes self-assembly. Among others, the micro-hydrodynamic focusing method represents the most commonly used microfluidic method for the formulation of liposomes. This method produces small and large unilamellar vesicles of 40-140nm with excellent uniformity (monodisperse property). Other microfluidic techniques include microfluidic droplets and pulsed jet flow microfluidic methods. The method of microfluidic droplets involves dissolving phospholipids in hexane to prepare giant liposomes (4-20 μ m). In the pulsed jet flow microfluidic method, the conventional film hydration method was modified by drying the lipid solution in microtubes. The resulting lipid film is hydrated in microtubes by a perfusion process that produces vesicles more giant than 200-534 μ m with remarkable encapsulation yield. As common advantages, microfluidic methods allow the production of vesicles of the desired size due to the versatility and flexibility of the methods. The disadvantages of these methods include the forced use of organic solvent and hard agitation, as well as the difficulty of large-scale production (158).

In proliposomes, the lipid and drug are coated onto a soluble carrier to form a free-flowing granular material; forms an isotonic liposomal suspension in hydration. The proliposome approach can provide an opportunity for low-cost, large-scale liposome production, especially involving lipophilic active ingredient (152).

Lyophilization involves freeze-drying (lyophilization), removing water from frozen products at low pressures. This technique has great potential as a method of solving long-term stability problems related to liposomal stability. There may be leakage of trapped materials during the frozen drying process and the reconstitution process. Recently, it has been shown that the freeze-dried liposomes retain 100% of their original contents in the presence of a sufficient amount of trehalose. Freeze dryers are available from pharmaceutical equipment suppliers ranging in size from small laboratory models to large industrial units. They are characterized by relatively short blood (152).

To overcome this problem of circulatory time, long-term circulating liposomes have been developed. These latent liposomes carry a polymer coating to achieve long circulation times. Targeted liposomes (immunoliposomes) may be conventionally or sterically stabilized and

may have specific antibodies or antibody fragments on their surface to enhance target site binding (157).

4.1.1.5. CHARACTERIZATION of LIPOSOMES

Characterization of liposomes should be performed immediately after preparation, as vesicle quality can change very quickly when stored. The most critical parameters of liposome characterization include visual appearance, light transmission, size distribution, lamellarity, entrapment concentration (encapsulation efficiency), composition, presence of degradation products, and stability.

4.1.1.5.1. DETERMINATION of ENCAPSULATION EFFICIENCY

Methods for determining the amount of material encapsulated within liposomes typically rely on the destruction of the lipid bilayer and liberation of the encapsulated material and then the quantification of the released material. In these measurements, the signal from the intact liposomes is typically monitored before the bilayer breakdown, and the signal after a breakdown is compared. Spectrophotometry is the most common method for quantifying the amount of the material. These techniques for quantification depend on the nature of the encapsulation and the type of spectrophotometric methods, such as fluorescence spectroscopy, enzyme-based methods, and electrochemical techniques (138).

4.1.1.5.2. DETERMINATION of LAMELLAR STRUCTURE

The degree of layering of liposomes made according to different lipids or preparation procedures varies. This is evidenced by reports showing that the phospholipid fraction exposed to the external environment ranges from 5% for the sizeable multilamellar vesicle to up to 70% for the unilamellar vesicle. The determination of liposome layers is generally carried out by ^{31}P -NMR. In this technique, the addition of Mn^{2+} interrupts the ^{31}P -NMR signal from the phospholipids on the outer surface of the liposomes. Mn^{2+} interacts with negatively charged phosphate groups of phospholipids and quantitatively causes the signal to broaden and reduce. The degree of the layer is determined from the signal ratio before and after the addition of Mn^{2+} (138).

Electron microscopy, visible or fluorescence microscopy, small-angle X-ray scattering are also used for the determination of lamellarity (159).

4.1.1.5.3. DETERMINATION of SIZE DISTRIBUTION and SURFACE CHARGE DETERMINATION

One of the essential criteria in the characterization of liposomes is the determination of size and size distribution. Various techniques are available to assess liposome size and size distribution, including static and dynamic light scattering (DLS), various microscopic techniques, size exclusion chromatography, and field-flow fractionation (160). The mean vesicle size and size distribution profile of the liposome is determined using the Malvern particle size analyzer, which follows Mie's theory of light scattering (161).

DLS, also known as photon correlation spectroscopy or semi-elastic light scattering, represents the most commonly used method for determining liposome size, polydispersity, and zeta potential (surface charge). DLS is made with an instrumental setting called Zetasizer Nano. The standard operating principle of DLS is based on the continuous motion of dispersed particles due to the bombardment of solvent molecules (Brownian motion). This phenomenon causes a significant scattering of the applied light. Since the degree of fluctuation in light intensity is related to the diffusion rate of particles emitted to the particle diameter (smaller particles emitting faster than the larger ones), the particle size is automatically deducted from the estimated amount of scattered light. In dealing with zeta potential measurements, DLS allows the determination of surface charge by reaching changes in the scattered light intensity caused by particle motion due to the applied electric field. In other words, for the surface charge zeta potential evaluation, changes in the intensity of scattered light are governed by the applied electric field, which causes intense motion of charged particles, unlike the size measurements, where Brownian motion is the main factor (162).

In addition to being a simple, fast, and reliable method for routine analysis, DLS offers many advantages from several nanometers to several micrometers, including taking measurements from a local environment and evaluating a wide range of sizes. However, DLS shows some limitations, such as the difficulty in distinguishing individual particles from aggregates and high sensitivity to contaminants (163).

Besides, DLS technically cannot provide the actual particle size but provides hydrodynamic diameter due to particle dissolution. Water layers on the particle surface cause misreading of particle diameters in the aqueous medium (164).

4.1.1.5.4. TRANSMISSION ELECTRON MICROSCOPY

Negative staining results in morphological appearance about liposome preparations of various variations on using cryo-electron microscopy (CEM). Liposomes prepared from phospholipids containing high purity phosphatidylcholine in the size of 100–300nm were reported to have higher stability. Therefore, the most crucial criterion in preparation methods will be particle size and particle size distribution. It is known that lamella does not have much effect on stability, but oligolamellar structures are said to be more stable. For active encapsulated liposomes, the encapsulation rate and active substance leakage will be another vital evaluation criterion. Liposomal batches prepared apart from these can be monitored in terms of their morphological properties using an optical microscope (165).

4.1.1.5.5. APPEARANCE

Liposome suspension may vary in appearance depending on composition and particle size. If the turbidity has a bluish shade, it means that the particles in the sample are homogeneous; a flat, gray color indicates the presence of a non-liposomal dispersion (152).

4.1.1.5.6. STABILITY of LIPOSOMES

The stability of a pharmaceutical product is generally defined as the capacity of the delivery system to remain within the specified or predetermined limits of the product itself, pharmacopeia (166).

Although liposome offers many advantages as a drug carrier system, its potential application as therapeutic agents is still challenged by physical and chemical imbalances in aqueous dispersions for long-term storage. Accordingly, many methods for the stabilization of liposomes such as osmification lyophilization, freezing, spray drying, and supercritical fluid technology have been investigated. Among these, lyophilization is the primary approach

used to extend the shelf life of liposomes, especially for heat-sensitive drugs containing liposomes (6).

Stability problems can also be solved by using inert nitrogen gas, using fresh solvents and freshly purified lipids, avoiding high temperatures, and adding antioxidants (167).

Classical models from colloidal science can be used to describe liposome stability. Colloidal systems are stabilized electrostatically, sterically. Besides, the self-assembled colloids may undergo association or phase change after collection (168).

The liposome exhibits both physical and chemical stability properties. In general, the physical property describes the preservation of the liposome structure, and the chemical property indicates the molecular structure of the liposomal components. Physically stable formulations maintain both the liposome size distribution and the amount of encapsulated material.

Table 8. Liposome stability tests(169)

TYPES	TEMPERATURE/°C	TIME
Shelf test	45	One month
Shelf test	4	One month
Shelf test	37	One month
Shelf test	25	12-14 month
3 rounds Freeze-thaw test	-20 < > 25	12-14 month
6 turns Heating-Cooling test	5 < > 45	

Previously, lecithins from egg and soybean containing unsaturated hydrocarbons lead yellowing color, however now modified phospholipids are used. The costs of purified lipids are quite high. Liposomes have also been prepared as synthetic and polymerizable lipids. Such liposome preparations generally have better stability (129, 152). There is no specific protocol for accelerated or long-term stability studies for liposome formulations. However, stability tests that a protocol may include are indicated in Table 7.

4.1.1.6. ETHOSOMES

Conventional liposomes have some disadvantage because of their ability to penetrate the stratum corneum barrier to the skin, different generation liposomes have been prepared to overcome this barrier effect. Niosomas (1st generation), Transferosomes (2nd generation), Ethosomes (3rd generation) were different generation flexible liposomes with different mechanisms for increasing the drug concentration in the skin.

A comparison of different vesicular carriers is given in Table 9 with different characteristics. Transferosomes are second-generation flexible liposomes with a combination of phospholipids and edge activator. An edge activator is usually a single chain surfactant that causes vesicle lipid bilayer destabilization and increases vesicle elasticity or fluidity (170, 171).

Transferosomes are ultra-deformable or ultra-flexible liposomes that quickly undergo a transepidermal effect on the skin water activity gradient. Transferasomas vesicles easily reach the stratum corneum of the skin in search of aqueous hydration. Ethosomes represent 3rd generation elastic lipid carriers developed by Touitou (172, 173).

Ethosomes are ethanol-modified liposomes, which act as reservoir systems and ensure the continuous delivery of drugs to the desired site. Ethosomes are malleable vesicles that act by the effect of ethanol and lipid penetration, results in the release of drugs into different skin layers. Ethanol can also provide vesicles with soft, resilient properties that allow them to penetrate deeper layers of the skin more easily into the deeper layers of the skin (174).

Ethosomes are non-invasive delivery systems that allow active substances to reach deeper skin layers, which may ultimately lead to the systemic circulation (175). For optimal skin delivery, the active ingredient must be effectively introduced into the ethosomal vesicles (176).

Touitou researched the vesicular lipid systems, which contain high concentrations of ethanol and called them ethosomes, and lead to the first patent (177, 178).

Table 9. Comparison of different characteristics of liposomes, transfersomes, and ethosomes

CHARACTERS	LIPOSOME	TRANSFEROSOMES	ETHOSOMES
Vesicles	Bilayer Lipid vesicle	2nd generation elastic lipid vesicle carriers	3rd generation elastic lipid vesicle carriers
Composition	Phospholipids and Cholesterol	Phospholipids and edge activator	Phospholipids and Ethanol
Characteristics	Microscopic Spheres (Vesicles)	Ultraflexible Liposome	Elastic Liposome
Flexibility	Rigid in nature	High deformability due to surfactant	High deformability and elasticity due to ethanol
Permeation Mechanism	Diffusion/Fusion/Lipolysis	Deformation of vesicle	Lipid Perturbation
The extent of Skin Penetration	The penetration rate is very less as the stiff shape and size does not allow to pass through stratum corneum	Can easily penetrate through paracellular space by a flexible structure	Can easily penetrate through paracellular space by ethanol effect
Route of administration	Oral, Parenteral. Topical and transdermal	Topical and Transdermal	Topical and Transdermal
Marketed products	Ambisome, DaunoXome, Doxil, Abelect	Transfersomes® (Idea AG)	Nanominox, Cellutight EF, Noicellex, Decorin Cream

Ethosomes are soft vesicles formed mainly by phospholipids, ethanol, and water; in other words, they are composed of hydroalcoholic phospholipids in which the concentration of alcohol or combination thereof is relatively high, and their sizes can range from 30nm to 3µm (179).

Ethosomes typically may contain phospholipids with various chemical structures such as phosphatidylcholine (PC), hydrogenated PC, phosphatidic acid (PA), phosphatidylserine (PS), phosphatidylethanolamine (PE), phosphatidylglycerol (PPG), phosphatidylinositol (PI), hydrogenated PC (PPG) (180). Generally, about 0.5 to 10% by weight of phospholipid is used. Cholesterol may also be added at concentrations ranging from 0.1 to 1%. The alcohol content of the final products can be between 20-50%. The proportion of water phase varies between 22-70% (178)

4.1.1.6.1. PRODUCTION of ETHOSOMES

The phospholipid and the active ingredient are mixed in a mixer, alcohol is added during mixing, and the mixture is heated in a water bath to 30°C. An additional amount of water is heated to 30°C in a separate vessel and added to this mixture and then stirred in a closed

vessel for 5 minutes. Sonication or extrusion method can be used to reduce the vesicle size of the etosomal formulation (181, 182).

4.1.2. LIPIDS

Lipids are naturally occurring compounds found in animals and plants and all cell types. They are distinctly different from other biomolecule groups, are water-insoluble, but are highly soluble in organic solvents such as chloroform. The long-chain hydrocarbon groups may also comprise chain hydrocarbon groups. Although they are composed primarily of carbon and hydrogen, lipid molecules may also contain oxygen, nitrogen, sulfur, and phosphorous. Lipids function biologically as fuel molecules, high concentration energy stores, signal molecules, and membrane components. For example, the three main types of membrane lipids are phospholipids, glycolipids, and cholesterol (183).

4.1.3. PHOSPHOLIPIDS

There are mainly two classes of phospholipids: glycerophospholipids and sphingophospholipids. There are two fatty acid phosphodiester attached to the glycerol. The head group moiety, which binds to phosphate, comprises nitrogenous bases amino alcohols or polyols. Glycerophospholipids are obtained from various natural sources as a mixture of various phospholipid species. In general, this glycerophospholipid mixture is called lecithin, which is used industrially as an emulsifier. The sphingophospholipid contains phosphorus as well as the sphingosine structure.

The most common in this class is the N-acylsphingosine phosphorylcholine ester called sphingomyelin 5. The backbone of glycerophospholipids as can be seen in Figure 10. The most commonly used phospholipid species is PC. They usually have a low critical micelle concentration. Natural, semi-synthetic, and synthetic phospholipids are mainly used in the preparation of liposomes. The most commonly used phospholipids are egg or soy PC, dipalmitoylphosphatidylcholine (DPPC), distearylphosphatidylcholine (DSPC), phosphatidylinositol (PI), sphingomyelin (SM), PS, and PE as shown in Figure 11.

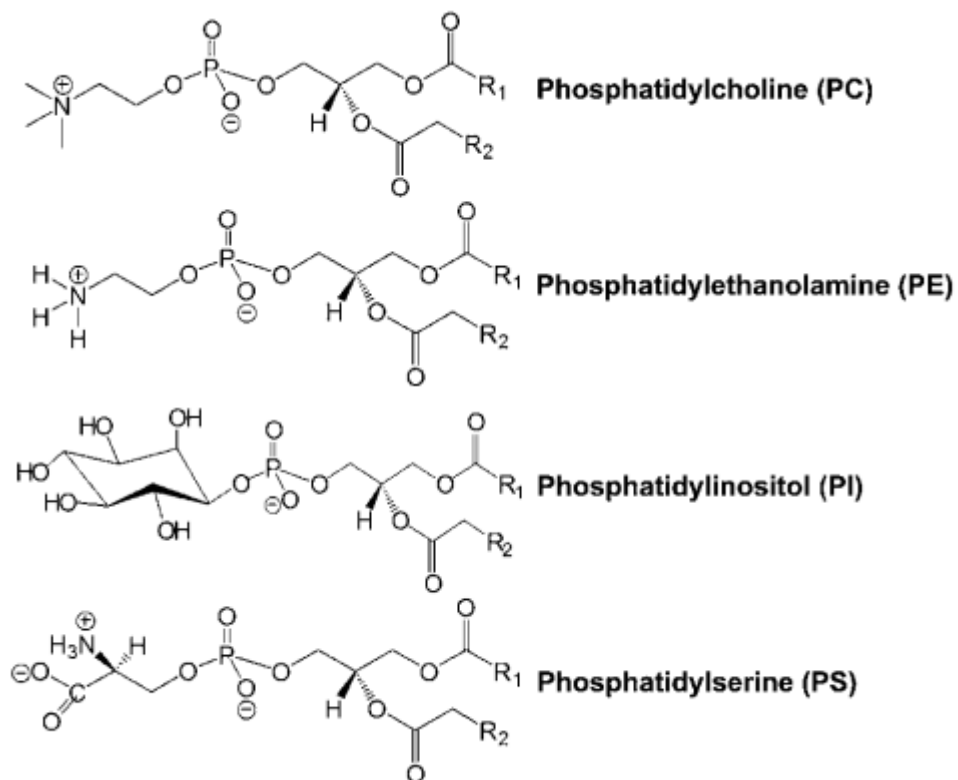


Figure 10. Glycerophospholipids (185)

Phospholipids are naturally found in cell membranes as bilayers. In a cell, the two-terminal portions of these layers face outwards, and an internal aqueous medium, non-polar portion, these polar regions stored from water from the structure of the cell membrane. As shown in Figure 12, phospholipids are predominantly found in the plasma membrane of mammalian cells. It is known that liposomes provide skin hydration (186).

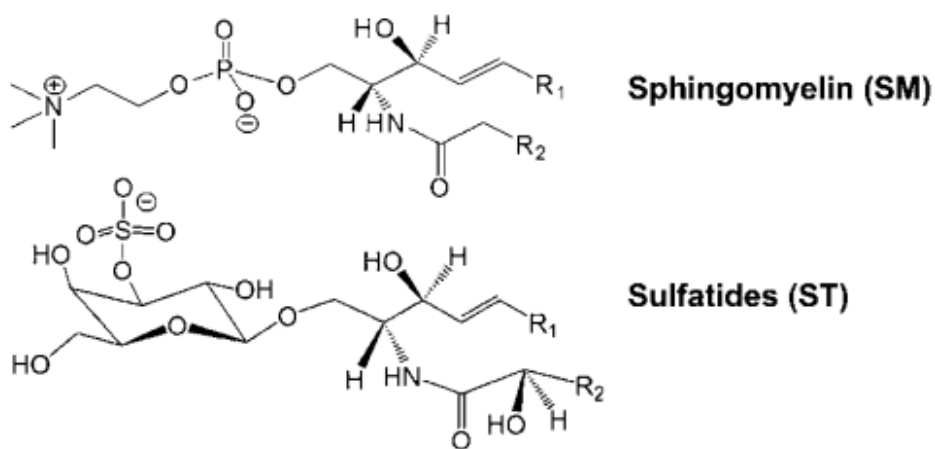


Figure 11. Sphingolipids

Phospholipids resemble cell membranes. They can encapsulate both water and oil-soluble actives. Interacts with the cell membrane and facilitates the penetration of compounds that cannot enter the skin structure in the usual way (187).

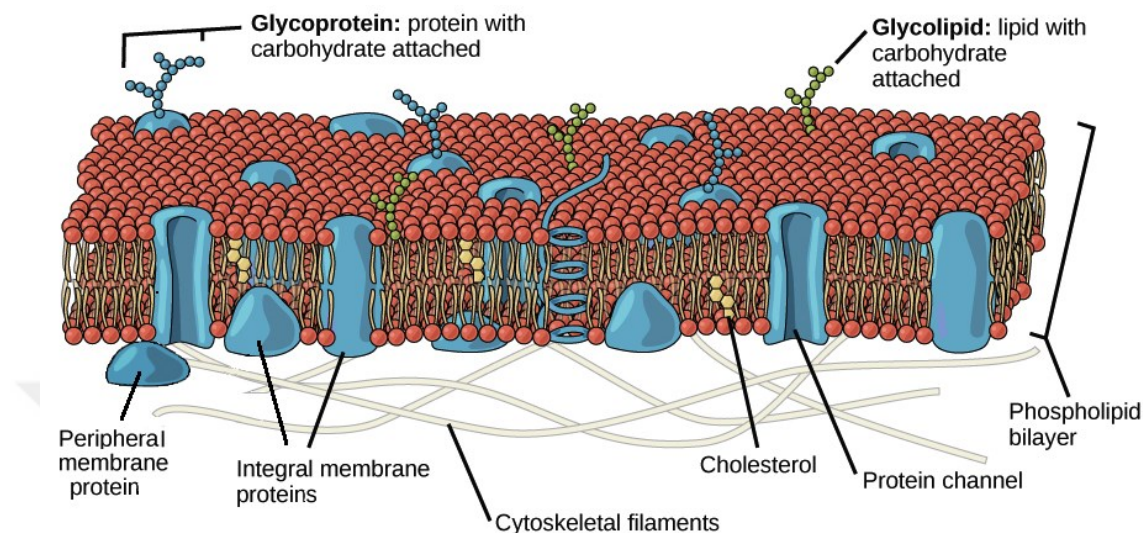


Figure 12. Structure of the cell membrane (188)

4.1.4. LIPOSOMES and SKIN

Although it is difficult for the active substances to enter the skin layers, the active substances can pass through the skin in many ways, and liposome delivery systems can enhance the penetration (189).

The carrier system properties of conventional phospholipid based vesicular liposomes have been extensively investigated, and their penetration enhancing effects have been shown by many researchers (190). Not only because of their convenience as a carrier for actives with different physicochemical properties but also their action as a reservoir for continuous delivery of actives that require local deposition make liposomes very convenient delivery systems (191).

In one study, the effect of liposomes on penetration through the skin was investigated, and it was concluded that penetration was inversely proportional to the size of the liposomal vesicle (192). Another critical factor for the dermal administration of such products was found to be the viscosity of the membrane of the vesicles (193). Many researchers have reported that increasing the deformability or elasticity of the vesicles leads to deeper

penetration of the active ingredients (194). This penetration enhancing effect was attributed to the mixing of liposomal bilayer lipids with intracellular lipids in the stratum corneum (195, 196).

5. FRANZCELL

Franz diffusion cell is an established system for diffusion tests measuring or estimating the amount of component that penetrates the epidermis or dermis and passes to systemic circulation from the topical preparations applied to human skin. Franzcell penetration/diffusion studies have become an important research method to investigate the efficacy of topical products (197).

The membranes used in franzcell diffusion tests can be biological (human, mouse, porcine) or synthetic (polymeric, cellulose-based) varieties. With the Franz diffusion cell apparatus, full-skin, dermatomed skin, only epidermis or stratum corneum can be used to test the penetration profiles of the materials into different layers of the skin.

The membranes are placed between the upper and lower chambers of the cell, and the temperature is generally set to 37°C or 32°C (Figure 13). Subsequently, various solutions are prepared and injected into the receptor cell to form a complete skin structure (198).

For hydrophilic components, salt or buffered saline solution may be recommended as the receptor solution, while other suitable solvents such as serum albumin or nonionic surfactants may be used to bind or solubilize the lipophilic components used in the topical formulation (199).

Solutions within the cell must be in continuous contact with the membrane and mixed well with a magnetic stirrer at a suitable rate. The preparations to be tested will be applied on the membrane at a measured, or infinite amounts. The samples from the receptor solution are collected to monitor the diffused amounts at predetermined times, such as at 1, 2, 4, 6, 8, 24 hours. For quantitative tests, the validated method (UV spectrophotometer, HPLC, LC-MS, etc.) is used.

The use of polymeric or synthetic membranes with Franz diffusion cell is a widespread practice, and these membranes are commercially available (Table 10). Synthetic membranes

are made of sheets of polymeric macromolecules that control the penetration of molecules formulated in products to be tested. These membranes may be polysulfone, polycarbonate, polyacrylonitrile, and polypropylene or semi-synthetic cellulose polymers (cellulose acetate, cellulose nitrate, and regenerated cellulose) which may also contain unique materials to provide mechanical support, drainage or adhesion (201).

Several studies have been conducted on the selectivity of semi-synthetic and synthetic membranes. In microfiltration membranes, the term ‘pore size’ is typically used, while for ultrafiltration membranes, the term ‘molecular weight cut-off’ (MWCO) is preferred, which are clear aids in the selection of synthetic membranes in drug diffusion studies. There are four different types of membranes that are used depending on the pore size and the molecular weight of the solute that membrane can reject. Although no absolute criteria are dividing these four membrane types, the following can be considered as a general classification (202).

Table 10. Summary of the synthetic membrane properties. All values are nominally provided by manufacturers (ρ -membrane porosity, τ -membrane tortuosity).

MEMBRANE	POLYMER	MWCO (kDa)	PORE SIZE (μm)	THICKNESS (μm)	ρ (%)	τ
<i>Cellulose-based</i>						
Visking	RC	Ara.14	-	20 ^b	-	-
Cuprophane	RC	10	-	10 ^b	-	-
Benzoylated tubing	RC	1.02.2002	-	35 ^b	-	-
Cellulose ester	CE	0.5	-	80 ^b	-	-
Cellulose nitrate	CN		0.45	125	66-84	-
<i>Polymeric-based</i>						
AN 69	PAN	40	-	25 ^b	-	-
Biodyne	PA	na	0.45	152	50-	-
Supor	PES	na	0.45	145	75	~1-1.5
Tuffryn	PS	na	0.45	145	80	~1-1.5
Nuclepore	PC	na	0.1	10	60	~1
Cyclopore	PC	na	0.1	10	8	~1
Celgard 3500	PP	na	0.05	20	4	-
Silicone	PDMS	na	-	400	35-48	-

RC - Regenerated cellulose, CE - Cellulose esters, CN - Cellulose nitrate, PAN - Polyacrylonitrile, PA – Polyamide (nylon), PES - Polyethersulfone, PS - Polysulfone, PC - Polycarbonate, PP - Polypropylene, PDMS – Polydimethylsiloxane^b. Dry thickness measured using a digital micrometer (Mitutoyo, UK).

Microfiltration, pore size is generally between 0.1 μm and 1 μm (202).

The ultra-membrane pore size is generally from 0.01 μm to 0.1 μm , as measured by the parameters. However, pore sizes are generally expressed as the MWCO measured by filtering carrier molecules of known molecular weights. MWCO ranges from 1,000 Da to 300,000 Da (202).

The nanomembranes, the pore size may range from 1nm to 10nm. MWCO may be in the range of 200 Da to 1,000 Da (203).

Parameters such as flow rate, membrane type, porosity, thickness, the molecular weight of the component to be tested are important for the correct selection of the membrane.

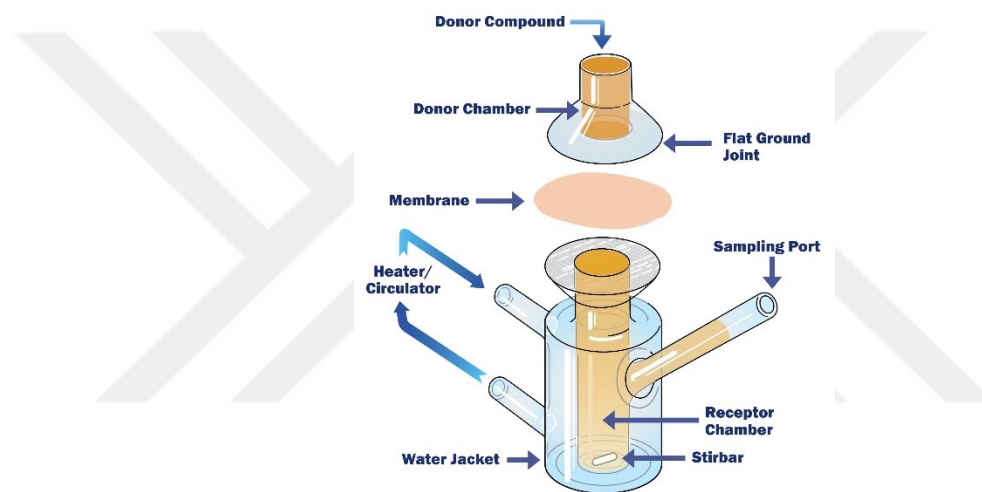


Figure 13. Franz cell diffusion cell (204)

In another study, the flow rates of membranes were examined for 6 hours, and it was found that the flow rate of ibuprofen was lower with polymeric membranes compared to cellulosic membranes. When Cellulose Nitrate was used as a membrane coefficient of variation was over 7%. Cellulose acetate membrane is classified as a low flow flux membrane whereas cellulose nitrate is a high flux cellulose derivative; the ibuprofen drug flow through the cellulose nitrate was very rapid ($17.65 \pm 2.06 \text{ mg/cm}^2/\text{h}$) (197).

The rapid flow of ibuprofen through the membranes was due to the high porosity of the cellulose nitrate membrane (66-84%) as shown in Table 11 and Table 12. Among the low flow cellulose membranes, cellulose acetate produced the highest ibuprofen flow. However, the membrane was found to be incompatible with the receptor fluid. In conclusion, the

authors commented that when studying diffusion, the investigators should always be cautious when selecting a membrane that is compatible with the receiving medium, especially if the test period to be used is too long (197).

Table 11. Properties of cellulose nitrate filter (ρ -membrane porosity, τ -membrane tortuosity) (197)

MEMBRANE	POLYMER	MWCO / (kDa)	SIZE (μm)	THICKNESS(μm)	P (%)	T
Cellulose Nitrate	CN-Cellulose Nitrate	-	0,1 - 0,45	125	66-84	-

The membrane must also be exposed to the chemical solvent for a long time to test compatibility. Franz diffusion cells can be used to examine the diffusion of a single raw material or more active substances in preparations such as semi-solid gels, creams, and ointments (197).

Table 12. Total diffusion flow of cellulose nitrate filter (197)

MEMBRANE	FLUX (mg/cm ² /h)	TOTAL DIFFUSION 6 HOURS AFTER H (mg/cm ²)	CV (%)	THICKNESS (μm)	P (%)	T
Cellulose Nitrate	17,65 \pm 2,06	97,89 \pm 5,79	11,7	125	66-84	-

There are several barriers to the use of human skin in *in-vitro* diffusion studies. Human skin has high variability from piece to piece, and the skin samples are expensive and not easy to obtain. The use of human tissue also poses experimental difficulties, such as poor stability, susceptibility to storage conditions, concerns of biohazards, and disposal costs. Recently, as an alternative to human skin, a synthetic-based membrane (Strat-M[®], Merck, USA) that correlates well with human skin has been developed. Strat-M[®] is constructed of two layers of polyethersulfone (PES, more resistant to diffusion) on top of one layer of polyolefin (more open and diffusive). These polymeric layers create a porous structure with a gradient across the membrane in terms of pore size and diffusivity. The porous structure is impregnated with a proprietary blend of synthetic lipids, imparting additional skin-like properties to the synthetic membrane. In a comparative study with human skin, it was reported that active diffusion correlated very closely with human skin, Also consistent with these observations, both encapsulation of avobenzone and octocrylene significantly reduced diffusion from the synthetic membrane (205).

In many diffusion experiments, the synthetic membranes used are not always dry but are conditioned in the same way. A magnetic bar is put into the receptor section, the membrane is placed on the receptor part of the cell by using clamps. Simulation of the stratum corneum by depositing cellulose or polymeric based synthetic membranes into IPM (isopropyl myristate) and filling the membrane pores of IPM is acceptable and can be applied in control group studies. The circulation of water through the jacket of the cells to maintain the temperature of the cells at a constant temperature and agitators are run to condition the system before the test solutions are filled in the donor site of the franzcell system. The test solution (formulation) is filled into the donor compartment. To prevent the back-penetration of the penetrant molecule, it should be ensured that the concentration in the receptor solution does not exceed 10% of its solubility in this solution.

6. DIFFUSION

Passive passage of molecules through solids, liquids, or gases is called diffusion. Diffusion as a scientific term referring to the 'the net movement of matter, attributed to the random movements of molecules, taking place from a region of high concentration to one of lower concentration' requires more excellent delineation and precision (206).

There are some mechanisms and systems through by release of molecules from drug formulations that can be studied: dissolution, diffusion, osmosis, partitioning, swelling, erosion, and targeting from solid or semi-solid systems. Diffusion is responsible most of the time, from drug molecules to biological systems. Besides, the passage of water vapor, gases, or active substances also is distributed through diffusion (207).

Any active substance needs to diffuse through the biological membranes in order to reach the target site to show its effect. A similar mechanism takes place when the drug is released from a product; in other words, the molecule must diffuse or move from a more concentrated medium to a less concentrated medium (208).

6.1. FICK'S 1st LAW

According to Fick's First Law, the movement of molecules must continue until the difference of the concentrations on both sides of the membrane is "zero" (209). The following equation can express this statement:

$$F = -Dx \left(\frac{dC}{dx} \right)$$

Equation 1. Fick's first law equation 7

The dC/dx concentration gradient is not time-dependent. This means that the concentration difference does not change over time during the transition of diffusion from very dense to less dense at each unit distance (209)

In Fick's 1st law (Equation 1). D is the diffusion coefficient (area/time, cm^2/sec) of the molecule; C is the concentration (quantity/volume, g/cm^3) and x is the distance traveled by the molecule (cm). F is flux; D shows how much area the molecule can pass in or out of the medium in the environment. In the above equation, "-" means that the molecular movement is from the denser region to the less dense region. The concentration decreases as we move away from the dense region, and therefore, the flux value will always be "+" (197).

6.2. FICK'S 2nd LAW

While concentration and time are independent in the Fick's First law, concentration and flux are both dependent on time and distance on Fick's second law. According to this;

$$-\frac{dC}{dt} = D \frac{d^2j}{dx^2}$$

Equation 2. Fick's second law equation

In Equation 2., flux is a function of time and distance. This equation is only one-way. The change in concentration over time is the ratio of the distance traveled to the rate of change of the concentration difference (209).

6.3. STEADY-STATE

In order to interpret the equilibrium state in diffusion, it is necessary to observe the change in the concentration of the molecule diffused from the membrane between the two compartments of the diffusion cells. Until the diffusion reaches a steady-state, there is a lag time. During the lag time, the diffusion from the donor to the receptor phase, the amount of the diffusing material is not the same. This is because of the membrane separating the two sides' movement from the donor side to membrane, then move within the membrane and movement from the membrane to the receiving side is the total process of the diffusion. At each media, the driving forces are due to the concentration gradients between donor and membrane, between each side of the membrane, and membrane and receptor solution. When the concentration gradient within the membrane becomes zero, the diffusion per unit time and the unit area becomes constant. This represents the steady-state diffusion (211).

7. MATERIALS and METHODS

7.1. MATERIALS

7.1.1. CHEMICALS

The list of chemicals used in the thesis is given in Table 13 with their Trade names and their intended use. Disodium Phosphate (Sigma-Aldrich), Mono Potassium Phosphate (Sigma-Aldrich), Sodium chloride (Merck, Germany), Potassium chloride (Merck, Germany) were used for the preparation of Phosphate Buffer solution (PBS). Ethyl alcohol (>99%, Merck), soybean lecithin containing phosphatidylcholine from lecithin genetically modified plants (Lipoid P75, Lipoid GmbH, Germany) was used for the preparation of the ethosomes. According to the certificate of analysis, it contains more than 70% phosphatidylcholine. Two different sources of phosphatidylcholine Phospholipon 85 G (>85%, Phospholipid, USA) and Epicron 170 (Epikuron 170, Cargill, USA) were used to expand the trials during this study. Hydrolyzed collagen (>98%, Kazlicesme, Turkey), trans-resveratrol (> 98.5% Organic herb, China), Retinol (RETINOL 10S>10%, BASF, Germany), vitamin E (BASF, Germany) were used. 2% Polysorbate 20 (Emulgin SML 20, BASF, Germany) was added to PBS in Franzcell cells. Ultra-pure water (Merck, Germany) was used in the analyses. Acetonitrile (Merck, Germany), methyl alcohol (Merck, Germany), ethyl alcohol (Merck,

Germany), isopropyl alcohol (Merck, Germany), phosphoric acid (Merck, Germany) were used in HPLC analyzes. XTT Cell Proliferation kit (Roche Diagnostics, Germany), DMEM (Sigma Aldrich, Germany) were used. Sodium carbonate to Lowry method (Merck, Germany), sodium hydroxide (Merck, Germany), sodium-potassium tartrate (ZAG Chemistry, Turkey), copper sulfate pentahydrate (Merck, Germany), Folin-Ciocalteu's (Sigma Aldrich, Germany), bovine serum albumin (BSA, Thermo Fischer) was used for protein analysis.

Table 13. Chemical materials

Trade Name	INCI Name	Function	Supplier
Disodium Phosphate	Disodium Phosphate	Phosphate Buffer	Sigma-Aldrich, Germany
Mono Potassium Phosphate	Mono Potassium Phosphate	Phosphate Buffer	Sigma-Aldrich, Germany
Sodium chloride	Sodium chloride	Phosphate Buffer	Merck, Germany
Potassium chloride	Potassium chloride	Phosphate Buffer	Merck, Germany
Ethyl alcohol	Ethyl alcohol	preparation of the ethosomes	Merck, Germany
Lipoid P75	phosphatidylcholine	preparation of the ethosomes	Lipoid GmbH, Germany
Phospholipon 85 G	phosphatidylcholine	preparation of the ethosomes	Lipoid GmbH, Germany
Epikuron 170	phosphatidylcholine	preparation of the ethosomes	Cargill, USA
Bovine Collagen	Hydrolyzed collagen	preparation of the ethosomes	Kazlicesme, Turkey
Resveratrol	<i>trans</i> - resveratrol	preparation of the ethosomes	Organic herb, China
RETINOL 10S	Retinol	preparation of the ethosomes	BASF, Germany
Vitamin E	vitamin E	preparation of the ethosomes	BASF, Germany
Emulgin SML 20,	Polysorbate 20	Phosphate Buffer	BASF, Germany
Ultra-pure water	Aqua	preparation of the ethosomes	Merck, Germany
Acetonitrile	Acetonitrile	HPLC analysis	Merck, Germany
isopropyl alcohol	isopropyl alcohol	HPLC analysis	Merck, Germany
phosphoric acid	phosphoric acid	HPLC analysis	Merck, Germany
XTT Cell Proliferation kit	Kit	Cell Culture	Merck, Germany
DMEM	DMEM	Cell Culture	Sigma-Aldrich, Germany
Sodium carbonate	Sodium carbonate	Lowry Analysis	Merck, Germany
Sodium hydroxide	sodium hydroxide	Lowry Analysis	Merck, Germany
Sodium-potassium tartrate	sodium-potassium tartrate	Lowry Analysis	ZAG Chemistry, Turkey
Copper sulfate pentahydrate	copper sulfate pentahydrate	Lowry Analysis	
Folin-Ciocalteu's	Folin	Lowry Analysis	Sigma-Aldrich, Germany
Bovine serum albumin	Albumine	Lowry Analysis	BSA, Thermo Fischer

Other chemicals and reagents used were analytical grades.

7.1.1.1. PBS (PHOSPHATE BUFFERED SOLUTION)

PBS solution was prepared in the laboratory and used as a reagent in many of the experiments. 8g of Sodium Chloride and 200mg of Potassium Chloride are added to 800mL of deionized water. After mixing to dissolve solids for a while, 1.44g of Disodium Phosphate

and 240mg of Mono Potassium Phosphate are added to the solution. The solution is adjusted to the desired pH (typically pH \approx 7.2). Deionized water is added to make a liter solution.

7.1.2. INSTRUMENTS/EQUIPMENT

The devices used in the thesis are listed as follows, given in Table 14.

Table 14. Instruments used in the study

Instruments/Equipment Trade name	Supplier	Function / Why used for
M-115P	Microfluidics	Microfluidizer High-Pressure Homogenizer;
Shimadzu 20A	Shimadzu	High-pressure liquid chromatography device (HPLC);
Mastersizer 2000	Malvern	Particle size analyzer
iD5 ATR Nicolet TM iS5	Thermo	The Fourier Transform Infrared Spectrometer (FTIR);
Litesizer TM 500	Anton-Paar	Zeta potential device
IMark TM Microplate Absorbance Reader	Bio-Rad,	Microplate absorbance reader
*PolarPrep 2000 cryo	Quorum Technologies	cryo-SEM
WTW pH 3110	WTW	pH meter
DMA38	Anton Paar	Density meter
Franzcell transdermal FDC-6	Logan	Franzcell
Strat-M	Merck	Artificial Membrane
12-14kD MWCO	Spectrum	Artificial Membrane

*This was provided by CfAM as an external service

7.1.2.1. MICROFLUIDIZER HIGH-PRESSURE HOMOGENIZER

It has an open, stainless steel chamber with dispersion included, a high-pressure piston pump, a diamond interaction chamber, and a piston of zirconium. The hopper volume is 1 liter. During operation, the pre-dispersion is put in the reservoir and is forced by the high-pressure pump through the interactive reservoir, subjected to very high speeds (typically several hundred meters per second), thereby exposing the dispersion to intense impact and

shear forces. System efficiency is correlated with the pressure difference between the inlet and outlet (212).

7.1.2.2. HIGH-PRESSURE LIQUID CHROMATOGRAPHY DEVICE (HPLC)

Reverse-phase HPLC is the most commonly used form of HPLC. HPLC is highly advanced column chromatography. It can operate under high pressures up to 400bar pressure. Thanks to improvements in solvent-delivery control firmware, solvent-delivery performance in the micro-flow-rate range below 50 μ L/min has been significantly improved. There is a total volume injection type Automatic Sampling Device that provides high-speed injection and multiple sample processing. It has a forced-air circulation-type column furnace. It provides temperature control from 10°C to 85°C of room temperature. It allows the setting of complex temperature programs such as direct or cascade heating and cooling (213).

7.1.2.3. PARTICLE SIZE ANALYZER

Particle size is an essential variable in encapsulation because it has a direct impact on the quality of the finished product. Laser diffraction particle size analysis is based on the fact that particles passing through a laser beam will scatter light at an angle directly related to their sizes. As the particle size decreases, the observed scattering angle increases logarithmically. The scattering intensity depends on both particle size and particle volume. Therefore, large particles scatter light at narrow angles of high intensity, while small particles emit wider angles (214).

The angular scattering intensity data is then analyzed to calculate the size of the particles responsible for creating the scattering pattern and the mean diameter, and the size distribution is determined (215).

7.1.2.4. FRANZCELL

Ex-vivo and *in-vitro* penetration testing, many different product formulations can be performed with manual and semi-automatic Franz diffusion cells. The cells are placed on the device, and water inlet/outlet connections of the jacket are attached to the temperature regulating water bath to keep the receiving solutions at a constant temperature. For water

circulation, 3/4 of the water tank is filled, and the desired temperature is adjusted (Franzcell transdermal FDC-6, Logan, USA).

7.1.2.5. UV-VIS SPECTROPHOTOMETER

Two different types of UV-Vis spectrophotometers were used to determine the amounts of active materials. The first device is a UV-Vis spectrophotometer for single-use quartz cuvettes. The other device is for measuring the UV-Vis spectrophotometer absorbance of tiny amounts of materials without the use of the quartz cuvettes of liposomal suspensions; only a drop of sample is sufficient for the measurement (216).

7.1.2.6. THE FOURIER TRANSFORM INFRARED SPECTROMETER

FT-IR is a technique used to obtain the infrared absorption spectrum or emission of a solid, liquid, or gas by molecular bond characterization. An FT-IR spectrometer simultaneously collects high spectral resolution data over a wide spectral range. Measure the vibration frequencies of various bonds in molecules and give qualitative information about the functional groups in the molecule. IR spectra are rarely used for quantitative analysis. The spectrometer consists of a beam source, detector, cuvette parts (iD5 ATR Nicolet™ iS5, Thermo, USA).

7.1.2.7. ZETA POTENTIAL DEVICE

It is used to characterize nano and microparticles in dispersions and solutions. By measuring the dynamic light scattering (DLS), electrophoretic light scattering (ELS), and static light scattering (SLS), it determines particle size, zeta potential, and molecular mass (Litesizer™ 500, Anton-Paar, Germany).

7.1.2.8. MICROPLATE ABSORBANCE READER

It is an eight-channel, vertical photometer that measures the absorbance of content in the wells of a 96-well microtiter plate. It can perform single or double wavelength measurements and report absorbance values to three decimal places (IMark™ Microplate Absorbance Reader, Bio-Rad, USA).

7.1.2.9. CRYO-SEM of LIPOSOMAL DELIVERY SYSTEMS

Ethosome samples are prepared with a particular device (PolarPrep 2000 cryo, Quorum Technologies, UK), which eliminates the need for conventional preparation methods such as chemical fixation and critical point drying and allows the monitoring of samples in their natural hydrated state. Imaging is performed by scanning electron microscopy (FEI Quanta 600F FEG, Thermo, USA) at -140°C . With Cryo-SEM. Images are analyzed using the scandium image analysis system (Olympus Soft Imaging Systems, Olympus, USA).

7.2. METHODS

7.2.1. FT-IR SPECTRUM ANALYSIS of ACTIVE SUBSTANCES

The spacing absorbance below 1500cm^{-1} is significant for deformation, bending, and ring vibrations. They can be very specific for a substance or different types of substitutions. This range is often referred to as the “fingerprint region un of a spectrum. The theoretical background for spectral analysis and interpretation is provided by various modern textbooks (217). The most commonly applied method of FT-IR spectroscopy is the transmission mode. Aqueous suspensions can be used as well. Attenuated total reflectance (ATR). As an analytical tool, ATR provides another possibility to directly investigate the chemical composition of the smooth surfaces of the various materials (218).

ATR apparatus can be achieved practically without any sample preparation. Concerning biofilm research, this provides a significant advantage for the sample to be searched in a relatively intact condition. Thus, it can be prevented from being removed from the support of a biofilm that significantly changes its structure. Besides, thin films and surface coatings that cannot be accessed by standard chemical methods can be examined. Especially in membrane and polymer research, ATR is a useful analytical tool (219).

FT-IR ATR spectrums are given as a mean of 16 replicates by adding samples at 32cm^{-1} resolution at $4000\text{-}400\text{cm}^{-1}$ wavelength, single reflection crystalline diamond double, and triple bonds show higher oscillations than single bonds (219).

7.2.2. STUDIES on RESVERATROL

Trans-resveratrol was used as it was received. No physicochemical analysis of the material was performed; only quantitative analysis was performed on resveratrol by using the HPLC method. The certificate of analysis of the supplier is provided in appendix B.

7.2.2.1. HPLC ANALYSIS PROCEDURE

Quantitative analysis of *trans*-resveratrol was performed by using HPLC. The HPLC equipment used consists of Shimadzu SIL-20AC Ht HPLC autosampler and pump. Inertsil ODS-3 column (250mm x 4.6mm, 5 μ m) was used for this analysis,

Test Solution: 5 mg of *trans*-resveratrol is weighed into 50 ml of the flask. 40 ml of ethanol was added to it, sonicated in the ultrasonic bath for 10 minutes, the solution is allowed to cool to room temperature, and its volume is completed with ethanol to 50 ml. Filtered through a 0.45 μ m PTFE filter attached to an injector.

Reference Solution 1: 10 mg of *trans*-resveratrol was weighed into 50 ml of the flask. 40 ml of ethanol was added to it, after sonicating in the ultrasonic bath for 10 minutes, it is allowed to cool to room temperature, and its volume is completed with ethanol. Filter through a 0.45 μ m PTFE injector was filtered.

Reference Solution 2: 12 mg of *trans*-resveratrol was weighed into 50 ml of the flask. 40 ml of ethanol was added to it, after sonicating in the ultrasonic bath for 10 minutes, it is allowed to cool to room temperature, and its volume is completed with ethanol. Filter through a 0.45 μ m PTFE injector was filtered.

Disolutions solution: Other concentrations were prepared by diluting from the reference solution 1. These solutions had concentrations of 0.2, 0.1, 0.05, 0.02, 0.01 (mg/ml).

Acetonitrile was used as mobile phase A; 0.2% formic acid was used as mobile phase B. 20 μ l of the sample was injected into the system at a gradient flow rate of 1.5 ml/min and with a column temperature of 40°C. *Trans*-resveratrol absorption was measured at 306 nm wavelength. The software Shimadzu LC post-run Analysis analyzed data.

In order to determine the reliability of the method, validation studies were performed by testing the following parameters according to ICH Q2(R1).

7.2.2.1.1. LINEARITY

The linearity of an analytical procedure is its ability within a given range to obtain test results which are directly proportional to the concentration of an analyte in the sample. For this purpose, the calibration curve of *trans*-resveratrol was prepared, and the correlation coefficient and linearity was determined (220).

7.2.2.1.2. ACCURACY

The accuracy is the proximity of the determined value to the real value. It shows the accuracy of the quantification method and is calculated by recovery, and it is expressed by calculating the percent recovery (%R) of analyte recovered. For this purpose, five solutions were prepared in 3 different concentrations (20, 50, 100µg/ml) from the stock solution of Resveratrol, and curved areas were replaced in the standard equation, and concentrations were calculated. The recovered amounts of the actual (spiked concentrations) concentrations were calculated with the help of the following equation:

$$\% Recovery = \frac{(C Spiked)}{(C Real)} \times 100$$

C Real : Concentration values of an active substance obtained from the calibration equation

C Spiked : 20, 50, 100µg/ml

7.2.2.1.3. PRECISION

The precision of an analytical procedure expresses the closeness of agreement degree of scattering between a series of measurements obtained from multiple sampling of the same homogeneous sample under the prescribed conditions (220). Precision may be considered at three levels: repeatability, intermediate precision, and repeatability.

7.2.2.1.3.1. REPEATABILITY 1

Repeatability expresses the precision under the same operating conditions over a short interval of time. Repeatability is also termed intra-assay precision. A concentration was selected from the stock solution prepared to form the standard correct equation. Under the curve of the three concentration solutions was measured three times in a row. The mean of the concentrations corresponding to the area under curve area values, standard deviation (σ) and variance (V) was calculated.

7.2.2.1.3.2. REPEATABILITY 2

Repeatability expresses the precision between laboratories(collaborative studies, usually applied to the standardization of methodology). For repeatability, the area under curve values of 6 solutions of the same concentration prepared by dilution from the same stock was measured, and the mean concentration, σ (st deviation), and V(variance) of the corresponding concentration values were calculated.

7.2.2.1.4. LIMIT of DETECTION (LOD)

The limit of detection (LOD) is the lowest concentration at which the active substance analyzed can be detected but not necessarily quantitated as an exact value. To estimate the detection limit, a signal-to-noise ratio of between 3 or 2:1 is generally considered acceptable.

7.2.2.1.5. LIMIT of QUANTITATION (LOQ)

The quantitation limit of an individual analytical procedure is the lowest amount of analyte in a sample, which can be quantitatively determined with suitable precision and accuracy (220).

The limit of quantitation (LOQ) is the lowest concentration at which the substance can be determined. A typical signal-to-noise ratio is 10:1.

$$QL = \frac{10\sigma}{S}$$

Equation 3. The quantitation limit (QL)

σ = the standard deviation of the response

S = the slope of the calibration curve

7.2.2.1.6. RANGE

The range of an analytical procedure is the interval between the upper and lower concentration amounts of analyte in the sample, including these concentrations, for which it has been demonstrated that the analytical procedure has a suitable level of precision, accuracy, and linearity.

7.2.2.1.7. ROBUSTNESS

The robustness of an analytical procedure is a measure of its capacity to remain unaffected by small, but deliberate variations in method parameters and indicates its reliability during normal usage (220).

The robustness is to see if the measurements are sensitive to small changes in analytical conditions; the analytical conditions should be appropriately controlled or included in a prudential expression procedure. The conformity parameter system should be established to ensure its validity every time.

7.2.2.1.8. SPECIFICITY

Specificity is the ability to assess the analyte unequivocally in the presence of components which may be expected to be present. Typically these might include impurities, degradants, matrix, etc. Lack of specificity of an individual analytical procedure may be compensated by other supporting analytical procedure(s).

The HPLC method should be able to separate the desired structure from other substances in the formulation or medium to be analyzed. To determine whether the curves of the substances coincide with the curve of the active substance, solutions of other components which do not contain active substance were prepared, and it was determined whether they formed any curve at the point where the active substance curve occurred in the system.

7.2.2.1.9. DETERMINATION OF SOLUBILITY OF RESVERATROL

To calculate the solubility of resveratrol in PBS solution, 1g of the active ingredient in PBS solution containing 30ml of 2% nonionic material was stirred at 150rpm at 25°C for 1 hour on a magnetic stirrer. Three parallel solubility studies were performed. Samples were filtered through a 0.45µm membrane filter, and a 1ml sample was taken. To calculate the solubility in ethyl alcohol solution, 1g of the active ingredient, 30ml ethyl alcohol, was stirred at 150rpm at 25°C for 1 hour on a magnetic stirrer. The solubility test in ethyl alcohol was repeated three times. Samples were filtered through a 0.45µm membrane filter, and 1 ml of sample was taken, and both samples were analyzed by the method of 7.2.2.1

7.2.3. STUDIES on RETINOL

Retinol was used as no physical-chemical analysis was performed; only quantitative analysis was performed of resveratrol quantitative analysis of retinol was performed by using the HPLC method.

7.2.3.1. HPLC ANALYSIS PROCEDURE

Quantitative analysis of retinol was performed by using HPLC. The HPLC equipment used was consists of Shimadzu SIL-20AC Ht HPLC autosampler and pump. Inertsil ODS-3 column (250mm x 4.6mm, 5µm) was used for this analysis,

Reference Solution 1: 15 mg of retinol was weighed into 50 ml of the flask. 40 ml of methanol was added to it, after waiting in the ultrasonic bath for 10 minutes, it is allowed to cool to room temperature, and its volume is completed with methanol. Filter through a 0.45 µm PTFE injector was filtered.

Other Solution: Other concentrations were prepared by dilution from the reference solution 1. These; 0.2, 0.15, 0.12, 0.075, 0.0375, 0.0075 (mg/ml).

The mobile phase, a methanol/water 95:5 (v/v) binary solvent, was used for analysis. 20µl of the sample was injected into the isocratic mobile phase was methanol/water 95:5 (v/v) at a flow-rate of 1.5 mL/min and with a column temperature of 40°C. Retinol absorption was measured at 325nm wavelength. Data were analyzed by the software Shimadzu LC post-run

analysis. In order to determine the reliability of the method, validation studies were performed by testing the following parameters according to ICH Q2(R1).

7.2.3.1.1. LINEARITY

The linearity of an analytical procedure is its ability within a given range to obtain test results which are directly proportional to the concentration amount of analyte in the sample. For this purpose, the calibration curve of retinol has been prepared, and the correlation coefficient and linearity have been determined (220).

7.2.3.1.2. ACCURACY

The accuracy is the proximity of the determined value to the real value. It shows the accuracy of the quantification method and is calculated by recovery, and it is expressed by calculating the percent recovery (%R) of analyte recovered. For this purpose, five solutions were prepared in 3 different concentrations (10, 20, 25 (µg/ml)) from the stock solution of Retinol, and curved areas were replaced in the standard equation, and concentrations were. The recovered values from the calculated concentrations were calculated with the help of the following equation.

$$\% Recovery = \frac{(C Spiked)}{(C Real)} \times 100$$

C Real : Concentration values of active substances obtained from the calibration equation

C Spiked : 10, 20, 25 (µg/ml)

7.2.3.1.3. PRECISION

The precision of an analytical procedure expresses the closeness of agreement degree of scattering between a series of measurements obtained from multiple sampling of the same homogeneous sample under the prescribed conditions (220).

Precision may be considered at three levels: repeatability, intermediate precision, and reproducibility.

7.2.3.1.3.1. REPEATABILITY 1

Repeatability expresses the precision under the same operating conditions over a short interval of time. Repeatability is also termed intra-assay precision. A concentration was selected from the stock solution prepared to form the standard correct equation. Under the curve of the three concentration solutions was measured three times in a row. The mean of the concentrations corresponding to the area under curve area values, standard deviation (σ) and variance (V) was calculated.

7.2.3.1.3.2. REPEATABILITY 2

Repeatability expresses the precision between laboratories collaborative studies, usually applied to the standardization of methodology. For repeatability, the area under curve values of 6 solutions of the same concentration prepared by dilution from the same stock was measured, and the mean concentration, σ (st deviation), and V(variance) of the corresponding concentration values were calculated.

7.2.3.1.4. LIMIT of DETECTION (LOD)

The limit of detection (LOD) is the lowest concentration at which the active substance analyzed can be determined with acceptable accuracy and repeatability. To estimate the detection limit, a signal-to-noise ratio of between 3 or 2:1 is generally considered acceptable.

7.2.3.1.5. LIMIT of QUANTITATION (LOQ)

The quantitation limit of an individual analytical procedure is the lowest amount of analyte in a sample, which can be quantitatively determined with suitable precision and accuracy (220).

The limit of quantitation (LOQ) is the lowest concentration at which the substance can be determined. A typical signal-to-noise ratio is 10:1.

$$QL = \frac{10\sigma}{S}$$

Equation 4. The quantitation limit (QL)

σ = the standard deviation of the response

S = the slope of the calibration curve

7.2.3.1.6. RANGE

The range of an analytical procedure is the interval between the upper and lower concentration amounts of analyte in the sample, including these concentrations, for which it has been demonstrated that the analytical procedure has a suitable level of precision, accuracy, and linearity.

7.2.3.1.7. ROBUSTNESS

The robustness of an analytical procedure is a measure of its capacity to remain unaffected by small but deliberate variations in method parameters and indicates its reliability during normal usage (220).

The robustness is to see if the measurements are sensitive to small changes in analytical conditions; the analytical conditions should be appropriately controlled or included in a prudential expression procedure. The conformity parameter system should be established to ensure its validity every time.

7.2.3.1.8. SPECIFICITY

Specificity is the ability to assess the analyte unequivocally in the presence of components which may be expected to be present. Typically these might include impurities, degradants, matrix, etc. Lack of specificity of an individual analytical procedure may be compensated by other supporting analytical procedure(s).

The HPLC method should be able to separate the desired structure from other substances in the formulation or medium to be analyzed. To determine whether the curves of the substances coincide with the curve of the active substance, solutions of other components which do not contain active substance were prepared, and it was determined whether they formed any curve at the point where the active substance curve occurred in the system.

7.2.3.1.9. DETERMINATION OF SOLUBILITY OF RETINOL

To calculate the solubility in PBS solution, 1g of the active ingredient in 30ml of PBS solution was stirred in a magnetic stirrer for 1 hour at 25°C at 150rpm. Three parallel studies were performed. Samples were filtered through a 0.45µm membrane filter, and a 1ml sample was taken. To calculate the solubility in ethyl alcohol solution, 1g of the active ingredient, 30ml ethyl alcohol, was stirred at 150rpm at 25°C for 1 hour on a magnetic stirrer.

To calculate the solubility in methyl alcohol solution, 1g of the active ingredient, 30ml methyl alcohol, was stirred at 150rpm at 25°C for 1 hour on a magnetic stirrer. The solubility test in ethyl alcohol was repeated three times. Samples were filtered through a 0.45µm membrane filter, and 1 ml of sample was taken, and both samples were analyzed by the method of 7.2.3.171.

7.2.4. STUDIES on HYDROLYZED COLLAGEN

Hydrolyzed collagen was used as no physicochemical analysis was performed; only quantitative analysis was performed of hydrolyzed collagen quantitative analysis of hydrolyzed collagen was performed by using the Lowry method.

7.2.4.1. HYDROLYZED COLLAGEN ANALYSIS

One of the oldest methods to determine the total amount of protein in solutions is the Lowry assay. The exact mechanism of color formation in the Lowry assay remains poorly understood.

The assay is performed in two distinct steps.

- a.** Protein is reacted with alkaline cupric sulfate in the presence of tartrate for 10 minutes at room temperature. During this incubation, a tetradentate copper complex forms from four peptide bonds and one atom of copper. This is the "biuret reaction."
- b.** Second, a phosphomolybdic-phosphotungstic acid solution is added. This compound (called Folin-phenol reagent) becomes reduced, producing an intense blue color.

It is believed that the color enhancement occurs when the tetradentate copper complex transfers electrons to the phosphomolybdic-phosphotungstic acid complex. The blue color continues to intensify during a 30-minute room temperature incubation. It has been suggested that during the 30-minute incubation, a rearrangement of the initial unstable blue

complex leads to the stable final blue colored complex, which has higher absorbance (221, 222).

The final blue color is optimally measured at 750nm, tyrosine, tryptophan, and cysteine amino acids participate in this reaction, and the color intensity is proportional to protein concentration. Color intensity the color gives absorbance at 750nm as a visible area. Lowry's 1951 paper describing this technique is the most cited article in the scientific literature with 300,000 times (221).

Conducting the test,

Solution A is taken up with 2.8598g sodium hydroxide and 14.3030g sodium carbonate and diluted to 500ml.

Solution B, 1.4232g of copper sulfate pentahydrate, is taken and diluted to 100ml. Solution C, 2,85299g sodium-potassium tartrate are taken and diluted to 100ml.

The ratio used when preparing the Lowry solution should be Solution A: Solution B: Solution C=100:1:1. 1N Folin and Ciocalteu's are prepared.

Different concentrations of protein solutions are prepared (20, 40, 60, 80, and 100 µg/ml) as follows: vortex it samples well to mix and transfer 0.5ml to a 10 ml glass tube, and 0.7ml of the Lowry solution is added, mixed, and allowed to stand for 20 minutes in a dark place. 0.1ml of 1N Folin and Ciocalteu's solution is added to the incubated tube, mixed, and left for 30 minutes. The absorbance of each solution is measured at 750nm (221).

7.2.4.2. LINEARITY

The linearity of an analytical procedure is its ability within a given range to obtain test results which are directly proportional to the concentration amount of analyte in the sample. For this purpose, the calibration curve of collagen was prepared, and the correlation coefficient and linearity were determined (220).

7.2.4.3. ACCURACY

The accuracy is the proximity of the determined value to the real value. It shows the accuracy of the quantification method and is calculated by recovery, and it is expressed by calculating

the percent recovery (%R) of analyte recovered. For this purpose, five solutions were prepared at 3 different concentrations (20, 60, 80 (µg/ml)) from the stock solution of hydrolyzed collagen, and curved areas were replaced in the standard equation, and concentrations were calculated. The recovered values from the absorbed concentrations were calculated with the help of the following equation.

$$\% Recovery = \frac{(C Spiked)}{(C Real)} \times 100$$

C Real : Concentration values of active substances obtained from the calibration equation

C Spiked : 20, 60 and 80µg/ml

7.2.4.4. PRECISION

The precision of an analytical procedure expresses the closeness of agreement degree of scattering between a series of measurements obtained from multiple sampling of the same homogeneous sample under the prescribed conditions (220).

Precision may be considered at three levels: repeatability, intermediate precision, and repeatability.

7.2.4.4.1. REPEATABILITY 1

Repeatability expresses the precision under the same operating conditions over a short interval of time. Repeatability is also termed intra-assay precision. A concentration was selected from the stock solution prepared to form the correct standard equation. Under the curve of the three concentration solutions was measured three times in a row. The mean of the concentrations corresponding to those areas under curve area values, standard deviation (σ) and variance (V) was calculated.

7.2.4.4.2. REPEATABILITY 2

Repeatability expresses the precision between laboratories collaborative studies, usually applied to the standardization of methodology. For repeatability, the area under curve values of 6 solutions of the same concentration prepared by dilution from the same stock was

measured, and the mean concentration, σ (st deviation), and V(variance) of the corresponding concentration values were calculated.

7.2.4.5. LIMIT of DETECTION (LOD)

The limit of detection (LOD) is the lowest concentration at which the active substance analyzed can be determined with acceptable accuracy and repeatability. To estimate the detection limit, a signal-to-noise ratio of between 3 or 2:1 is generally considered acceptable.

7.2.4.6. LIMIT of QUANTITATION (LOQ)

The quantitation limit of an individual analytical procedure is the lowest amount of analyte in a sample, which can be quantitatively determined with suitable precision and accuracy (220).

The limit of quantitation (LOQ) is the lowest concentration at which the substance can be determined. A typical signal-to-noise ratio is 10:1.

$$QL = \frac{10\sigma}{S}$$

Equation 5. The quantitation limit (QL)

σ = the standard deviation of the response

S = the slope of the calibration curve

7.2.4.7. RANGE

The range of an analytical procedure is the interval between the upper and lower concentration amounts of analyte in the sample, including these concentrations, for which it has been demonstrated that the analytical procedure has a suitable level of precision, accuracy, and linearity.

7.2.4.8. ROBUSTNESS

The robustness of an analytical procedure is a measure of its capacity to remain unaffected by small but deliberate variations in method parameters and indicates its reliability during normal usage (220).

The robustness is to see if the measurements are sensitive to small changes in analytical conditions; the analytical conditions should be appropriately controlled or included in a prudential expression procedure. The conformity parameter system should be established to ensure its validity every time.

7.2.4.9. SPECIFICITY

Specificity is the ability to assess the analyte unequivocally in the presence of components which may be expected to be present. Typically these might include impurities, degradants, matrix, etc. Lack of specificity of an individual analytical procedure may be compensated by other supporting analytical procedure(s).

Lowry method will analyze the total amount of protein in the formulation or medium to be analyzed for the desired structure. In order to determine whether the curves of the amount of protein coincide with the curve of the active substance, solutions of other components without active substance were prepared, and it was determined whether they formed any curve at the point at which the active substance curve formed.

7.2.4.10. DETERMINATION of the SOLUBILITY of HYDROLYZED COLLAGEN

In order to calculate the solubility in PBS solution, 1g of the active ingredient in 30ml of PBS solution was stirred on a magnetic stirrer for 1 hour at 25°C and 150rpm. Three parallel test studies were performed. Samples were filtered through a 0.45µm membrane filter, and a 1ml sample was taken for quantitative analysis by using the method described in section 7.2.4.1.

7.2.5. PREPARATION of LIPOSOMES and ETHOSOMES

In this study, liposomes were prepared in order to select the appropriate phosphatidylcholine source three differently the sourced phosphatidylcholine available,

which were animal-based (egg yolk, Phospholipon 85G), plant-based (soybean, Epikuron 170), and synthetic (lipoid P75).

In this study, the “cold method” was used in the preparation of liposomes. This method involved mixing all of the materials in the formulations in water with a mechanical stirrer at room temperature. This mixture was used to prepare the final formulation by reducing the size (section 7.2.5.1.)

The prepared liposome formulations contained 10% phosphatidylcholine (w/v), 0.5% vitamin E (w/v) and up to 100% water.

After selecting the phosphatidylcholine (Lipoid P75), for encapsulation studies of the actives, only ethosomes were prepared.

Ethosomes were prepared by using a mechanical stirrer. In this study, both “hot method” and “cold method” were used in the preparation of ethosomes. The prepared ethosomes contained 1.5% active materials, 2-6% phosphatidylcholine (w/v) which was the synthetic material as a result of the liposome studies maintained at the beginning of this section, 10-45% ethanol (w/v), 0.3% vitamin E (w/v) and up to 100% water.

Hot method: The active ingredient was dissolved in a mixture of water, and vitamin E and ethanol were added to the phospholipid dispersion at 40°C by using a mechanical stirrer, the mixing rate used was 300 rpm, and mixing duration was 5 minutes. This mixture was used to prepare the final formulation by reducing the size (section 7.2.5.1.)

Cold method: The active ingredient, ethanol, phospholipid, and vitamin E were mixed in the same beaker and stirred with a mechanical stirrer at 300rpm. Water was slowly added to the system at 30°C and mixed for 5 minutes. This mixture was used to prepare the final formulation by reducing the size (section 7.2.5.1.)

7.2.5.1. REDUCING the SIZES of LIPOSOMES and ETHOSOMES

In order to obtain nano-sized liposomes and ethosomes, the pre-formulations solution was homogenized by using a high-pressure homogenizer with microfluidizer, under a pressure of 500, 750, 1000 bar, and adjusted to 1, 3, 5 and 7 cycles. The temperature was kept at 25°C

during the size reduction processes. Microfluidizer used was a Microfluidics M110-P (Newton, MA, USA), which is used on a commercial design bench (224).

7.2.6. STUDIES CONDUCTED on LIPOSOMES and ETHOSOMES

7.2.6.1. DETERMINATION of ETHOSOMES ENCAPSULATION EFFICIENCY

Encapsulation efficiency (EE) of the ethosomal vesicular systems was determined by the ultracentrifugation method. In order to determine the encapsulation efficiency, a 0.5ml ethosome solution was diluted with distilled water, and it was centrifuged with Allegra X-30R centrifuge (Beckman Coulter, USA) for 45 min at a speed of 16.000g. Samples from the supernatant were analyzed by the appropriate method of the active ingredient *trans*-resveratrol, retinol, and hydrolyzed collagen. When T is the total amount of active ingredient, C is only the amount of activity detected in the supernatant, retention capacity of the ethosome is calculated as (Equation 5):

$$\% RE = \frac{T - C}{T} \times 100$$

Equation 6. Encapsulation efficiency

7.2.6.2. PARTICLE SIZE ANALYSIS

The particle size and uniformity of empty and loaded ethosomes and empty liposomes vesicular systems were determined by the DLS technique using a computerized Mastersizer 2000 (Mastersizer 2000, Malvern, USA) and a computerized nanosizer (Litesizer TM500, Anton Paar, Germany). The measurements were made 25±2°C, and the scattering angle was 90°. The mean values were determined by calculating the average of the readings of 5 repeated measurements.

7.2.6.3. UV-VIS SPECTROPHOTOMETER ANALYSIS

In this study, a UV spectrophotometer (Thermo ScientificTM GENESYSTM 10S) was used to read the UV absorbance of micro-materials with quartz cuvettes of hydrolyzed collagen ethosomes. 2mL of the sample was put into the quartz cuvettes, and the absorbance equipped

with a 10 mm optical path quartz cell, and the spectral resolution was measured. All measurements were repeated five times, and averages were calculated in 750nm.

7.2.6.4. ZETA POTENTIAL ANALYSIS of ETHOSOMES

Zeta potential (ζ) measurements were performed by using Litesizer 500 (Litesizer™ 500, Anton-Paar, Germany). The particle size distribution of both empty and loaded ethosomes was determined at $25\pm 2^\circ\text{C}$. The formulations were tested by diluting the dispersions at 1:20 dilution factor with deionized water in 100 omega-type zeta cuvettes.

7.2.6.5. IMAGING of ETHOSOMES BY SCANNING ELECTRON MICROSCOPE

The samples were prepared with a Quorum Technologies PolarPrep 2000 cryo preparation system. Frozen in a nitrogen slush at -210°C , then fractured at -180°C sublimed at -90°C for 5-25 min. (as indicated by experimentation) to achieve optimum surface relief and then Coated with Platinum.

Imaging was done with an FEI Quanta 600F FEG Scanning Electron Microscope at a temperature of -140°C . It is possible with cryo-SEM that sample shape has been affected by the growth of ice crystals during the preparation process. Analysis of the images was performed using the Scandium Image Analysis System from Olympus Soft Imaging Systems. The spatial calibration of the images is taken directly from the calibration data of the microscope.

7.2.6.6. PH MEASUREMENT

pH measurements of ethosomes were made using a tabletop pH meter (WTW pH 3110, WTW, Germany). All measurements were repeated five times, and average values and the standard deviation were calculated.

7.2.6.7. CONDUCTIVITY MEASUREMENT

Conductivity measurements of ethosomes were made a tabletop conductivity meter (WTW pH 3110, WTW, Germany). All measurements were repeated five times, and average values and the standard deviation were calculated.

7.2.6.8. DENSITY MEASUREMENT

Density measurements of ethosomes were made by using tabletop density meter (DMA38, Anton Paar, USA). All measurements were repeated five times, and average values and the standard deviation were calculated.

7.2.6.9. CONDUCTING STABILITY STUDIES

In order to select the correct lipid and to determine the suitable formulations, the stability of empty liposomes were tested for only 14 days. After the selection of the appropriate formulations, the stability of the vesicles was determined by keeping them at room temperature ($25\pm 2^{\circ}\text{C}$) for 180 days. The samples were subjected to tests like particle size/particle size distribution, uniformity, and zeta potential, as instructed in the user guidelines of the specific instruments used. Besides these, physical properties such as color and appearance were also examined at the end of 1, 7, 30 days, and six months.

7.2.6.10. CYTOTOXICITY ANALYSIS

Cytotoxicity analysis was performed with XTT Cell Proliferation Assay using the recommended method ISO 10993-5. Cytotoxicity analysis consists of cell cultivation, adding different concentrations of ethosomes and active materials (Resveratrol, Retinol, Hydrolyzed collagen), incubating with this mixture, and adding a yellow XTT solution at the end of incubation. Cytotoxicity analysis by XTT is based on the principle of converting the yellow tetrazolium salt into orange formazan crystals by metabolically active cells. Formazan crystals are water-soluble and can be read spectrophotometrically at a certain wavelength density. The amount of dye absorbance is proportional to the number of metabolically active cells.

Based on this principle, cytotoxicity analysis was performed with keratinocyte cells (HaCaT cell line). Cells were removed from the surface of the petri dish according to the passaging protocol. Cells were counted with a hemocytometer under an inverted microscope. Cells were seeded into 96-well plates with 10,000 cells in each well and incubated for 24 hours at 37°C , 5% CO_2 than the next day the medium was removed.

Test Sample: Ethosomes and active materials (Resveratrol, Retinol, Hydrolyzed collagen) were diluted with the medium (DMEM). (S1: 25%; S2: 10%; S3: 1% and S4: 0.1%).

Positive control: Sodium lauryl sulfate (SLS) was used as a positive control (PC 1: 0.1% and PC 2: 0.01%)

Blank control: DMEM medium was used as a negative control.

The samples prepared from the 16 blank samples, 4 test samples, 4 positive control, 8 negative control wells were added and 37 ° C, incubated in 5% CO₂ for 24 hours. The samples prepared the 16-blank sample, 4 test sample, 4 positive control, 8 negative control wells were added and incubated at 37°C, 5% CO₂ for 24 hours. At the end of the 24-hour incubation, XTT solution and activator were added to the final concentration to make up a concentration of 0.3mg/mL and incubated for 4 hours at 37°C, under 5% CO₂. Then, the absorbance of the cells at 450 nm was measured using a Microplate reader (Biorad-iMark), and based on this, the proportion of viable cells at different concentrations is determined. All of the cytotoxicity analysis was conducted in two replicates. Cells were seeded in four separate wells for each concentration. The reliability of the test was increased with both biological and technical replicates by doing three readings per well. The mean values of all readings were taken, and the ratio of live cells at different extract concentrations to the non-extracted cells was plotted, and the results of the analysis were plotted. The cell viability was calculated by using the formula below:

$$\text{Cell viability (\%)} = [\text{Mean A of test group} / \text{Mean A of control group}] \times 100$$

A: Absorbance

7.2.6.11. FRANZCELL *in-vitro* DIFFUSION TESTS

In-vitro diffusion test of resveratrol, retinol, hydrolyzed collagen, which were entrapped in ethosomes, was conducted by using a semi-automatic Franz diffusion cell working device (Franzcell transdermal FDC-6, Logan, USA). The volume of the receptor part of the cell was 1 ml, and the receptor solution was continuously stirred with a magnetic stirring bar. The temperature of the cells kept constant with a recirculating water bath at 37±1°C. The barrier used between donor and receptor cells was either a synthetic membrane, either cellulose acetate or Strat-M[®]. 1 ml of ethosomes solution of the active ingredient (resveratrol, retinol,

hydrolyzed collagen) as well as the was used as the donor phase. 1ml samples were taken from the receptor solution was withdrawn after 1, 2, 4, 8, 12, 24, 48 hours and this sample was taken each time point was analyzed to determine the concentration of the active ingredient in the receptor solution, as given in the relevant methods (7.2.2.1, 7.2.3.1, 7.2.4.1). In this study, membrane samples were immersed in distilled water for 2 hours before use. 2% Nonionic surfactant in phosphate buffer was used as a receptor solution for resveratrol and hydrolyzed collagen diffusion experiments. Ethyl alcohol was used solution to enable diffusion retinol due to its extremely low solubility in PBS.

In order to prevent the back-penetration of the penetrant molecule, it should be ensured that the concentration in the receptor solution does not exceed 10% of the solubility of the penetrant (active materials) tested. In the diffusion study control experiment, 1.5% solutions of the same actives were prepared and worked in parallel. Prepared hydrolyzed collagen and resveratrol at PBS, retinol at ethyl alcohol.

7.2.7. STATICAL ANALYSIS

All the experiments in the thesis were conducted at least three replicates and average, and \pm S.S. (Standard Deviation) values were calculated. Statistical analysis of the results was performed by using one-way ANOVA (Variance Analysis) and Turkey's multiple comparison test. If the P (probability) value between the two groups was less than $P < 0.05$, the difference was regarded as statistically significant

8. RESULTS

8.1. RESULTS of LIPOSOME FORMULATION STUDIES

Twenty-seven liposome formulations were prepared by using different lipids and different compositions with the cold method preparation method, as given in section 7.2.5. The percent composition of the formulations is shown in Table 15.

Table 15. Formulations of liposomes obtained with different sources of lecithin

Brand	CODE	Deionized Water (%)	Lecithin (%)	Vitamin E (%l)	Pressure	Cycle
Lipoid P75	F1	89,5	10	0,5	500	1
	F2	89,5	10	0,5	500	3
	F3	89,5	10	0,5	500	5
	F4	89,5	10	0,5	750	1
	F5	89,5	10	0,5	750	3
	F6	89,5	10	0,5	750	5
	F7	89,5	10	0,5	1000	1
	F8	89,5	10	0,5	1000	3
	F9	89,5	10	0,5	1000	5
Epikron 170	F10	89,5	10	0,5	500	1
	F11	89,5	10	0,5	500	3
	F12	89,5	10	0,5	500	5
	F13	89,5	10	0,5	750	1
	F14	89,5	10	0,5	750	3
	F15	89,5	10	0,5	750	5
	F16	89,5	10	0,5	1000	1
	F17	89,5	10	0,5	1000	3
	F18	89,5	10	0,5	1000	5
Phospholipon 85 G	F19	89,5	10	0,5	500	1
	F20	89,5	10	0,5	500	3
	F21	89,5	10	0,5	500	5
	F22	89,5	10	0,5	750	1
	F23	89,5	10	0,5	750	3
	F24	89,5	10	0,5	750	5
	F25	89,5	10	0,5	1000	1
	F26	89,5	10	0,5	1000	3
	F27	89,5	10	0,5	1000	5

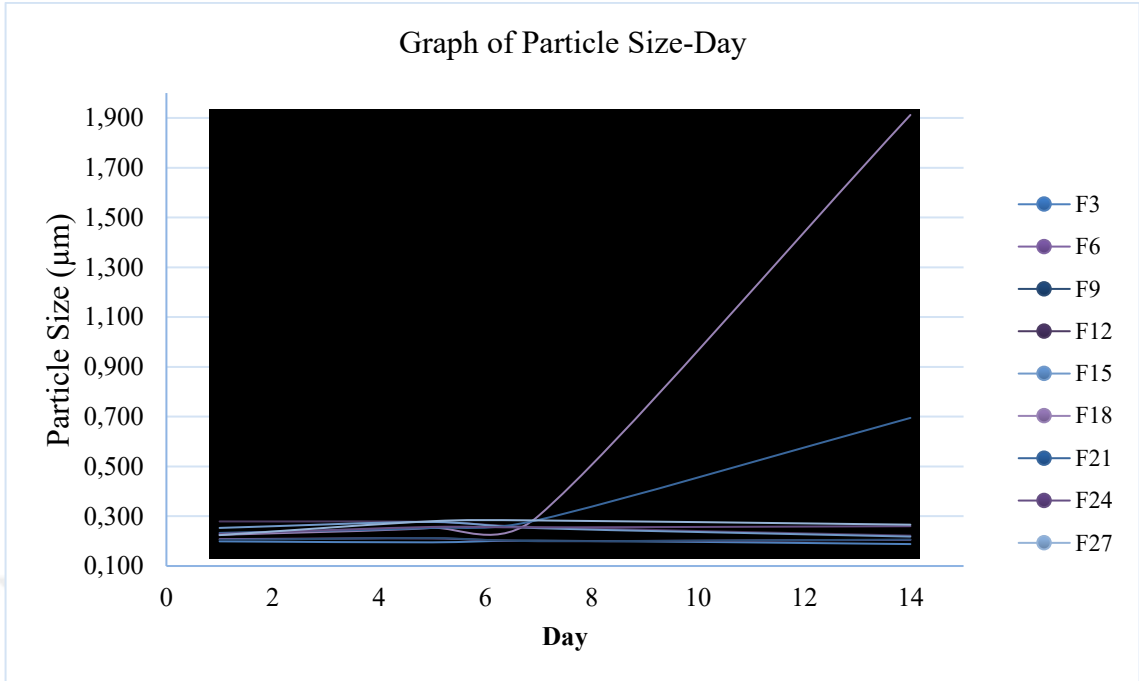
The stability of the empty liposome formulations were monitored for 14 days, as given in section 7.2.6.9. According to these initial results, it was concluded that Lipoid P75 produced the most stable liposomes compared to the other two raw materials. Therefore, it was decided to continue the study by using Lipoid P75.

Stability studies of liposome formulations were performed, as given in section 7.2.6.9. The time-dependence of particle size and uniformity changes of the formulations which were kept at $25\pm 2^{\circ}\text{C}$ are given in Table 16. Table 16 annotation (the stability was not recorded) means that these formulations were not tested on days 1, 5, 7, 14, because they either showed immediate phase separation or liposomes were not formed properly during the production.

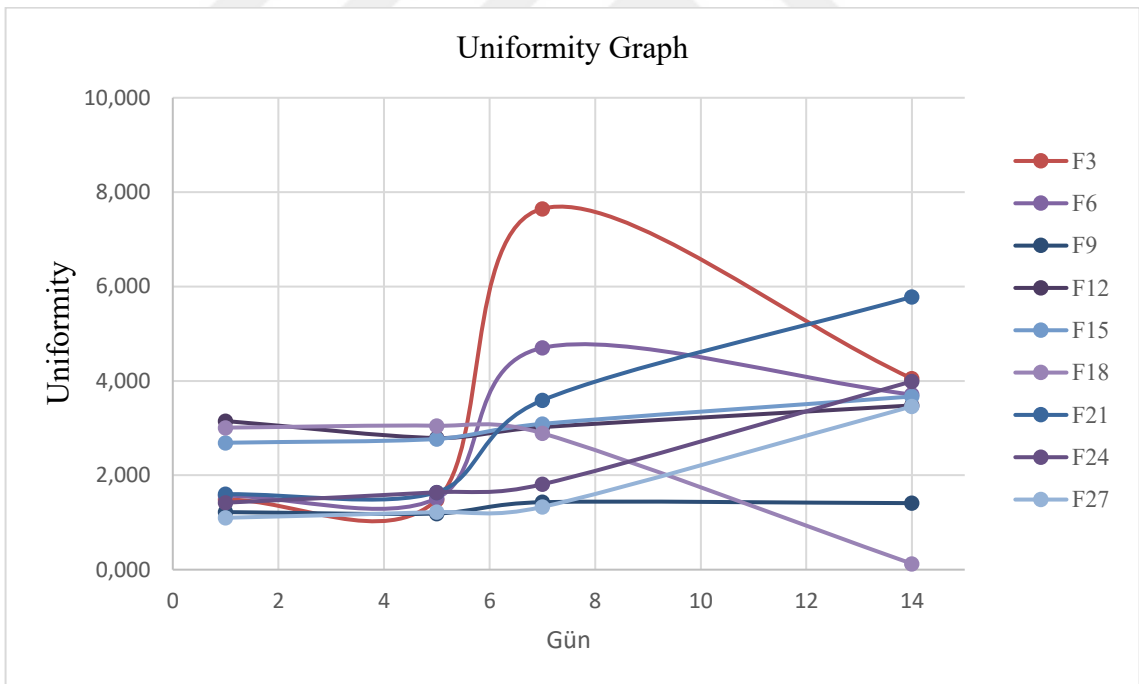
Table 16. Particle Size and Uniformity Analysis of Empty liposomes

	1 day	5 day	7 day	14 day		1 day	5 day	7 day	14 day
CODE	d (0.5) (µm)				CODE	Uniformity			
F1	The stability was not recorded.				F1	The stability was not recorded.			
F2	The stability was not recorded.				F2	The stability was not recorded.			
F3	0,199	0,195	0,202	0,188	F3	1,490	1,480	7,650	4,050
F4	The stability was not recorded.				F4	The stability was not recorded.			
F5	The stability was not recorded.				F5	The stability was not recorded.			
F6	0,208	0,211	0,200	0,205	F6	1,570	1,510	14,700	3,710
F7	The stability was not recorded.				F7	The stability was not recorded.			
F8	The stability was not recorded.				F8	The stability was not recorded.			
F9	0,205	0,212	0,200	0,206	F9	1,220	1,190	1,430	1,410
F10	The stability was not recorded.				F10	The stability was not recorded.			
F11	The stability was not recorded.				F11	The stability was not recorded.			
F12	0,279	0,277	0,256	0,222	F12	3,150	2,790	3,020	3,480
F13	The stability was not recorded.				F13	The stability was not recorded.			
F14	The stability was not recorded.				F14	The stability was not recorded.			
F15	0,253	0,277	0,252	0,218	F15	2,690	2,770	3,090	3,670
F16	The stability was not recorded.				F16	The stability was not recorded.			
F17	The stability was not recorded.				F17	The stability was not recorded.			
F18	0,225	0,253	0,301	1,912	F18	3,010	3,050	2,890	0,126
F19	The stability was not recorded.				F19	The stability was not recorded.			
F20	The stability was not recorded.				F20	The stability was not recorded.			
F21	0,233	0,253	0,285	0,695	F21	1,600	1,640	3,590	5,780
F22	The stability was not recorded.				F22	The stability was not recorded.			
F23	The stability was not recorded.				F23	The stability was not recorded.			
F24	0,229	0,257	0,255	0,260	F24	1,420	1,640	1,810	3,990
F25	The stability was not recorded.				F25	The stability was not recorded.			
F26	The stability was not recorded.				F26	The stability was not recorded.			
F27	0,224	0,280	0,283	0,266	F27	1,100	1,220	1,330	3,460

As can be seen in Table 16, a considerable amount of particle size growth was observed in the formulations of F18 and F21. The summary of the particle size measurements is given in Graph 1. Similarly, the stability of loaded liposome formulations was examined for 14 days. The shape uniformity versus time results of the liposome formulations is shown in Graph 3. The shape uniformity versus time of formulations coded as F3, F6, F12, F15, F18, F21, F24, F27 was found to be unsuitable. Formulation F9 was the best formulation according to the particle size versus time experiments.



Graph 1. Day-Particle Size Graph of liposomes



Graph 2. Uniformity graph of liposomes

In the analyses, the stability of ethosome formulations was best in L13, L14, and L15 formulation. Ethosomes studies were continued with this formulation method.

Table 17. Ethosome formulations with suitable Lipoid P75

CODE	Deionized Water (%)	Lecithin (%) (Lipoid P75)	Vitamin E (%)	Ethanol (%)	Pressure	Cycle
L1	89,5	10	0,5		500	1
L2	89,5	10	0,5		500	3
L3	89,5	10	0,5		500	5
L4	89,5	10	0,5		750	1
L5	89,5	10	0,5		750	3
L6	89,5	10	0,5		750	5
L7	89,5	10	0,5		1000	1
L8	89,5	10	0,5		1000	3
L9	89,5	10	0,5		1000	5
L10	59,5	10	0,5	30	1000	1
L11	59,5	10	0,5	30	1000	3
L12	59,5	10	0,5	30	1000	5
L13	64,7	5	0,3	30	1000	1
L14	64,7	5	0,3	30	1000	3
L15	64,7	5	0,3	30	1000	5

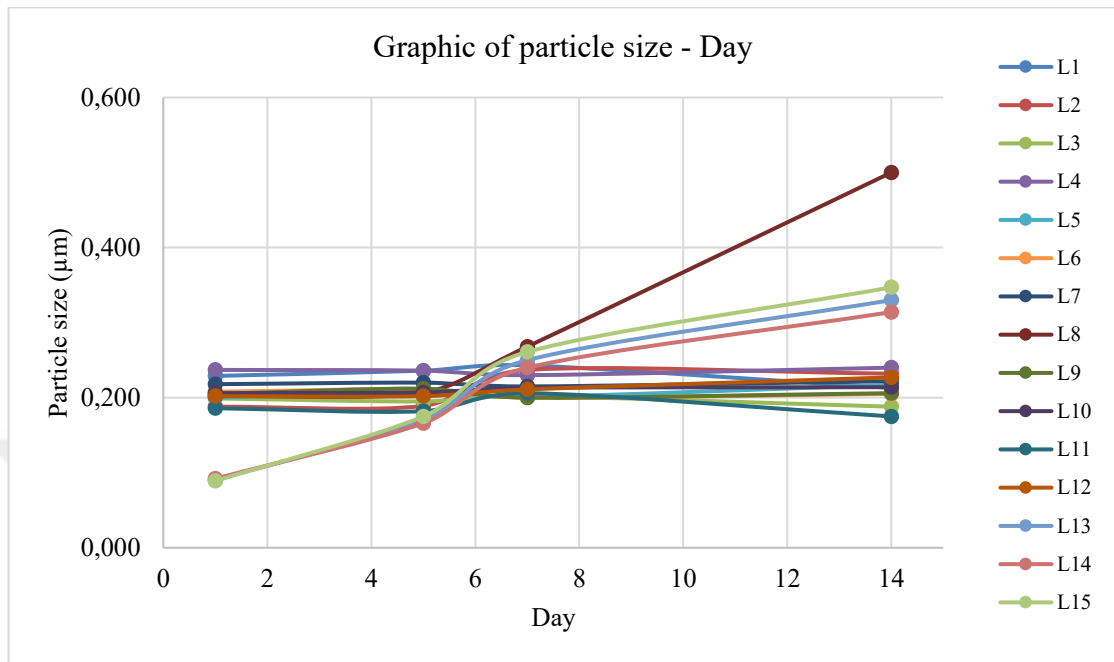
The particle size and uniformity of the particles starting with L were examined. The results are shown in Table 18 as empty formulations made with Lipoid P75.

Table 18. Particle Size and Uniformity Analysis for Empty liposome formulations and ethosomes with lipoid P75

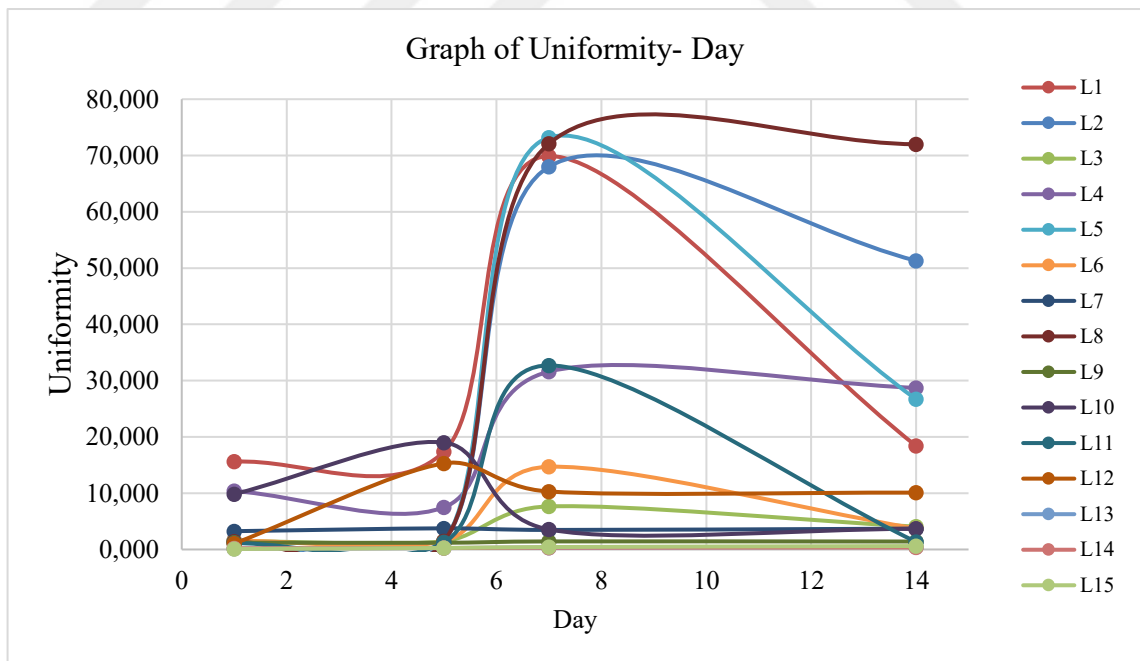
CODE	Pressure / BAR	Day cycle	1	5	7	14	1	5	7	14
			d (0.5) (nm)				Uniformty			
L1	500	1	0,229	0,236	0,243	0,213	15,6	17,4	69,9	18,4
L2	500	3	0,188	0,189	0,237	0,232	1,64	1,54	68	51,3
L3	500	5	0,199	0,195	0,202	0,188	1,49	1,48	7,65	4,05
L4	750	1	0,237	0,236	0,23	0,24	10,4	7,5	31,6	28,7
L5	750	3	0,2	0,207	0,201	0,217	1,59	1,48	73,2	26,7
L6	750	5	0,208	0,211	0,2	0,205	1,57	1,51	14,7	3,71
L7	1000	1	0,218	0,22	0,215	0,222	3,25	3,76	3,47	3,7
L8	1000	3	0,202	0,207	0,268	0,5	1,4	1,47	72,1	72
L9	1000	5	0,205	0,212	0,2	0,206	1,22	1,19	1,43	1,41
L10	1000	1	0,206	0,207	0,213	0,214	9,84	19	3,56	3,68
L11	1000	3	0,186	0,182	0,206	0,175	1,13	1,28	32,7	1,35
L12	1000	5	0,202	0,202	0,211	0,227	1,05	15,3	10,3	10,1
L13	1000	1	0,090	0,170	0,250	0,330	0,155	0,250	0,345	0,440
L14	1000	3	0,092	0,166	0,240	0,314	0,207	0,259	0,311	0,363
L15	1000	5	0,089	0,175	0,261	0,347	0,096	0,266	0,436	0,605

The results of particle size and size uniformity of the samples coded with L, which are empty liposomes made with Lipoid P75, are shown in Table 18, as it is seen from the results, the

uniformity of the ethosomes was better when pressure applied during production was 1000 bars. At lower pressures, uniformity values were unacceptable.



Graph 3. Particle size graph of formulations made with Lipoid P75



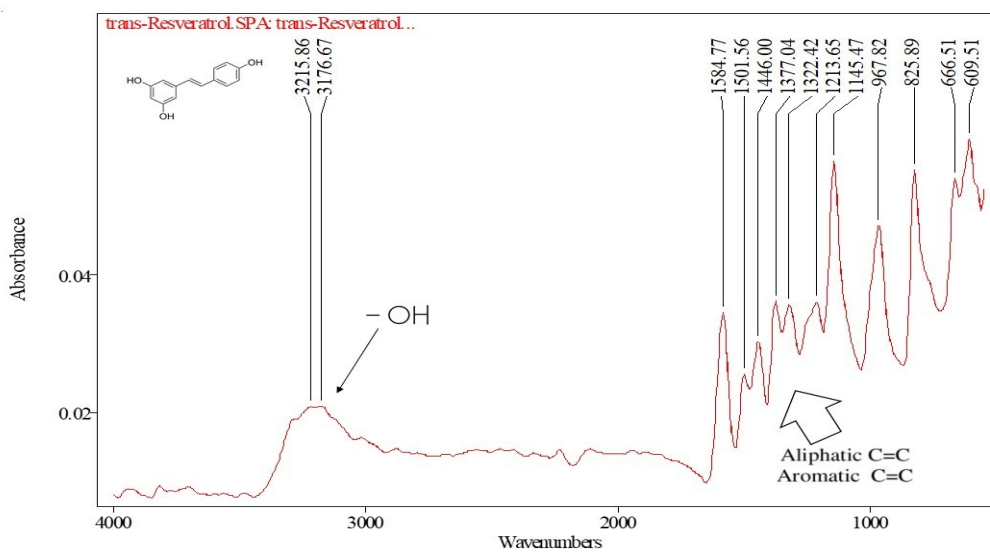
Graph 4. Uniformity graph of formulations made with lipoid P75

8.2. RESULTS of the RESVERATROL

8.2.1. RESULTS of ANALYTICAL VALIDATION of RESVERATROL ASSAY

8.2.1.1. FT-IR SPECTRUM

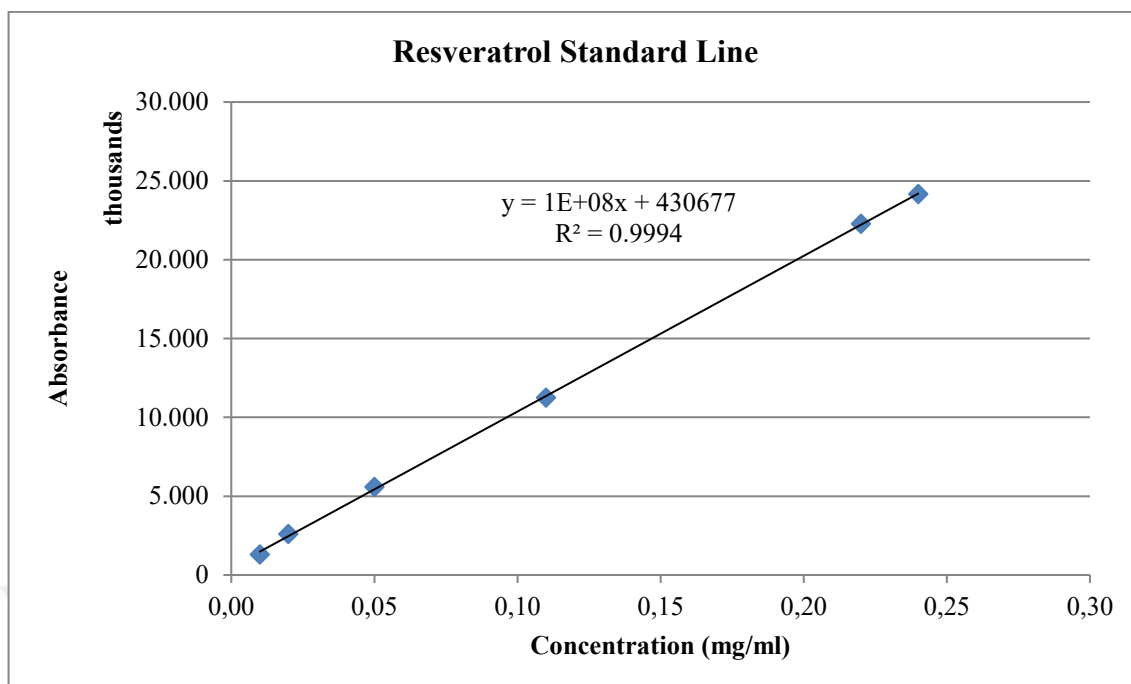
FT-IR results of resveratrol were presented in Graph 5.



Graph 5. IR spectrum of resveratrol

8.2.1.2. LINEARITY

Trans-resveratrol solutions were prepared in ethyl alcohol at six different concentrations by applying the test method given in 7.2.2.1. It was shown that within the range of concentration used, the calibration curve produced a linear regression equation of $y = 1E+08x + 430677$ and a squared correlation coefficient of $R^2 = 0.9994$. The calibration curve of Trans-resveratrol is presented in Graph 6. The linear regression equation, squared correlation coefficient (R^2), is shown in Graph 6. The limit of detection (LOD), and the limit of quantification (LOQ), is reported in section 8.2.1.5 and 8.2.1.6, respectively.



Graph 6. The standard line of *trans-resveratrol* obtained by HPLC method

8.2.1.3. ACCURACY

Samples of *trans-resveratrol* were prepared in ethyl alcohol at concentrations of 21, 50, and 100 $\mu\text{g/ml}$ were measured five times by HPLC at the wavelength of 306nm. The corresponding concentration values ($\mu\text{g/ml}$) were calculated with the help of standard linear formula.

Table 19. Accuracy of *trans-resveratrol* in ethyl alcohol

Sample	1st concentration		2nd concentration		3rd concentration	
	21 $\mu\text{g/ml}$		50 $\mu\text{g/ml}$		100 $\mu\text{g/ml}$	
	Account value	% recovery	Account value	% recovery	Account value	% recovery
1	21,54	102,59	51,61	103,22	104,25	104,25
2	21,60	102,85	51,64	103,28	104,23	104,23
3	21,60	102,84	51,66	103,33	104,24	104,24
4	21,60	102,85	51,53	103,07	104,11	104,11
5	21,61	102,89	51,58	103,15	104,27	104,27
Average	102,80		103,21		104,22	
Reliability level	0,01		0,05		0,05	
Standard deviation	0,12		0,10		0,06	
Coefficient of Variation	0,001		0,001		0,001	
n (sample size)	5		5		5	
Confidence interval	0,11		0,09		0,05	

The calculated concentrations and % recoveries are shown in table 19. The mean recovery amounts calculated were within the range 102,59–104,25 %, which are within the 90–110% range that is considered acceptable. The standard calibration curve of *trans*-resveratrol is shown in Graph 6. The general acceptance criteria for linearity is a correlation coefficient of 0,998 or higher. Therefore, the calibration curve of *trans*-resveratrol was shown to be linear with the squared correlation coefficient (R^2) of 0.9994 and showed good linearity in the tested range.

8.2.1.4. PRECISION

8.2.1.4.1. REPEATABILITY 1

Samples of *trans*-resveratrol prepared at 10, 20, 110 μ g/ml concentrations in ethyl alcohol were measured three times consecutively by HPLC at 306 nm. The area under curve, mean, and standard deviation values and coefficients of variation are given in Table 20. As the coefficients of variation were less than 2%, it was concluded that the method used is repeatable.

Table 20. *Trans*-resveratrol repeatability test results in ethyl alcohol

Sample	1st concentration	2nd concentration	3rd concentration
	10 μ g/ml	20 μ g/ml	110 μ g/ml
	Area	Area	Area
1	1.305.456	2.589.521	10.854.041
2	1.304.629	2.587.271	11.196.350
3	1.309.664	2.590.834	11.248.291
Average	1.306.583	2.589.209	11.099.561
Reliability level	0,05	0,05	0,05
Standard deviation	2.700	1.802	214.206
Coefficient of Variation	0,002	0,001	0,019
n (sample size)	3	3	3
Confidence interval	3.055	2.039	242.393

8.2.1.4.2. REPEATABILITY 2

As described in method 7.2.2.1, the area under the curve of six resveratrol samples that were prepared at a concentration of 220 μ g/ml from the same stock solution was measured with HPLC at 306 nm wavelength. The results are given in Table 21 the variation coefficient value is less than 2%, indicating that the method is reproducible.

Table 21. *Trans-resveratrol* repeatability test results in ethyl alcohol

Sample	Concentration
	220 µg/ml
	Area
1	22.308.380
2	22.295.155
3	22.071.170
4	22.013.907
5	21.991.941
6	21.787.250
Average	22.224.902
Reliability level	0,05
Standard deviation	133.300
Coefficient of Variation	0,0060
n (sample size)	6
Confidence interval	106.660

8.2.1.5. LIMIT of DETECTION (LOD)

According to the results, the lowest concentration at which *trans-resveratrol* can be determined with acceptable accuracy and repeatability was calculated as 4,8µg/ml.

8.2.1.6. LIMIT of QUANTITATION (LOQ)

According to the results, the lowest concentration at which *trans-resveratrol* can be detected with acceptable accuracy and repeatability was calculated as 14,5µg/ml.

8.2.1.7. ROBUSTNESS

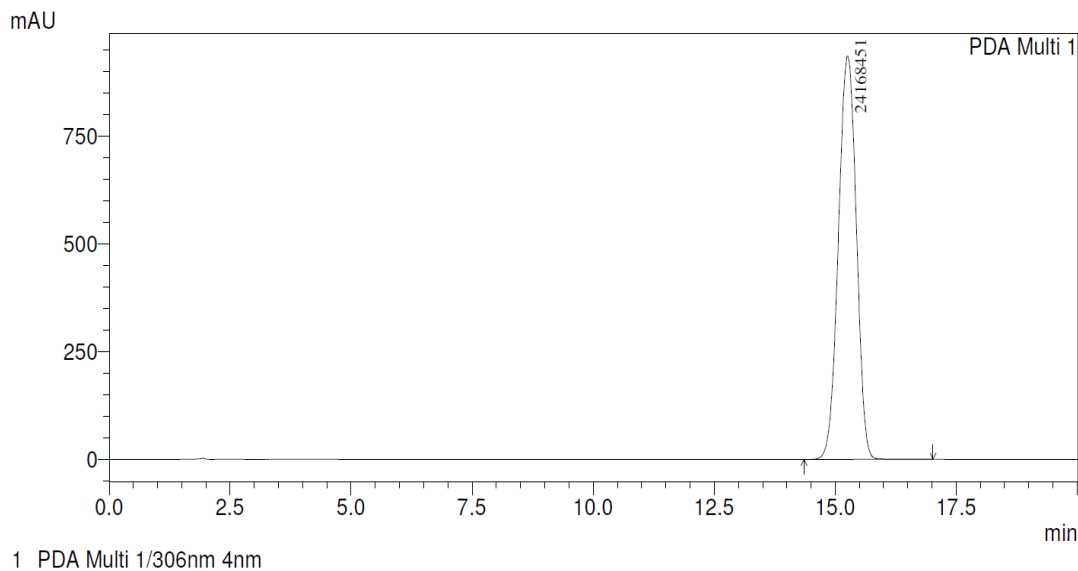
In order to determine the stability of *trans-resveratrol* in the dissolution media, the sample of 200 µg/ml resveratrol was subjected measured two times within 24 hours by HPLC. No significant change was observed in the area under curve values, as given in Table 22.

Table 22. *Trans-resveratrol* stability test results in ethyl alcohol

Concentration	1 st measurement	2 nd measurement	% Difference
200 µg/ml	21.787.250	21.968.899	0,83

8.2.1.8. SPECIFICITY

HPLC absorbance of *trans*-resveratrol free ethosome formulation was measured as a blank reading. This method was found to be specific for the analysis of *trans*-resveratrol since there was no other peaks on the *trans*-resveratrol curve coincided with the peaks of the other substances. In other words, resveratrol peak was specific as shown in Graph 7.



Graph 7. *Trans*-resveratrol peak in HPLC

8.2.1.9. SOLUBILITY

The solubility of *Trans*-resveratrol in ethyl alcohol is about 65mg/ml. The solubility in PBS (phosphate-buffered saline) prepared at pH 7.2 is about 100µg/ml. The solubility in 2% nonionic surfactant (Polysorbate 20) PBS is 500µg/ml.

8.2.2. FORMULATIONS of RESVERATROL ETHOSOMES

Table 23. Empty and loaded ethosomes formulations

	CODE	Deionized Water (%)	Lecithin (%) (Lipoid P75)	Vitamin E (%)	Ethanol (%)	(%) Active Substance	Cycle
<i>Trans</i> resveratrol	T13	63,2	5	0,3	30	1,5	1
	T14	63,2	5	0,3	30	1,5	3
	T15	63,2	5	0,3	30	1,5	5
	T16	63,2	5	0,3	30	1,5	7
Blank	T21	64,7	5	0,3	30	-	1
	T22	64,7	5	0,3	30	-	3
	T23	64,7	5	0,3	30	-	5
	T24	64,7	5	0,3	30	-	7

Particle size and uniformity of resveratrol loaded ethosomes were determined as given in section 7.2.7.9. The resveratrol loaded ethosomal formulation were coded as T, and their compositions are given in Table 23.

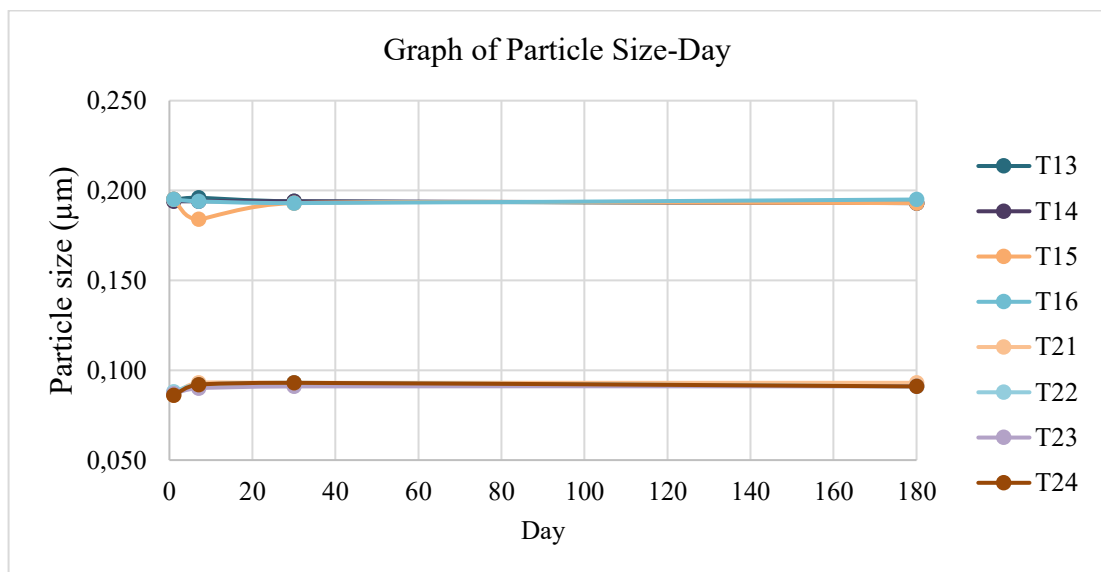
8.2.2.1. PARTICLE SIZE and STABILITY of ETHOSOMES FORMULATIONS

The changes seen in the particle size and shape uniformity of Trans-resveratrol ethosomes with time are given in Graph 8, Graph 9. All of these formulations showed acceptable stability; in other words, the size of the ethosomes did not change significantly at the time points tested. The results are summarized in Table 24.

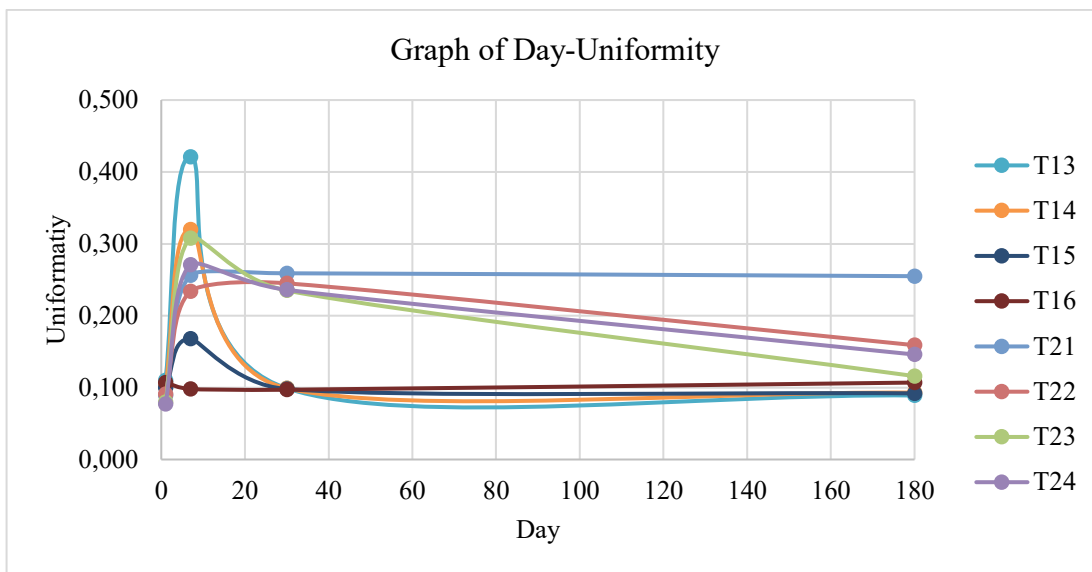
Table 24. Particle size and uniformity of ethosome formulations

	CODE	T*	d (0.5) (μm)				Uniformity				t
			1	7	30	180	1	7	30	180	
Trans resveratrol	T13	1	0,195	0,196	0,194	0,193	0,110	0,421	0,099	0,089	25 °C
	T14	3	0,194	0,194	0,194	0,193	0,102	0,320	0,099	0,093	25 °C
	T15	5	0,195	0,184	0,193	0,193	0,100	0,168	0,098	0,092	25 °C
	T16	7	0,195	0,194	0,193	0,195	0,107	0,098	0,097	0,107	25 °C
Empty	T21	1	0,086	0,093	0,093	0,093	0,089	0,256	0,259	0,255	25 °C
	T22	3	0,088	0,092	0,093	0,091	0,091	0,234	0,245	0,159	25 °C
	T23	5	0,087	0,090	0,091	0,091	0,080	0,308	0,235	0,116	25 °C
	T24	7	0,086	0,092	0,093	0,091	0,077	0,271	0,236	0,146	25 °C

- * Number of passes through a high-pressure homogenizer



Graph 8. The particle size of Resveratrol ethosome formulations vs empty ethosomes



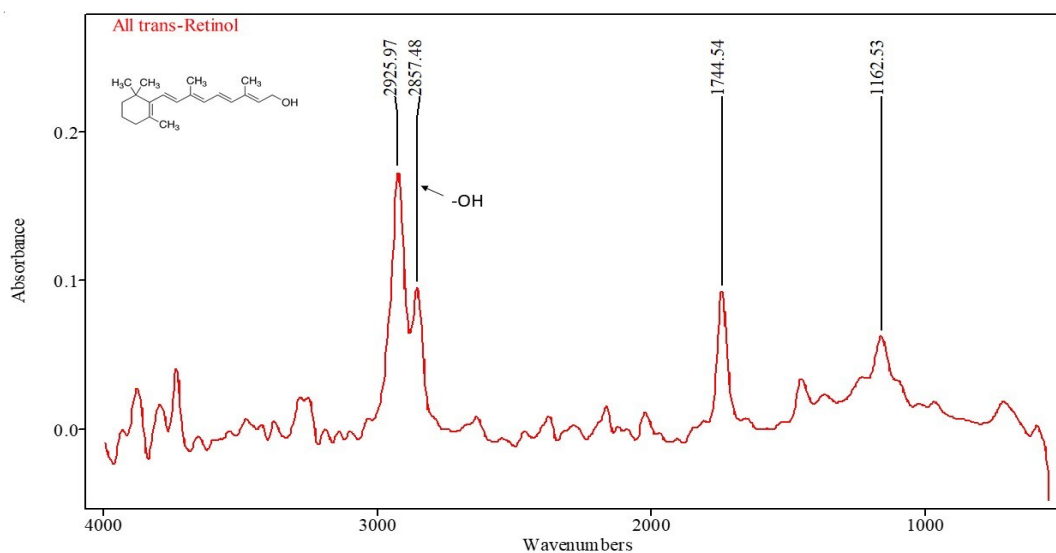
Graph 9. Uniformity of ethosomes formulations

8.3. RESULTS of the RETINOL

8.3.1. RESULTS of ANALYTICAL VALIDATION of RETINOL ASSAY

8.3.1.1. FT-IR SPECTRUM

FT-IR results of retinol were presented in Graph 10.

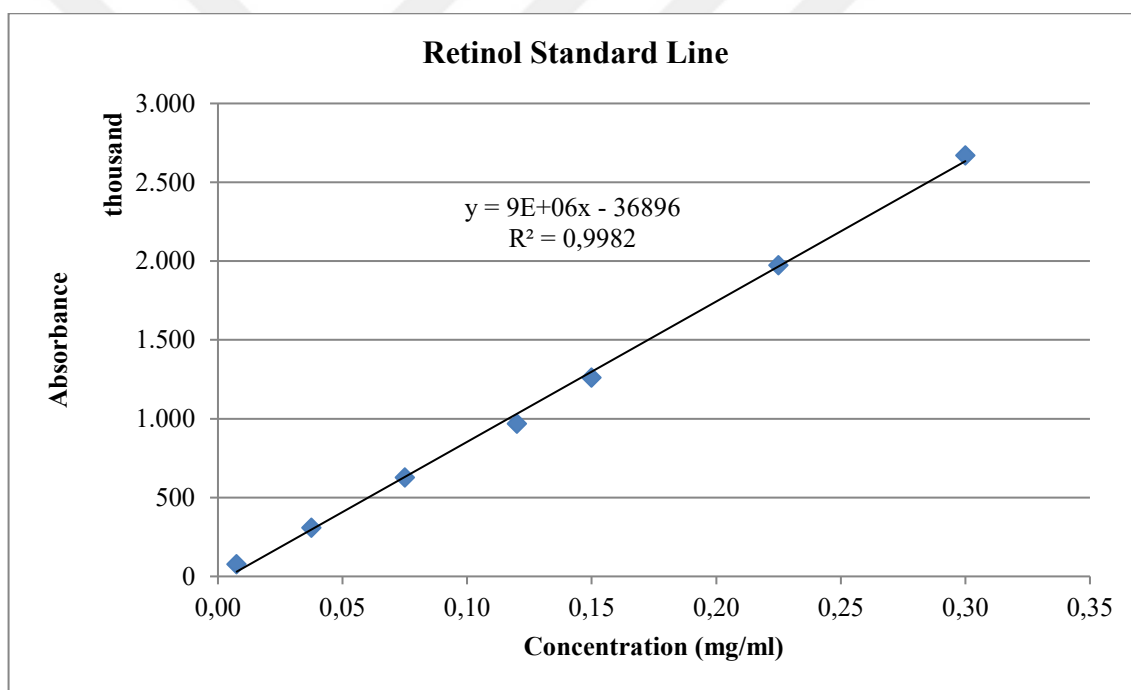


Graph 10. IR spectrum of retinol

8.3.1.2. LINEARITY

Retinol solutions were prepared in 7 different concentrations in methyl alcohol by applying the test method of 7.2.3.1. To determine linearity, the calibration curve of standard retinol is prepared, and it is given in Graph 11. The linear regression equation and squared correlation coefficient (R^2) is calculated and are given on the graph 11. The Limit of detection (LOD) and limit of quantification (LOQ) were calculated and presented in sections of 8.3.1.5. and 8.3.1.6. respectively.

The general acceptance criteria for linearity is a correlation coefficient of 0,998 or higher. Therefore, the calibration curve of retinol was shown to be linear with a squared correlation coefficient (R^2) of 0.9982 and showed excellent linearity in the tested range.



Graph 11. The standard line of retinol obtained by HPLC method

8.3.1.3. ACCURACY

The *Retinol* solutions were prepared in ethyl alcohol at concentrations of 10, 20, and 25 $\mu\text{g/ml}$. The absorbance of the solutions were measured five times consecutively by HPLC at 325 nm wavelength, and the corresponding concentration values ($\mu\text{g/ml}$) were calculated with the help of the standard calibration curve formula. The recovery percentages were calculated, as indicated in the method as given in 7.2.2.1. The results (the theoretical and

calculated concentrations, and the mean recovery percentages) are given in Table 25. The mean recovery rates calculated were within the range of 92,27-105,79 %. Since the recoveries are within the 90–110% range, the test method is considered acceptable.

The standard calibration curve of retinol is shown in Graph 11. The general acceptance criteria for linearity is a correlation coefficient of 0,998 or higher. Therefore, the calibration curve of retinol was shown to be linear with the squared correlation coefficient (R^2) of 0.9994 and showed excellent good linearity in the tested range.

The standard calibration curve of retinol is shown in Graph 11. The general acceptance criteria for linearity is a correlation coefficient of 0,998 or higher. Therefore, the calibration curve of retinol was shown to be linear with a squared correlation coefficient (R^2) of 0.9982 and showed excellent linearity in the tested range.

Table 25. Results of the accuracy test of retinol in ethyl alcohol

Sample	1st concentration		2nd concentration		3rd concentration	
	10 µg/ml		20 µg/ml		25 µg/ml	
	Account value	% recovery	Account value	% recovery	Account value	% recovery
1	12,66	105,47	20,59	102,93	23,82	95,27
2	12,67	105,55	20,59	102,97	23,83	95,32
3	12,67	105,57	20,60	103,01	23,84	95,35
4	12,68	105,69	20,60	103,01	23,84	95,35
5	12,69	105,79	20,62	103,09	23,84	95,35
Average	105,61		103,00		95,33	
Reliability level	0,05		0,05		0,05	
Standard deviation	0,13		0,06		0,04	
Coefficient of Variation	0,0012		0,0006		0,0004	
n (sample size)	5		5		5	
Confidence interval	0,11		0,05		0,03	

8.3.1.4. PRECISION

8.3.1.4.1. REPEATABILITY 1

Retinol samples were prepared at the concentration of 150, 75, and 37.5µg/ml in methyl alcohol medium were measured by HPLC three times at 325nm. Show the sub-curve area, mean, standard deviation values, and variation coefficients in Table 26. As the coefficient of variation was less than 2%, the method was found to be reproducible.

Table 26. Retinol repeatability test results in ethyl alcohol

Sample	1st concentration	2nd concentration	3rd concentration
	37,5 µg/ml	75 µg/ml	150 µg/ml
	Area	Area	Area
1	305.536	703.989	1.364.918
2	305.905	705.817	1.364.919
3	305.982	707.328	1.366.096
Average	305.808	705.711	1.365.311
Reliability level	0,05	0,05	0,05
Standard deviation	238	1.672	680
Coefficient of Variation	0,0008	0,0024	0,0005
n (sample size)	3	3	3
Confidence interval	270	1.892	769

8.3.1.4.2. REPEATABILITY 2

As described in Method 7.2.3.1, sub-curve areas of six samples that were prepared at a concentration of 120µg/ml from the same stock solution were read with HPLC at 325nm wavelength. The results are given in 7.2.3.1. The variation coefficient value is less than 2%, indicating that the method is reproducible.

Table 27. Retinol recoverability test results in ethyl alcohol

Sample	Concentration
	120 µg/ml
	Area
1	1.043.436
2	1.044.066
3	1.044.512
4	1.044.736
5	1.044.948
6	1.045.331
Average	1.044.005
Reliability level	0,05
Standard deviation	541
Coefficient of Variation	0,0005
n (sample size)	6
Confidence interval	433

8.3.1.5. LIMIT of DETECTION (LOD)

According to the results, the lowest concentration at which retinol can be detected with acceptable accuracy and repeatability was calculated as 15,7µg/ml.

8.3.1.6. LIMIT of QUANTITATION (LOQ)

According to the results, the lowest concentration at which retinol can be determined with acceptable accuracy and repeatability was calculated as 47,6µg/ml.

8.3.1.7. ROBUSTNESS

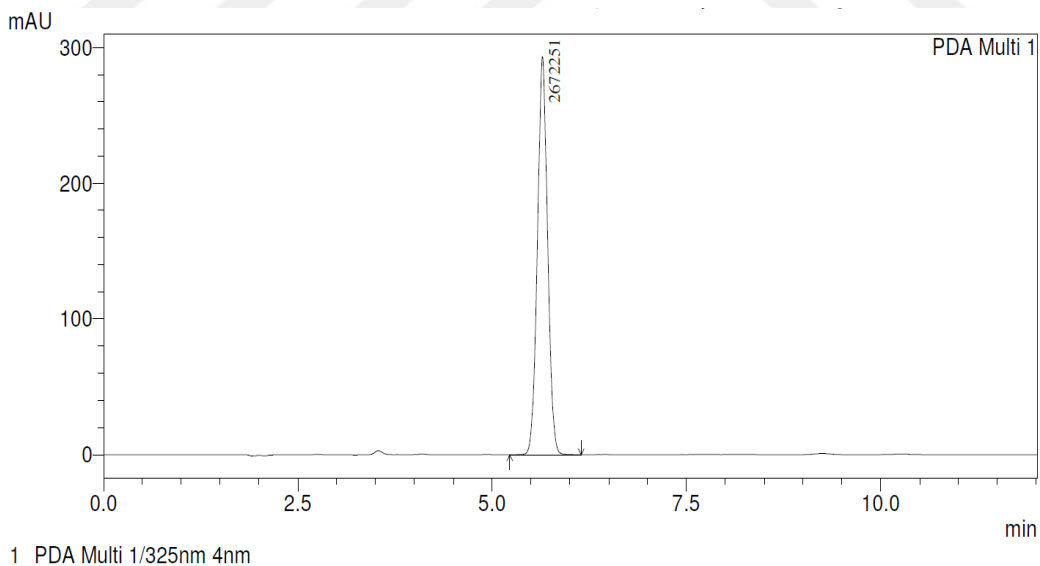
In order to examine the stability of retinol in dissolution media, the sample of 100µg/ml retinol was subjected to two HPLC measurements in 24 hours. No significant change was observed in the sub-curve values, as given in Table 28.

Table 28. *Trans-resveratrol stability test results in ethyl alcohol*

Concentration	1 st measurement	2 nd measurement	% Difference
100µg/ml	961.329	917.835	-4,52

8.3.1.8. ORIGINALITY, SELECTIVITY

HPLC absorbances of retinol free ethosomes formulation were analyzed. This method was found to be specific for the analysis of *retinol* since there were no other peaks close to the retinol. This is shown in Graph 12.



Graph 12. *Retinol peak in HPLC*

8.3.1.9. SOLUTION STUDY

The solubility of retinol in methyl alcohol is about 715mg/ml. The solubility of retinol in ethyl alcohol is about 721mg/ml. The solubility in PBS (phosphate-buffered saline) prepared at pH 7.2 is approximately 0.017 μ g/ml. The solubility in PBS containing 2% nonionic surfactant (polysorbate 20) into PBS is 0.08 μ g/ml.

8.3.2. FORMULATIONS of RETINOL ETHOSOMES

Particle size and uniformity measurement retinol loaded ethosomes were studied as given in section 7.2.6.2. The retinol loaded ethosome formulations were coded as T, and their compositions are given in Table 29.

Table 29. Empty and loaded retinol ethosomes formulations

	CODE	Deionized Water (%)	Lecithin (%) (Lipoid P75)	Vitamin E (%)	Ethanol (%)	(%) Active Substance	Cycle
Retinol	T17	63,2	5	0,3	30	1,5	1
	T18	63,2	5	0,3	30	1,5	3
	T19	63,2	5	0,3	30	1,5	5
	T20	63,2	5	0,3	30	1,5	7
Blank	T21	64,7	5	0,3	30	-	1
	T22	64,7	5	0,3	30	-	3
	T23	64,7	5	0,3	30	-	5
	T24	64,7	5	0,3	30	-	7

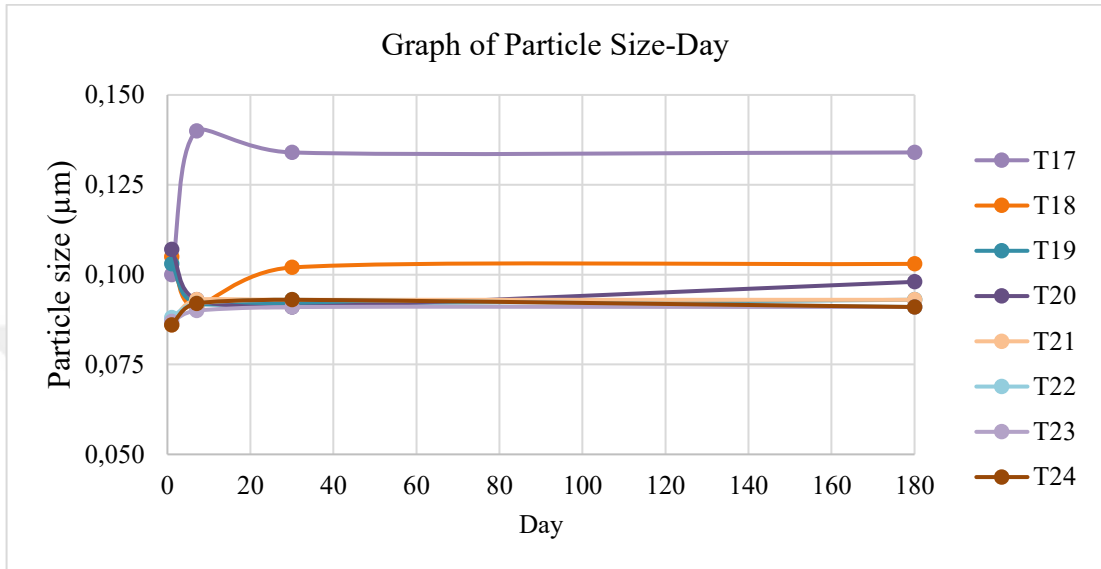
8.3.2.1. PARTICLE SIZE and STABILITY of RETINOL ETHOSOMES FORMULATIONS

Table 30. Particle size and uniformity of retinol ethosomes formulations

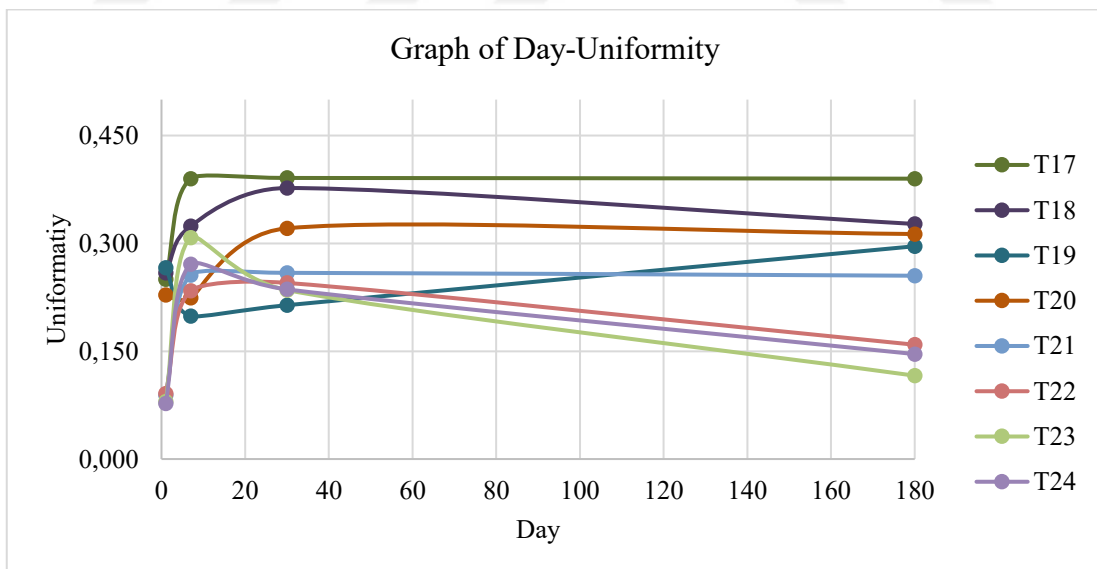
	CODE	T*	d (0.5) (μ m)				Uniformity				SK
			1	7	30	180	1	7	30	180	
Retinol	T17	1	0,100	0,140	0,134	0,134	0,250	0,390	0,391	0,390	25 °C
	T18	3	0,105	0,091	0,102	0,103	0,259	0,324	0,377	0,327	25 °C
	T19	5	0,103	0,092	0,092	0,093	0,266	0,199	0,214	0,296	25 °C
	T20	7	0,107	0,093	0,091	0,098	0,228	0,224	0,321	0,313	25 °C
Empty	T21	1	0,086	0,093	0,093	0,093	0,089	0,256	0,259	0,255	25 °C
	T22	3	0,088	0,092	0,093	0,091	0,091	0,234	0,245	0,159	25 °C
	T23	5	0,087	0,090	0,091	0,091	0,080	0,308	0,235	0,116	25 °C
	T24	7	0,086	0,092	0,093	0,091	0,077	0,271	0,236	0,146	25 °C

* Number of passes through a high-pressure homogenizer

The changes seen in the particle size and shape uniformity of retinol ethosomes with time are given in Graph 13, and Graph 14. All of these formulations showed acceptable stability; in other words, the size of the ethosomes did not change significantly at the time points tested. The results are shown in Table 30.



Graph 13. Particle size of retinol ethosomes formulations



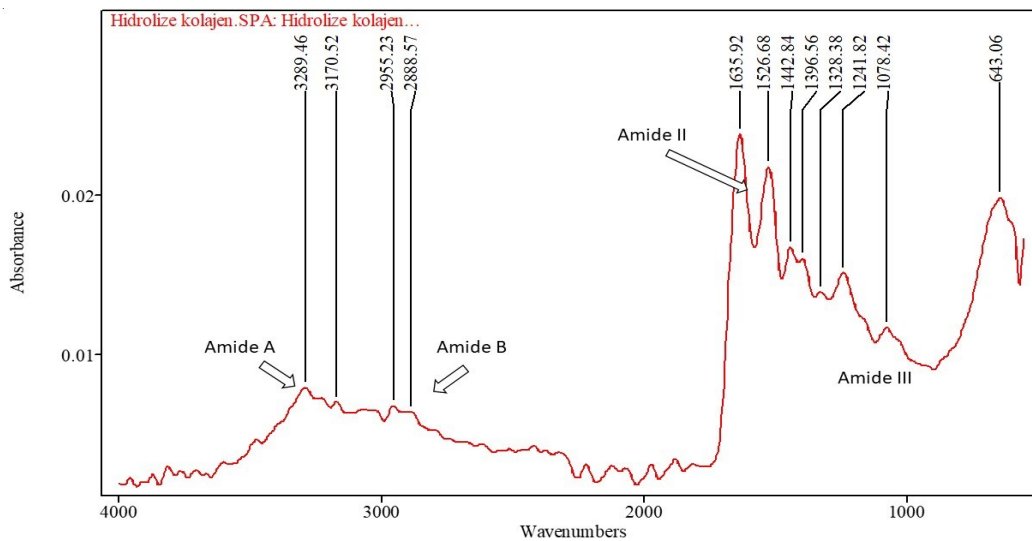
Graph 14. Uniformity of retinol ethosomes formulation

8.4. RESULTS of the HYDROLYZED COLLAGEN

8.4.1. RESULTS of ANALYTICAL VALIDATION of HYDROLYZED COLLAGEN ASSAY

8.4.1.1. FT-IR SPECTRUM

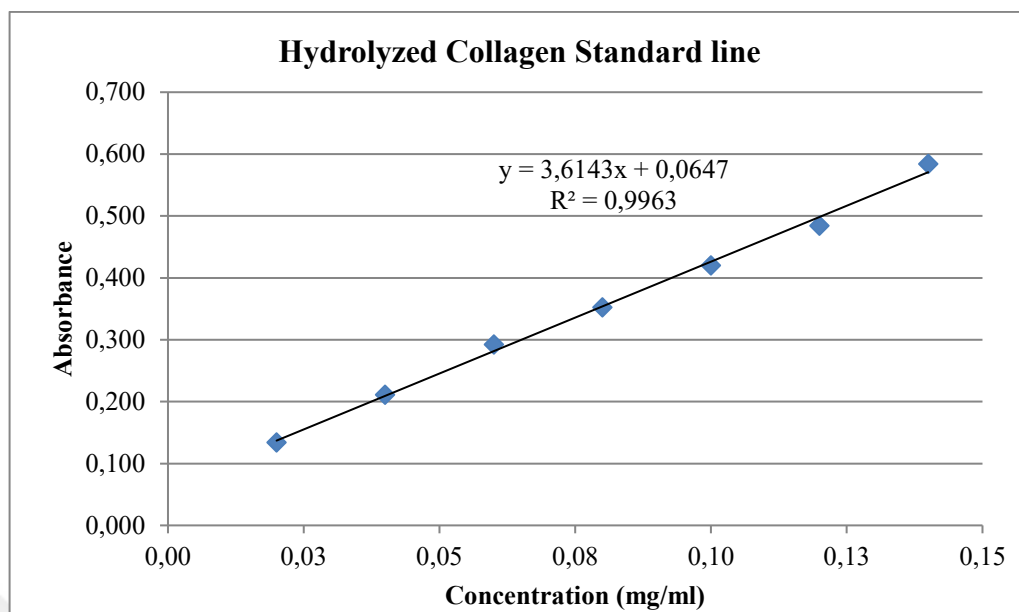
FT-IR result of hydrolyzed collagen is presented in Graph 5.



Graph 15. IR spectrum of hydrolyzed collagen

8.4.1.2. LINEARITY

Hydrolyzed Collagen solutions were prepared in PBS at seven different concentrations by applying the test method given in 7.2.4.1. It was shown that within the range of the concentrations used, the calibration curve produced a linear regression equation of $y = 3,6143x + 0,0647$ and a squared correlation coefficient of $R^2 = 0.9963$. The calibration curve of *hydrolyzed collagen* is presented in Graph 16. LOD and LOQ are reported in section 8.2.1.5 and 8.2.1.6, respectively.



Graph 16. The standard line of hydrolyzed collagen obtained by lowry method

8.4.1.3. ACCURACY

Samples of *hydrolyzed Collagen* prepared in PBS were prepared at concentrations of 20, 60, and 80 $\mu\text{g/ml}$. The absorbance of the solutions was read five times consecutively with a UV-Visible spectrometer at 750nm wavelength, and the corresponding concentration values ($\mu\text{g/ml}$) were calculated with the help of the standard calibration curve formula.

Table 31. Data on the accuracy test of Hydrolyzed Collagen

Sample	1st concentration		2nd concentration		3rd concentration	
	20 $\mu\text{g/ml}$		60 $\mu\text{g/ml}$		80 $\mu\text{g/ml}$	
	Account value	% recovery	Account value	% recovery	Account value	% recovery
1	18,62	93,10	62,06	103,43	78,38	97,98
2	18,34	91,72	62,06	103,43	78,94	98,67
3	18,07	90,34	61,51	102,51	77,83	97,29
4	17,51	87,57	61,51	102,51	77,83	97,29
5	17,51	87,57	62,34	103,89	77,55	96,94
Average	90,06		103,16		97,63	
Reliability level	0,05		0,05		0,05	
Standard deviation	2,47		0,62		0,69	
Coefficient of Variation	0,0275		0,0060		0,0071	
n (sample size)	5		5		5	
Confidence interval	2,17		0,54		0,61	

The recovery values were calculated, as indicated in the method 7.2.2.1, and the results are given in Table 31. The theoretical and calculated concentrations and the mean recovery percentages are given in Table 31. The mean recovery amounts calculated were within the range of 90,06–103,16 %. Therefore, the method is considered acceptable.

The calibration curve of hydrolyzed collagen was shown to be linear with the squared correlation coefficient (R^2) of 0.9963 and showed good linearity in the tested range. The standard calibration curve of hydrolyzed collagen is shown in Graph 16. The general acceptance criteria for linearity is a correlation coefficient of 0,998 or higher.

8.4.1.4. PRECISION

8.4.1.4.1. REPEATABILITY 1

Samples of hydrolyzed collagen prepared at 20, 60, and 80µg/ml concentrations in PBS were measured three times consecutively by UV-Vis Spectrophotometer at 750nm. The mean and standard deviation values and coefficients of variation are given in Table 32. As the coefficients of variation were less than 2%, it was concluded that the method used is reproducible

Table 32. Hydrolyzed Collagen repeatability test results in PBS

Sample	1st concentration	2nd concentration	3rd concentration
	20 µg/ml	60 µg/ml	90 µg/ml
1	18,62	62,06	93,05
2	18,34	61,51	92,77
3	18,07	61,51	93,32
Average	18,34	61,69	93,05
Reliability level	0,05	0,05	0,05
Standard deviation	0,28	0,32	0,28
Coefficient of Variation	0,0151	0,0052	0,0030
n (sample size)	3	3	3
Confidence interval	0,31	0,36	0,31

8.4.1.4.2. REPEATABILITY 2

As described in method 7.2.4.1, for repeatability, 6 solutions of the same concentration was prepared by dilution from the same stock solution. The concentration of the solution was 100µg / ml. The absorbance values were measured by UV-Vis spectrophotometer at 750nm.

From the absorbances, the concentrations were calculated, and the mean concentration, σ , V of the corresponding concentrations values were calculated, and all are summarized in Table 33. Since the coefficient of variation is less than 2%, the method is accepted as reproducible.

Table 33. Hydrolyzed collagen repeatability test results in PBS

Sample	Concentration
	100 μ g/ml
1	0,428
2	0,428
3	0,428
4	0,435
5	0,484
6	0,476
Average	0,447
Reliability level	0,05
Standard deviation	0,026
Coefficient of Variation	0,0589
n (sample size)	6
Confidence interval	0,021

8.4.1.5. LIMIT of DETECTION (LOD)

According to the results, the lowest concentration at which hydrolyzed collagen can be detected with acceptable accuracy and repeatability was calculated as 20 μ g/ml.

8.4.1.6. LIMIT of QUANTITATION (LOQ)

According to the results, the lowest concentration at which hydrolyzed collagen can be determined with acceptable accuracy and repeatability was calculated as 60 μ g/ml.

8.4.1.7. ROBUSTNESS

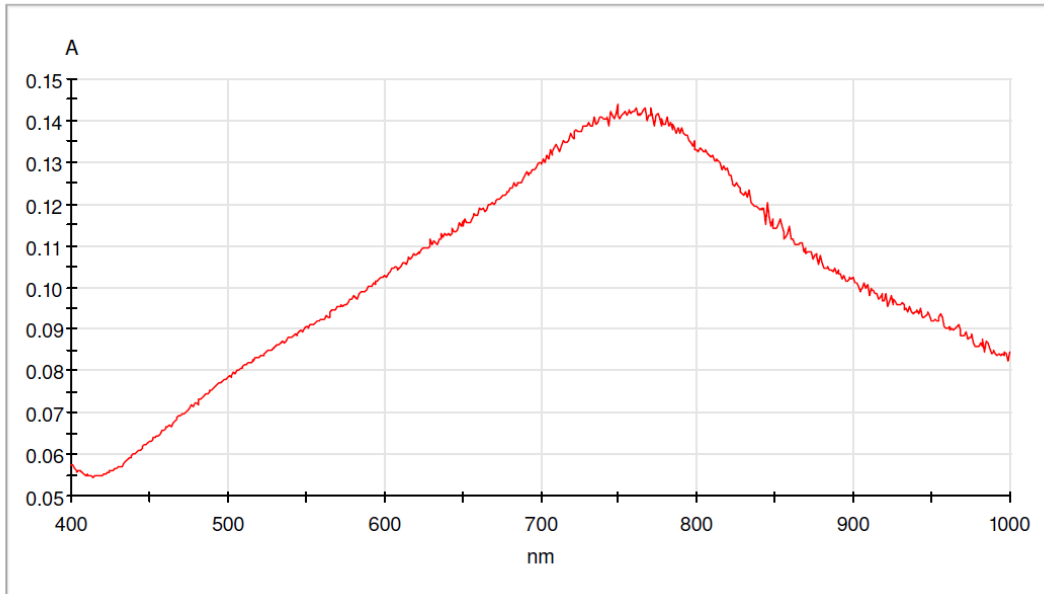
In order to determine the stability of hydrolyzed collagen in the dissolution media, the sample of 100 μ g/ml hydrolyzed collagen was subjected to two UV-Vis measurements in 24 hrs. No significant change was observed in the absorbance. As given in Table 34.

Table 34. Hydrolyzed collagen stability test results in PBS

Concentration	1st Measurement (A)	2nd Measurement (A)	% Difference
100 μ g/ml	0,456	0,420	7,89

8.4.1.8. SPECIFICITY

UV-Vis absorbance at 750nm wavelength of a hydrolyzed collagen-free formulation was examined. This method was found to be specific for the analysis of hydrolyzed collagen since there was no other peaks observed when the spectrum of the solution was taken. This spectrum is presented in Graph 17.



Graph 17. Hydrolyzed collagen in Uv-Vis

8.4.1.9. SOLUTION STUDY

The solubility in PBS (phosphate-buffered saline) at pH 7.2 is about 100µg/ml.

8.4.2. FORMULATIONS of HYDROLYZED COLLAGEN ETHOSOMES

Table 35. Empty and loaded hydrolyzed collagen ethosomes formulations

	CODE	Deionized Water (%)	Lecithin (%) (Lipoid P75)	Vitamin E (%)	Ethanol (%)	(%) Active Substance	Cycle
Hydrolyzed Collagen	T9	63,2	5	0,3	30	1,5	1
	T10	63,2	5	0,3	30	1,5	3
	T11	63,2	5	0,3	30	1,5	5
	T12	63,2	5	0,3	30	1,5	7
Blank	T21	64,7	5	0,3	30	-	1
	T22	64,7	5	0,3	30	-	3
	T23	64,7	5	0,3	30	-	5
	T24	64,7	5	0,3	30	-	7

Particle size and uniformity tests for hydrolyzed collagen loaded ethosomes are studied as given in section 7.2.6.9. The hydrolyzed collagen loaded ethosome formulations were coded as T, and their compositions are given in Table 35.

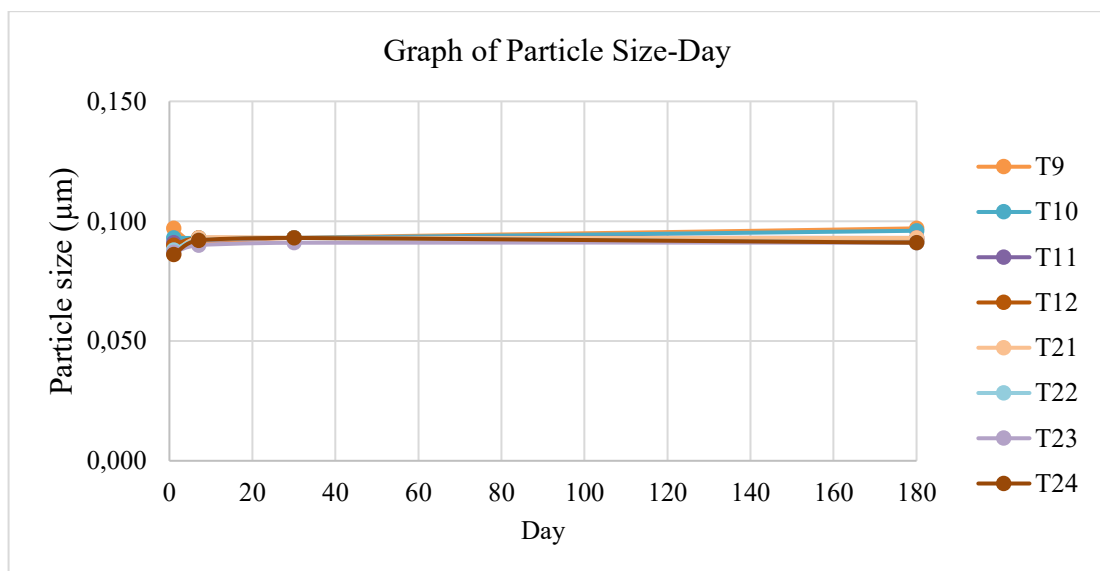
8.4.2.1. PARTICLE SIZE and STABILITY of ETHOSOMES FORMULATIONS

The changes seen in the particle size and shape uniformity of hydrolyzed collagen ethosomes with time are also in Graph 18, Graph 19. All of these formulations showed acceptable stability; in other words, the size of the ethosomes did not change significantly at the time points tested. The results are shared in Table 36.

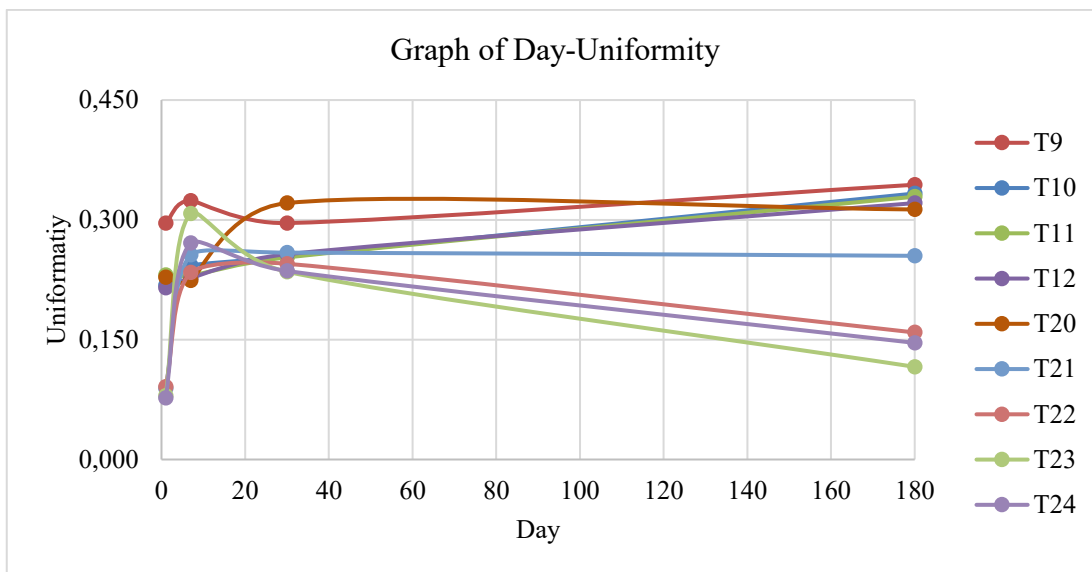
Table 36. Particle size and uniformity of hydrolyzed collagen ethosomes

	CODE	T*	d (0.5) (μm)				Uniformity				t
			1	7	30	180	1	7	30	180	
Hydrolyzed Collagen	T9	1	0,097	0,091	0,093	0,097	0,296	0,324	0,296	0,344	25 °C
	T10	3	0,093	0,093	0,093	0,096	0,218	0,243	0,254	0,333	25 °C
	T11	5	0,091	0,092	0,093	0,093	0,231	0,230	0,253	0,329	25 °C
	T12	7	0,090	0,093	0,093	0,092	0,215	0,227	0,257	0,321	25 °C
Empty	T21	1	0,086	0,093	0,093	0,093	0,089	0,256	0,259	0,255	25 °C
	T22	3	0,088	0,092	0,093	0,091	0,091	0,234	0,245	0,159	25 °C
	T23	5	0,087	0,090	0,091	0,091	0,080	0,308	0,235	0,116	25 °C
	T24	7	0,086	0,092	0,093	0,091	0,077	0,271	0,236	0,146	25 °C

* Number of passes through a high-pressure homogenizer



Graph 18. Particle size of hydrolyzed collagen ethosomes

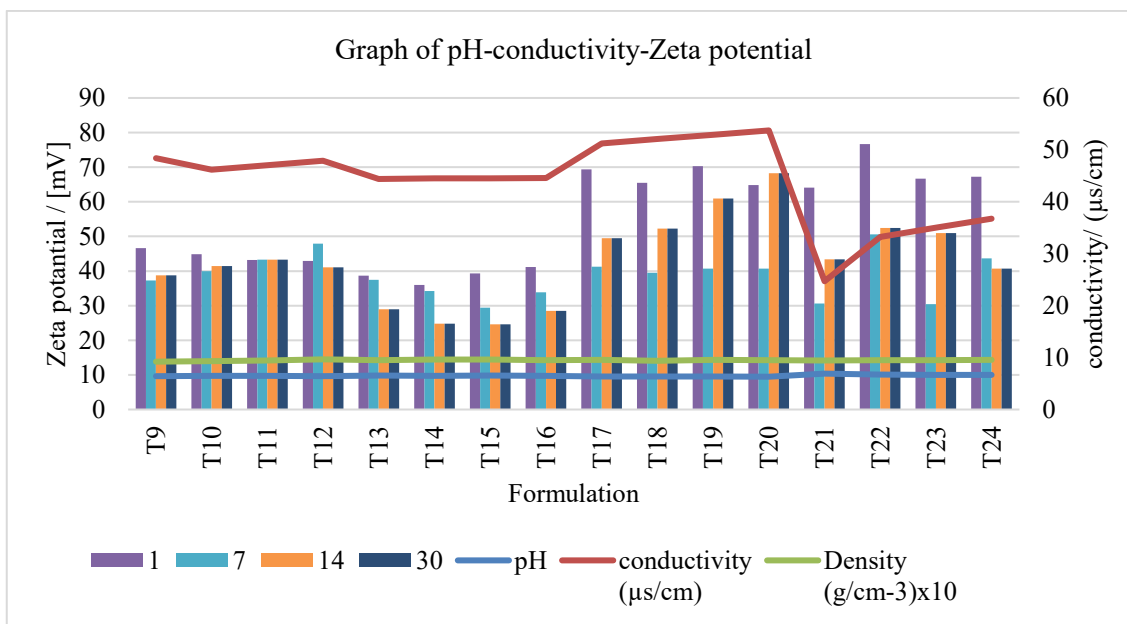


Graph 19. Uniformity of hydrolyzed collagen ethosomes

8.5. CHARACTERIZATION of ETHOSOMES FORMULATIONS

8.5.1. DETERMINATION of PH, CONDUCTIVITY, DENSITY and ZETA POTENTIALS of ETHOSOMES FORMULATIONS

Zeta potential measurement of ethosome formulations was performed as given in the method 7.2.6.6, 7.2.6.7, 7.2.6.8, 7.2.6.4. The Zeta Potentials change during the stability tests (at day 1,7,14 and 30 days) was measured. The results are given in Table 37.



Graph 20. PH-Conductivity-Zeta potential measurements of ethosomes

Zeta potential values provide information about the colloidal stability of vesicular systems. The zeta potential is the electric potential difference between the dispersion medium and the surface of the dispersed particle. The zeta potential of ethosomes is usually negative when ethosomes are made of phospholipids because the functional groups of the phospholipids are negative (244). However, the sign of the charge is not the most important point. Normally, a zeta potential value of $> 30\text{mV}$ indicates good stability. $>30\text{mV}$ zeta potential provides enough repulsion between the particles, which prevents agglomeration.

Table 37. The pH, conductivity and Zeta potential values of ethosomes formulations

CODE	pH	Conductivity ($\mu\text{s}/\text{cm}$)	Density (g/cm^3)	1 st day	7 th day	14 th day	30 th day
				Zeta Potential			
T9	6,430	48,4	0,921	46,6	37,3	38,8	47,4
T10	6,473	46,2	0,931	44,9	40,0	41,4	43,8
T11	6,455	47,1	0,943	43,2	43,3	43,3	47,2
T12	6,438	47,9	0,966	42,9	47,9	41,1	43,9
T13	6,540	44,4	0,951	38,7	37,5	29,0	29,3
T14	6,508	44,5	0,961	36,0	34,2	24,8	33,1
T15	6,518	44,5	0,961	39,3	29,4	24,6	25,6
T16	6,500	44,6	0,949	41,2	33,9	28,5	25,8
T17	6,368	51,2	0,953	69,4	41,3	49,5	50,9
T18	6,350	52,1	0,939	65,5	39,5	52,3	57,2
T19	6,333	52,9	0,957	70,3	40,7	61,0	59,5
T20	6,315	53,8	0,951	64,8	40,7	68,3	64,2
T21	6,910	44,7	0,945	64,1	30,6	43,4	39,6
T22	6,721	53,2	0,948	76,7	50,6	52,4	54,4
T23	6,687	55,0	0,952	66,7	30,4	51,0	52,9
T24	6,653	56,8	0,956	67,2	43,7	40,7	55,6

8.5.2. ELECTRON MICROSCOPY (SEM) IMAGES of ETHOSOMES FORMULATIONS

Some growth was observed in the images of empty ethosomes and *trans*-resveratrol containing ethosomes. It is possible that the growth of ice crystals influenced the growth of the sample particles with a cryo-SEM spaceman preparation process. The average values, standard deviations, and PDI are given in Table 35. The following PDI formula was used for the calculations:

$$PDI = (\text{Average value})^2 \times (\text{Standard deviation})^2$$

Equation 7.PDI

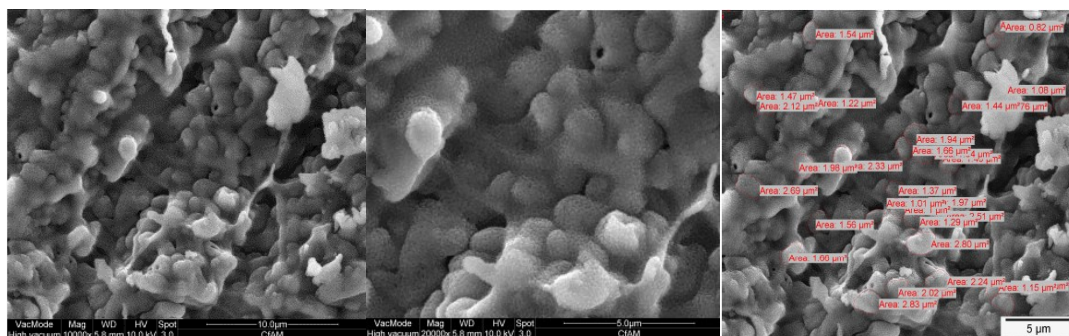


Figure 14. Cryo-SEM images of the active substance-free ethosomes (T24)

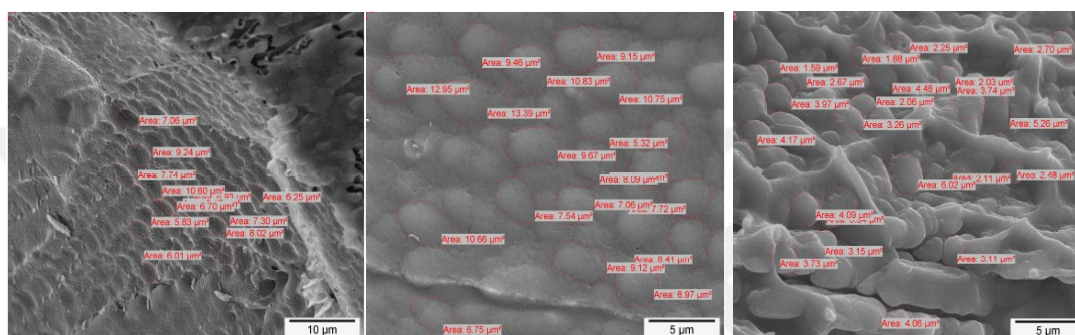


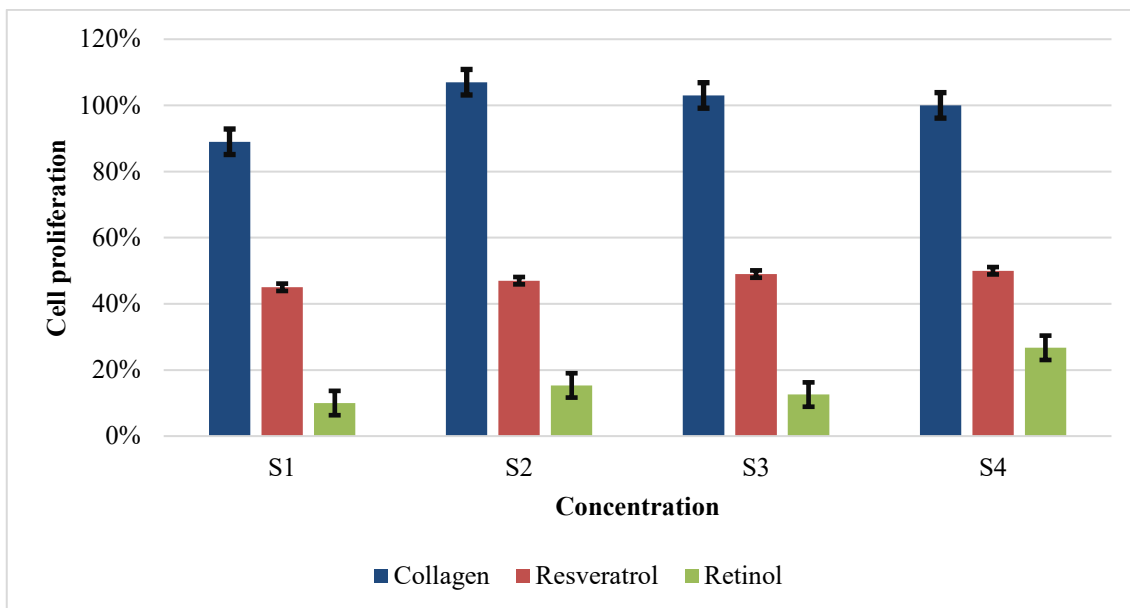
Figure 15. Cryo-SEM images of the active substance containing ethosomes (T12, T16, T20)

Table 38. PDI values of ethosomes formulations

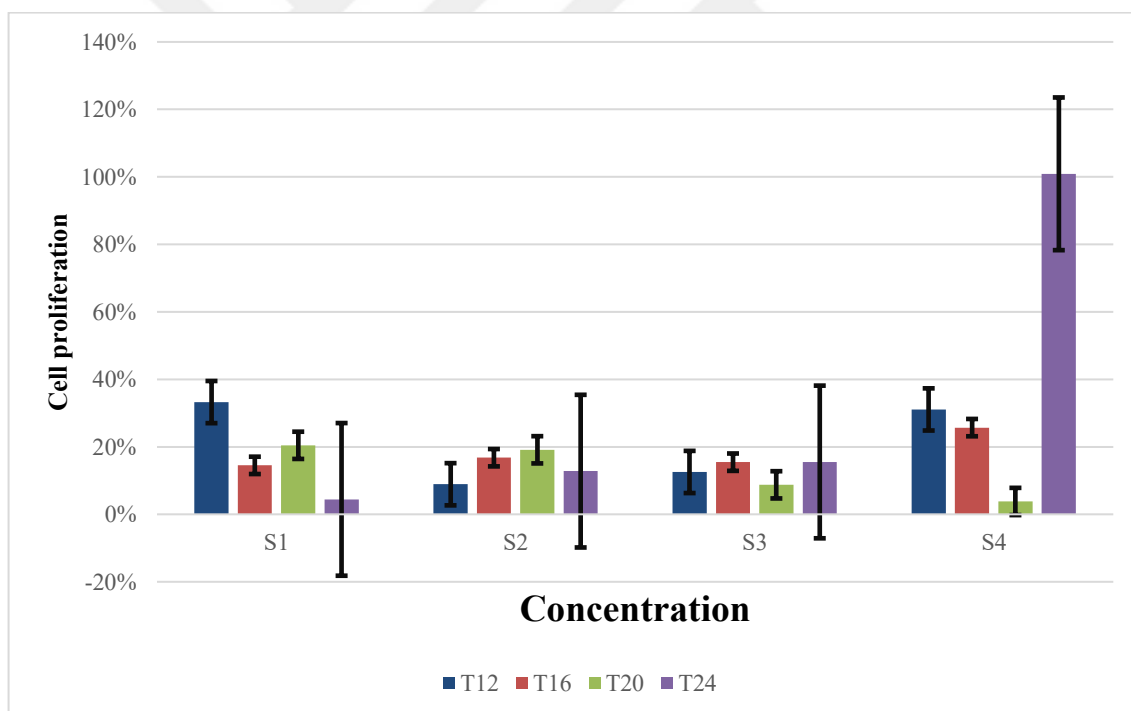
CODE	Mean Aspect ratio	Standard deviation	PDI
T12	1,34	0,26	0,038
T16	1,43	0,28	0,038
T20	1,58	0,23	0,021
T24	1,37	0,22	0,026

8.5.3. DETERMINATION of CYTOTOXICITY of ETHOSOMES FORMULATIONS

Solutions of pure raw materials T12, T16, and T20 ethosomes were toxic at concentrations of 0,1% and above probably due to. The T24 ethosome provided 100% viability at a concentration of 0,1%. The solutions were prepared as 25, 10, 1, and 0,1 % at the water.



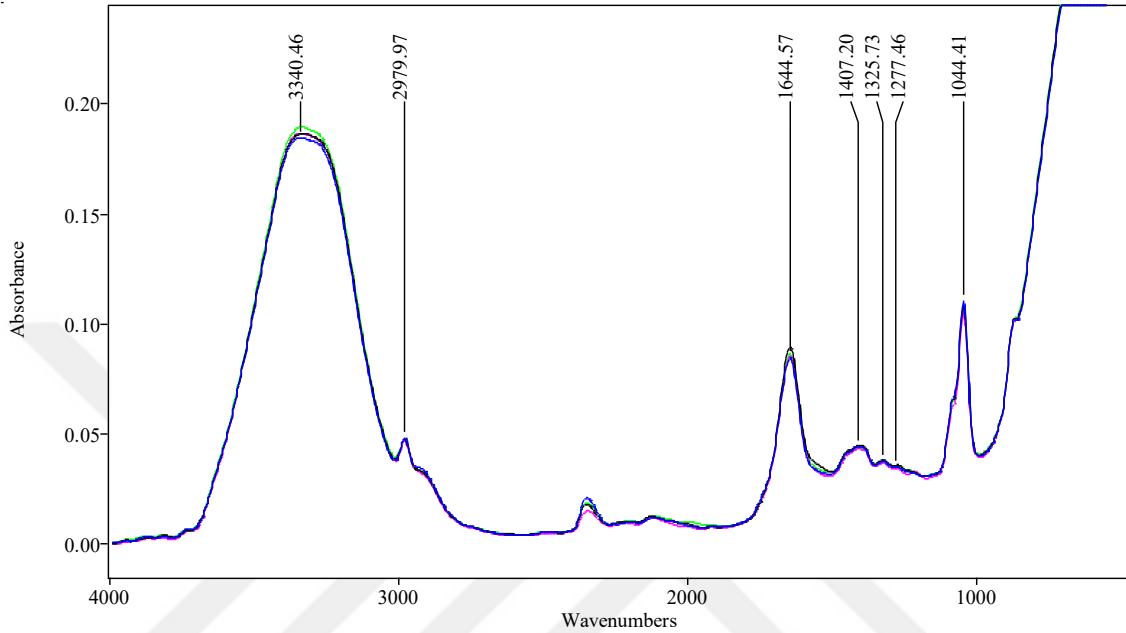
Graph 21. Cytotoxicity results of actives on HaCaT cells



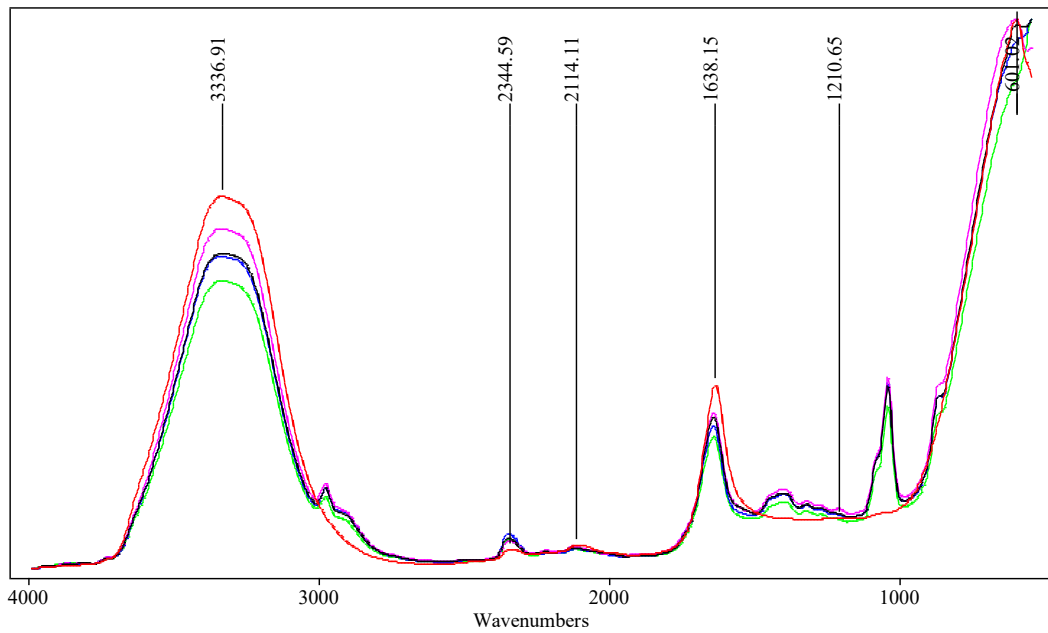
Graph 22. Cytotoxicity results of ethosomes on HaCaT cells

8.5.4. INFRARED FOURIER TRANSFORMATION SPECTROSCOPY (FT-IR) ANALYSIS of ETHOSOMES FORMULATIONS

Infrared Fourier transform spectra of ethosomes are given. Comparative FT-IR analyzes with PBS are shown in Graph 13, Graph 14.



Graph 23. FT-IR absorbances of T12, T16, T20, T24 formulations



Graph 24. FT-IR absorbances of T12, T16, T20, T24 formulations and PBS

8.5.5. MEASUREMENT of ACTIVE SUBSTANCE CONTENT in ETHOSOMES FORMULATIONS

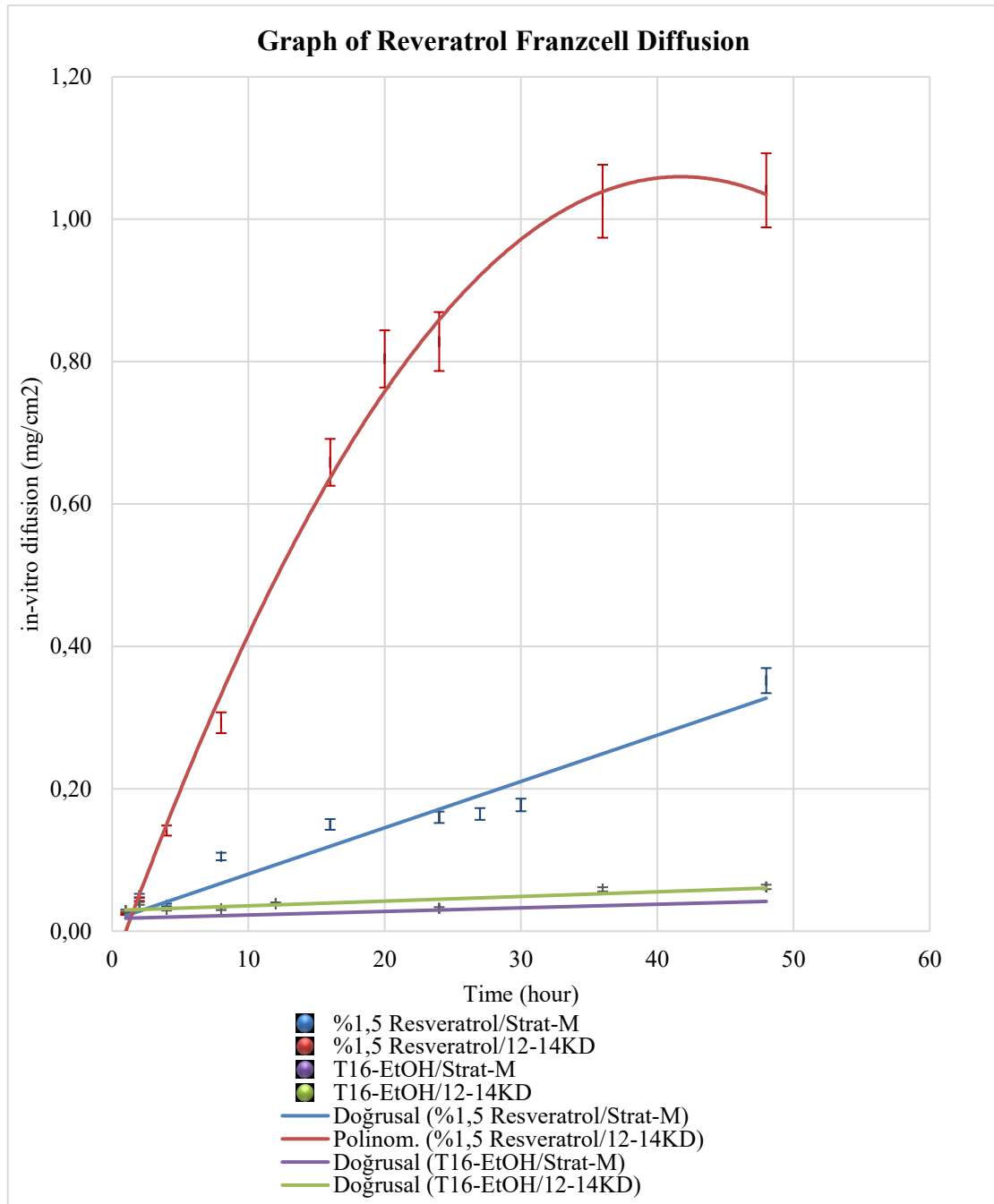
The amount of active ingredient in the ethosome formulations was determined by HPLC for resveratrol and retinol, as described in Method 7.2.2.1 and 7.2.3.1, and by Lowry method for hydrolyzed collagen, as described in method 7.2.4.1. Table 34 shows the amount of encapsulated and non-encapsulated active ingredient. The amount of encapsulation of ethosomes passed through the reduced with high-pressure homogenizer as of the first day is greater.

Table 39. % amount of encapsulated active ingredient of ethosomes and the solutions

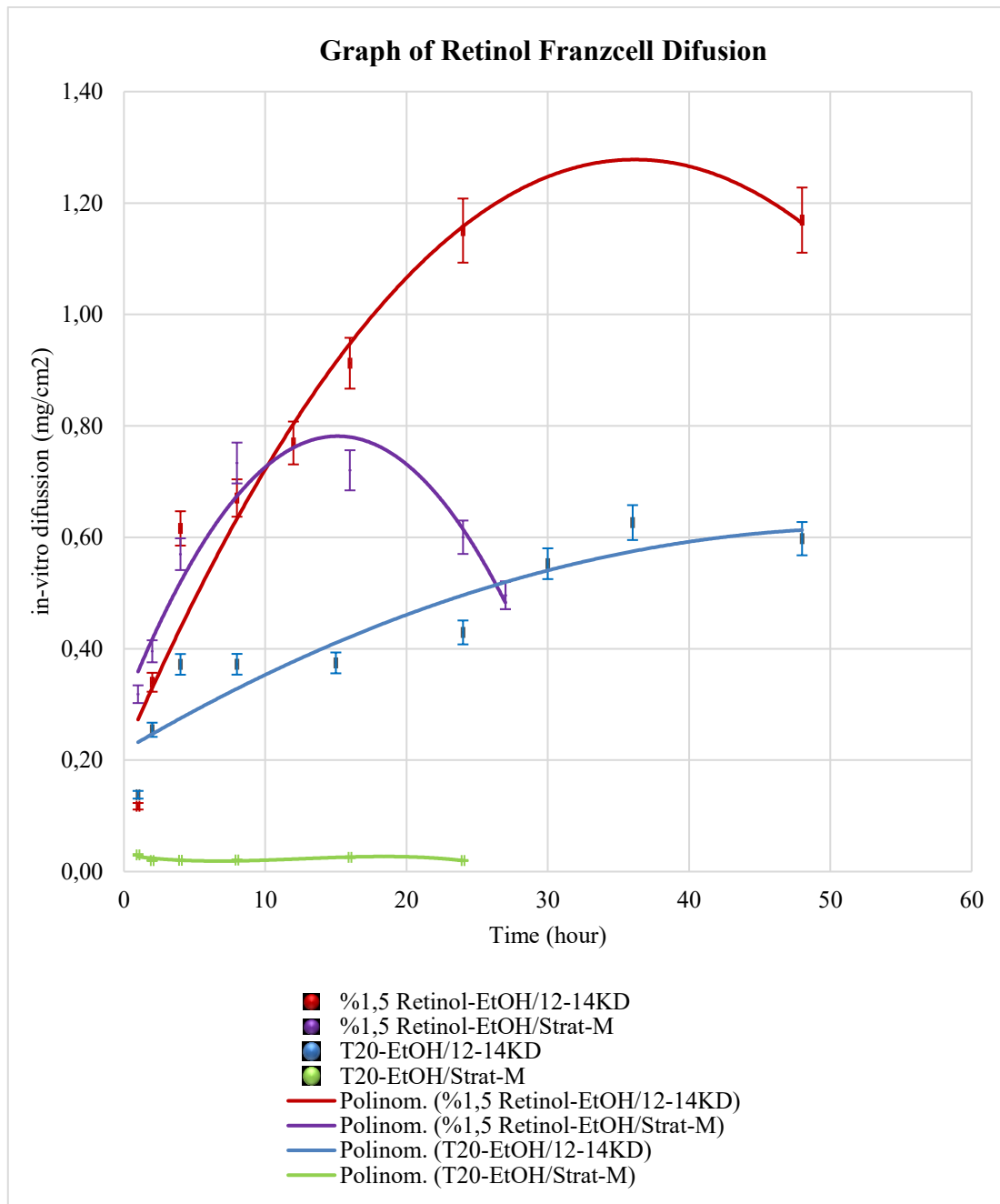
	% Unencapsulated		% Encapsulated	
	day 1	day 180	day 1	day 180
T12	13,66%	29,48%	86,34%	70,52%
T16	4,51%	15,79%	95,49%	84,21%
T20	11,44%	22,04%	88,56%	77,96%

8.5.6. *In-vitro* RELEASE STUDIES of ETHOSOME FORMULATIONS

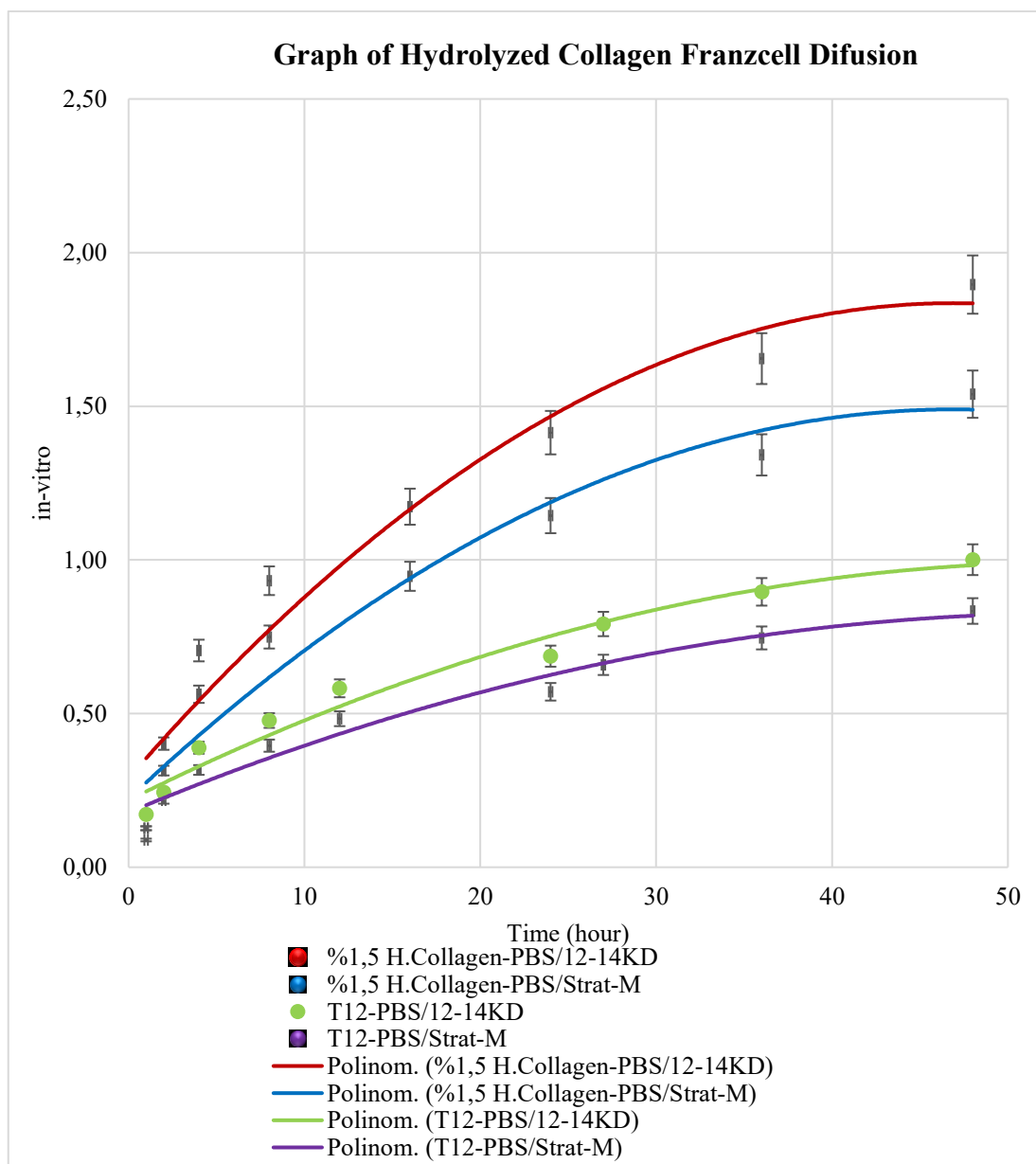
In vitro release studies of ethosome formulations were performed using the cellulose acetate (12-14KD) dialysis membrane and Strat-M. The surface area of the membranes used is 0,21cm². Ethosomes were analyzed of T12, T16, T20, T24 formulations release studies of the prepared formulations were made using the Franzcell method, and the graph of the active substance per unit time is shown.



Graph 25. Graph of trans-resveratrol Franzcell Diffusion T16 formulation



Graph 26. Graph of Retinol Franzcell Diffusion T20 formulation



Graph 27. Graph of Hydrolyzed collagen Franzcell Diffusion T12 formulation

The release from ethosome formulations was conducted by using the diffusion cell systems described in 7.2.6.11. The formulations used for these tests are summarized in Table 39 and Table 40. In each set of active material ethosome formulation and 1,5%, a simple solution of the active material in the appropriate medium was used as a comparison. The release diffusion results for resveratrol ethosome and 1,5% PBS solution, Retinol Athosome, and 1,5% ethyl alcohol solution and hydrolyzed collagen ethosome and 1,5% PBS solution are shown in Graph 25, Graph 26, Graph 27 respectively.

9. DISCUSSION

9.1. The CHOICE of ACTIVE SUBSTANCES, IDENTIFICATION, and VALIDATION STUDIES

Skin is not only one of the largest, but also an important and one of the largest organs in the human body. It has great importance since it provides the overall cosmetic appearance of every person. The outermost side of the skin is covered with the SC, which forms an epidermal barrier to prevent water and electrolyte loss (8, 22).

Skin aging is a very complex biological process that is caused by internal and external factors. The internal factors or intrinsic factors are chronological and mainly related to hormonal and physiological changes (28). The external factors include all of the other factors like photoaging, smoking, and other environmental factors (27). Both the natural or premature aging causes many changes in the skin; like the appearance of fine and coarse wrinkles, reduced elasticity, loss of radiance, and dryness (28).

There are several ingredients, both synthetic chemicals, and herbal extract, that is used in cosmetics/cosmeceuticals for their different favorable functions (51). Resveratrol, Retinol, and Hydrolyzed Collagen are among the commonly used active materials in cosmetic/cosmeceutical products in order to both prevent the effects of skin aging as well as in improving the appearance of the aged skin.

Resveratrol is a polyphenol found in grapes (*Vitis vinifera*) and various other fruits, peanuts, and Japanese plants (*Polygonum cuspidatum*). It has received widespread interest as a preventive agent against numerous diseases that are caused by free radicals. There have been several clinical trials conducted to demonstrate the safety, efficacy, and bioavailability of resveratrol. Despite the interest shown in resveratrol as a topical anti-aging compound, most of the literature available is focusing on the anti-oxidant effects of resveratrol. Some *in-vitro* studies showed that resveratrol protects normal human fibroblasts from the harmful effects of hydrogen peroxide, possibly in a dose-dependent manner, by binding the specific receptors of the epidermis (225). The potent antioxidant properties of resveratrol in the grape peels are 50 times more than vitamin E and 30 times more than vitamin C 9. Resveratrol binds to specific binding sites which are mainly located in human epidermis and delays the

normal process of skin aging by blocking mitochondrial dysfunction in keratinocytes and apoptotic events (85).

Collagens are the most abundant proteins in mammals, which are deposited in the extracellular matrix. There are about 28 types of collagens, but 80-90% of the collagen in the body is collagen I, II, and III. The collagen interacts with cells via several receptor families and regulates their proliferation, migration, and differentiation (93). They are responsible for skin strength and elasticity, and when they are degraded, skin wrinkles increase. Collagen is also the main structural protein of different connective tissues found in animals. It is mostly found in fibrous tissues such as tendons and ligaments and is also abundant in cornea, cartilage, bones, blood vessels, intestines, and intervertebral discs (226), which make up 25 to 35% of the total protein mass in mammals and provide stiffness (227). Collagen is a large molecule with an MW of 100,000. Cosmetic uses of collagens include skincare and haircare products.

Retinol is the most popular substance known as a moisturizer in cosmeceutical anti-aging products. It is a derivative of vitamin A. Vitamin A is a substance that captures free radicals to protect against UV radiation damage (70). The potential of retinol in the treatment of photoaging was first realized by Kang et al. (79). According to many studies conducted, the vehicle used for retinol delivery would also play a crucial role in eliciting its efficacy, as well as to protect retinol, which is extremely unstable and easily gets degraded to biologically inactive forms on exposure to light and air.

In this thesis, resveratrol, retinol, and collagen were selected for their anti-aging effects. These three molecules are slightly different in terms of their MW, solubilities in PBS and ethyl alcohol.

As much as the ingredients used in the cosmetic formulations, the delivery systems carrying the actives into the skin are also important for the overall effectiveness of the cosmetic products (52). In recent years, new delivery systems have been developed and used to improve the efficacy of the products. As a result, emulsions, nanoemulsions, vesicular systems such as liposomes, niosomes, ethosomes have gained importance as novel delivery systems. Ethosome is one of these new delivery systems which could be used in the industry for its individual advantages.

One part of the study aimed to evaluate and discuss the *in-vitro* test methods to estimate the efficacy of the delivery systems. Therefore, the ethosomes of resveratrol, retinol, and hydrolyzed collagen were selected as a possibility of developing new delivery systems for these anti-aging ingredients. The results showed that both the cold and hot methods that were tried, as explained in method 7.2.5., were rather easy compared to the well-known thin film method that is widely used to prepare liposomes.

In order to fulfill one of the purposes of this study, the release characteristics of ethosomes were studied by Franz cell diffusion experiments with two different membranes.

Analytical method development and validation studies were another important part of this thesis. As presented in the results, the calibration curves of all actives tested for this study were linear at the selected concentration ranges, as shown in Graph 6, Graph 11, and Graph 16 (the calibration curves of Trans-resveratrol, retinol, and hydrolyzed collagen, respectively). The calibration curves had strong linearity with good correlation coefficients of more than 0,998 and good squared correlation coefficients (R^2).

The IR spectrum shown in Graph 5 of resveratrol is compatible with the IR bands given in the literature (228).

In the selected concentration range of resveratrol, a linear relationship was obtained between the absorbance (at 306 nm) and concentration as shown in Graph 6. The calibration curve was prepared with six different resveratrol concentrations of standard solutions that were in the range of 0,0075-0,25 mg/ml, and all injections were repeated three times ($n=3$). Selected calibration ranges deliberately included the amounts of resveratrol present in the samples to be tested for the studies related to resveratrol such as encapsulation efficiency, release studies, etc. The regression analysis shows that there was an excellent relationship between the absorbances and the concentrations used. The six repetitive injections of standard solutions were analyzed in terms of retention time and relative absorbances. Resveratrol samples that were prepared at the concentrations of 10, 20, 110 $\mu\text{g/ml}$ in PBS were measured by HPLC for three times at 306nm. The absorbances, averages, standard deviation values, and variation coefficients proved that the test method was reproducible in Table 20 and Table 21; the coefficient of variation was less than 2%. Besides, in spiked samples ($n=5$), the concentration of the resveratrol was increased by 21, 50, and 100 $\mu\text{g/ml}$, and the amount of

the analyte recovered was calculated. The recovery data presented in Table 19 was satisfactory to prove the accuracy of the method,

The IR spectrum shown in Graph 10 of retinol is compatible with the IR bands given in the literature (229).

In the selected concentration range of retinol, a linear relationship was obtained between the absorbance at 325 nm and concentration, as shown in Graph 11. The calibration curve was prepared with six different retinol concentrations of standard solutions that were in the range of 0,0075-0,3 mg/ml, and all injections were repeated three times (n=3). Selected calibration ranges deliberately included the amounts of retinol present in the samples to be tested for the studies related to retinol such as encapsulation efficiency, release studies etc. The regression analysis shows that there was an excellent relationship between the absorbances and the concentrations used. The six repetitive injections of standard solutions were analyzed in terms of retention time and relative absorbances. Retinol samples that were prepared at the concentrations of 37.5, 75 and 150µg/ml in ethyl alcohol were measured by HPLC for three times at 325nm. The absorbances, averages, standard deviation values, and variation coefficients proved that the test method was reproducible (Table 26 and Table 27).; the coefficient of variation was less than 2%. Besides, in spiked samples (n=5), the concentration of the retinol was increased by 12.5, 20, and 25 µg/ml, and the amount of the analyte recovered was calculated. The recovery data presented in Table 25 was satisfactory to prove the accuracy of the method,

The IR spectrum of hydrolyzed collagen, which is shown in Graph 15, is compatible with the IR bands given in the literature 10. The lowry method (7.2.4.1.) was chosen as the analytical method of hydrolyzed collagen in order to measure the quantity of hydrolyzed collagen.

In the selected concentration range, a linear relationship was obtained between the absorbances at 750nm and the concentrations, as shown in Graph 16. The calibration curve was constructed with seven different hydrolyzed collagen standard solutions where the concentrations were in the range of 0,020-0,140 mg/ml. All readings were repeated three times (n = 3). The correlation coefficient of the regression analysis of the calibration curve was 0,9963, showing that there was an excellent linear relationship between the UV-Vis absorbance reading at 750nm and the concentrations tested. The repeatability of the method

was evaluated with six repetitive readings of the standard solutions. The average values and the standard deviations of the concentrations calculated are listed in Table 32, as described in method 7.2.4.1. for repeatability, the absorbances of 6 solutions of the same concentration prepared by dilution from the same stock solution were measured. The concentration of the solution was 100 μ g/ml. The absorbance values read by the UV-Vis spectrophotometer at the wavelength of 750nm. From the absorbances, the concentrations, the average concentrations, σ , V of the corresponding concentration values were calculated, and all are summarized in 8.4.1.2. Since the coefficient of variation is less than 2%, the method is accepted as reproducible (Table 33). The standard deviations for accuracy and repeatability were also very good. The recovery percentages were determined by the standard addition method on selected samples. In the spiked samples (n=5), the concentrations of the hydrolyzed collagen were increased by 20, 60, and 80 μ g/ml. This recovery of collagen in these spiked samples was analyzed (n = 5). As shown in Table 31, the recoveries were between 93% and 103% and were satisfactory.

9.2. The ETHOSOMES FORMULATION of *trans*-RESVERATROL, RETINOL, and HYDROLYZED COLLAGEN

Liposomes were prepared by using three different phosphatidylcholine samples which represented animal and plant-derived sources and synthetic material. Liposomes were prepared with these materials by using a high-pressure homogenizing device by which the pressure was adjusted as required. The formulations were prepared by varying the percentages of the materials as well as the applied pressures by the homogenizing system. The pressures applied were at 500, 750, 1000 bars and the pre-mixtures were passed through an orifice under these pressures 1, 3, and 5 times. Based on short-term stability tests for two weeks conducted at 25 °C. The particle size range and the uniformity test were the basis for selecting the best formulation. Among these formulations prepared by using synthetic material, Lipoid P 75, as coded F9, was found to be the most stable formulation, based on its average particle size, particle size distribution and the uniformity results measured at day 1 and day 14.

After the selection of the phosphatidylcholine and the appropriate method, ethosome formulation was prepared. The active material percentage was decided to be 1,5. After the

preparation of several different formulations, as summarized in Table 23, Table 29, and Table 35, the best ethosomal formulations were selected based on their stability test results, as summarized in Table 24, Table 30 and Table 36. The best formulation was T12, T16, and T20 for trans-resveratrol, retinol, and hydrolyzed collagen respectively.

9.3. STABILITY STUDIES of ETHOSOME FORMULATIONS

The mean particle sizes of all ethosome formulations, both empty or loaded, were given in Table 23, Table 29, and Table 35 for resveratrol, retinol, and hydrolyzed collagen, respectively. According to the results of the average particle size and particle size distribution, the best formulations were T12, T16, and T20 with the average particle sizes of 0.092, 0.194, 0.097 μm respectively.

In all of the ethosomes formulations, no phase separation or bottom precipitation was observed. The pH, density, and conductivity results of the ethosomes were also stable, as shown in Table 37. The pH was between 6.3-6.9, the conductivity was between 44-56 ($\mu\text{s}/\text{cm}$), and the average density was 0.9 g/cm^3 .

9.4. EVALUATION of ENTRAPMENT EFFICACY, POLY DISPERSITY INDEX, PARTICLE SIZE, ZETA POTENTIAL, and ELECTRON MICROSCOPY IMAGES

Zeta potential is the potential difference between the stationary layer of the dispersion media attached to the particle and the dispersion medium. The nanoparticle has a charge that attracts a thin layer of counter ions to their surfaces. The magnitude of zeta potential has a valuable meaning in terms of predicting the stability of colloidal particles as well as nanoparticles (231). The nanoparticles with more than 30mV zeta potential are rather stable, and dispersions with less than 25mV may agglomerate because of the overcoming van der Waals interactions and lower electrostatic repulsion. As clearly stated by DLVO theory, when the zeta potential drops below the critical value of 25 mV, the attractive forces become dominant than repulsive electrostatic forces and this is the reason for the agglomeration.

In our study, the zeta potential values of ethosomes were measured on the days of 1,7,14 and 30 the ethosome formulation that was selected, which had more than 25mV (in fact, because

of a sign, less than -25mV). The most stable ethosomes had a zeta potential between 25mV to 70mV. These results showed a good agreement with the literature in terms of zeta potential values and stability. There was no agglomeration, creaming, sedimentation or phase separation (Table 37).

In the novel delivery systems, entrapment efficiency is an important feature. Ethosomes are regarded to be more stable as well as better carrier systems due to the presence of alcohol systems (232). The presence of alcohol increases the solubility of both lipophilic and amphiphilic ingredients resulting in better loading. However, some researchers have also reported unfavorable properties. This is mainly due to the increased permeability (leakage of actives) of the membrane as a result of the higher alcohol content of ethosomes (233) and the optimum ethyl alcohol amounts are generally around 20-40% for good stability and higher entrapment.

In our studies, the optimum ethyl alcohol concentration used in the formulations was also 30% which produced good stability (Table 23, Table 24 for resveratrol; Table 29, Table 30 for retinol; Tables 35 and 36 for hydrolyzed collagen). On the other hand, the selected formulation that was coded as T12 (hydrolyzed collagen), T16 (resveratrol) and T20 (retinol) entrapped respective active materials at a minimum of 86 % (Table 39) and retained the entrapped the respective actives at a minimum 71% after 180 days. These results showed that the formulations developed can be a good candidate for carrier systems for the active ingredients studied (234-236).

Microscopic observations of the ethosomes were made by Scanning electron microscope imaging techniques, as given in chapter 7.1.2.9. The cryo-SEM images showed homogeneous bilayer structure (T12, T16, T20), but the bilayers were not always intact, and there were gaps on the surface of the bilayer structure Figure 15. Cryo-SEM images of the active substance containing ethosomes (T12, T16, T20). Furthermore, SEM images were in good agreement with the results of the average particle size distribution (Graph 15). However, it is possible that the shape of the ethosomes was affected by the growth of ice crystals during the preparation process (T12, T16, T20). As a result, the sizes of the images by cryo-SEM are larger than what was measured by DLS, as shown in Table 38. The average PDI $0,031 \pm 0,009$ mean is given as reliability level $p < 0,05$.

Images that were taken under normal light and crossed polarized light also showed the liquid crystal bilayer structure of the ethosomes give shown figure16, 17, and 18 in appendix I.

9.5. EVALUATION of *in-vitro* RELEASE STUDIES on FRANZCELL

Transdermal delivery systems have many advantages, such as avoidance of the first-pass opportunity and less frequent dosing. These advantages together with improved patient compliance due to the easy self-administration possibility. Makes transdermal delivery an important route of drug administration. In recent years, there have been many researchers conducting the test on the new transdermal delivery systems. Among these novel delivery systems, ethosomes are also going important. As summarized in some of the review articles, ethosomes has been tested for many different types of active ingredients and reported as being a promising drug delivery alternative (237).

Dialysis membrane and Strat-M were used *in-vitro* release studies by the Franzcell diffusion system for the ethosome formulations. Ethosome formulations used were formulations T12 (Hydrolyzed Collagen), T16 (Resveratrol), T20 (Retinol), T24 (Empty Ethosomes).

During *in-vitro* diffusion/penetration studies of the active two different synthetic membranes; Strat-M (layered skin mimicking) and 12-14KD cellulose acetate dialysis membrane, was used. The diffusion rates were calculated for 1 to 48 hours in terms of the mean cumulative amount of active dialyzed and percent diffused amount \pm SD.

The diffusion rates were calculated at predetermined times (1,2,4,8,16,24, and 48 hours). The amount of active ingredients at the specific time points were calculated as the mean cumulative amount released then converted to as diffused amount per unit area (mg/cm^2). The release/diffusion experiments from the ethosomes were compared with the simple solutions of the respective active. The two membranes used were different in their structure. The cellulose acetate membrane is used as a rate-controlling membrane but not regarded as similar to the skin. On the contrary, Strat-M which is also a synthetic membrane but is regarded as being a predictive membrane of the diffusion through human skin. It is constructed of two layers of polysulphone, and the porous structure is impregnated with some lipophilic materials to give it a more skin-like structure. According to the other studies, strat-M diffusion correlates very closely to the skin (5).

In our experiments, we expected to have fewer amounts of the active ingredients to diffuse through the Strat-M than cellulose acetate (12-14KD). In all of the experiments, these results were seen clearly except for retinol diffusion studies. The release from resveratrol (Graph 25) and hydrolyzed collagen ethosomes (Graph 27) showed the following release patterns:

1. The release from the simple solution (1,5%) was fastest with cellulose acetate membrane
2. The release from simple solution was the second fast from the Strat-M membrane
3. The release from the loaded ethosome formulations as through cellulose acetate was in the third place
4. The release from ethosomes formulation through Strat-M was the slowest

The results clearly showed that the ethosomes encapsulation provides a sustained release; these results were one of the expectations of the study and are similar to the results shown by many other researcher results (237, 238).

Our diffusion test results for retinol with the strat-M membrane were not as expected. Some additional studies were made in order to enlighten the unexpected release profiles from retinol solution and ethosomes. The results with the cellulose acetate membrane (12-14KD) were similar to the other test results and as expected.

The diffusion test results with the Strat-M membrane were erratic. Further studies and investigations about the properties of the Strat-M revealed that these results were due to an incompatibility between Strat-M and the receptor solution, ethyl alcohol used for retinol diffusion studies. The manufacturer provided information that makes a clear statement that the use of ethyl alcohol with Strat-M is not recommended (239).

The release experiments from retinol ethosome should be repeated by using an appropriate receptor solution that is compatible with the Strat-M membrane. During the studies, the reason for selecting ethyl alcohol as the receptor solution can be explained as below:

Retinol has a low solubility (0,017 μ g/ml) in PBS at pH 7.2, as reported in section 8.3.1.7. Retinol solubility in PBS containing 2% polysorbate 20 increased solubility to approximately 0,08 μ g/ml, but this was well below the LOQ (47,6 μ m/ml). The selection of ethyl alcohol as a receptor solution; however, increased the solubility of retinol, due to

incompatibility, the structure of Strat-M changed after probably 4-8 hours. Therefore, the release pattern of retinol became erratic. Further studies need to be performed to investigate retinol release from ethosomes by using Strat-M.

9.6. CONCLUSION

In this study, ethosome formulations were developed to entrap the three well known anti-aging ingredients, namely trans-resveratrol, retinol, and hydrolyzed collagen.

First of all, the base formulations to produce stable ethosomes were developed by using synthetic phosphatidylcholine (Lipoid P75), ethyl alcohol, vitamin E, and water. The stable ethosomes were produced by using a high-shear homogenizer. Reduction was achieved with a microfluidizer. Following the formulations studies, the active materials were entrapped in the ethosomes with an acceptable entrapment efficiency (not less than 89%). The results obtained from the characterization and stability studies showed that the selected formulations were stable during the 180 days that they were tested. The particle size, size distribution, polydispersity index, uniformity, pH were the measurements used to monitor stability. Besides, microscopic imaging was used as part of characterization.

One of the purposes of this study was to show that the ethosomes that are developed can entrap a high amount of those active ingredients used, and they could be good candidates for the new delivery systems. In order to measure the amount of actives, entrapped, analytical methods were developed and validated according to the ICH guidelines. By using these validated methods, the encapsulation efficiency and the release profiles were investigated. The results showed that the ethosomes developed were good candidates to deliver the active ingredients.

On the other hand, the release profiles compared to the simple solutions clearly showed that the ethosomes provided a retarded/sustained release delivery opportunity. When compared, the Strat-M membrane was less permeable to all of the actives than the cellulose acetate membrane (12-14KD). However, due to the ethyl alcohol incompatibility of the strat-M membrane, the release profile of retinol was not evaluated as planned.

One of the future recommendations will be to further investigate the diffusion profiles of the three ingredients through the skin. Also, release profiles of the ethosomes, which are

incorporated into different topical products such as gels, creams with different formulations, can be investigated.



10. REFERENCES

- 1) Bozzuto G, Molinari A. Liposomes as nanomedical devices. *Int J Nanomedicine*. 2015:975–999.
- 2) Touitou E, Dayan N, Bergelson L, Godin B, Eliaz M. Ethosomes - novel vesicular carriers for enhanced delivery: characterization and skin penetration properties. *J Control Release*. 2000:403-18.
- 3) Lasic DD. Applications of Liposomes. *Handbook of Biological Physics*. 1995:491-519.
- 4) Uchida T, Kadhum W, Kanai S, Todo H, Oshizaka T, Sugibayashi K. Prediction of skin permeation by chemical compounds using the artificial membrane, Strat-M™. *Eur J Pharm Sci*. 2015:113-118.
- 5) Zsikó S, Csányi E, Kovács A, et al. Methods to Evaluate Skin Penetration In Vitro. *Scientia Pharmaceutica*. 2019:87,19.
- 6) Chen C, Han D, Cai C, Tang X. An overview of liposome lyophilization and its future potential. *Journal of Controlled Release*. 2010:299-311.
- 7) Holbrook K, Haake A, Scott GA. Structure and function of the developing human skin. *Advances in biology of skin*. 2001:64-101.
- 8) Baumann L. Basic science of the Epidermis. *Cosmetic Dermatology*. Miami: The McGraw-Hill companies; 2002.
- 9) McGrath JA, Eady RAJ, Pope FM. Anatomy and Organization of human skin. *Rook's textbook of dermatology*; 2004.
- 10) Breathnach A. Aspects of epidermal ultrastructure. *J Invest Dermatol*. 1975:2-15.
- 11) Odland G. Structure of the skin. *Physiology, Biochemistry, and Molecular Biology of the Skin*. New York; 1991.
- 12) Lavker R, Matoltsy A. Substructure of keratohyalin granules of the epidermis as revealed by high resolution electron microscopy. *J Ultrastruct Res*. 1971:575-581.
- 13) Lynley A, Dale B. The characterisation of human epidermal filaggrin, a histidine-rich keratin filament-aggregating protein. *Biochim Biophys Acta*. 1983:28-35.
- 14) Rawlings A, Scott I, Harding C, Bowser P. Stratum corneum moisturization at the molecular level. *J Invest Dermatol*. 2004:731-41.
- 15) fowler J. Understanding the Role of Natural Moisturizing Factor in Skin Hydration. *PRACTICAL DERMATOLOGY*. 2012:36-40.
- 16) Baumann L. Acne. *Cosmetic Dermatology*; 2002.
- 17) Sato S, Hiraga K, Nishijima A. Neonatal sebaceous glands: fine structure of sebaceous and dendritic cells. *Acta Derm Venereol*. 1977:279-87.
- 18) Accessory Structures of the Skin. *Boundless Anatomy and Physiology*. 2012.
- 19) Yapar EA. Cilt Beyazlatıcılara Genel Bakış. *Marmara Pharmaceutical Journal*. 2017:48-53.
- 20) Freinkel DRK, Woodley DT. Basic biology of the skin. *The Biology of the Skin: Bartlett, Jones*; 2001.
- 21) Breathnach A, Robins J. Ultrastructural observations on Merkel cells in human foetal skin. *J Anat*. 1970:106-411.
- 22) Pillai S, Cornell M, Oresajo C. Epidermal barrier. *Cosmetic Dermatology*. Durham: Wiley Blasckwell; 2010.
- 23) Wertz PW. Lipids and barrier function of the skin. *Acta Derm Venereol Suppl (Stockh)*. 2000:7-11.

- 24) Weller RB, Hunter HJA, Mann MW. The Function and Structure of the Skin. *Clinical Dermatology*, 2014:10-33.
- 25) Baumann L. Basic of the dermis. *Cosmetic Dermatology*. Miami: The McGraw-Hill companies; 2002.
- 26) Paul A.J. Kolarsick BMAKCG. Anatomy and Physiology of the Skin; 2011.
- 27) Shuster S, Black M, McVitie E. The influence of age and sex on skin thickness, skin collagen and density. *Br J Dermatol*. 1975:639-43.
- 28) Baumann L. Skin ageing and its treatment. *J Pathol*. 2007:241-251.
- 29) El-Domyati M, Attia S, Saleh F, et al. Intrinsic aging vs. photoaging: a comparative histopathological, immunohistochemical, and ultrastructural study of skin. *Exp Dermatol*. 2002:398-405.
- 30) Farage M, Miller K, Elsner P, Maibach H. Structural characteristics of the aging skin: a review. *Cutan Ocul Toxicol*. 2007:343-57.
- 31) Stevenson S, Thornton J. Effect of estrogens on skin aging and the potential role of SERMs. *Clinical Interventions in Aging*. 2007:283-97.
- 32) Baumann L. Hormones and Aging skin. *Cosmetic dermatology*. USA: The McGraw-Hill Companies; 2002.
- 33) Kim DU, Chung HC, Choi J, Sakai Y, Lee BY. Oral Intake of Low-Molecular-Weight Collagen Peptide Improves Hydration, Elasticity, and Wrinkling in Human Skin: A Randomized, Double-Blind, Placebo-Controlled Study. *Nutrients*. 2018:1-13.
- 34) Gordon J, Brieva J. Images in clinical medicine. Unilateral dermatoheliosis. *N Engl J Med*. 2012:366-382.
- 35) Baumann L. Photoaging. *Cosmetic dermatology*. Miami: The McGraw-Hill Companies; 2002.
- 36) Varani J, Dame MK, Voorhees JJ, et al. Decreased Collagen Production in Chronologically Aged Skin. *Am J Pathol*. 2006:1861-1868.
- 37) Chung JH, Seo JY, Choi HR, et al. Modulation of Skin Collagen Metabolism in Aged and Photoaged Human Skin In Vivo. *J Invest Dermatol*. 2001:1218-24.
- 38) Şen T. Deri Yaşlanması ve Antioksidanların Önemi. *Ankara Ecz. Fak. Derg*. 2016:36-53.
- 39) Pittayapruerk P, Meehansan J, Prapapan O, Komine M, Ohtsuki M. Role of Matrix Metalloproteinases in Photoaging and Photocarcinogenesis. *Int J Mol Sci*. 2016:868.
- 40) Chung J, Seo J, Lee M, et al. Ultraviolet modulation of human macrophage metalloelastase in human skin in vivo. *J Invest Dermatol*. 2002:507-12.
- 41) Taylor C, Stern R, Leyden J, Gilchrest B. Photoaging/photodamage and photoprotection. *J Am Acad Dermatol*. 1990:1-15.
- 42) Seite S, Zucchi H, Septier D, Igondjo-Tchen S, Senni K, Godeau G. Elastin changes during chronological and photo-ageing: the important role of lysozyme. *J Eur Acad Dermatol Venereol*. 2006:980-7.
- 43) Bernstein E, Underhill C, Hahn P, Brown D, Uitto J. Chronic sun exposure alters both the content and distribution of dermal glycosaminoglycans. *Br J Dermatol*. 1996:255-62.
- 44) Tobin D. Introduction to skin aging. *J Tissue Viability*. 2017:37-46.
- 45) Baumann L, Lazarus MC. The use of cosmeceutical moisturizers. *Dermatologic Therapy*. 2002: Volume 14, Issue 3.

- 46) Kışlalıoğlu MS. Dermakozmetik/Kozmesötik kavramına genel bakış. *Dermakozmetik/Kozmesötik Madde ve Ürünler*. İstanbul: Nobel kitapevi; 2016.
- 47) Kligman A. Cosmetics. A dermatologist looks to the future: promises and problems. *Dermatologic Clinics*. 2000:699-709.
- 48) Eken A, Uzun Polat M. Kozmesötik Nemlendiricilerin Yapısına Katılan Biyolojik Aktif Maddeler. *Türkiye Klinikleri J Cosmetol*. 2002:200-205.
- 49) Kligman A. Cosmeceuticals: Do We Need a new category? *Cosmeceuticals*. Pennsylvania: Marcel Dekker, Inc; 2000.
- 50) Epstein H. Cosmeceutical vehicles. *Clinics in Dermatology*. 2009:453-460.
- 51) Laxmi S Joshi HAP. Herbal Cosmetics and Cosmeceuticals: An Overview. *Natural Products Chemistry & Research*. 2015:2-8.
- 52) Lorencini M, Brohem C, Dieamant G, Zanchin N, Maibach H. Active ingredients against human epidermal aging. *Ageing Res Rev*. 2014:100-15.
- 53) Ackermann M, Ajello M, Allafort A, et al. Detection of the Characteristic Pion-Decay Signature in Supernova Remnants. *Science*. 2013:807-811.
- 54) Francois B, Francisco HGF, Marta M. Inequality of Opportunity in Brazil: A Corrigendum. *Income and Wealth*. 2013:551-555.
- 55) Wu G, Xiao M, Yang C, Yu, Y. U2 snRNA is inducibly pseudouridylated at novel sites by Pus7p and snR81 RNP. *EMBO J*. 2011:79-89.
- 56) Rabe J, Mamelak A, McElgunn P, Morison W, Sauder D. Photoaging: Mechanisms and repair. *Journal of the American Academy of Dermatology*. 2006:1-19.
- 57) Yaar M, Gilchrist B. Photoageing: mechanism, prevention and therapy. *Br J Dermatol*. 2007:874-87.
- 58) Fisher G, Kang S, Varani J, et al. Mechanisms of photoaging and chronological skin aging. *Arch Dermatol*. 2002:1462-70.
- 59) Sander C, Chang H, Salzman S, et al. Photoaging is associated with protein oxidation in human skin in vivo. *J Invest Dermatol*. 2002:618-25.
- 60) Murray J, Burch J, Streilein R, Iannacchione M, Hall R, Pinnell S. A topical antioxidant solution containing vitamins C and E stabilized by ferulic acid provides protection for human skin against damage caused by ultraviolet irradiation. *J Am Acad Dermatol*. 2008:418-25.
- 61) Ramos Silva M CLRSSFCA. Anti-aging cosmetics: facts and controversies. *Clin Dermatol*. 2013:750-758.
- 62) Green HN, Mellanby E. VITAMIN A AS AN ANTI-INFECTIVE AGENT. *Br Med J*. 1928:691-696.
- 63) Ramos-e-Silva M, Hexsel D, Rutowitsch M, Zechmeister M. Hydroxy acids and retinoids in cosmetics. *Clin Dermatol*. 2001:460-466.
- 64) Antille C, Tran C, Sorg O, Saurat J. Penetration and metabolism of topical retinoids in ex vivo organ-cultured full-thickness human skin explants. *Skin Pharmacol Physiol*. 2004:124-8.
- 65) Chytil F. Retinoic acid: Biochemistry and metabolism. *J Am Acad Dermatol*. 1986:741-747.
- 66) Aström A, Tavakkol A, Pettersson U, Cromie M, Elder J, Voorhees J. Molecular cloning of two human cellular retinoic acid-binding proteins (CRABP). Retinoic acid-induced expression of CRABP-II but not CRABP-I in adult human skin in vivo and in skin fibroblasts in vitro. *J Biol Chem*. 1991:17662-6.
- 67) Giguere V, Ong E, Segui P, Evans R. Identification of a receptor for the morphogen retinoic acid. *Nature*. 1987:624-9.

- 68) Griffiths C, Finkel L, Tranfaglia M, Hamilton T, Voorhees J. An in vivo experimental model for effects of topical retinoic acid in human skin. *Br J Dermatol.* 1993:389-94.
- 69) Maddin S, Lauharanta J, Agache P, Burrows L, Zultak M, Bulger L. Isotretinoin improves the appearance of photodamaged skin: results of a 36-week, multicenter, double-blind, placebo-controlled trial. *J Am Acad Dermatol.* 2000:56-63.
- 70) Orfanos CE, Zouboulis CC, Almond-Roesler B, Geilen CC. Current use and future potential role of retinoids in Dermatology. *Drugs.* 1997:358-88.
- 71) Helander SD. Treatment of Photoaged Skin, Efficacy, tolerability and costs of available agents. *Drugs & Aging.* 1996:12-16.
- 72) Griffiths C, Russman AN, Majmudar G, Singer RS, Hamilton TA, Voorhees aJJ. Restoration of Collagen Formation in Photodamaged Human Skin by Tretinoin (Retinoic Acid). *N Engl J Med.* 1993:530-535.
- 73) Kligman L, Duo C, Kligman A. Topical retinoic acid enhances the repair of ultraviolet damaged dermal connective tissue. *Connect Tissue Res.* 1984:139-50.
- 74) Keller KL, Fenske NA. Uses of vitamins A, C, and E and related compounds in dermatology:a review. *J Am Acad Dermatol.* 1998:611-625.
- 75) Oğuz O, Garip F. Deri Yaşlanmasında Beslenmenin Önemi. *Türkiye Klinikleri Journal of Internal Medical Sciences.* 2005:7-11.
- 76) Sendagorta ELJAR. Topical isotretinoin for photodamaged skin. *J Am Acad Dermatol.* 1992:15-8.
- 77) Griffiths C, Maddin S, Wiedow O, Marks R, Donald A, Kahlon G. Treatment of photoaged skin with a cream containing 0.05% isotretinoin and sunscreens. *J Dermatolog Treat.* 2005:79-86.
- 78) Rolewski S. Clinical review: topical retinoids. *Dermatol Nurs.* 2003:459-65.
- 79) Kang S, Duell E, Fisher G, et al. Application of retinol to human skin in vivo induces epidermal hyperplasia and cellular retinoid binding proteins characteristic of retinoic acid but without measurable retinoic acid levels or irritation. *J Invest Dermatol.* 1995:549-56.
- 80) Antille C, Tran, C, Sorg O, Carraux P, Didierjean L, Saurat J. Vitamin A exerts a photoprotective action in skin by absorbing UVB radiations. *J Invest Dermatol.* 2003:1163-1167.
- 81) Huang Z, Liu Y, Qi G, Zheng SG. Role of Vitamin A in the Immune System. *Journal of Clinical Medicine.* 2018:258.
- 82) Kavas G, Aribal-Kocatürk P, Büyükkaygıncı D. Resveratrol: Is There Any Effect on Healthy Subject? *Biological Trace Element Research.* 2007:250–254.
- 83) Harman D. Aging: A Theory Based on Free Radical and Radiation Chemistry
- 84) Baumann L. Antioxidants. *Cosmetic Dermatology.* Miami: The McGraw-Hill Companies; 2002.
- 85) Addor FAS. Antioxidants in dermatology. *A Bras Dermatol.* 2017:356-362.
- 86) Dunaway S, Odin R, Zhou L, Ji L, Zhang Y, Kadekaro A. Natural Antioxidants: Multiple Mechanisms to Protect Skin from Solar Radiation. *Front Pharmacol.* 2018:392.
- 87) Haigis M, Sinclair D. Mammalian Sirtuins: Biological Insights and Disease Relevance. *Annu Rev Pathol.* 2010:253-95.
- 88) Bayram A, İğci M. Sirtuin Genleri ve İşlevleri. *Fırat Tıp Derg.* 2013:136-140.
- 89) Cameron D. *New study validates longevity pathway: Findings identify universal mechanism for activating anti-aging pathway.* Cambridge 2013.

- 90) Masaki H. Role of antioxidants in the skin: Anti-aging effects. *J Dermatol Sci*. 2010:85-90.
- 91) Lorencini M, Brohem CA, Dieamant GC, Zanchin NIT, Maibach HI. Active ingredients against human epidermal aging. *Ageing Research Reviews*. 2012:100-15.
- 92) Karabulut AB. Resveratrol ve Etkileri. *Turkiye Klinikleri J Med Sci*. 2008:166-169.
- 93) Ricard-Blum S. The Collagen Family. *Cold Spring Harb Perspect Biol*. 2011:1-19.
- 94) Kadler K. Extracellular matrix 1: Fibril-forming collagens. *Protein Profile*. 1995:491-619.
- 95) Martel-Pelletier J, Boileau C, Pelletier J, Roughley P. Cartilage in normal and osteoarthritis conditions. *Best Pract Res Clin Rheumatol*. 2008:351-84.
- 96) Bruckner-Tuderman L, Mitsushashi Y, Schnyder U, Bruckner P. Anchoring Fibrils and Type VII collagen are Absent from Skin in Severe Recessive Dystrophic Epidermolysis Bullosa. *J Invest Dermatol*. 1989:3-9.
- 97) Fratzl P. Collagen. *Collagen: Structure and Mechanics, an Introduction*. Boston, MA: Springer; 2008.
- 98) Miller A, Wray J. Molecular Packing in Collagen. *Nature*. 1971:437-439.
- 99) Fleischmajer R, MacDonald E, Perlish J, Burgeson R, Fisher L. Dermal collagen fibrils are hybrids of type I and type III collagen molecules. *J Struct Biol*. 1990:162-9.
- 100) Niyibizi C, Eyre D. Bone type V collagen: chain composition and location of a trypsin cleavage site. *Connect Tissue Res*. 1989:247-50.
- 101) Biewenga G, Haenen G, Aalst B. The pharmacology of the antioxidant lipoic acid. *Gen Pharmacol*. 1997:315-31.
- 102) Perricone N. Dr. Perricone's 7 Secrets to Beauty, Health, and Longevity: The Miracle of Cellular Rejuvenation; 2006.
- 103) Vinson J, Anamandla S. Comparative topical absorption and antioxidant effectiveness of two forms of coenzyme q10 after a single dose and after long-term supplementation in the skin of young and middle-aged subjects. *international journal of cosmetic science*. 2006:148-148.
- 104) Knott A, Achterberg V, Smuda C, et al. Topical treatment with coenzyme Q10-containing formulas improves skin's Q10 level and provides antioxidative effects. *Biofactors*. 2015:383-90.
- 105) Shindo Y, Witt E, Han D, Epstein W, Packer L. Enzymic and non-enzymic antioxidants in epidermis and dermis of human skin. *J Invest Dermatol*. 1994:122-4.
- 106) Pullar JM, Carr AC, Vissers MCM. The Roles of Vitamin C in Skin Health. *Nutrients*. 2017:866.
- 107) Kishimoto Y, Saito N, Kurita K, Shimokado K, Maruyama N, Ishigami A. Ascorbic acid enhances the expression of type 1 and type 4 collagen and SVCT2 in cultured human skin fibroblasts. *Biochem Biophys Res Commun*. 2013:579-84.
- 108) Parsons K, Maeda N, Yamauchi M, Banes AKB. Ascorbic acid-independent synthesis of collagen in mice. *Am J Physiol Endocrinol Metab*. 2006:1131-1139.
- 109) Tajima S, Pinnell S. Ascorbic acid preferentially enhances type I and III collagen gene transcription in human skin fibroblasts. *J Dermatol Sci*. 1996:250-3.

- 110) Bissett D, Chatterjee R, Hannon D. Photoprotective effect of superoxide-scavenging antioxidants against ultraviolet radiation-induced chronic skin damage in the hairless mouse. *Photodermatol Photoimmunol Photomed*. 1990:56-62.
- 111) Shukla ARAPG. Depletion of reduced glutathione, ascorbic acid, vitamin E and antioxidant defence enzymes in a healing cutaneous wound. *Free Radic Res*. 1997:93-101.
- 112) Lin J, Selim M, Shea C, et al. UV photoprotection by combination topical antioxidants vitamin C and vitamin E. *J Am Acad Dermatol*. 2003:866-74.
- 113) Kameyama K, Sakai C, Kondoh S, et al. Inhibitory effect of magnesium L-ascorbyl-2-phosphate (VC-PMG) on melanogenesis in vitro and in vivo. *J Am Acad Dermatol*. 1996:29-33.
- 114) Matsuda S SHHMOMIM. Inhibitory effects of a novel ascorbic derivative, disodium isostearyl 2-O-L-ascorbyl phosphate on melanogenesis. *Chem Pharm Bull*. 2008.
- 115) Pasonen-Seppänen, Suhonen T, Kirjavainen M, et al. Vitamin C enhances differentiation of a continuous keratinocyte cell line (REK) into epidermis with normal stratum corneum ultrastructure and functional permeability barrier. *Histochem Cell Biol*. 2001:287-97.
- 116) Uchida Y BMQDEPHW. Vitamin C stimulates sphingolipid production and markers of barrier formation in submerged human keratinocyte cultures. *J Invest Dermatol*. 2001:1037-13.
- 117) Mock D. Skin manifestations of biotin deficiency. *Semin Dermatol*. 1991:296-302.
- 118) Gupta A, Bluhm R, Cooper E, Summerbell R, Batra R. Seborrheic dermatitis. *Dermatol Clin*. 2003:401-12.
- 119) Patel D, Swink S, Castelo-Soccio L. A Review of the Use of Biotin for Hair Loss. *Skin Appendage Disord*. 2017:166-169.
- 120) Herman A, Herman A. Caffeine's mechanisms of action and its cosmetic use. *Skin Pharmacol Physiol*. 2013:8-14.
- 121) Koo S, Hirakawa S, Fujii S, Kawasumi M, Nghiem P. Protection from photodamage by topical application of caffeine after ultraviolet irradiation. *Br J Dermatol*. 2007:957-64.
- 122) Kerzendorfer C, O'Driscoll M. UVB and caffeine: inhibiting the DNA damage response to protect against the adverse effects of UVB. *J Invest Dermatol*. 2009:1611-3.
- 123) León-Carmona J, Galano A. Is caffeine a good scavenger of oxygenated free radicals. *J Phys Chem B*. 2011:4538-46.
- 124) Kaul S, Gulati N, Verma D, Mukherjee S, Nagaich U. Role of Nanotechnology in Cosmeceuticals: A Review of Recent Advances. *J Pharm*. 2018:19.
- 125) Radha GV, Sudha Rani T, Sarvani B. A review on proniosomal drug delivery system for targeted drug action. *Journal of Basic and Clinical Pharmacy*. 2013:42-48.
- 126) Patravale VB, Mandawgade SD. Novel cosmetic delivery systems: an application update. *International Journal of Cosmetic Science*. 2008:19-33.
- 127) Hougeir FG, Kircik L. A review of delivery systems in cosmetics. *Dermatologic Ther*. 2012:234-237.
- 128) Nelson Monteiro AMRLRaNMN. Liposomes in tissue engineering and regenerative medicine. *J R Soc Interface*. 2014:11(101).

- 129) Gökçe EH, Özer Ö. Dermakozmetik/Kozmesötik ürünlerde kullanılan yeni taşıyıcı sistemler. *Dermakozmetik*. İstanbul: Nobel kitapevi; 2016.
- 130) Mishra J, Mishra AK. Significant bile salt induced perturbation of niosome membrane: A molecular level interaction study using 1-Naphthol fluorescence. *Colloids and Surfaces B: Biointerfaces*. 2020:1-7.
- 131) Akbarzadeh A, Rezaei-Sadabady R, Davaran S, et al. Liposome: Classification, Preparation, and Applications. *Nanoscale Research Letters*. 2013:1-9.
- 132) Gupta A, Aggarwal G, Singla S, Arora R. Transfersomes: A Novel Vesicular Carrier for Enhanced Transdermal Delivery of Sertraline: Development, Characterization, and Performance Evaluation. *Sci Pharm*. 2012:1061-80.
- 133) Song Y, Kim C. Topical delivery of low-molecular-weight heparin with surface-charged flexible liposomes. *Biomaterials*. 2006:271-80.
- 134) Amnuakitt T, Limsuwan T, Khongkow PBP. Vesicular carriers containing phenylethyl resorcinol for topical delivery system; liposomes, transfersomes and invasomes. *Asian Journal of Pharmaceutical Sciences*. 2018:472-484.
- 135) Kisk ET, Coldren B, Evans CA, Boyer C, Zasadzinski JA. The Vesosome – A Multicompartment Drug Delivery Vehicle. *Current Medicinal Chemistry*. 2004:1241-1253.
- 136) Fan Y, Fang Y, Ma L. The self-crosslinked ufasome of conjugated linoleic acid: Investigation of morphology, bilayer membrane and stability. *Colloids and Surfaces B: Biointerfaces*. 2014:8-14.
- 137) Aguilar ZP. Targeted Drug Delivery. *Nanomaterials for Medical Applications*; 2013.
- 138) Edwards KA, Baeumner AJ. Analysis of liposomes. *Talanta*. 2006:1432-41.
- 139) Bangham AD, Watkins JC, Standish MM. Diffusion of univalent ions across the lamellae of swollen phospholipids. *Journal of Molecular Biology*. 1965:238-252.
- 140) Sessa G, Weissmann G. Phospholipid spherules (liposomes) as a model for biological membranes. *JOURNAL OF LIPID RESEARCH*. 1968:310-318.
- 141) Mazda F, Özer AY. Kozmetoloji ve Dermatolojide Lipozom ve Niozomlar. *J.PHARM. Sci*. 1993:121-128.
- 142) Xing H, Hwang K, Lu Y. Recent Developments of Liposomes as Nanocarriers for Theranostic Applications. *Theranostics*. 2016:1336–1352.
- 143) Sharma A, S. Sharma U. Liposomes in drug delivery: progress and limitations. *International Journal of Pharmaceutics*. 1997:123-140.
- 144) Ceh B, Winterhalter M, Frederok PM, Valliner JJ, Lasic DD. Stealth® liposomes: from theory to product. *Advanced Drug Delivery Reviews*. 1997:165-177.
- 145) Yurdakul A. Lipozomların Yapısı ve Sınıflandırılması. *TEKSTİL ve KONFEKSİYON*. 2007:243-247.
- 146) Papahadjopoulos D, K.Kimelberg H. Phospholipid vesicles (liposomes) as models for biological membranes: Their properties and interactions with cholesterol and proteins. *Progress in Surface Science*. 1974:145-232.
- 147) Yu B, Lee R, Lee L. Microfluidic methods for production of liposomes. *Methods Enzymol*. 2009:129-41.
- 148) Gubernator J. Active methods of drug loading into liposomes: Recent strategies for stable drug entrapment and increased in vivo activity. *Informa Healthcare*. 2011:565-80.

- 149) Dua JS, Rana AC, Bhandari AK. Liposome: Methods of Preparation and Applications. *International Journal of Pharmaceutical Studies and Research*. 2012:14-20.
- 150) Anderson M, Omri A. The Effect of Different Lipid Components on the In Vitro Stability and Release Kinetics of Liposome Formulations. *Journal Drug delivery*. 2004:33-9.
- 151) Burgess,S.<https://www.sigmaaldrich.com/technicaldocuments/articles/biology/liposome-preparation.html>. <https://www.sigmaaldrich.com>. 1998.
- 152) Anwekar H, Patel S, Singhai AK. Liposome- as drug carriers. *International Journal of Pharmacy & Life Sciences*. 2011:945-951.
- 153) Sahil K, Premjeet S, Ajay B, Middha A, Bhawna K. STEALTH LIPOSOMES: A REVIEW. *International Journal of Research in Ayurveda & Pharmacy*. 2011:1534-1538.
- 154) Shashi K, Satinder K, Bharat P. A complete review on:liposomes. *I.Research journal of PHARMACY*. 2012:10-16.
- 155) Andreas W, Karola VU. Liposome Technology for Industrial Purposes. *Journal of Drug Delivery*. 2011(Article ID 591325):1-9.
- 156) Schubert R. Liposome Preparation by Detergent Removal. *Methods Enzymol*. 2003:46-70.
- 157) Singh RA, Sharma Narendra JRC, Tiwari R, Sharma G. A Review on Liposomes as a Topical Drug Delivery. *Indo American Journal of Pharmaceutical Research*. 2013:3420-3432.
- 158) Nkanga CI, Bapolisi AM, Okafor NI, Krause RWM. General Perception of Liposomes: Formation, Manufacturing and Applications. *Liposomes - Advances and Perspectives*. South Africa; 2019.
- 159) Fröhlich M, Brecht V, Peschka-Süss R. Parameters influencing the determination of liposome lamellarity by 31P-NMR. *Chem Phys Lipids*. 2001:103-112.
- 160) Hupfeld S, Holsaeter A, Skar M, Frantzen C, Brandl M. Liposome Size Analysis by Dynamic/Static Light Scattering upon Size Exclusion-/Field Flow-Fractionation. *J Nanosci Nanotechnol*. 2006:3025-31.
- 161) Matsuzaki K, Murase O, Sugishita K, et al. Optical characterization of liposomes by right angle light scattering and turbidity measurement. *Biochimica et Biophysica Acta (BBA) - Biomembranes*. 2000:219-226.
- 162) Hadinoto K, Sundaresan A, Cheow W. Lipid-polymer hybrid nanoparticles as a new generation therapeutic delivery platform: A review. *European Journal of Pharmaceutics and Biopharmaceutics*. 2019:427-443.
- 163) Fissan H, Ristig S, Kaminski H, Asbach C, Epple M. Comparison of different characterization methods for nanoparticle dispersions before and after aerosolization. *Analytical Methods*. 2014:7324-7334.
- 164) Eaton P, Quaresma P, Soares C, Neves C, Almeida M, Pereira E. A direct comparison of experimental methods to measure dimensions of synthetic nanoparticles. *Ultramicroscopy*. 2017:179-190.
- 165) Lars I, Martin B. Determination of the size distribution of liposomes by SEC fractionation, and PCS analysis and enzymatic assay of lipid content. *AAPS PharmSciTech*. 2002: E7.
- 166) GMP guide for manufacturing plants of human medicinal products. 2018.
- 167) Yadav AV, Murthy MS, Shete AS, Sfurti S. Stability Aspects of Liposomes. *Indian Journal of Pharmaceutical Education and Research*. 2010:402-413.

- 168) Li J, Wang X, Zhang T, et al. A review on phospholipids and their main applications in drug delivery systems. *Asian Journal of Pharmaceutical Sciences*. 2014:81-98.
- 169) BOZKIR A, KOÇYİĞİT S. An Investigation of Physical and Chemical Stabilities on Liposomes. *Ankara Üniversitesi Eczacılık Fakültesi Dergisi*. 1995:42-52.
- 170) Negi LM, Garg AK, Chauhan M. Ultradeformable Vesicles: Concept and Execution. *Pharma Times*. 2009:11-14.
- 171) Ita K. Current status of ethosomes and elastic liposomes in dermal and transdermal drug delivery. *Curr Pharm Des*. 2016:5120-5126.
- 172) Jain S, Tiwary, A, Sapra B, Jain, N. Formulation and evaluation of ethosomes for transdermal delivery of lamivudine. *AAPS PharmSciTech*. 2007:1-9.
- 173) Cevc G, Blume G. New, highly efficient formulation of diclofenac for the topical, transdermal administration in ultradeformable drug carriers, Transfersomes. *Biochim Biophys Acta*. 2001:191-205.
- 174) Cevc G. SA, BG. Transdermal drug carriers: Basic properties, optimization and transfer efficiency in the case of epicutaneously applied peptides. *J Control Release*. 1995.
- 175) Rajan R, Jose S, Mukund VPB, Vasudevan DT. Transferosomes - A vesicular transdermal delivery system for enhanced drug permeation. *J Adv Pharm Technol Res*. 2011:138-143.
- 176) Poonam V, Pathak K. Therapeutic and cosmeceutical potential of ethosomes: An overview. *J Adv Pharm Technol Res*. 2010:274-82.
- 177) Touitou E, Inventor. 5,716,638, 1998.
- 178) Kumar KP, P.R.Radhika, T.Sivakumar. Ethosomes-A Priority in Transdermal Drug Delivery. *International Journal of Advances in Pharmaceutical Sciences*. 2010:111-121.
- 179) Gupta NB, Loona S, Khan MU. ETHOSOMES AS ELASTIC VESICLES IN TRANSDERMAL DRUG DELIVERY: AN OVERVIEW. *INTERNATIONAL JOURNAL OF PHARMACEUTICAL SCIENCES AND RESEARCH*. 2017:682-687.
- 180) Patel A, Sharma RK, Trivedi M, Shivaprakash, Panicker A. Ethosomes: A Novel Tool for Transdermal Drug Delivery. *Asian Journal of Research in Chemistry*. 2013:838-841.
- 181) Verma D, Fahr A. Synergistic penetration enhancement effect of ethanol and phospholipids on the topical delivery of cyclosporin A. *J Control Release*. 2004:55-66.
- 182) Elsayed M, Abdallah O, Naggar V, Khalafallah N. Deformable liposomes and ethosomes: Mechanism of enhanced skin delivery. *Int J Pharm*. 2006:60-66.
- 183) JM B, JL T, L. S. There Are Three Common Types of Membrane Lipids. *Biochemistry*. 5th edition. New york: W H Freeman; 2002.
- 184) [Basics on Lipid Chemistry. http://ocw.nagoya-u.jp/files/1/chap1.pdf.](http://ocw.nagoya-u.jp/files/1/chap1.pdf)
- 185) Amina W, Shelley J. Brain Tissue Lipidomics: Direct Probing Using Matrix-assisted Laser. *The AAPS Journal*. 2006: E391-E395.
- 186) Röding J, Ghyczy M. Control of skin Humidity with liposomes, stabilization of skin care oils and lipophilic active substances with liposomes. *SÖFW*. 1991:372-378.

- 187) Lautenschlager H. Liposomes in Dermatological: Part 1. *Cosmet&Toilet*. 1990:89-96.
- 188) OpenStax.
<https://www.wikizeroo.org/index.php?q=aHR0cHM6Ly9lbi53aWtpcGVkaWEub3JnL3dpa2kvTGJwaWQtYW5jaG9yZWRFcHJvdGVpbG>.
<https://www.wikizeroo.org>. Mayıs 18, 2016.
- 189) Hagen M, Baker M. Skin penetration and tissue permeation after topical administration of diclofenac. *Curr Med Res Opin*. 2017:1623-1634.
- 190) Vanić Ž. Phospholipid Vesicles for Enhanced Drug Delivery in Dermatology. *J Drug Discov Develop and Deliv*. 2014:2-9.
- 191) González-Rodríguez M, Rabasco A. Charged liposomes as carriers to enhance the permeation through the skin. *Journal Expert Opinion on Drug Delivery*. 2011:857-871.
- 192) Peralta F, Guzmán L, Pérez P, et al. Liposomes can both enhance or reduce drugs penetration through the skin. *Scientific Reports*. 2018.
- 193) Verma DD, Verma S, Blume G, Fahr A. Particle size of liposomes influences dermal delivery of substances into skin. *Int J Pharm*. 2003:141-51.
- 194) Hussain A, Singh S, Sharma D, Webster T, Shafaat K, Faruk A. Elastic liposomes as novel carriers: recent advances in drug delivery. *Int J Nanomedicine*. 2017:5087-5108.
- 195) Guo J, Ping Q, Sun G, Jiao C. Lecithin vesicular carriers for transdermal delivery of cyclosporin A. *International Journal of Pharmaceutics*. 2000:201-207.
- 196) Honeywell-Nguyen PL, Graaff AMD, Groenink HWW, Bouwstra JA. The in vivo and in vitro interactions of elastic and rigid vesicles with human skin. *Biochimica et Biophysica Acta*. 2002:130-140.
- 197) Shio FN, Jennifer R, Dominic S, Eccleston G. A Comparative Study of Transmembrane Diffusion and Permeation of Ibuprofen across Synthetic Membranes Using Franz Diffusion Cells. *Pharmaceutics*. 2010:209-223.
- 198) Kailas DT, Wendy HC. Development and Validation of In Vitro Release Tests for Semisolid Dosage Form Case Study. *Disolution Technology*. 2003:10-15.
- 199) Gharbavi M, Amani J, Kheiri-Manjili H, Danafar H, Sharafi A. Niosome: A Promising Nanocarrier for Natural Drug Delivery through Blood-Brain Barrier. *Adv Pharmacol Sci*. 2018:1-15.
- 200) Wilna L, Engelbrecht E, Wessels A, et al. A Comparative Study of the Release of Active Ingredients from Semisolid Cosmeceuticals Measured with Franz, Enhancer or Flow-Through Cell Diffusion Apparatus. *Journal of Food and Drug Analysis*. 2003:90-99.
- 201) Ng S, Rouse J, Sanderson F, Eccleston G. The relevance of polymeric synthetic membranes in topical formulation assessment and drug diffusion study. *Arch Pharm Res*. 2012:579-93.
- 202) Baker RW. MEMBRANE SEPARATION. *Handbook of Industrial Membranes*; 2015.
- 203) Yoon SH. *Membrane Bioreactor Processes: Processes and Applications*: CRC Press ; 2015.
- 204) Sonam Vats CSTEVS. Emulsion Based Gel Technique: Novel Approach for Enhancing Topical Drug. *International Journal for Pharmaceutical Research Scholars*. 2014:649-660.

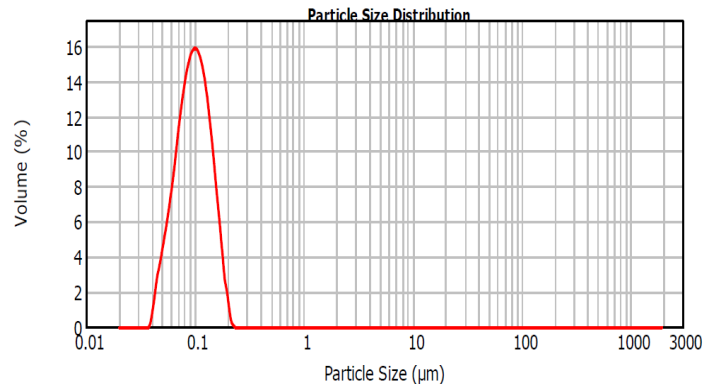
- 205) Joshi V. Substituting Strat-M® membrane for human skin in evaluating effect of encapsulation on diffusion of screen formulations. 2014.
- 206) Agutter P, Malone P, Wheatley D. Diffusion Theory in Biology: A Relic of Mechanistic Materialism. *J Hist Biol.* 2012:71-111.
- 207) Bruschi ML. *Strategies to Modify the Drug Release from Pharmaceutical Systems*: Woodhead Publishing; 2015.
- 208) Watson H. Biological membranes. *Essays Biochem.* 2015:43-69.
- 209) Tırnaksız F. Difüzyon. *Modern Farmasötik Teknoloji*; 2007.
- 210) Florence A, Atwood D. Physicochemical properties of drugs in solution. *Physicochemical Principles of Pharmacy*. London: MacMillan Press; 1988.
- 211) Tırnaksız F. Difüzyon. *Modern Farmasötik Teknoloji*. Ankara: TEB Eczacılık Akademisi; 2009.
- 212) KÜCHLER S, SCHNEIDER C, LERCHE D, SOBISCH T. Process optimisation for making stable emulsions using accelerated dispersion analysis. September 2006.
- 213) [Clark J. High performance liquid chromatography - HPLC.](https://www.chemguide.co.uk) <https://www.chemguide.co.uk>. 2007. Available at: <https://www.chemguide.co.uk/analysis/chromatography/hplc.html>.
- 214) Kippax P. Measuring Particle Size Using Modern Laser Diffraction Techniques. *CHINA COATINGS JOURNAL*. 2008:30-36.
- 215) Malvern. www.malvernpanalytical.com/en/products/technology/light-scattering/laser-diffraction. www.malvernpanalytical.com. 2019.
- 216) Rojas FS, Cano Pavón JM. Spectrophotometry | Overview. *Reference Module in Chemistry, Molecular Sciences and Chemical Engineering*. 2019:244-248.
- 217) Nichols P, Henson J, Guckert J, Nivens D, White D. Fourier transform-infrared spectroscopic methods for microbial ecology: analysis of bacteria, bacteria-polymer mixtures and biofilms. *J Microbiol Methods*. 1998:79-94.
- 218) Beckmann NJ, Harrick KH. Internal Reflection Spectroscopy. *Optics and Photonics Journal*. 1974:215-245.
- 219) Ojeda JJ, Dittrich M. Fourier Transform Infrared Spectroscopy for Molecular Analysis of Microbial Cells. *Methods Mol Biol*. 2012:187-211.
- 220) *Validation of Analytical Procedures: Text and Methodology*. UK 1995.
- 221) LOWRY O, ROSEBROUGH N, FARR A, RANDALL R. Protein measurement with the Folin phenol reagent. *J Biol Chem*. 1951:265-75.
- 222) Legler G, Müller-Platz C, Mentges-Hettkamp M, Pflieger G, Jülich E. On the chemical basis of the Lowry protein determination. *Anal Biochem*. 1985:278-87.
- 223) Bhalaria MK, Naik S, Misra AN. Ethosomes: a novel delivery system for antifungal drugs in the treatment of topical fungal diseases. *Indian journal of Experimental biology*. 2009:368-375.
- 224) Rakesh R, Anoop KR. Formulation and optimization of nano-sized ethosomes for enhanced transdermal delivery of cromolyn sodium. *J Pharm Bioallied Sci*. 2012:333-40.
- 225) Buonocore D, Lazzeretti A, Tocabens P, et al. Resveratrol-procyanidin blend: nutraceutical and antiaging efficacy evaluated in a placebocontrolled, double-blind study. *Clin Cosmet Investig Dermatol*. 2012:159–165.
- 226) Fratzl P. *Collagen Structure and Mechanics*. USA: Springer US; 2008.
- 227) Sibilla S, Godfrey M, Brewer S, Budh-Raja A, Genovese L. An Overview of the Beneficial Effects of Hydrolysed Collagen as a Nutraceutical on Skin Properties:

- Scientific Background and Clinical Studies. *The Open Nutraceuticals Journal*. 2015:29-42.
- 228) Lozano-Pérez A, A RN, V OC, et al. Silk fibroin nanoparticles constitute a vector for controlled release of resveratrol in an experimental model of inflammatory bowel disease in rats. *PubMed Central - PubMed*. 2014:1-21.
- 229) Pezeshki A, Ghanbarzadeh B, Mohammadi M, Fathollahi I, Hamishehkar, H. Encapsulation of Vitamin A Palmitate in Nanostructured Lipid Carrier (NLC)-Effect of Surfactant Concentration on the Formulation Properties. *Adv Pharm Bull*. 2014:563-568.
- 230) Krishnamoorthi J, Ramasamy P, Shanmugam V, Shanmugam A. Isolation and partial characterization of collagen from outer skin of Sepiapharaonis (Ehrenberg, 1831) from Puducherry coast. *Biochemistry and Biophysics Reports*. 2017:39-45.
- 231) Kumar A, Kumar Dixit C. methods for characterization of nanoparticles. *advances in nanomedicine for the delivery of the therapeutic nucleic acids*. UK: Elviesier; 2017.
- 232) Jain NK. Transfersomes - A Novel Vesicular Carrier for Enhanced Transdermal Delivery: Development, Characterization, and Performance Evaluation. *Drug Development and Industrial Pharmacy*. 2003:013-26.
- 233) Prasanthi D, Lakshmi P. Development of ethosomes with taguchi robust design-based studies for transdermal delivery of alfuzosin hydrochloride. *International Current Pharmaceutical Journal*. 2012:370-375.
- 234) Prasanthi D, Lakshmi P. Vesicles-mechanism of transdermal permeation: a review. *Asian J Pharm Clin Res*. 2012:1-21.
- 235) Dave V, Kumar D, Lewis S, Paliwal S. Ethosome for Enhanced Transdermal Drug Delivery of Aceclofenac. *International Journal of Drug Delivery*. 2010:81-92.
- 236) Pandey V, Golhani D, Shukla R. Ethosomes: versatile vesicular carriers for efficient transdermal delivery of therapeutic agents. *Drug Delivery*. 2015:988-1002.
- 237) Abdulbaqi I, Darwis Y, Khan N, Assi R, Khan A. Ethosomal nanocarriers: the impact of constituents and formulation techniques on ethosomal properties, in vivo studies, and clinical trials. *Int J Nanomedicine*. May 2016;25(11):2279-304.
- 238) Pandey A,VD,CS,SS,NG,KCD. Long-term dietary exposure to low concentration of dichloroacetic acid promoted longevity and attenuated cellular and functional declines in aged Drosophila melanogaster. *Age (Dordr)*. 2014:36(3): 9628.
- 239) https://www.merckmillipore.com/TR/tr/product/Strat-M-Membrane-for-Transdermal-Diffusion-Testing,MM_NF-C112892.
https://www.merckmillipore.com/TR/tr/product/Strat-M-Membrane-for-Transdermal-Diffusion-Testing,MM_NF-C112892. 2020.
- 240) Komsa-Penkova R, Spirova R, Bechev B. Modification of Lowry's method for collagen concentration measurement. *J Biochem Biophys Methods*. 1996:33-43.
- 241) Kane M, Folias A, Napoli J. HPLC/UV quantitation of retinal, retinol, and retinyl esters in serum and tissues. *Anal Biochem*. 2008:71-9.
- 242) Baumann L. Fat and the Subcutaneous Layer. *Cosmetic Dermatology*. Miami: The McGraw-Hill companies; 2002.
- 243) Saurat, JH., Didierjean, L., Masgrau, E., et al. Topiical retinaldehyde on human skin: biologic effects and tolerance. *J Invest Dermatol*. 1994:770-4

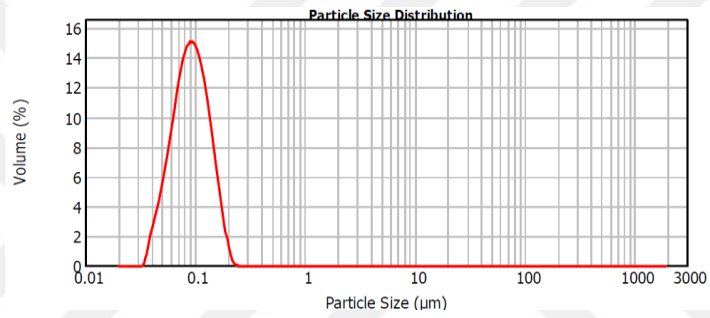
- 244) Salvati, A., Ristori, S., Oberdisse, J., et al. Small angle scattering and zeta potential of Liposomes loaded with octa(carboranyl)porphyrazine. *Journal of Physical Chemistry*.2007:10357-10364



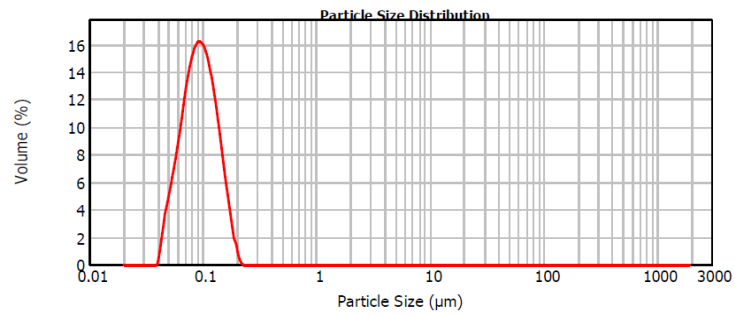
11. ANNEX A: DEVICE OUTPUTS of ANALYZES



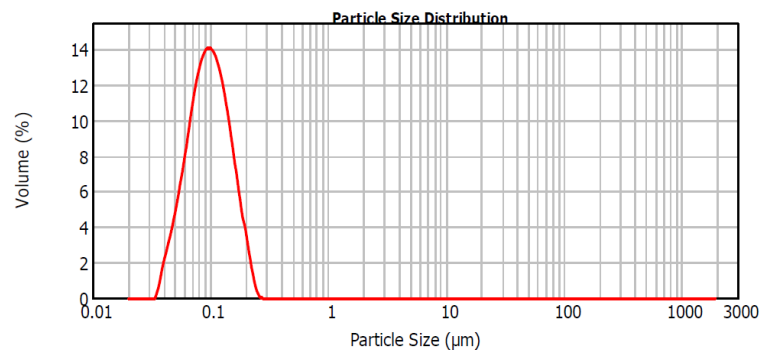
Graph 28.T9 1st-day particle size analysis



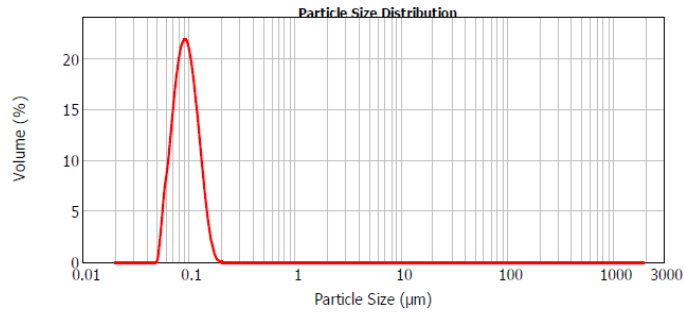
Graph 29.T9 5th-day particle size analysis



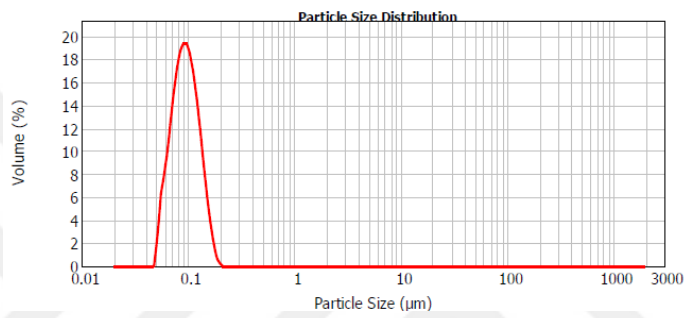
Graph 30.T9 15th-day particle size analysis



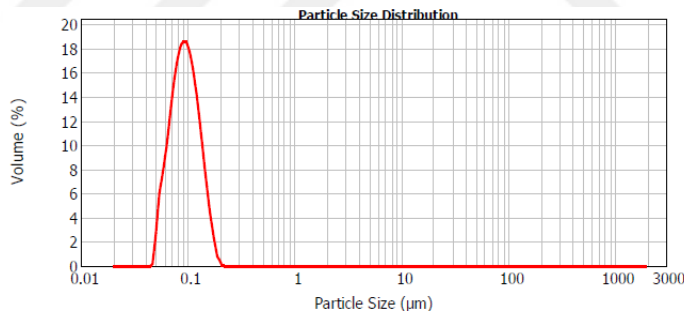
Graph 31.T9 180th-day particle size analysis



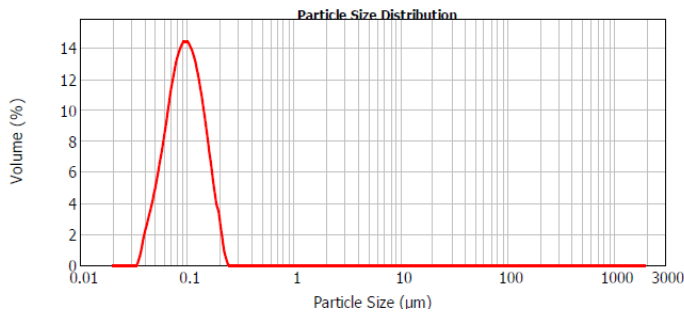
Graph 32.T10 1st-day particle size analysis



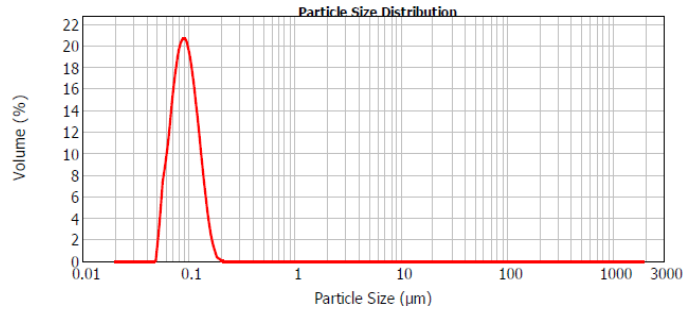
Graph 33.T10 5th-day particle size analysis



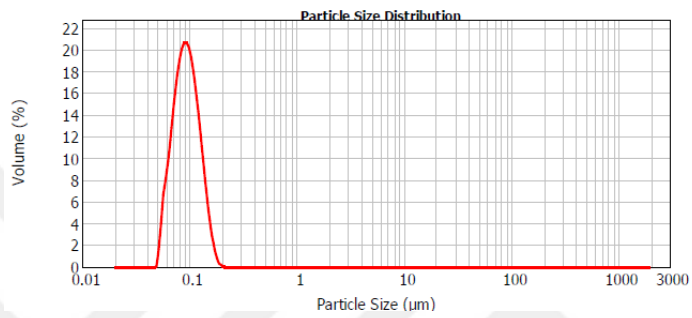
Graph 34.T10 15th-day particle size analysis



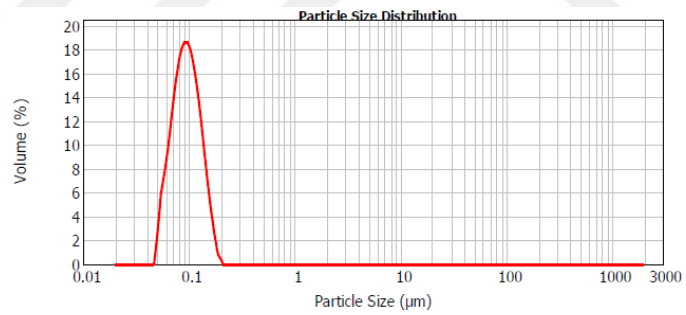
Graph 35.T10 180th-day particle size analysis



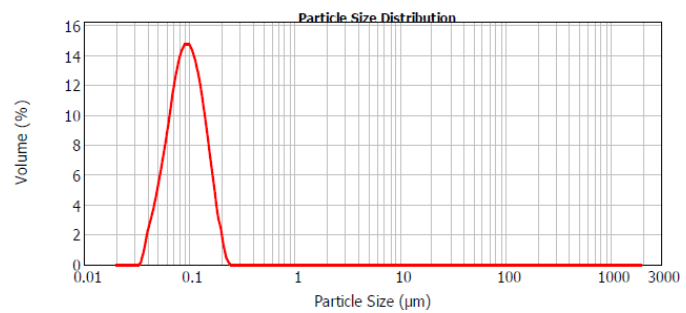
Graph 36.T11 1st-day particle size analysis



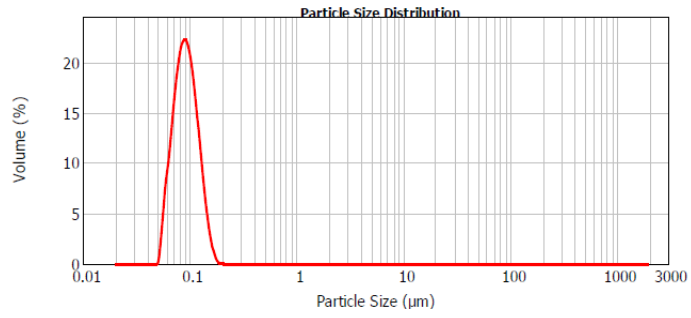
Graph 37.T11 5th-day particle size analysis



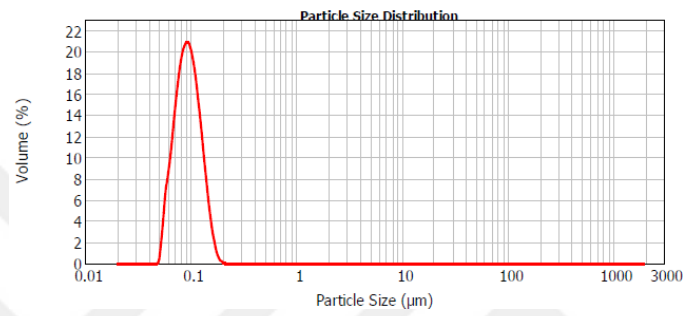
Graph 38.T11 15th-day particle size analysis



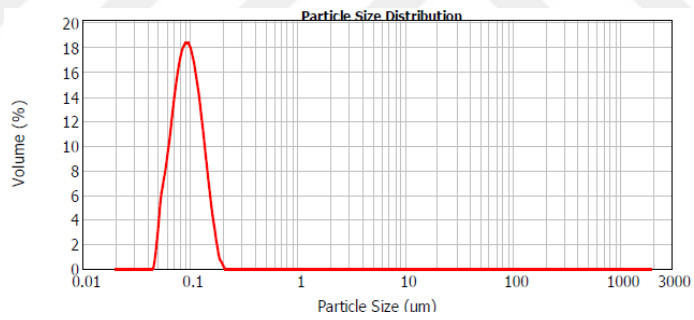
Graph 39.T11 180th-day particle size analysis



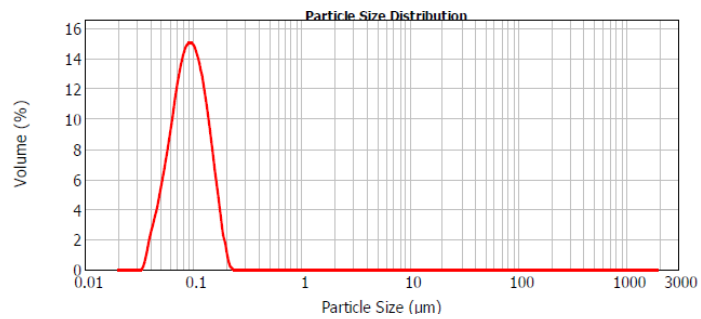
Graph 40.T12 1st-day particle size analysis



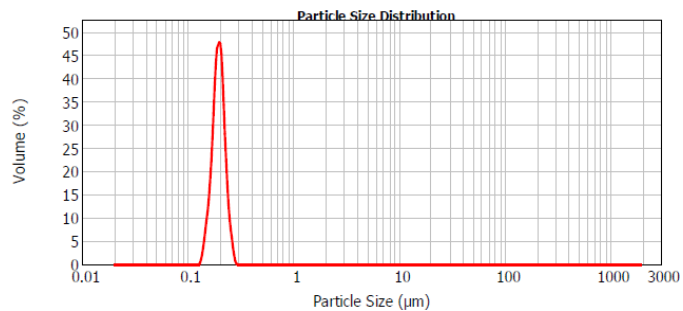
Graph 41.T12 5th-day particle size analysis



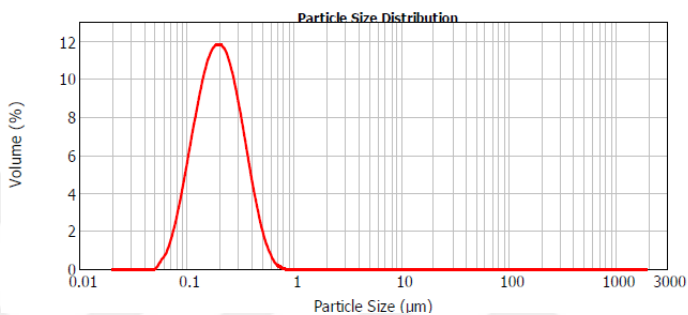
Graph 42.T12 15th-day particle size analysis



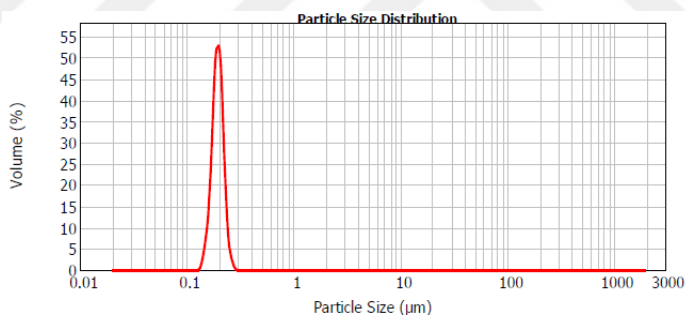
Graph 43.T12 180th-day particle size analysis



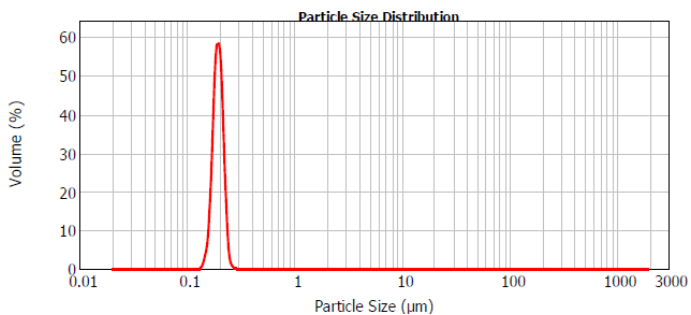
Graph 44.T13 1st-day particle size analysis



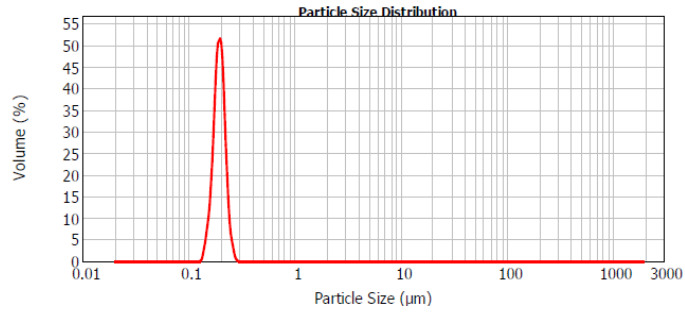
Graph 45.T13 5th-day particle size analysis



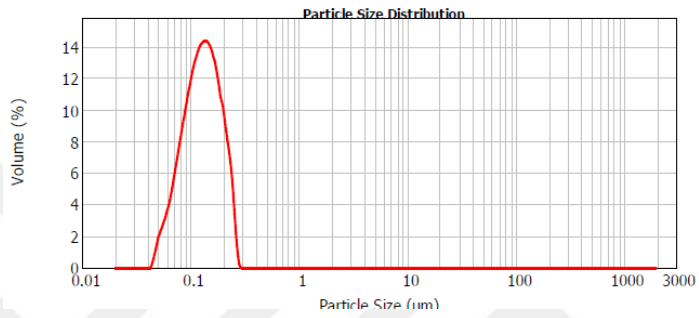
Graph 46.T13 15th-day particle size analysis



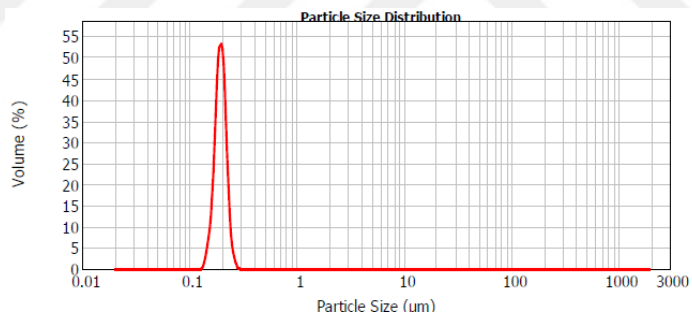
Graph 47.T13 180th-day particle size analysis



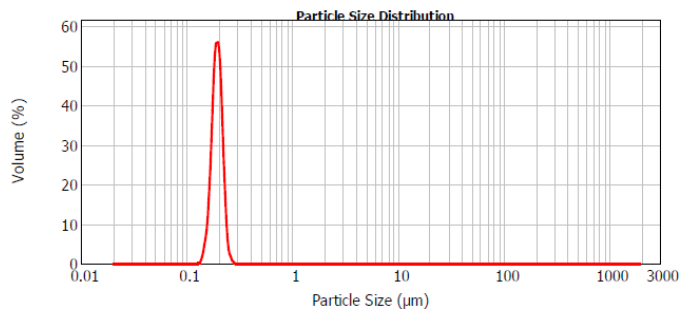
Graph 48.T14 1st-day particle size analysis



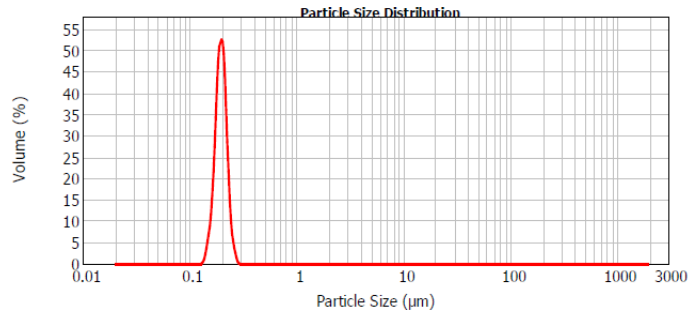
Graph 49.T14 5th-day particle size analysis



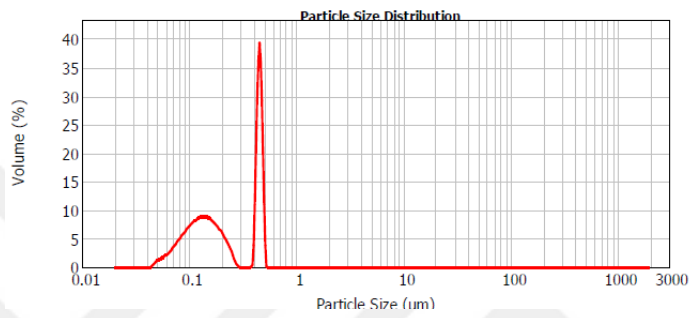
Graph 50.T14 15th-day particle size analysis



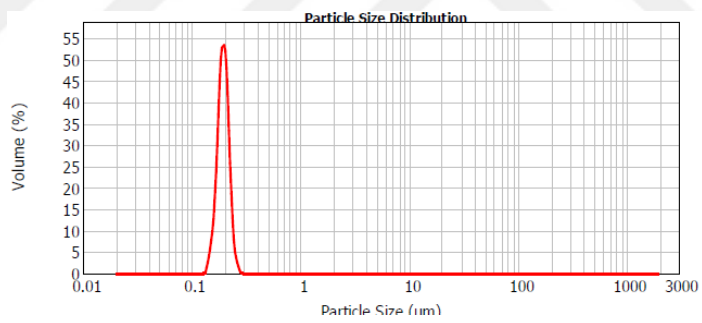
Graph 51.T14 180th-day particle size analysis



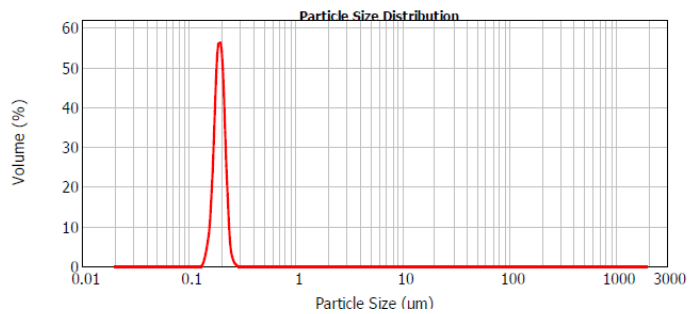
Graph 52.T15 1st-day particle size analysis



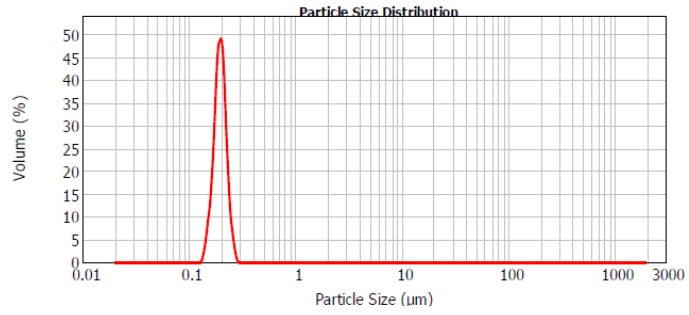
Graph 53.T15 5th-day particle size analysis



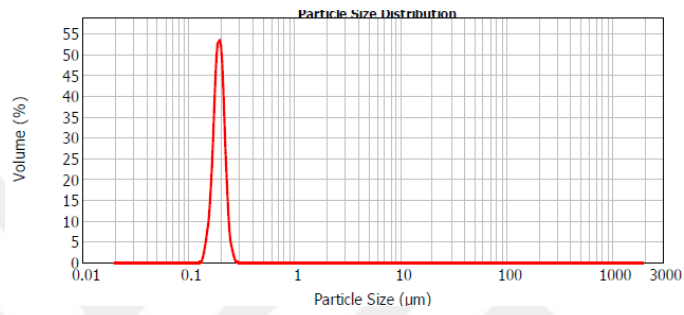
Graph 54.T15 15th-day particle size analysis



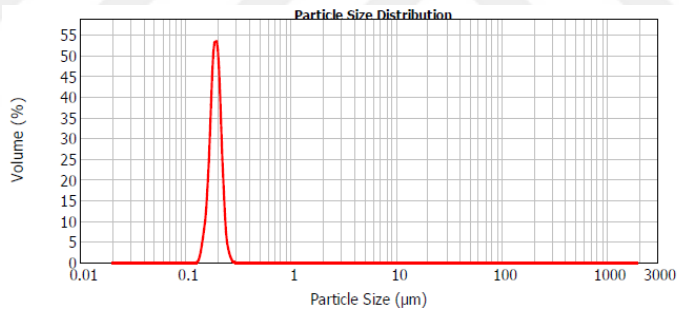
Graph 55.T15 180th-day particle size analysis



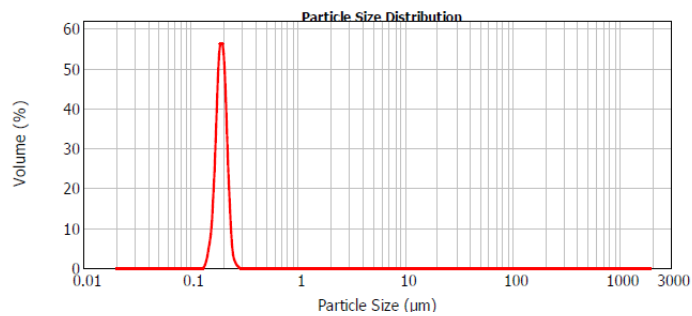
Graph 56.T16 1st-day particle size analysis



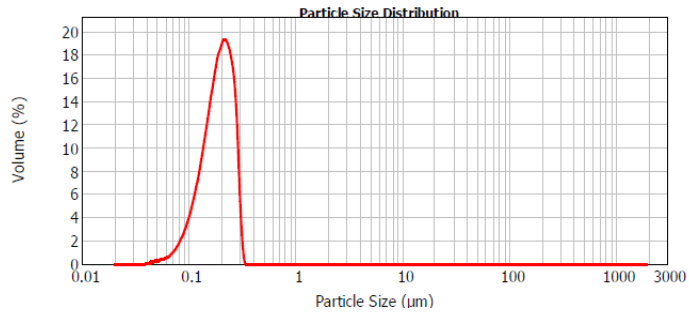
Graph 57.T16 5th-day particle size analysis



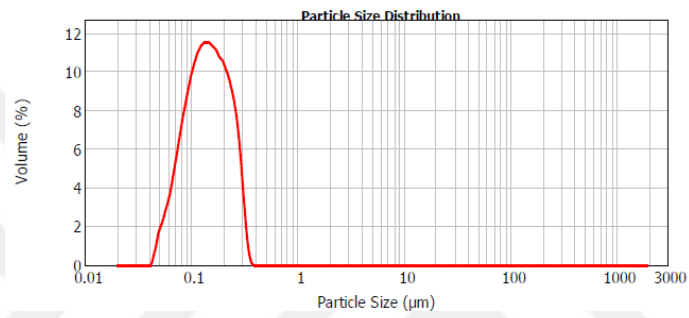
Graph 58.T16 15th-day particle size analysis



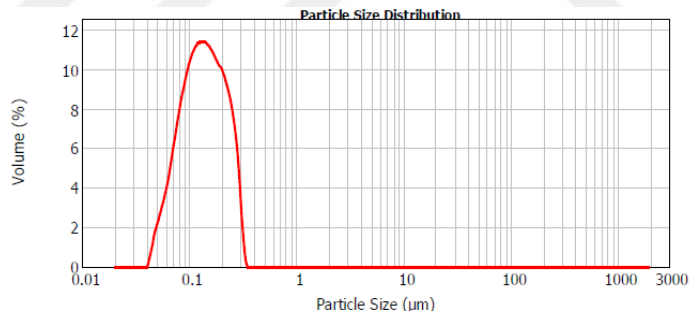
Graph 59.T16 180th-day particle size analysis



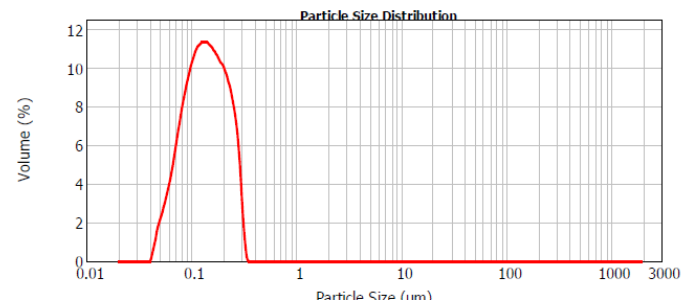
Graph 60.T17 1st-day particle size analysis



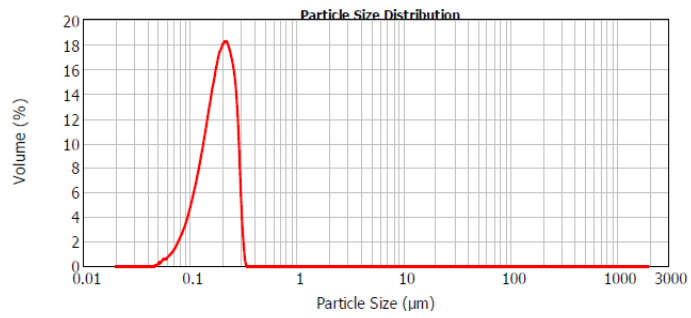
Graph 61.T17 5th-day particle size analysis



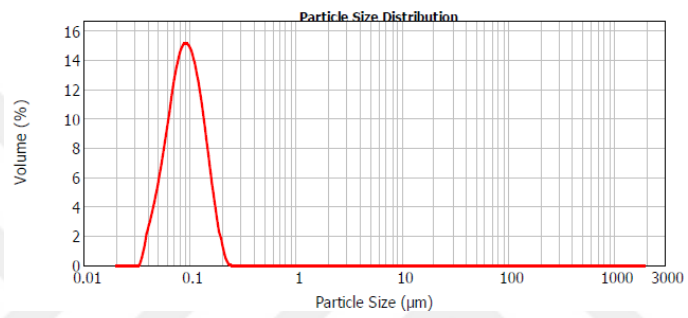
Graph 62.T17 15th-day particle size analysis



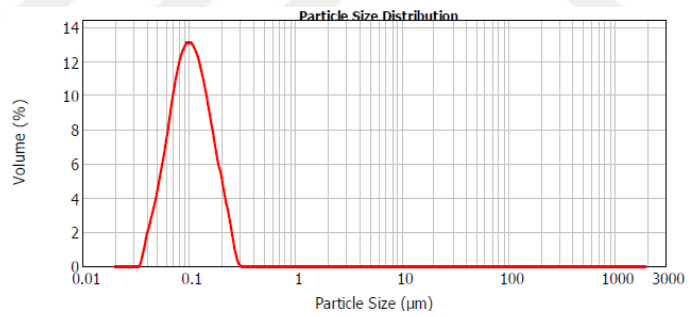
Graph 63.T17 180th-day particle size analysis



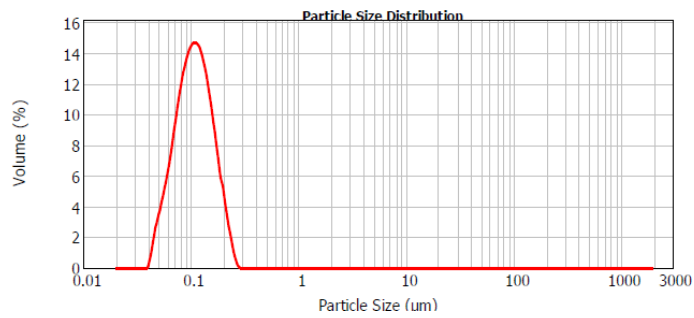
Graph 64.T18 1st-day particle size analysis



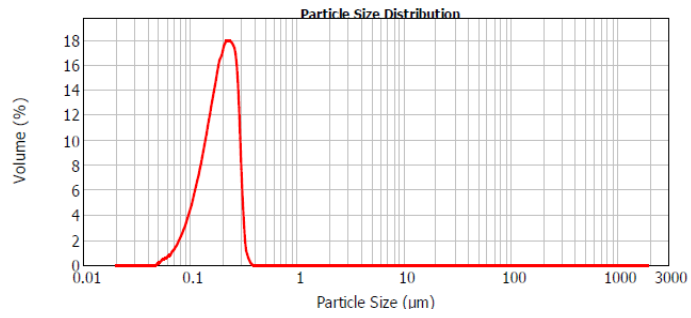
Graph 65.T18 1st-day particle size analysis



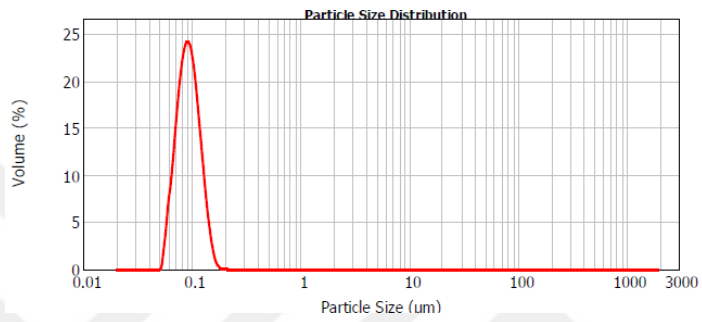
Graph 66.T18 1st-day particle size analysis



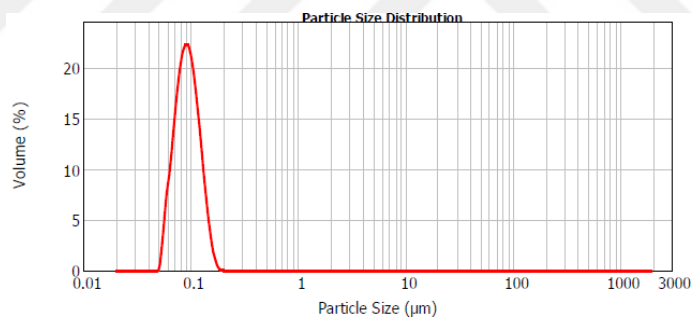
Graph 67.T18 1st-day particle size analysis



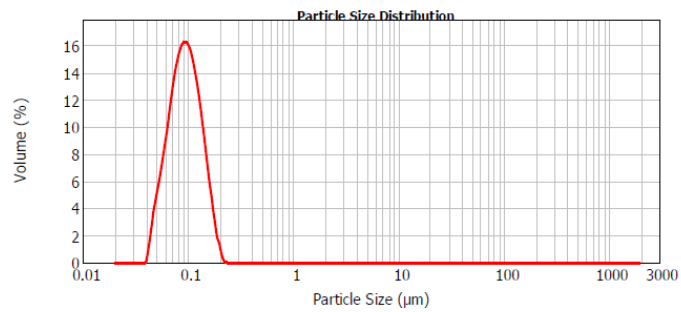
Graph 68.T19 1st-day particle size analysis



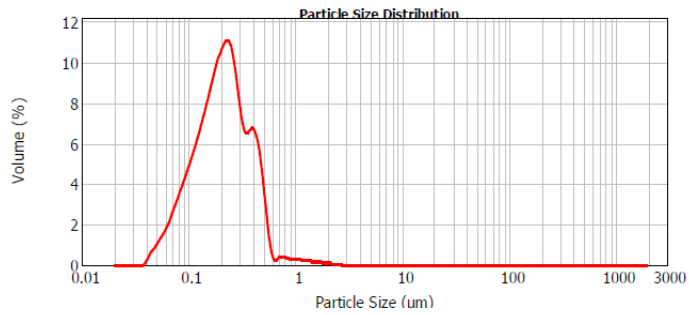
Graph 69.T19 5th-day particle size analysis



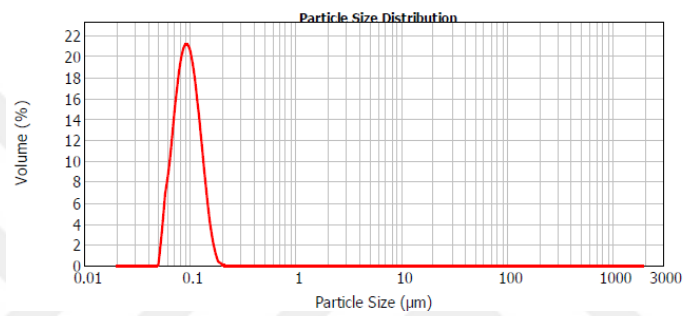
Graph 70.T19 15th-day particle size analysis



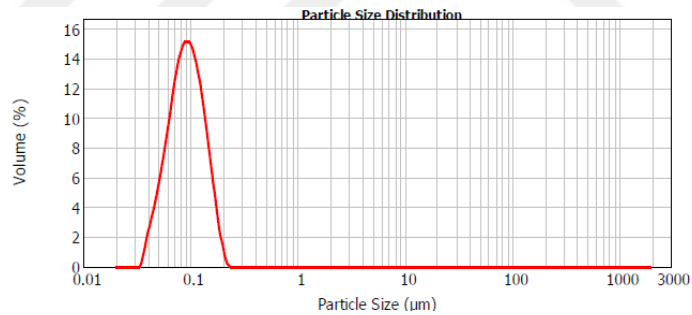
Graph 71.T19 180th-day particle size analysis



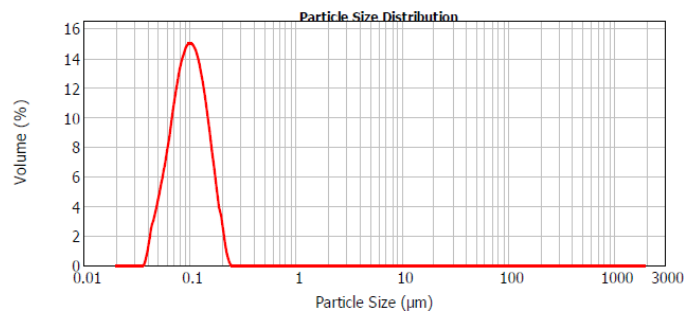
Graph 72.T20 1th day particle size analysis



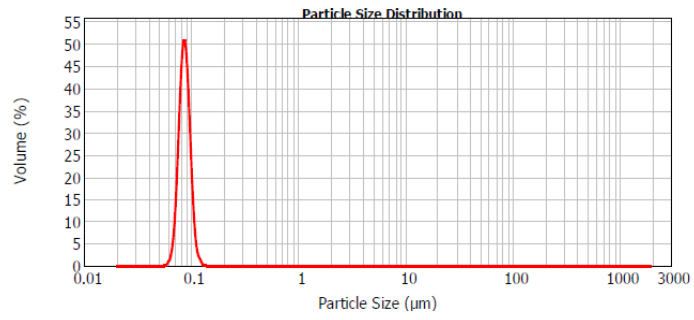
Graph 73.T20 5th-day particle size analysis



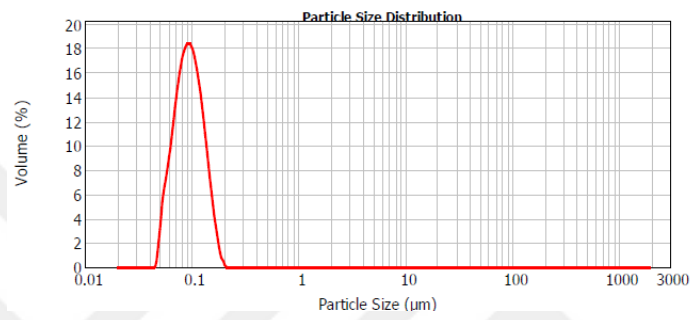
Graph 74.T20 15th-day particle size analysis



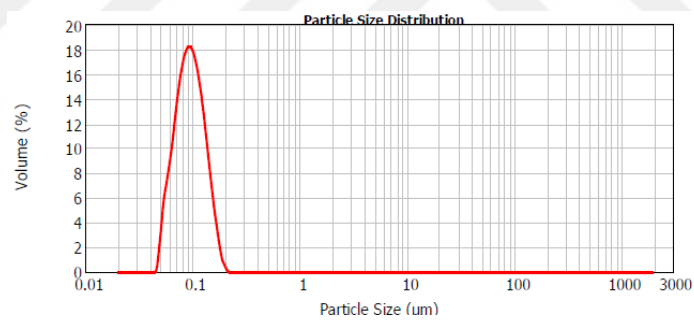
Graph 75.T20 180th-day particle size analysis



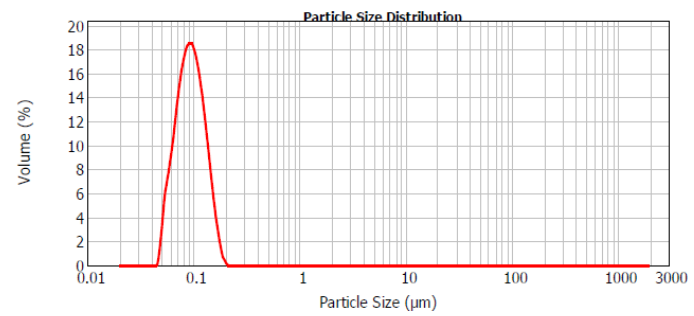
Graph 76.T21 1st-day particle size analysis



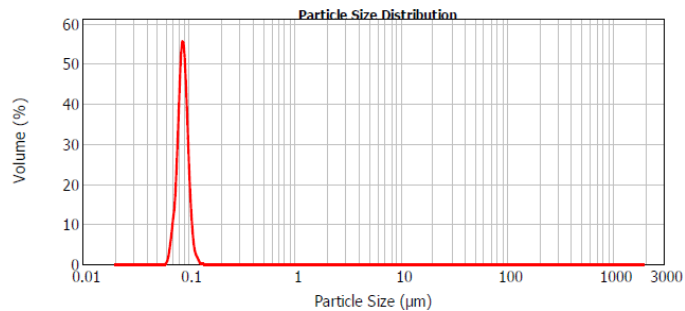
Graph 77.T21 5th-day particle size analysis



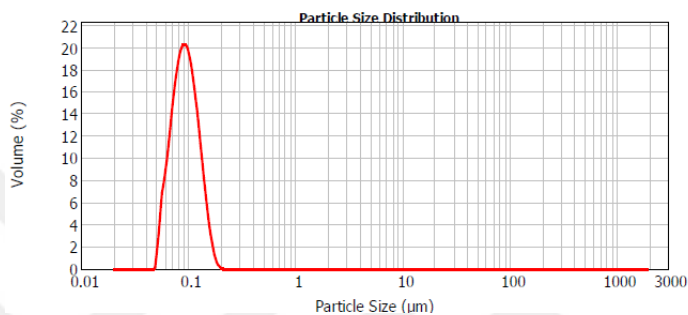
Graph 78.T21 15th-day particle size analysis



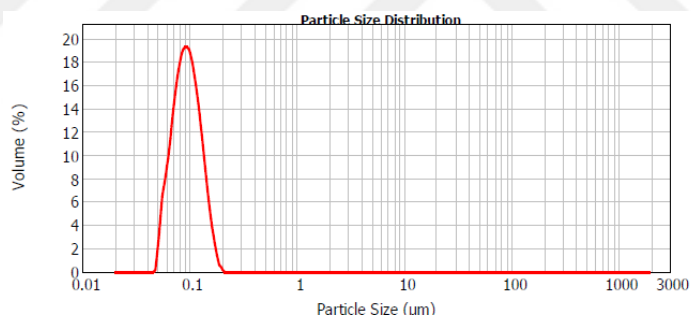
Graph 79.T21 180th-day particle size analysis



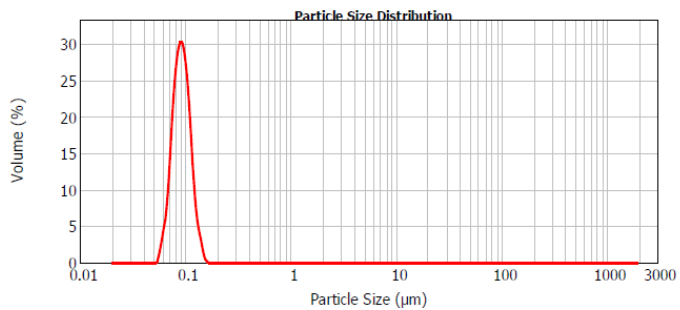
Graph 80.T22 1st-day particle size analysis



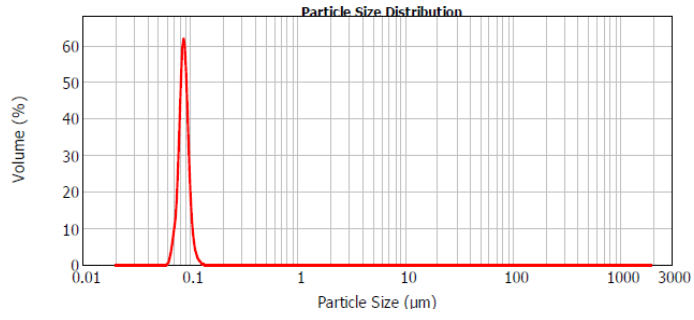
Graph 81.T22 5th-day particle size analysis



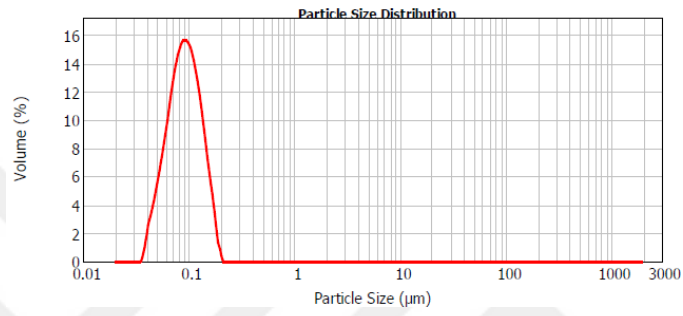
Graph 82.T22 15th-day particle size analysis



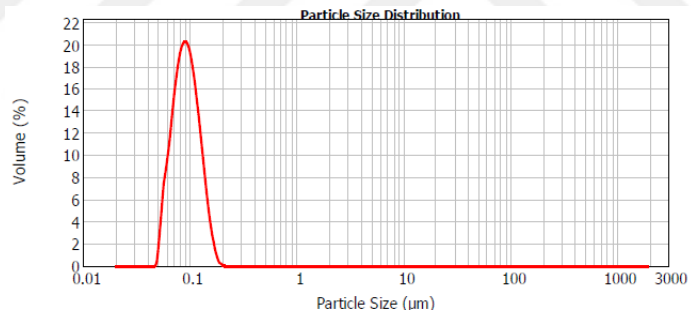
Graph 83.T22 180th-day particle size analysis



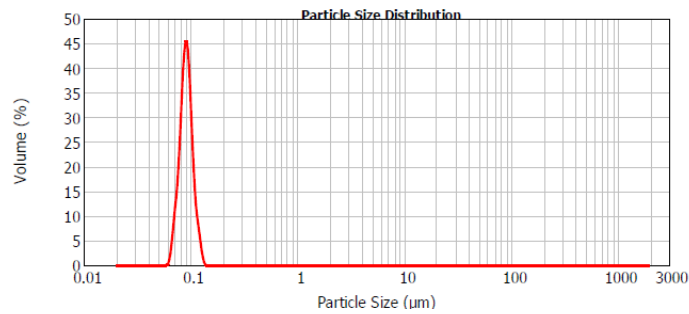
Graph 84.T23 1st-day particle size analysis



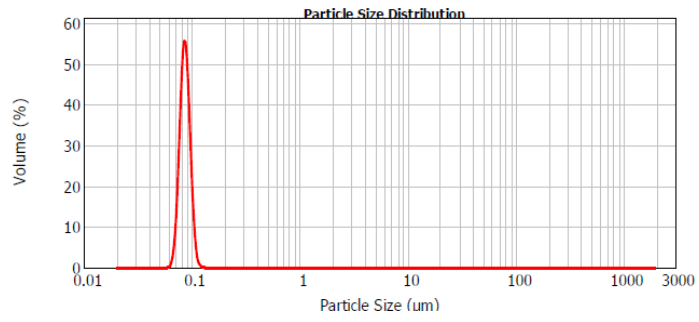
Graph 85.T23 5th-day particle size analysis



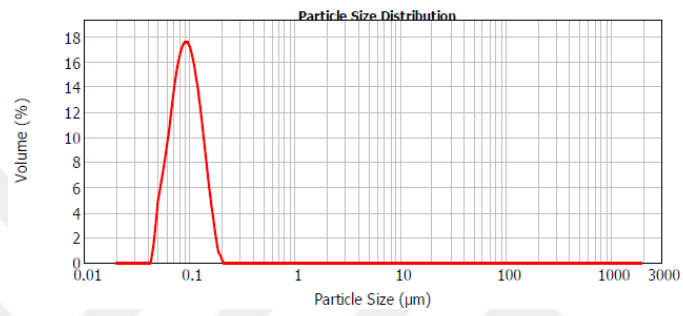
Graph 86.T23 15th-day particle size analysis



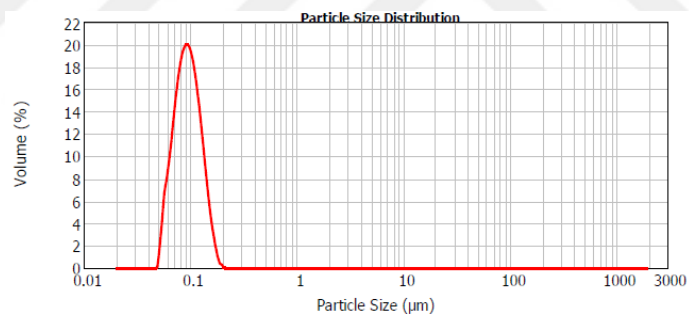
Graph 87.T23 180th-day particle size analysis



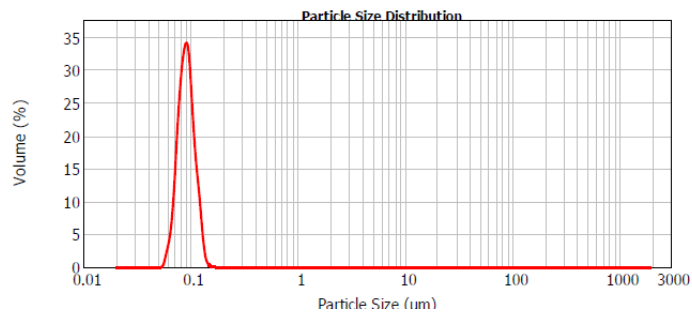
Graph 88.T24 1st-day particle size analysis



Graph 89.T24 5th-day particle size analysis



Graph 90.T24 15th-day particle size analysis

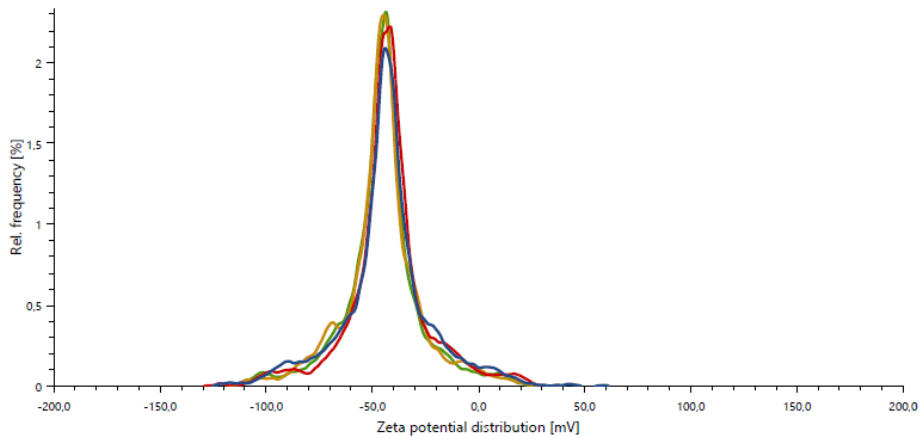


Graph 91.T24 180th-day particle size analysis

Measurements

Name	Temperature [°C]	Processed runs	Mean zeta potential [mV]	Distribution peak [mV]	Conductivity [mS/cm]	Electrophoretic Mobility [μm ² cm/Vs]	Color
T9	25,0	100	-46,6	-43,5	0,040	-3,6334	—
T10	25,0	100	-44,9	-44,6	0,028	-3,4985	—
T11	25,0	100	-43,2	-41,9	0,025	-3,3647	—
T12	25,0	100	-42,9	-44,1	0,025	-3,3454	—

Zeta potential distribution

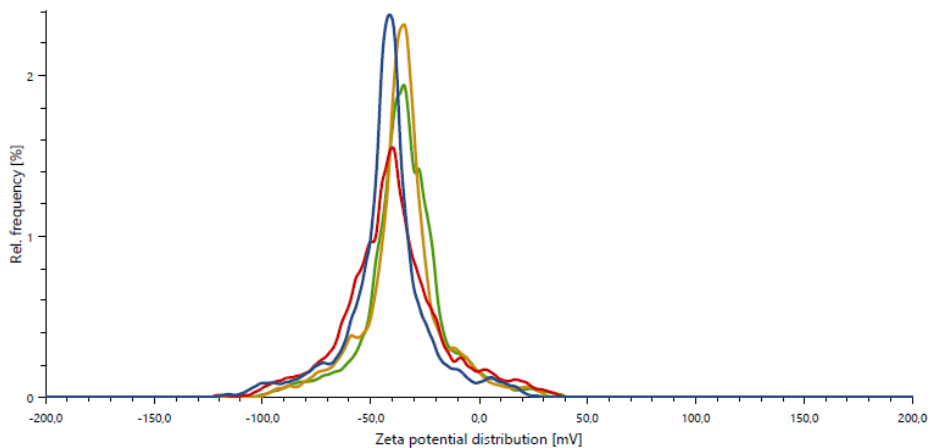


Graph 92. T9-T10-T11-T12 1st-day zeta potentials

Measurements

Name	Temperature [°C]	Processed runs	Mean zeta potential [mV]	Distribution peak [mV]	Conductivity [mS/cm]	Electrophoretic Mobility [μm ² cm/Vs]	Color
T13	25,0	100	-38,7	-34,7	0,010	-3,0178	—
T14	25,0	100	-36,0	-34,8	0,011	-2,8086	—
T15	25,0	100	-39,3	-39,8	0,014	-3,0595	—
T16	25,0	100	-41,2	-41,6	0,011	-3,2096	—

Zeta potential distribution

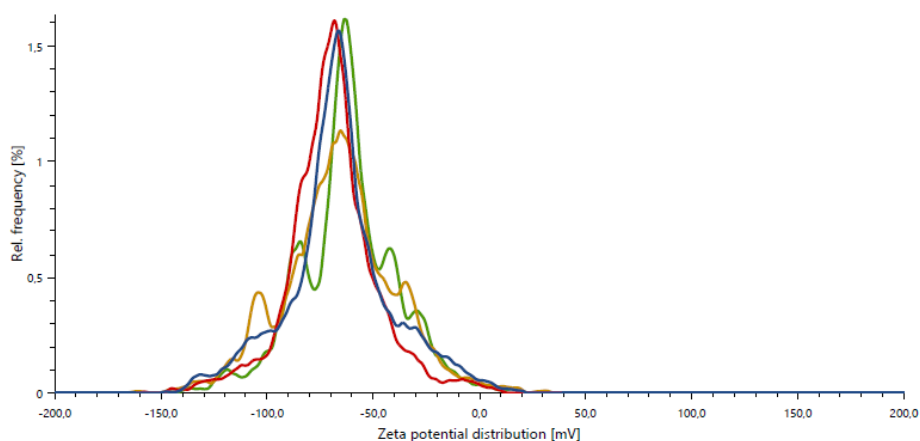


Graph 93. T13-T14-T15-T16 1st-day zeta potentials

Measurements

Name	Temperature [°C]	Processed runs	Mean zeta potential [mV]	Distribution peak [mV]	Conductivity [mS/cm]	Electrophoretic Mobility [$\mu\text{m}^2\text{cm/Vs}$]	Color
T17	25,0	100	-64,1	-63,1	0,015	-4,9934	—
T18	25,0	100	-76,7	-65,6	0,014	-5,9777	—
T19	25,0	100	-66,7	-68,0	0,019	-5,1961	—
T20	25,0	100	-67,2	-66,1	0,014	-5,2399	—

Zeta potential distribution

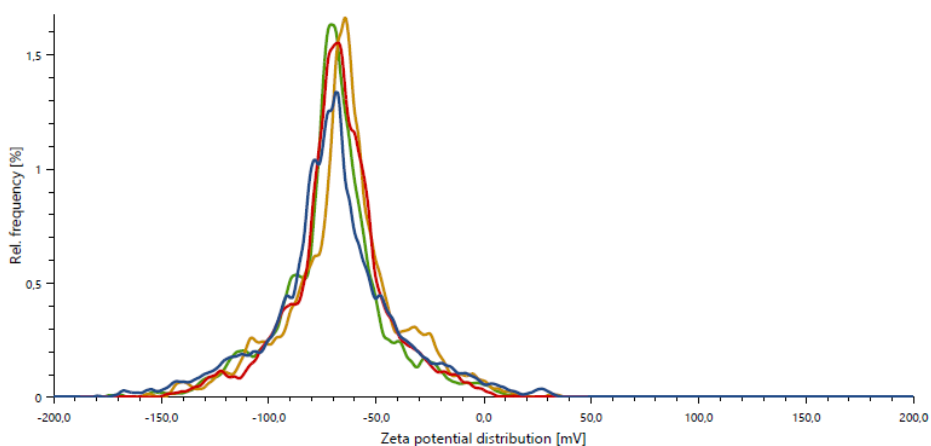


Graph 94.T17-T18-T19-T20 1st-day zeta potentials

Measurements

Name	Temperature [°C]	Processed runs	Mean zeta potential [mV]	Distribution peak [mV]	Conductivity [mS/cm]	Electrophoretic Mobility [$\mu\text{m}^2\text{cm/Vs}$]	Color
T21	25,0	100	-69,4	-70,8	0,039	-5,4121	—
T22	25,0	100	-65,5	-64,6	0,014	-5,1066	—
T23	25,0	100	-70,3	-68,0	0,016	-5,4754	—
T24	25,0	100	-64,8	-68,3	0,015	-5,0519	—

Zeta potential distribution

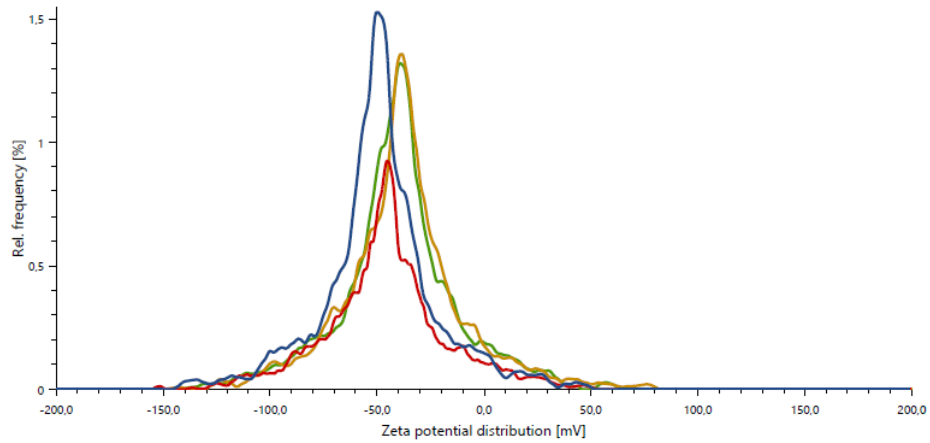


Graph 95.T21-T22-T23-T24 1st-day zeta potentials

Measurements

Name	Temperature [°C]	Processed runs	Mean zeta potential [mV]	Distribution peak [mV]	Conductivity [mS/cm]	Electrophoretic Mobility [μm ² cm/Vs]	Color
T9	25,0	100	-37,3	-39,0	0,034	-2,9032	—
T10	25,0	100	-40,0	-38,6	0,034	-3,1156	—
T11	25,0	180	-43,3	-45,1	0,034	-3,3750	—
T12	25,0	100	-47,9	-49,9	0,034	-3,7326	—

Zeta potential distribution

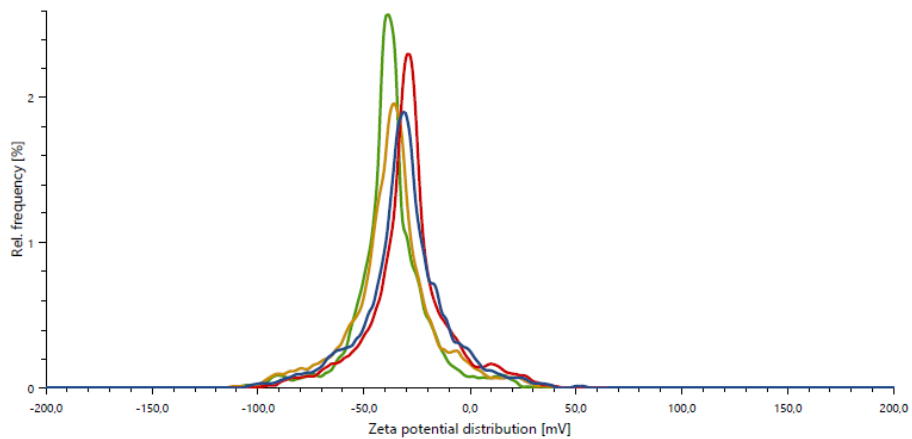


Graph 96.T21-T22-T23-T24 1st-day zeta potentials

Measurements

Name	Temperature [°C]	Processed runs	Mean zeta potential [mV]	Distribution peak [mV]	Conductivity [mS/cm]	Electrophoretic Mobility [μm ² cm/Vs]	Color
T14	25,0	100	-37,5	-39,0	0,017	-2,9242	—
T15	25,0	100	-34,2	-36,1	0,018	-2,6669	—
T16	25,0	100	-29,4	-29,0	0,018	-2,2883	—
T13	25,0	100	-33,9	-31,1	0,018	-2,6434	—

Zeta potential distribution

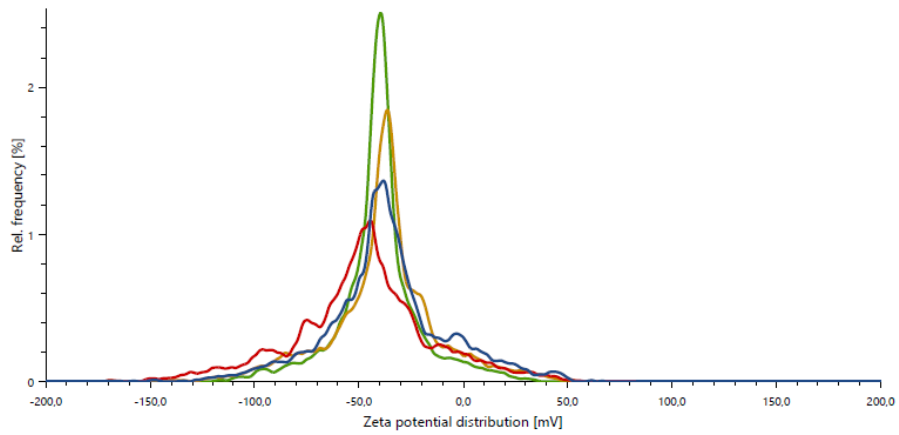


Graph 97.T13-T14-T15-T16 7th-day zeta potentials

Measurements

Name	Temperature [°C]	Processed runs	Mean zeta potential [mV]	Distribution peak [mV]	Conductivity [mS/cm]	Electrophoretic Mobility [μm ² cm/Vs]	Color
T17	25,0	100	-41,3	-39,6	0,022	-3,2152	Green
T18	25,0	100	-39,5	-36,2	0,020	-3,0773	Yellow
T19	25,0	100	-40,7	-44,6	0,022	-3,1709	Red
T20	25,0	100	-40,7	-38,2	0,021	-3,1703	Blue

Zeta potential distribution

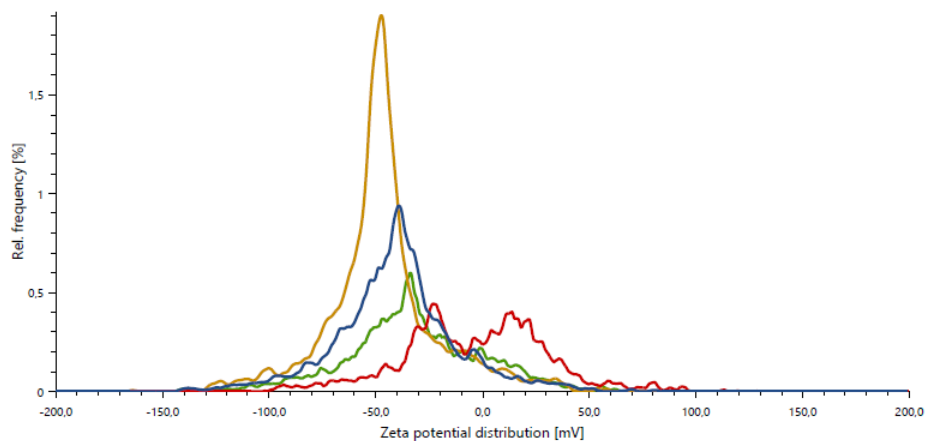


Graph 98. T17-T18-T19-T20 7th-day zeta potentials

Measurements

Name	Temperature [°C]	Processed runs	Mean zeta potential [mV]	Distribution peak [mV]	Conductivity [mS/cm]	Electrophoretic Mobility [μm ² cm/Vs]	Color
T21	25,0	1000	-30,6	-33,7	0,020	-2,3812	Green
T22	25,0	100	-50,6	-47,3	0,020	-3,9398	Yellow
T23	25,0	1000	-30,4	-23,4	0,020	-2,3697	Red
T24	25,0	160	-43,7	-39,1	0,021	-3,4033	Blue

Zeta potential distribution

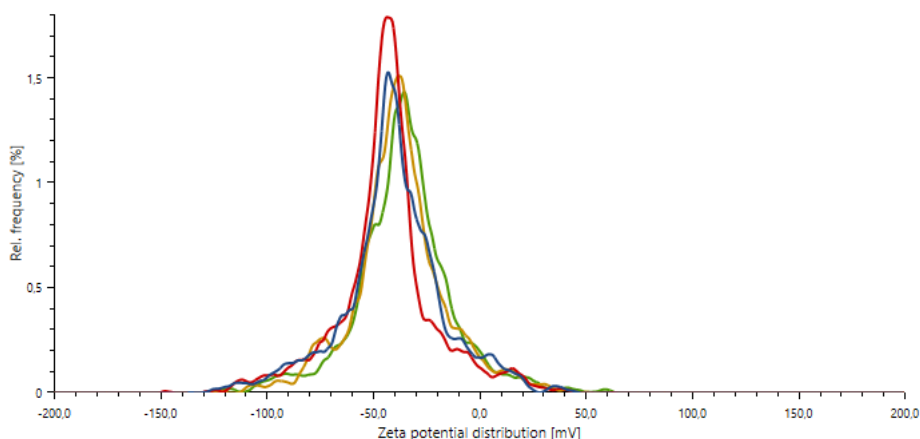


Graph 99. T21-T22-T23-T24 7th-day zeta potentials

Measurements

Name	Temperature [°C]	Processed runs	Mean zeta potential [mV]	Distribution peak [mV]	Conductivity [mS/cm]	Electrophoretic Mobility [μm ² cm/Vs]	Color
T9	25,0	100	-38,8	-35,3	0,043	-3,0274	—
T10	25,0	100	-41,4	-37,6	0,039	-3,2231	—
T11	25,0	100	-43,3	-43,7	0,042	-3,3783	—
T12	25,0	100	-41,1	-42,7	0,041	-3,2039	—

Zeta potential distribution

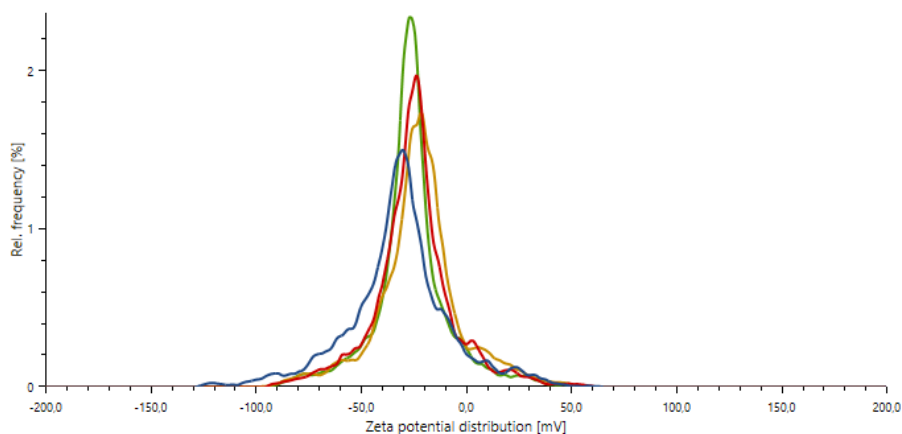


Graph 100. T9-T10-T11-T12 15th-day zeta potentials

Measurements

Name	Temperature [°C]	Processed runs	Mean zeta potential [mV]	Distribution peak [mV]	Conductivity [mS/cm]	Electrophoretic Mobility [μm ² cm/Vs]	Color
T13	25,0	100	-29,0	-26,5	0,025	-2,2578	—
T14	25,0	100	-24,8	-21,3	0,023	-1,9301	—
T15	25,0	100	-24,6	-23,7	0,023	-1,9140	—
T16	25,0	100	-28,5	-30,0	0,023	-2,2186	—

Zeta potential distribution

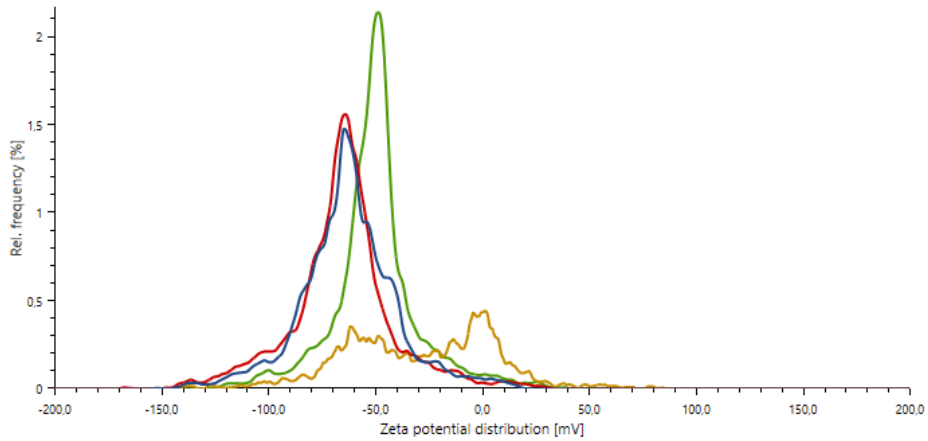


Graph 101. T13-T14-T15-T16 15th-day zeta potentials

Measurements

Name	Temperature [°C]	Processed runs	Mean zeta potential [mV]	Distribution peak [mV]	Conductivity [mS/cm]	Electrophoretic Mobility [μm ² cm/Vs]	Color
T17	25,0	100	-49,5	-48,6	0,028	-3,8575	—
T18	25,0	1000	-52,3	1,3	0,035	-4,0725	—
T19	25,0	100	-61,0	-64,1	0,032	-4,7503	—
T20	25,0	100	-68,3	-64,3	0,034	-5,3222	—

Zeta potential distribution

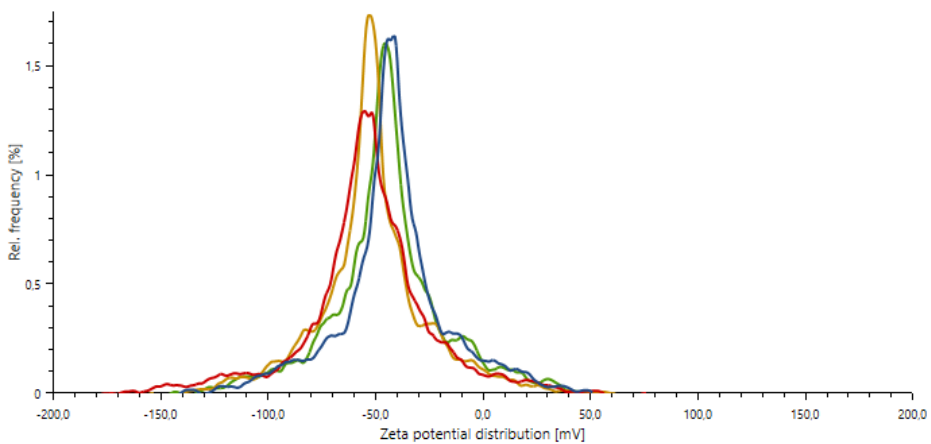


Graph 102.T17-T18-T19-T20 15th-day zeta potentials

Measurements

Name	Temperature [°C]	Processed runs	Mean zeta potential [mV]	Distribution peak [mV]	Conductivity [mS/cm]	Electrophoretic Mobility [μm ² cm/Vs]	Color
T21	25,0	100	-43,4	-45,2	0,025	-3,3863	—
T22	25,0	100	-52,4	-52,7	0,030	-4,0819	—
T23	25,0	100	-51,0	-55,3	0,030	-3,9768	—
T24	25,0	100	-40,7	-41,4	0,026	-3,1723	—

Zeta potential distribution

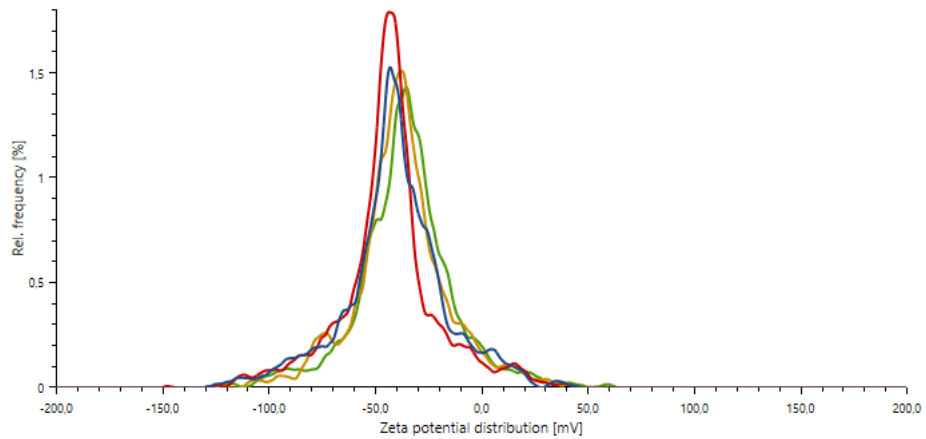


Graph 103.T21-T22-T23-T24 15th-day zeta potentials

Measurements

Name	Temperature [°C]	Processed runs	Mean zeta potential [mV]	Distribution peak [mV]	Conductivity [mS/cm]	Electrophoretic Mobility [μm ² cm/Vs]	Color
T9	25,0	100	-38,8	-35,3	0,043	-3,0274	—
T10	25,0	100	-41,4	-37,6	0,039	-3,2231	—
T11	25,0	100	-43,3	-43,7	0,042	-3,3783	—
T12	25,0	100	-41,1	-42,7	0,041	-3,2039	—

Zeta potential distribution

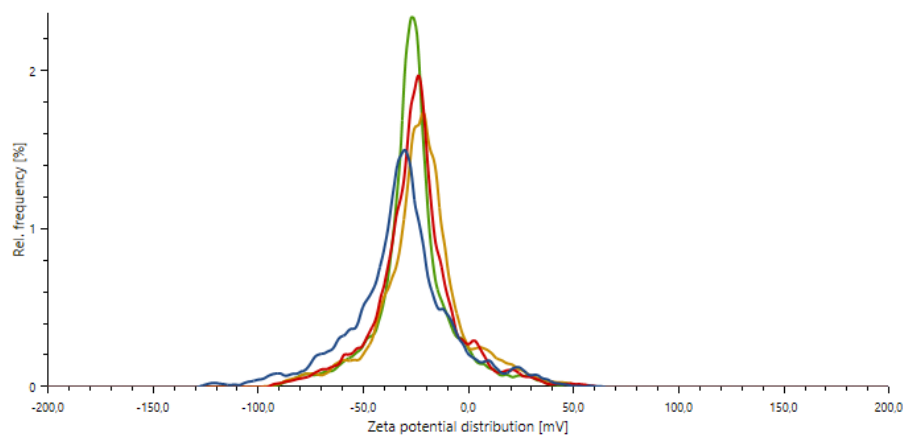


Graph 104. T9-T10-T11-T12 30th-day zeta potentials

Measurements

Name	Temperature [°C]	Processed runs	Mean zeta potential [mV]	Distribution peak [mV]	Conductivity [mS/cm]	Electrophoretic Mobility [μm ² cm/Vs]	Color
T13	25,0	100	-29,0	-26,5	0,025	-2,2578	—
T14	25,0	100	-24,8	-21,3	0,023	-1,9301	—
T15	25,0	100	-24,6	-23,7	0,023	-1,9140	—
T16	25,0	100	-28,5	-30,0	0,023	-2,2186	—

Zeta potential distribution

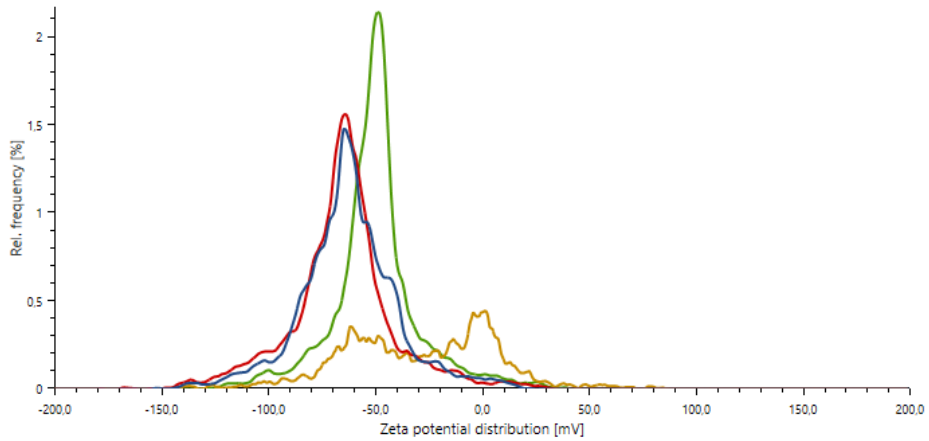


Graph 105. T13-T14-T15-T16 30th-day zeta potentials

Measurements

Name	Temperature [°C]	Processed runs	Mean zeta potential [mV]	Distribution peak [mV]	Conductivity [mS/cm]	Electrophoretic Mobility [μm ² cm/Vs]	Color
T17	25,0	100	-49,5	-48,6	0,028	-3,8575	—
T18	25,0	1000	-52,3	1,3	0,035	-4,0725	—
T19	25,0	100	-61,0	-64,1	0,032	-4,7503	—
T20	25,0	100	-68,3	-64,3	0,034	-5,3222	—

Zeta potential distribution

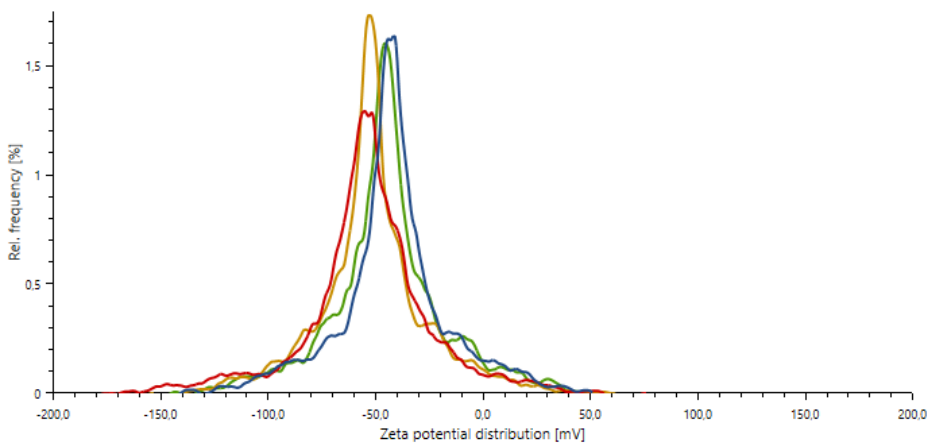


Graph 106.T17-T18-T19-T20 30th-day zeta potentials

Measurements

Name	Temperature [°C]	Processed runs	Mean zeta potential [mV]	Distribution peak [mV]	Conductivity [mS/cm]	Electrophoretic Mobility [μm ² cm/Vs]	Color
T21	25,0	100	-43,4	-45,2	0,025	-3,3863	—
T22	25,0	100	-52,4	-52,7	0,030	-4,0819	—
T23	25,0	100	-51,0	-55,3	0,030	-3,9768	—
T24	25,0	100	-40,7	-41,4	0,026	-3,1723	—

Zeta potential distribution



Graph 107.T21-T22-T23-T24 30th-day zeta potentials

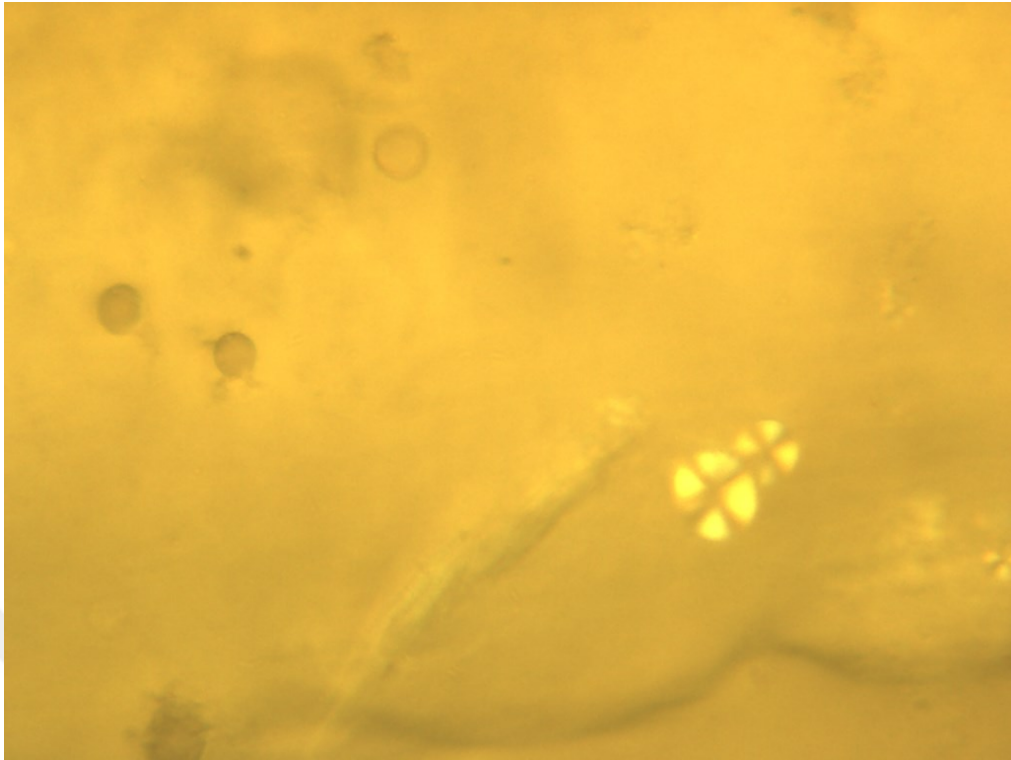


Figure 16. Light refraction image of bilayer layer with a microscope of ethosome

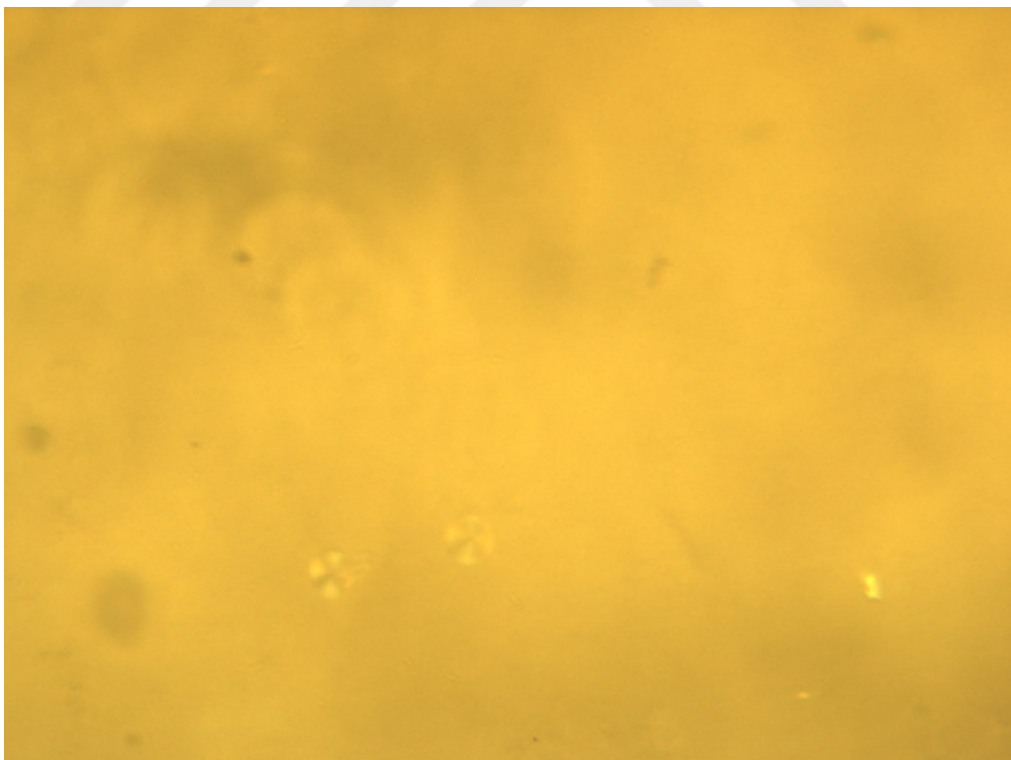


Figure 17. Light refraction image of bilayer layer with a microscope of ethosome

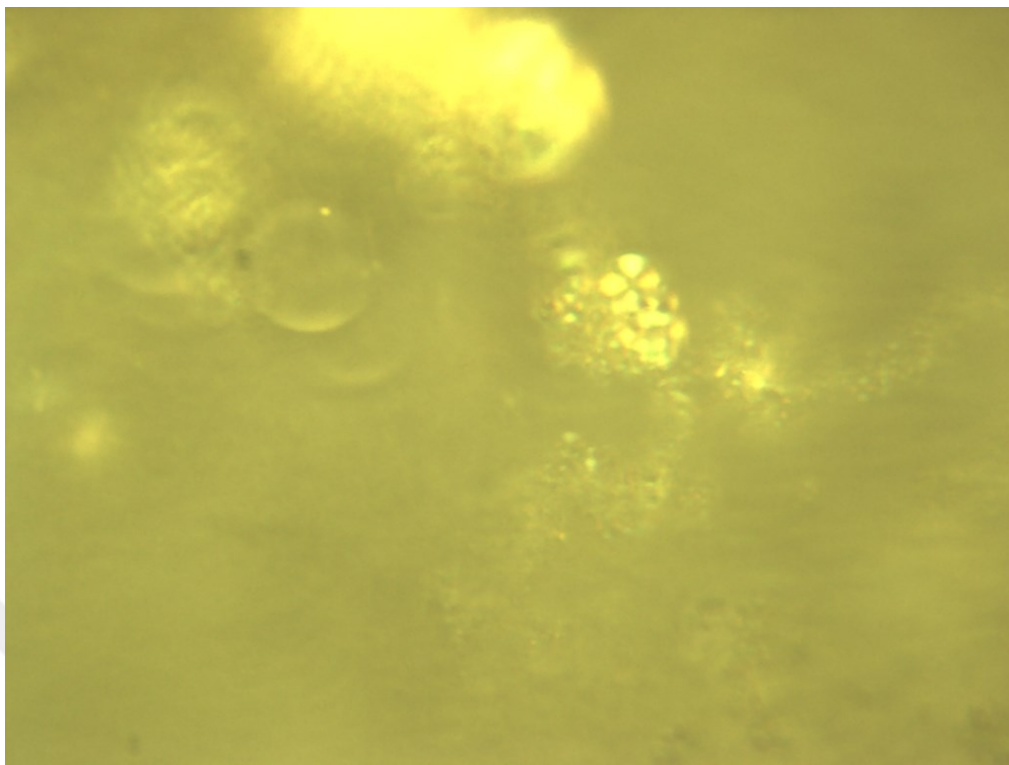


Figure 18. Light refraction image of bilayer layer with a microscope of ethosome

12. ÖZGEÇMİŞ

Kişisel Bilgiler

Adı	Hakan	Soyadı	Sevinç
Doğum Yeri	Gölcük	Doğum Tarihi	2.01.1982
Uyruğu	TC	TC Kimlik No	
E-mail	hakansevinc@gmail.com	Tel	+905424141061

Öğrenim Durumu

Derece	Alan	Mezun Olduğu Kurumun Adı	Mezuniyet Yılı
Doktora	-		
Yüksek Lisans	-		
Lisans	Kimya	Cumhuriyet Üniversitesi	2005
Lise	-		

Bildiği Yabancı Dilleri	Yabancı Dil Sınav Notu (#)

İş Deneyimi (Sondan geçmişe doğru sıralayın)

Görevi	Kurum	Süre (Yıl - Yıl)
Sabun Üretim Müh.	Hayat Kimya A.Ş.	2006-2007
Toz Üretim ve Paketleme Müh.	Hayat Kimya A.Ş.	2007-2008
Kalite Kontrol Sorumlusu	Derma-Cos Kozmetik San.Tic.ith ve ihr.ltd. Şti,	2008-2009
Ar-Ge Proje Sorumlusu- Sap Key User	Derma-Cos Kozmetik San.Tic.ith ve ihr.ltd. Şti,	2009-2011
Ar-Ge Proje Sorumlusu	Biota Bitkisel İlaç ve Kozmetik lab. A.Ş.	2011-2012
Ar-Ge Bölüm Şefi	Biota Bitkisel İlaç ve Kozmetik lab. A.Ş.	2012-2016
Ar-Ge Formülasyon Müdürü	Biota Bitkisel İlaç ve Kozmetik lab. A.Ş.	2016-2019
Ar-Ge Müdürü	Biota Bitkisel İlaç ve Kozmetik lab. A.Ş.	2019-devam ediyor

Bilgisayar Bilgisi

Program	Kullanma becerisi
Ms Office	Çok iyi
SAP R3	Çok iyi
VB, SQL	Orta

*Çok iyi, iyi, orta, zayıf olarak değerlendirin

Bilimsel Çalışmaları

SCI, SSCI, AHCI indekslerine giren dergilerde yayınlanan makaleler

A Comparative Study to Test a Plant Extract against Minoxidil in HaCaT Cells, 01 Haz 2017, American Journal of Dermatology and Venereology
Effect of Ficus carica leaf extract on the gene expression of selected factors in HaCaT cells, 15 Mar 2017, Journal of Cosmetic Dermatology

In vitro Evaluation of Natural Thermal Waters in HaCaT Cells, EADV - european academy of dermatology and venereology

Diğer dergilerde yayımlanan makaleler

-

Uluslararası bilimsel toplantılarda sunulan ve bildiri kitabında (*Proceedings*) basılan bildiriler

Gene expression levels of selected factors in HaCaT cells upon treatment with plant extracts against hair loss, Abstract submitted for IFSCC Conference 2015- Poster Submission ID: 215

Hakemli konferans/sempozyumların bildiri kitaplarında yer alan yayınlar

-

Diğer (Görev Aldığı Projeler/Sertifikalari/Ödülleri)

TEYDEB 1501 - CİSTUS CRETICUS L. (TÜYLÜ LADEN) BİTKİSİNDEN STANDARDİZE EKSTRELERİN HAZIRLANMASI TAKVİYE EDİCİ GIDA VE KOZMETİK ÜRÜNLER GELİŞTİRİLMESİ

7100629-BOŞ VE DOLU LİPOZOMAL TAŞIYICI SİSTEMLER GELİŞTİRİLEREK ANTİ-AKNE, NEMLENDİRİCİ VE ANTİ-AGİNG ÜRÜNLERİNE UYGULANMASI

3130970-SAÇ VE DERİYE ETKİLİ BİTKİSEL EKSTRELER GELİŞTİRİLEREK GEN İFADELERİNİN BELİRLENMESİ VE BİTKİSEL BAZLI DERMOKOZMETİK ÜRÜNLERİN ELDE EDİLMESİ

3140857-KARAYEMİŞ MEYVESİNİN GIDA VE GIDA TAKVİYELERİNDE KULLANIMINA YÖNELİK STANDARDİZE EDİLMİŞ ÜRÜNLER ELDE EDİLMESİ